A novel role for PRC2 activity in light signalling in Arabidopsis thaliana

JOSEPH FRANCIS NELSON

A novel role for PRC2 activity in light signalling in *Arabidopsis thaliana*

Joseph Francis Nelson

Submitted for the qualification of Doctor of Philosophy

Department of Biosciences, Durham University

July 2021

Abstract

Light is the major regulator of plant development, controlling a number of key stages throughout the plant life cycle. One of these is the transition from skotomorphogenesis to photomorphogenesis in seedlings upon exposure to light. Perception of light via a suite of photoreceptors initiates a massive reorganisation at the transcriptional, translational and post-translational levels across the seedling. In recent years, increasing evidence has also been presented showing epigenetic changes also play a crucial role in this process. The work in this thesis seeks to contribute to this growing field by identifying that the Polycomb Repressive Complex 2 (PRC2) plays a key role in photomorphogenesis via the deposition of H3K27me3, mediated by the histone methyltransferase CURLYLEAF (CLF).

Phenotypic and genetic analysis shows that CLF activity is upregulated by blue light in a CRY1-dependent manner, and that loss of CLF leads to elongated hypocotyls – a classic phenotypic trait which has been long used to identify deficiencies in light signalling. RNA-seq and ChIP-qPCR analysis indicates that CLF inhibits hypocotyl elongation via the deposition of the silencing chromatin modification H3K27me3 at expansins and *XTH* genes. It is also shown that CLF further contributes to the enhancement of auxin signalling in cotyledons via the H3K27me3-mediated silencing of *AUX*/*IAA* and GH3 genes. Additional phenotypic analysis indicates that CLF also plays a role in other auxin-regulated processes such as phototropism. Finally, a candidate interaction is identified between CLF and the skotomorphogenesis-promoting transcription factor PIF4, indicating an intriguing possible mechanism for CLF regulation during light responses.

Table of Contents

List of Figures

Chapter 1 - Introduction

Chapter 3 – Identification of a role for CURLYLEAF during photomorphogenesis

Chapter 5 – Further investigations to characterise the role of *CLF* in light signalling

Chapter 6

List of Tables

Chapter 2 – Methods and Materials

Appendices

Statement of authorship

I certify that all of the work described in this thesis is my own original research unless otherwise acknowledged in the text or by references, and has not been previously submitted for a degree in this or any other university.

Statement of copyright

Abbreviations and naming conventions

The standard scientific conventions for protein and gene naming have been followed: wild type genes and proteins are in capitals and mutants are denoted by lower case, gene names are italicized whereas protein names are not. Standard scientific abbreviations have been used for units of weight, length, amount, molarity, temperature and time. Standard chemical element symbols, nucleic acid and amino acid codes are used

MS	Murashige & Skoog media
Col-0	Columbia
BR	Brassinosteroids
bHLH	Basic Helix-Loop-Helix
DEGs	Differentially expressed genes
DMSO	Dimethyl sulfoxide
DNA	Deoxyribonucleic acid
GA	Gibberellic acid

GFP	Green fluorescent protein
GO	Gene ontology
GUS	β-glucuronidase
HAT	Histone Acetyl Transferase
HDAC	Histone De-Acetylase
IAA	Indole-3-acetic acid
Log2fc	Log2 fold change
NGS	Next generation sequencing
PCR	Polymerase chain reaction
RT-qPCR	Reverse transcription-quantitative PCR
RNA	Ribonucleic acid
RNA-seq	RNA-sequencing
TF	Transcription factor
WT	Wild type
Y2H	Yeast-two hybrid

Acknowledgements

Production of this thesis has been a long, and not always smooth road, and I wouldn't have made it to this point without support from a whole host of people in various ways. It gives me great pleasure to thank them here.

Firstly, I must sincerely thank my supervisor, Miguel de Lucas, for all your help throughout the PhD. Your insight and assistance were invaluable and essential in the production of this thesis, and thank you for always being on hand at literally a moment's notice to offer help throughout the years. I also must register my gratitude to the BBSRC Newcastle-Liverpool-Durham Doctoral Training partnership for financial support of the project and Dr Wenbin Wei of Durham University for carrying out the initial bioinformatic steps of the RNA-seq analysis, aligning the raw reads to the *Arabidopsis* genome.

Next, thanks to my fellow students of the De Lucas research group, and in other groups of Lab 1003/1004. Grace, I couldn't have found a better person to spend first year with, or be a better co-"lab parent" to the summer students! And Lauren, you were such a wonderful person to have around in the lab, and thanks for demonstrating an amazing ability to never get annoyed no matter how many times I grumbled about protein extractions! Thanks also to Amy (biosis!), Flora and May for always being there for me for chats about science and everything else and somehow ensuring that a pub trip always happened when it needed to. To Cian, George and Julian for all the rugby, football and joint excitement about stocks and cryptocurrency. And finally to Chris, Geoff, Naomi, Shauni, Becca, Catherine, Perrine, Rodrigo and Fahad, thanks making the lab and the office such a great place to be.

Huge thanks also to all my friends who have helped keep me sane throughout the years, particularly during the final year and lockdown! Thanks to Boro friends Kate, Tom, Laura, Joe, Sammy, Zeeshan, Ceyda, Matt and Chris for all the walks, dog playtime and Boro matches. To my fellow Uqbar adventurers Amy, Jack, Andy, Liv, May and Flora and our leader John for the hours of fun with the dungeons and the singular dragon. To the Krakens Lucinda, Michael, Imogen, Rob, Danielle, Sophie, Jess, Adam and Jo for all the pub trips and zoom calls, and particularly Lucinda thanks for listening to my many stressed splurges during the final few months despite having your own PhD to contend with! And of course thanks to the many friends from Chad's who have given me such a wonderful community through the years, especially my wonderful committee of 2017-18 Yanmin, Emily, Cate, Liz, Tom, Michael, Alastair, George and Julian for giving me such a great year when I decided to take on being president alongside the PhD!

And finally I must say a huge thank you to my mum and my sister Victoria. Thank you for always being there for me whenever I needed to collapse and go somewhere else, and even taking it on yourselves to drive up and feed Max the cat when I needed to spend all day writing! I couldn't have made it to the finish line without both of you!

Chapter 1 – Introduction

1.1 Skotomorphogenesis, photomorphogenesis and light signalling in *Arabidopsis thaliana*

1.1.1 Photomorphogenesis is major developmental transition in *Arabidopsis thaliana*

All organisms must respond to their environment in order to survive. As sessile organisms, plants such as *Arabidopsis thaliana* are unable to change their location, and instead must utilise their highly plastic development in order to accomplish this. The most important environmental factor regulating plant development is light. As autotrophs, plants are dependent on light to provide the energy for photosynthesis, and light signalling governs key steps of the plant life cycle such as germination and the transition from vegetative to reproductive development (Fankhauser and Chory, 1997). In addition, light also provides key signals to plants about neighbour density and photoperiod, and plants show drastically different development in different light regimes (Reviewed in Kami et al., 2010). These various processes are summarised in (Fig. 1.1).

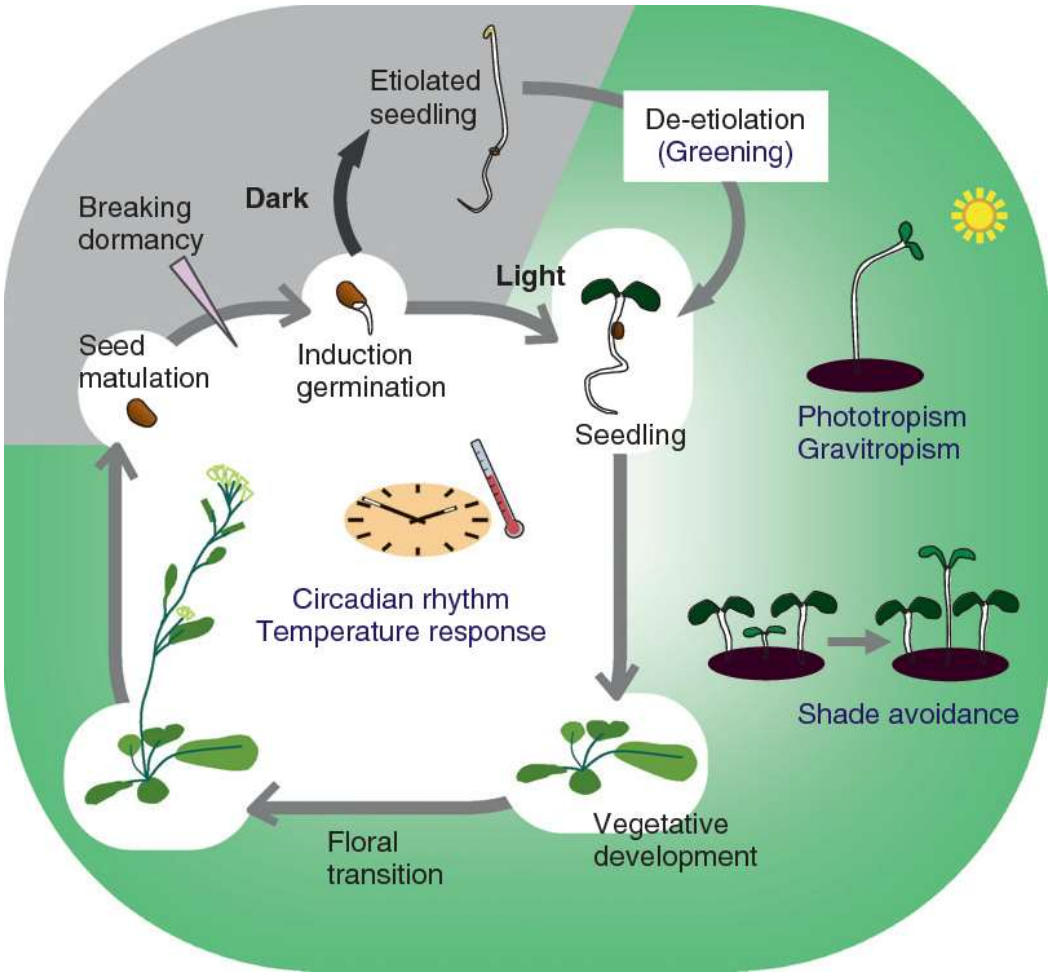

Fig. 1.1 Summary of the involvement of light at various stages of plant development – Reproduced from (Kami et al., 2010)

Light regulates a number of key developmental transitions in plants, including germination, photomorphogenesis/de-etiolation, vegetative development and floral transition. Plants also display distinct responses to different light regimes such as shade avoidance, in response to a low red:far-red ratio, and phototropism in response to light from a certain direction. These processes are summarised in the figure above.

Another process governed by light is known as photomorphogenesis, or de-etiolation, and is one of the most significant developmental shifts seen in the plant life cycle. When angiosperms such as *Arabidopsis thaliana* are grown in darkness, a distinct form of growth known as etiolation or skotomorphogenesis is displayed. Whilst in darkness, seedlings are unable to produce energy via photosynthesis and must instead rely on seed reserves. Skotomorphogenesis prioritises rapid upwards growth, to ensure that the shoot

tip can reach the light and begin photosynthesis before this finite supply of energy is exhausted (Josse and Halliday, 2008). Skotomorphogenesis is characterised by several distinct architectural traits which can be clearly seen in dark-grown seedlings, as shown in (Fig 1. 2). Firstly, the hypocotyl undergoes rapid elongation, providing the growth necessary to reach the surface (Koornneef et al., 1980), (Cowling and Harberd, 1999). In addition, the cotyledons are small and folded and together with the upper hypocotyl form a bent structure known as the apical hook, which is vital to protect the shoot tip as the plant grows through soil (Harpham et al., 1991).

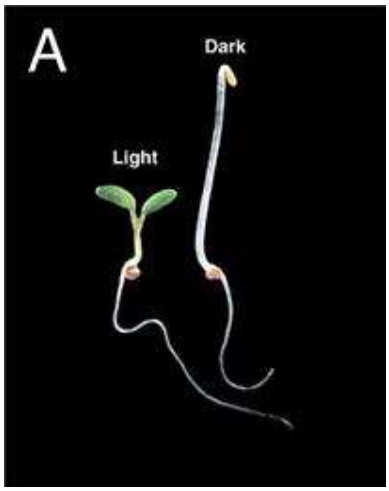

Fig. 1.2 – Illustration of architectural differences between etiolated and de-etiolated plants.

Arabidopsis seedlings grown in the presence of light exhibit deetiolation/photomorphogenesis (left), characterised by open cotyledons, inhibition of hypocotyl elongation, unfolding of the apical hook and greening. Those grown in the dark exhibit etiolation/skotomorphogenesis (right), characterised by closed, folded cotyledons, yellowing, an apical hook and elongation of the hypocotyl. Adapted from (Nemhauser and Chory, 2002).

Upon exposure to light, etiolated seedlings undergo a process known as de-etiolation, or photomorphogenesis. Photomorphogenesis is a distinct morphological shift which includes inhibition of hypocotyl expansion, straightening of the apical hook, and the unfolding and expansion of the cotyledons. The morphological differences between

skotomorphogenesis and photomorphogenesis is illustrated in (Fig. 1.2). There is also a distinct greening of the seedlings, particularly in the cotyledons, driven by the conversion of undifferentiated etioplasts into chloroplasts and the accumulation of chlorophyll (Huq et al., 2004), (Wang et al., 2018).

1.1.2 COP1 and PIFs are crucial to the maintenance of skotomorphogenesis in the darkness

The process of skotomorphogenesis requires the active repression of genes promoting photomorphogenic light-responsive growth (Josse and Halliday, 2008).

One crucial factor in maintaining skotomorphogenesis is CONSTITUTIVELY PHOTOMORPHOGENIC 1 (COP1). *cop1* loss-of-function mutants display a photomorphogenic phenotype even when grown in darkness, and do not display the typical skotomorphogenic traits of hypocotyl elongation, apical hook or folded cotyledons (Deng et al., 1991). COP1, along with SUPPRESSOR OF PHYA-105 (SPA), functions in substrate recognition for the CUL4 E3 ubiquitin ligase. In darkness COP1 accumulates in the nucleus, where it targets key factors involved in promotion of photomorphogenesis and targets them for proteasome-mediated degradation via ubiquitination, most notably ENLONGATED HYPOCOTYL 5 (HY5) (Osterlund et al., 2000) (Hoecker, 2005). HY5 is a basic leucine zipper (bZIP) transcription factor which is considered the master regulator of light-induced transcription during photomorphogenesis (Gangappa and Botto, 2016). HY5 has been shown to regulate the transcription of over 1000 genes in a light-dependent fashion (Zhang et al., 2011), and is crucial to the regulation of photomorphogenic traits such as the inhibition of cell elongation and promotion of chloroplast development (Koorneef, 1980), (Oyama et al., 1997), (Jing et al., 2013). Notably, *hy5* mutants exhibit dramatically elongated hypocotyls under all light wavelengths (Koornneef et al., 1980), (Holm et al.,

2002), (Oravecz et al., 2006), (Sibout et al., 2006). Other transcription factors have also been identified as targets of COP1-promoted degradation, including HY5-HOMOLOG (HYH) and LONG HYPOCOTYL IN FAR-RED (HFR1), which are involved in blue- and far-red-mediated repression of hypocotyl elongation respectively (Fairchild et al., 2000), (Holm et al., 2002). Upon light perception, COP1 is excluded from the nucleus, facilitating the de-repression of downstream light signalling components such as HY5 (Osterlund and Deng, 1998).

Another group of vital components promoting skotomorphogenesis are the family of PHYTOCHROME INTERACTING FACTORS (PIFs), a group of basic Helix-Loop-Helix (bHLH) transcription factors. Eight PIFs have been identified in Arabidopsis and named PIFs 1 through 8, with the closely-related *PIF1*, *PIF3*, *PIF4* and *PIF5* being the best characterised and playing the most distinct roles in the light response (Reviewed in Lee and Choi, 2017). PIFs promote transcriptional programmes that maintain skotomorphogenesis in the darkness (Shin et al., 2009). High redundancy between PIFs means that the loss of individual PIFs rarely has an effect, but loss of the four core PIFs (PIF1, PIF3, PIF4 and PIF5) together in the *pif* quadruple mutant (*pifq*) results in a constitutive photomorphogenic phenotype even in darkness (Shin et al., 2009). Upon light perception, PIF activity is inhibited, allowing photomorphogenesis to proceed. As the names suggest, PIFs are primarily known to be regulated by phytochromes, which repress PIF activity both by inhibiting their binding to target promoters (Park et al., 2012) and inducing their degradation (Al-Sady et al., 2006). Notably, however, other photoreceptors such as cryptochromes are also known to have functions in regulating PIF activity (Pedmale et al., 2016), (Ma et al., 2016).

1.1.3 Light Perception in *Arabidopsis thaliana*

Light in *Arabidopsis thaliana* is perceived by several classes of light-receptive proteins known as photoreceptors. Plants are responsive to light across the visible and ultraviolet spectrum, with each photoreceptor primarily responding primarily to a subset of light wavelengths. It should be noted, however, that such responses are not exclusive, and many photoreceptors have some sensitivity to a broad range of wavelengths, as shown in (Fig. 1.3).

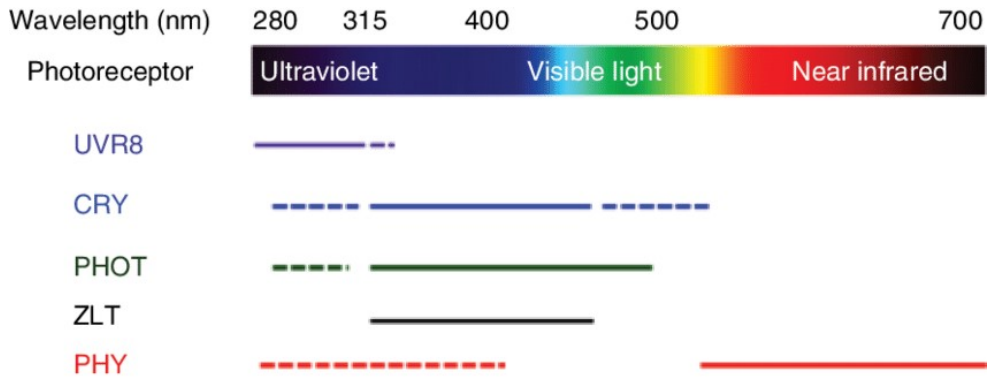

Fig. 1.3 – Absorption wavelengths of plant photoreceptors – reproduced from (Gupta et al., 2017).

Illustration of light wavelengths to which each group of photoreceptors is responsive. Primary absorption regions indicated by solid lines, sensitivity towards other wavelengths shown by dashed lines.

The PHYTOCHROMES (PHY) primarily absorb light in the red and far-red wavelengths, with some sensitivity to blue light. Three groups of photoreceptors primarily respond to blue and UV-A light – the CRYPTOCHROMES (CRY), the PHOTOTROPINS (PHOT) and three members of the ZEITLUPPE family (ZLT). One photoreceptor is known to respond to UV-B light, known as the UV RESISTANCE LOCUS 8 (UVR8).

Red and Far-Red light is predominantly perceived by the phytochrome family of photoreceptors, which has five members known as PHYTOCHROME A-E (PHYA-E). Blue and UV-A light is perceived by several families of photoreceptors: The cryptochromes CRYPTOCHROME 1 (CRY1) and 2 (CRY2); The phototropins PHOTOTROPIN 1 (PHOT1) and 2 (PHOT2); and the three members of the Zeitlupe family ZEITLUPE (ZTL), FLAVIN-

BINDING KELCH REPEAT F-BOX1 (FKF1) and LOV KELCH PROTEIN 2 (LKP2) (Suetsugu and Wada, 2013). There is one known protein responsible for UV-B light perception, known as UV RESISTANCE LOCUS 8 (UVR8) (Rizzini et al., 2011). Although effects of green light wavelengths have been reported, they are minor compared to the effects of the other wavelengths mentioned here (Wang and Folta, 2013). Correspondingly, there are no known photoreceptors which primarily respond to green light, although these wavelengths can have minor effects thanks to the broad spectrum of light absorption of other photoreceptors, particularly through the repression of CRY activity (Wang and Folta, 2013).

Among the various photoreceptors, analyses of photomorphogenesis in the literature predominantly discuss the effects of PHYs and CRYs, and focus on the effects of blue, red, and far-red light (e.g. (Nemhauser et al., 2002), (Arsovski et al., 2012), (Favero et al., 2020)). This thesis will follow this pattern.

1.1.4 Phytochromes

The Phytochrome family were the first photoreceptors to be identified and characterised (Siegelman and Hendricks, 1965), (Siegelman et al., 1966). In the cell, phytochromes exist as dimers of two chromoproteins. Each individual phytochrome protein consists of two subunits: An N-terminal sensory domain; and a C-terminal regulatory domain. The N-terminal domain is covalently bound to a light-sensitive chromophore named phytochromobilin, which is responsible for the phytochrome's light-perceptive activity (Siegelman et al., 1966). Meanwhile, the regulatory domain interacts with various factors and is responsible for the downstream signalling effected by the phytochrome (Reviewed in (Quail, 2010)).

Phytochromes exist in two morphological states, known as Pr and Pfr, and display reversible conversion between the two upon light perception. The Pr form is biologically inactive, with the Pfr form responsible for the downstream effects of phytochromes. Phytochromes are synthesised in the cytosol, in the inactive Pr form, and accumulate here during etiolated growth, remaining inactive in darkness. When the plant first encounters light, PHYs are rapidly converted to the biologically active Pfr form, and translocated to the nucleus, where they interact with downstream factors to promote the transition to photomorphogenesis. Predominant effects of phytochromes in photomorphogenesis include the inhibition of PIFs and the exclusion of COP1 from the nucleus (Osterlund and Deng, 1998), (Al-Sady et al., 2006), (Park et al., 2012).

Additionally, the Pr and Pfr have different absorption spectra, with Pr primarily absorbing red light, and Pfr absorbing far-red light (Rockwell et al., 2009), and the conversion process governs how the phytochromes differentially respond to different wavelengths of light. A high ratio of red:far-red light will result in greater abundance of Pfr relative to Pr, whilst a low ratio will result in higher levels of Pr relative to Pfr. However, the two conformations overlap in their absorption spectrum, with Pr and Pfr showing some absorption of far-red and red light, respectively. As such, in the presence of light, a photoequilibrium between the two states will be reached depending on the balance of red/far-red wavelengths present (Klose et al., 2015). The balance between Pr and Pfr is particularly important for regulating the shade avoidance response, where low red:far-red light ratios caused by shade from neighbouring plants result in distinct developmental responses such as repression of seed germination, the promotion of hypocotyl and petiole growth and early flowering (Casal, 2012).

In the absence of light, meanwhile, biologically-active Pfr will gradually revert to the inactive Pr form in a process known as dark or thermal reversion (Eichenberg et al., 2000).

Notably in the case of PHYB, the process of dark reversion is increased at higher temperatures (Legris et al., 2016). This represented a novel property of PHYB and demonstrated that as well as responding to light, it can also function as a temperature sensor (Legris et al., 2016) (Jung et al., 2016). This dual property of PHYB means it can function to integrate light and temperature signals during development, and helps to explain observations that higher ambient temperatures can promote skotomorphogenic traits such as hypocotyl elongation, a process referred to as thermomorphogenesis (Legris et al., 2016), (Jung et al., 2016), (Casal and Balasubramanian, 2019).

This core mechanism of phytochrome action is illustrated in (Fig. 1. 4).

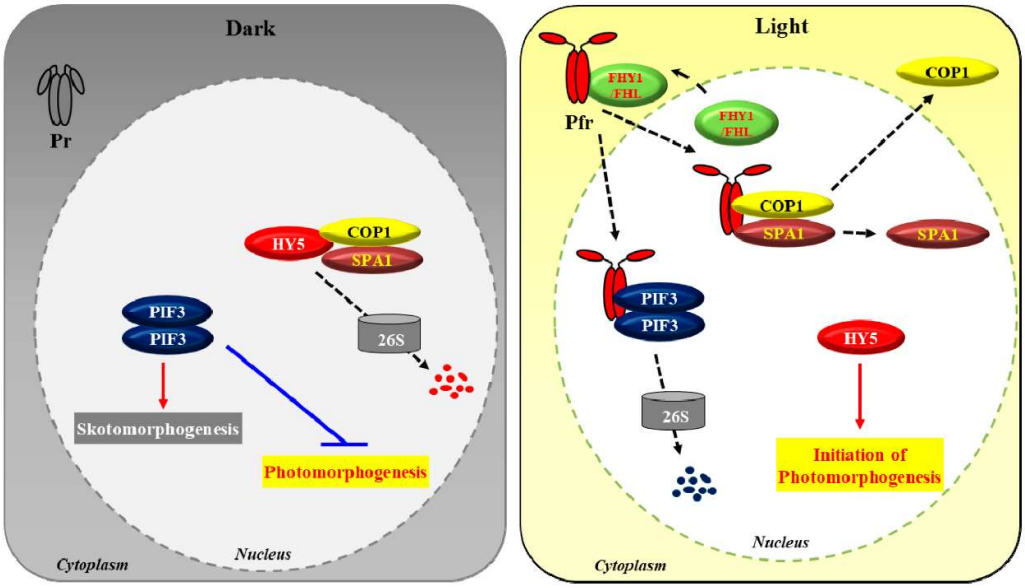

Figure 1.4 Mechanisms of phytochrome mediated photomorphogenesis (Reproduced from (Hoang et al., 2019)).

This figure summarises the core mechanisms by which phytochromes promote photomorphogenesis. In darkness, transcription factors known as PIFs such as PIF3 promote skotomorphogenesis and inhibit photomorphogenesis. Meanwhile, HY5, a master regulator of light-promoted transcription is targeted for degradation via the 26s proteasome by a complex consisting of CONSTITUTIVE PHOTOMORPHOGENIC 1 (COP1) and SUPPRESSOR OF PHYA 1 (SPA1). Upon perception of light, phytochromes are converted to the biologically active Pfr form and translocated to the nucleus where they induce degradation of PHYTOCHROME INTERACTING FACTORS (PIFs) via the 26s proteasome and promote the nuclear exclusion of (COP1), inhibiting the COP1-SPA1 complex , facilitating photomorphogenesis. This figure also shows the involvement of FHY1 (FAR-RED ELONGATED HYPOCOTYL 1)/FHL (FHY1-LIKE), which is crucial for the nuclear accumulation of PHYA.

The phytochrome family is primarily divided into two classes known as Type I and Type II phytochromes, also known as Light-labile phytochrome and light-stable phytochrome, with different patterns of activation and light sensitivity. PHYA is the sole Type I phytochrome in *Arabidopsis*, whilst PHYB, PHYC, PHYD and PHYE are all members of the Type II sub-family (Sharrock and Clack, 2002).

The light-labile phytochrome, PHYA, is primarily responsible for mediating responses to far-red light (Reviewed in Li et al., 2011). PHYA shows the highest expression in darkness, accumulating in the Pr form, but the Pfr form has a very short half-life, meaning that upon light perception PHYA is rapidly degraded (Debrieux and Fankhauser, 2010). This has the curious effect that although red light promotes transition into the biologically active Pfr form, it is actually the environments with high levels of far-red light that result in the highest active PHYA, as the conversion to the stable Pr form is more prominent, resulting in higher overall levels of PHYA protein. This can be seen in the fact that *phyA* mutation has no phenotypic effect on seedlings grown in red light, but results in longer hypocotyls in seedlings grown under far-red light (Li et al., 2011). It is also known that PHYA plays a role in responses to blue light (Lin, 2000).

The other four phytochromes (PHYB-E) are all more stable in the light. High levels of red light promote a photoequilibrium favouring the biologically active Pfr form, whilst high levels of far-red promote reversion to the Pr inactive form (Li et al., 2011). PHYB predominates during light growth and is largely responsible for the responses to red light (Reviewed in Li et al, 2011 and Tang et al., 2016). In R-light, PHYB mutants display elongated hypocotyls and smaller cotyledons, although apical hook unfolding does still occur (Li et al., 2011). PHYC-E perform overlapping functions with PHYB but with reduced impact in plant development. Thus, PHYB is often discussed in isolation when referring to phytochrome-mediated red light responses in the literature (e.g. Li et al., 2011; Tang et al., 2016; Legris et al., 2016). The work in this thesis will follow this precedent and focus on the activity of PHYA and PHYB during de-etiolation.

1.1.5 Cryptochromes

Cryptochromes were characterised later than phytochromes, having originally been named for their “cryptic” nature (Gressel, 1979). Cryptochromes consist of two key domains: an N-terminal light-sensory domain known as the PHR or CNT domain, which is bound to a chromophore; and a C-terminal domain which facilitates downstream cryptochrome-mediated effects known as the CCT domain (Yang et al., 2000). Unlike the phytochromes, however, the synthesis and subcellular localisation of the two cryptochromes differs markedly.

CRY1 was the first cryptochrome to be identified (Lin et al., 1995), and has the most prominent effects on blue light-mediated photomorphogenesic traits such as inhibition of hypocotyl elongation (Lin et al., 1998). The light-induced activation of CRY1 follows a comparable pattern to that of PHYB. CRY1 is synthesised in the cytoplasm, in a biologically inactive form. Upon blue light perception, CRY1 undergoes a conformational change, probably involving a repositioning of the PHR and CCT domains (Reviewed in Wang and Lin, 2020). The photoactivated CRY1 molecule is then translocated to the nucleus, initiating downstream signalling.

CRY2, meanwhile, shows a different pattern of localisation and is localised to the nucleus throughout its post-translational life, with no re-localisation after blue light perception (Yu et al., 2007). Like CRY1, however, it exists in an inactive form in the dark, and undergoes a conformational change upon light perception to activate downstream signalling (Reviewed in Wang and Lin, 2020). Comparably to PHYA, CRY2 exhibits rapid degradation upon light perception (Yu et al., 2007). CRY2 has an effect in promoting photomorphogenesis, although minor compared to CRY1, and also has effects in promoting photoperiod-mediated floral transition (Lin et al., 1998), (Guo et al., 1998).

After activation by blue light, the cryptochromes interact with a range of partners to mediate signalling promoting photomorphogenesis. The first CRY-interacting proteins were a group of bHLH transcription factors known as CIBs (CRYPTOCHROME INTERACTING BASIC HELIX-LOOP-HELIX) (Liu et al., 2008). Interactions between both CRYs and members of this family have been shown to mediate several cryptochrome-mediated processes including CRY1-mediated inhibition of hypocotyl elongation (Wang et al., 2018) and CRY2-mediated leaf senescence and regulation of flowering (Liu et al., 2008), (Meng et al., 2013), (Liu et al., 2018). As research into cryptochromes has progressed it has also been found that they regulate a number of other targets, showing partial redundancy with other photoreceptors such as the phytochromes. Firstly, both CRY1 and CRY2 interact and inhibit the action of the COP1-SPA complex (Wang et al., 2001). Cryptochromes are also known to interact with PIF4 and PIF5, inhibiting their activity and thus facilitating blue light-inhibition of skotomorphogenic transcriptional programmes (Pedmale et al., 2016), (Ma et al., 2016). Finally, cryptochromes are also known to interact with hormone signalling components which play a key role in promoting skotomorphogenesis (Reviewed in Wang et al., 2020).

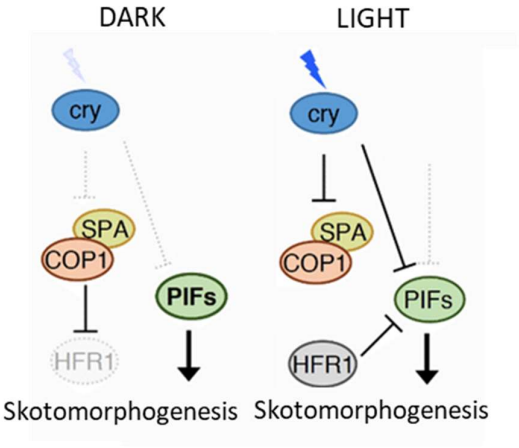

Figure 1.5 Mechanisms of cryptochrome mediated photomorphogenesis (Adapted from (Su et al., 2017)).

This figure summarises the core mechanisms by which cryptochromes promote photomorphogenesis. In darkness, the COP1-SPA complex targets LONG HYPOCOTYLS IN FAR-RED (HFR1) for degradation, whilst the PIF transcription factors promote skotomorphogenesis. Upon perception of light, CRY proteins undergo a conformational change and become activated. The photoactivated CRY proteins the COP1-SPA complex, which de-represses HFR1, allowing it to inhibit PIFs. The photoactivated CRY proteins also directly inhibit PIF activity.

1.2 The regulation of hypocotyl elongation by hormone and light signalling

1.2.1 Skotomorphogenesis involves hypocotyl elongation, which is driven by cell expansion and frequently used to assess photomorphogenesis

Of the various architectural traits seen in skotomorphogenesis, the elongated hypocotyl is arguably the most easily observable, and also the most easily quanitified. Correspondingly, hypocotyl lengths in darkness and light have been frequently used throughout the history of research into the light response as a key phenotypic indicator of deficiencies in light sensitivity. For example, the first genes to be identified as part of photomorphogenesis were identified in 1980 in a screen for mutants displaying elongated hypocotyls in white light (Koornneef et al., 1980). The distinct importance of hypocotyl elongation as a trait to identify deficiencies in light signalling can be seen in the nomenclature for several of the major promoters of photomorphogenesis. The master transcriptional regulator of photomorphogenesis, HY5, is named for the elongated hypocotyls in the mutant (Oyama et al., 1997), and the photoreceptors PHYB, CRY1 and PHYA were also originally identified from a long-hypocotyl mutant phenotype, and their genetic loci were previously known as *hy3*, *hy4* and *hy8* respectively (Somers et al., 1991), (Ahmad and Cashmore, 1993), (Dehesh et al., 1993). Concurrently, hypocotyl lengths in far-red light, red light and blue light was key evidence for the differential roles of PHYA, PHYB and CRY1 in these pathways (Neff and Chory, 1998), and was the primary phenotypic evidence indicating that CRY2 plays a minor role in blue light-mediated photomorphogenesis compared to CRY1 at high levels of blue light irradiance (Lin et al., 1998). Work in this thesis will follow this precedent, and utilise analysis of hypocotyl lengths as a phenotypic indicator of deficiency in light signalling.

The process of hypocotyl elongation is driven by cell elongation, with hypocotyl cells formed during embryogenesis and exhibiting little to no cell division during skotomorphogenic seedling growth after germination, whilst cell size increases potentially more than 100-fold (Gendrau et al., 1997). Correspondingly, regulation of cell walls is a key factor in control of skotomorphogenesis and photomorphogenesis. Cell expansion largely involves loosening of the cell wall, facilitating expansion by vacuole-driven turgor pressure (Cosgrove, 1993), (Cosgrove, 2016).

As discussed in Chapter 1.1, the elongation of the hypocotyl during skotomorphogenesis is under strict control of light signalling machinery, with COP1 and PIFs playing vital roles in its promotion in darkness, and is antagonized by photoreceptors. In addition to these factors, a suite of endogenous hormones also play vital roles in this process, and its inhibition after light perception. In particular, the signalling pathways of Auxin, Brassinosteroids and Gibberellins are known to act co-operatively with light signalling machinery in regulating hypocotyl growth during skotomorphogenesis and photomorphogenesis, and these varying signalling pathways display extensive crosstalk (Favero et al., 2020).

1.2.2 Auxin

Auxin is a crucial hormone which is involved in most aspects of plant development and produces a range of differential responses across different tissues. There are four native auxin compounds in *Arabidopsis*, with Indole-3-Acetic Acid being the most abundant. The core of the auxin signalling pathways consists of three main factors: The F-Box TRANSPORT INHIBITOR RESPONSE 1/AUXIN F-BOX PROTEIN (TIR1/AFB) Auxin co-receptors; The Auxin/INDOLE-3-ACETIC ACID (Aux/IAA) family; and the AUXIN RESPONSE FACTOR (ARF) family (Wang and Estelle, 2014). ARFs are transcription factors which bind

to auxin-responsive genes via Auxin response elements (AuxREs) and promote their expression. Aux/IAA proteins are transcriptional repressors which, in the absence of Auxin, repress the transcriptional activity of ARFs. When auxins are present in the cell, they bind to TIR1 and favour its association with Aux/IAA. This leads to Aux/IAA ubiquitination and degradation by the proteasome. This leads to the de-repression of ARFs, allowing for the transcriptional induction of auxin-responsive genes. This core mechanism of auxin signalling is illustrated in (Fig. 1. 3).

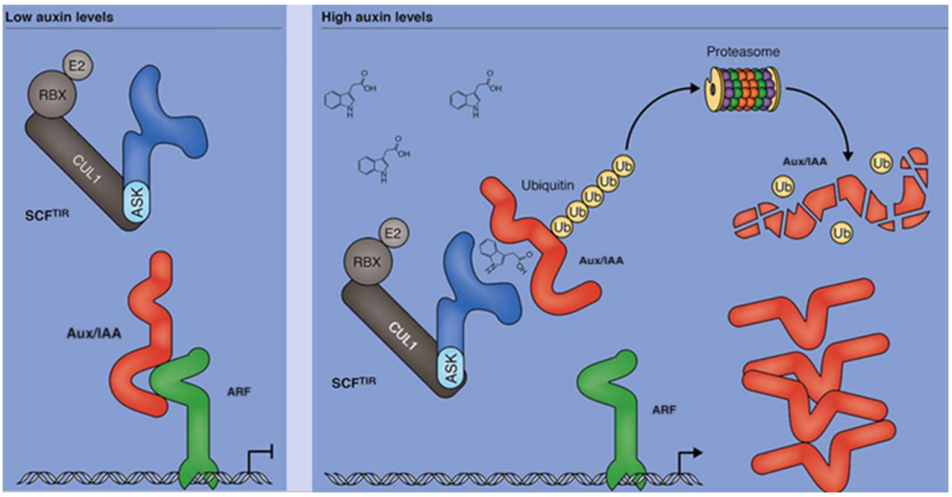

Figure 1.6 Auxin perception in *Arabidopsis thaliana* (Adapted from Larvy and Estelle, 2016).

This figure summarises the key mechanisms of auxin perception in *Arabidopsis thaliana*. When auxin levels are low, Aux/IAA proteins bind to ARF (AUXIN RESPONSE FACTOR) transcription factors, and inhibit their activity. When auxin levels are high, TIR1 forms an SCF E3 ubiquitin ligase complex along with the proteins SKP (ASK1), CULLIN1 (CUL1) and RBX. This complex binds to and mediates the ubiquitination of Aux/IAA proteins, targeting them for proteasomal degradation. The degradation of Aux/IAA proteins derepresses ARFs, allowing promotion of auxin-responsive gene expression.

Auxin signalling plays a key role in hypocotyl elongation by facilitating cell expansion. A number of genes involved in promoting cell expansion are transcriptionally induced by auxin treatment, including EXPANSINS, XYLOGLUCAN ENDOTRANSGLUCOSYLASE/HYDROLASE-related genes, CELLULOSE SYNTHASE GENES and various pectin-related genes (Nemhauser et al., 2006). Auxin is also known to induce protonation of the cell wall via activating H+ATPase proton pumps in the cell membrane, which promotes loosening of the cell wall and thus cell expansion (Takahashi et al., 2012), (Spartz et al., 2014).

Various plant mutants with altered auxin signalling show hypocotyl length defects. For example, loss of function mutations in the ARF genes *ARF6*, *ARF7* and *ARF8* cause shortened hypocotyls in dark-grown seedlings, with an additive effect when 2 or more of these genes are lost (Reed et al., 2018). Correspondingly, gain of function mutations in IAA genes *IAA3*, *IAA7* and *IAA17* have been shown to result in de-etiolated phenotypes in dark-grown seedlings, with short hypocotyls as well as unfolded cotyledons and lack of an apical hook (Nagpal et al., 2000), (Reed et al., 2018). In these gain-of-function mutants, the AUX/IAA protein is stabilised and is not degraded upon auxin perception, resulting in decreased levels of ARF activity and lack of auxin sensitivity. Conversely, null-mutants lacking these *AUX*/*IAA* genes display higher levels of ARF activity/auxin signalling when auxin levels are low, and this has been seen to result in increased hypocotyl lengths in light-grown seedlings (Nagpal et al., 2000).

1.2.3 Brassinosteroids

Another group of key signalling hormones in plants are the brassinosteroids . In fact, the role of Brassinosteroids in promoting skotomorphogenesis and hypocotyl elongation was highlighted by some of the first findings showing the roles of Brassinosteroids as signalling hormones (Li et al., 1996), (Szekeres et al., 1996).

Brassinosteroid signalling involves a de-repression downstream-acting transcription factors upon perception of BR. In the absence of Brassinosteroids, a GSK3-like kinase known as BRASSINOSTEROID-INSENSITIVE 2 (BIN2) phosphorylates and inactivates two transcription factors: BRASSINOZOLE-RESISTANT 1 (BZR1) and BRI1-1-EMS-SUPPRESSOR 1 (BES1, sometimes referred to as BZR2) (Li and Nam, 2002), (Yin et al., 2002), (He et al., 2002). Brassinosteroids bind to the receptor kinase a BRASSINOSTEROID-INSENSITIVE 1 (BRI1) and initiate a phosphorylation cascade (Wang et al., 2001), (Kinoshita et al., 2005). BRI1 phosphorylates two families of membrane-bound cytoplasmic kinases: the BR-SIGNALING KINASE (BSK) family and the CONSTITUTIVE DIFFERENTIAL GROWTH (CDG1) family (Tang et al., 2008), (Kim et al., 2011). These in turn phosphorylate BRI1-SUPPRESSOR-1 (BSU1) a phosphatase which then de-phosphorylates BIN2 (Kim et al., 2011). De-phosphorylated BIN2 is inactive and susceptible for proteasomal degradation (Li and Nam, 2002). Inactivation of BIN2 leads to BZR1 and BES1 dephosphorylation by PROTEIN PHOSPHATASE 2 A (PP2A), upon which they accumulate in the nucleus and regulate brassinosteroid-responsive transcription (Sun et al., 2010), (Yin et al., 2005). This mechanism of brassinosteroid signalling is illustrated in (Fig. 1.4).

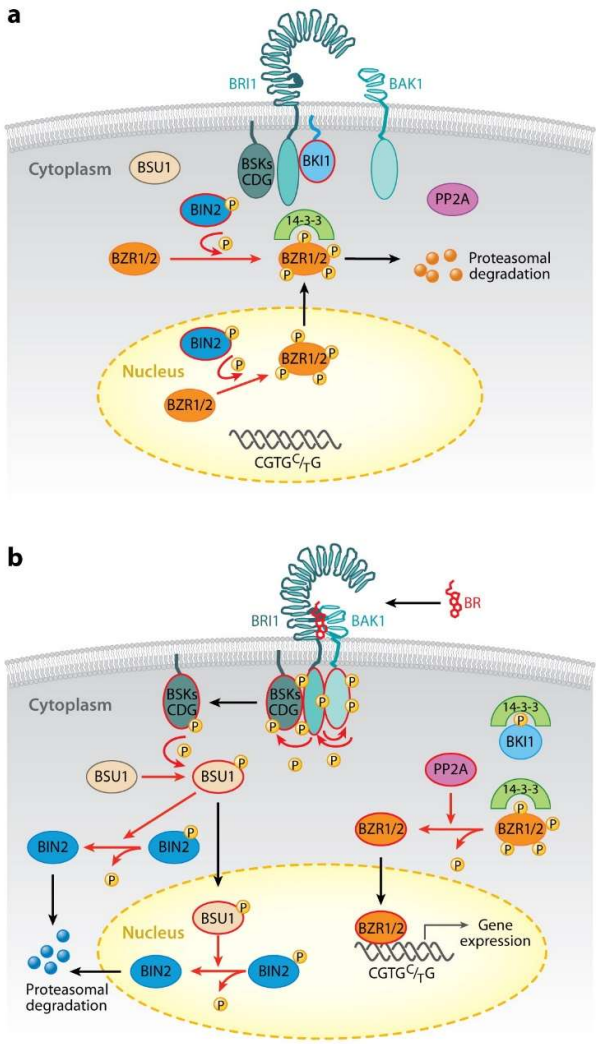

Figure 1.7 Brassinosteroid signalling in *Arabidopsis thaliana* (Reproduced from Wang et al., 2012).

This figure summarises the key mechanisms of brassinosteroid perception in *Arabidopsis thaliana*. When brassinosteroid (BR) levels are low, the GSK3-like kinase BRASSINOSTEROID INSENSITIVE 2 (BIN2) phosphorylates the transcription factors BZR1 and BZR2 (also known as BES1), targeting them for proteasomal degradation.

Binding of BR to the receptor BRI1 causes its activation. The inhibitory protein BRI1 KINASE INHIBITOR1 (BKI1) dissociates and the co-receptor kinase BRI1-ASSOCIATED RECEPTOR KINASE1 (BAK1) associates. A phosphorylation cascade is initiated by BRI1, which phosphorylates the kinases BRASSINOSTEROID-SIGNALLING KINASE1 (BSK1) and CONSTITUTIVE DIFFERENTIAL GROWTH1 (CDG1). These kinases then phosphorylate and activate the phosphatase BRI1-SUPPRESSOR1 (BSU1), which then de-phosphorylates BIN2. This inactivates BIN2 and targets it for proteasomal degradation. In the absence of BIN2 activity, BZR1 and BZR2/BES1 are dephosphorylated by PROTEIN PHOSPHATASE 2 A (PP2A). This stabilises and de-represses BZR1 BZR2/BES1, which activate BR-responsive gene expression.

Auxin and Brassinosteroids show partially overlapping functions. Both hormones promote hypocotyl elongation via cell wall expansion and repress photomorphogenesis (Reviewed in Wang et al., 2012). Furthermore, BR-mediated transcriptional targets include genes involves in cell wall synthesis/modification, cellular transport, and cytoskeleton organization, and a number of genes relating to chloroplast development are repressed by BR signalling (Sun et al., 2010).

The first BR mutants such as *de-etiolated 2* (*det-2*) (Li et al., 1996) and *constitutive photomorphogenesis and dwarfism* (*cpd*) (Szekeres et al., 1996) were identified to display constitutive photomorphogenic phenotypes. Further brassinosteroid-related signalling mutants have reinforced this view, indicating the crucial role of BR during skotomorphogenesis. For example *bin2.1* gain-of-function mutants (in which BIN2 is constitutively active and repressing BZR1 and BES1) and *bri1* mutants (in which *bri1* function is lost, leading to BR-insensitivity) both display a constitutive photomorphogenic phenotype in the dark (Peng et al., 2008), (Oh et al., 2012).

1.2.4 Gibberellin

Gibberellins (GAs) are one of the longest known classes of plant hormones and play roles in various developmental phases including germination, growth and flowering. GAs are required for skotomorphogenic growth, playing an antagonistic role to light (Alabadí et al., 2004), (de Lucas et al., 2008).

As for Auxin, GA signalling transduction involves the degradation of a repressor. *Arabidopsis* possesses three redundantly-acting GA-repressors, homologs of the rice gene *GIBERELLIN INSENSITIVE DWARF 1* (*GID1*), known as *GID1a*, *GID1b* and *GID1c* (Griffiths et al., 2006). When GAs bind to GID1 proteins, they repress the activity of several DELLA proteins, which in the absence of GAs function to repress GA-induced activity such as

growth and germination. In *Arabidopsis* there are 5 such DELLA proteins: GIBBERELLIC ACID INSENSITIVE (GAI); REPRESSOR-OF-ga1-3 (RGA); and RGA-LIKE1, 2 and 3 (RGL1),(RGL2),(RGL3) (Schwechheimer, 2012). The GA-GID1 complex binds to the DELLA proteins along with the F-Box proteins GIBBERELLIN INSENSITIVE DWARF 2 (GID2) and SLEEPY1 (SLY1) and facilitates their ubiquitination via the SCF E3 ubiquitin ligase complex. This leads to the degradation of DELLA proteins and the promotion of GA-induced responses, as illustrated in (Fig. 1. 5).

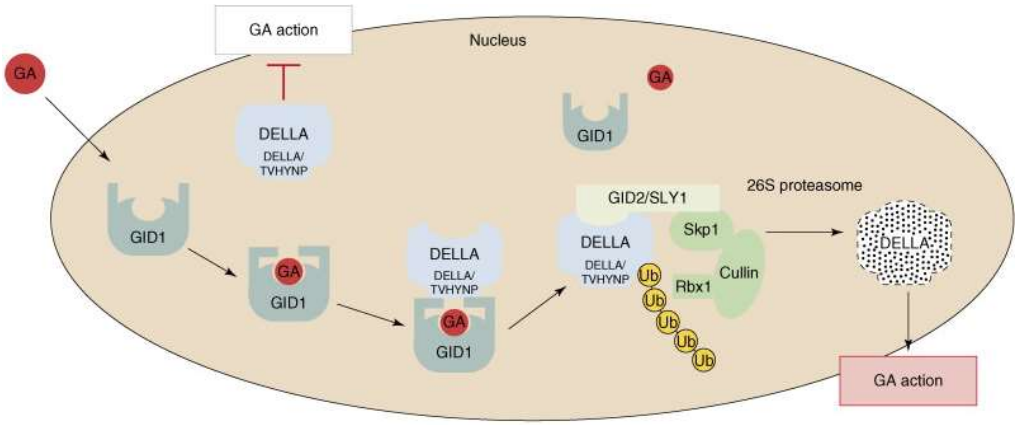

Figure 1.8 Gibberellic Acid (GA) signalling in *Arabidopsis thaliana*. (Reproduced from (Hirano et al., 2008)).

This figure summarises the key mechanisms of GA perception in *Arabidopsis thaliana*.

When GA levels are low, GA-induced responses are repressed by DELLA proteins.

When GA is present, it binds to one of three GIBBERELLIN-INSENSITIVE DWARF1 (GID1) proteins, which then binds to DELLA proteins. The GID1-bound DELLA proteins are then targeted by an SCF ubiquitin ligase complex consisting of SKP1, CULLIN, and RBX1 along with GIBBERELLIN INSENSITIVE DWARF 2 (GID2) and SLEEPY1 (SLY1). This results in their ubiquitination, which targets them for proteasomal degradation, thus de-repressing GA-induced action.

DELLAs are known to interact with and inhibit PIF3 and PIF4, and *pif4* mutants show increased sensitivity to GA biosynthesis inhibition, but reduced sensitivity to application of GAs (de Lucas et al., 2008). As such, by inhibiting the action of DELLAs, GA-signalling enhances photmorphogenesis by depression of the crucial PIF transcriptional factors.

1.2.5 Crosstalk between hormones and light signalling pathways

These three hormone pathways are extensively integrated with the central regulators of skotomorphogenesis. Two of these key hormone-regulated transcription factors, ARF6 and BZR1 show significant integration with the action of the PIF transcription factors, and together these three factors have been described as forming a single transcriptional module regulating light responses termed the BAP module (**B**ZR/**A**RF/**P**IF – module) (Bouré et al., 2019).

Numerous studies have highlighted the interconnectivity between these hormone- and light-signalling pathways. Disruption of the activity of PIF4 or BZR1-mediated brassinosteroid signalling reduces the sensitivity of hypocotyls to auxin-stimulated growth whilst disruption of PIF4 or ARF activity also inhibits the ability of *bzr1-d* gain-of-function mutation to induce long hypocotyls (Oh et al., 2014). Correspondingly, the long-hypocotyl phenotype of a *PIF4ox* mutant was also substantially reduced by disruption of brassinosteroid signalling in a *bri1* mutant (Oh et al., 2014). Much of this interconnectivity stems from the members of the BAP module regulating common transcriptional targets. In particular, ARF6-, PIF4- and BZR1-regulated genomic targets have substantial overlap (Oh et al., 2014). A number of genes which are known to promote growth are interdependently upregulated by the action of these three transcription factors (Oh et al., 2012), (Oh et al., 2014). These genes have also been shown to physically interact with

each other, facilitating their synergistic action (Oh et al., 2012), (Oh et al., 2014). Notably, PIF4 has also been observed to interact with BES1 (Martínez et al., 2018). BR-regulated transcription has also been found to overlap substantially with targets of the key photomorphogenesis-inducing transcription factor ELONGATED HYPOCOTYL 5 (HY5) (Sun et al., 2010).

Meanwhile, gibberellins relieve the actions of DELLA proteins which act antagonistically to growth promoting factors, including the BAP module transcription factors, thus facilitating hypocotyl elongation in darkness (de Lucas et al., 2008). GA signalling is also known to be substantially affected by BR signalling, and plants showing impaired BR signalling show reduced sensitivity to GAs, which is rescued in the *bzr1-1D* gain of function mutant (Bai et al., 2012). GA-enriched genes also heavily overlap with targets bound by BAP module member ARF6, BZR1 and PIF4 (Oh et al., 2014).

As well as mediating hypocotyl growth during skotomorphogenesis, the regulation of these hormones is also linked with photoreceptor activity in the light. For example, BIN2 promotes the phosphorylation and degradation of PIFs, in addition to its core targets BZR1 and BES1 (Bernardo- García et al., 2014). In the light this is promoted by HY5, which plays an important role in repression of hypocotyl elongation (Li et al., 2020). CRY1 has been observed to inhibit PIF4-mediated activation of the auxin synthesis gene YUCCA8, facilitating a decrease in auxin levels (Ma et al., 2016).

Crosslinks between hormone signalling and PIF activity to promote growth of hypocotyls during skotomorphogenesis is illustrated in (Fig. 1.7).

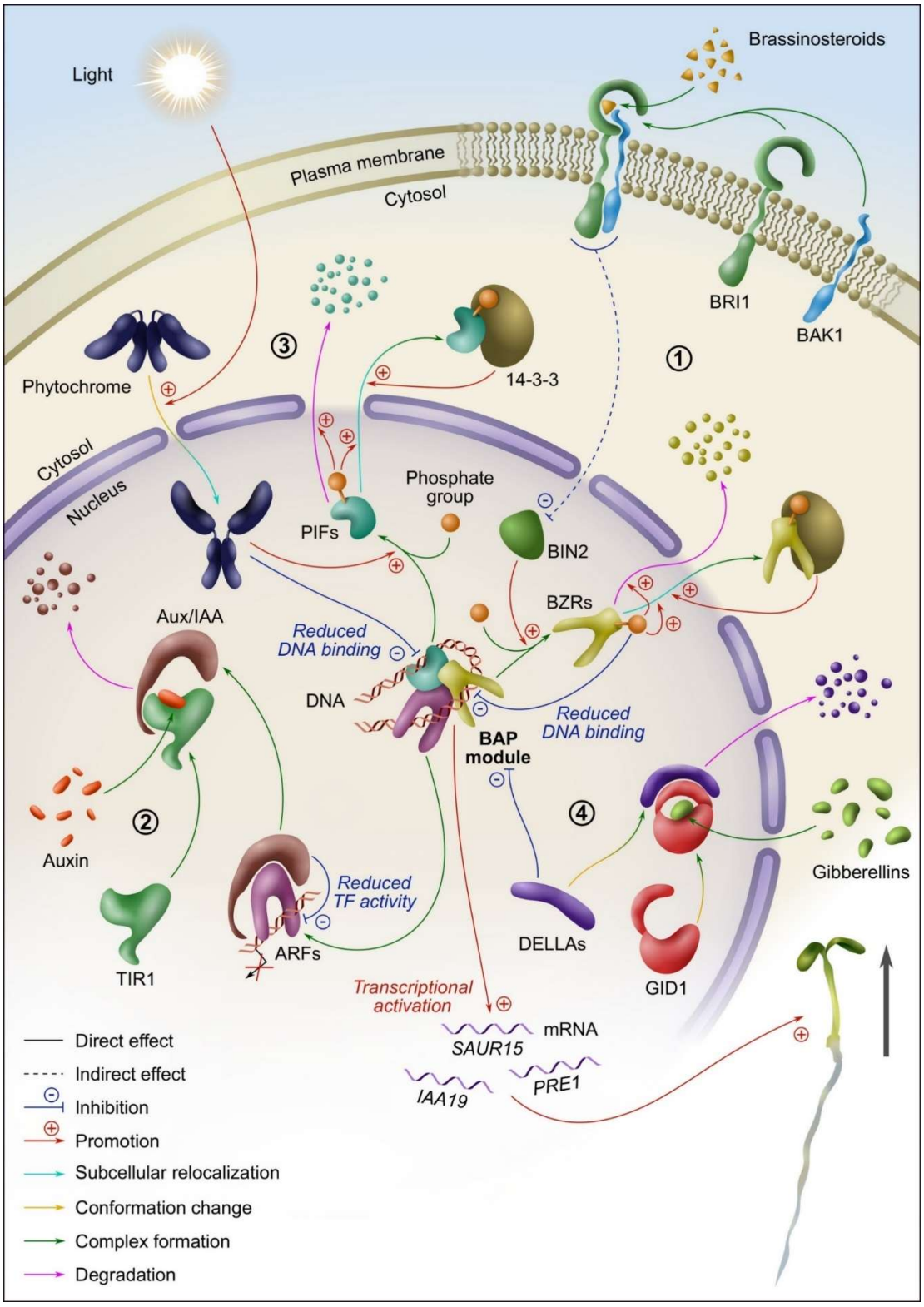

(Fig 1.9 legend on next page)

Figure 1.9 Crosslinks between hormone signalling and PIFs in promoting hypocotyl growth during skotomorphogenesis (Reproduced from Favero et al., 2020).

This figure shows various ways in which hormone signalling and light signalling pathways interact during skotomorphogenesis and photomorphogenesis. The BAP module consisting of the three transcription factors BRASSINOZOLE RESISTANT 1 (BZR1), AUXIN RESPONSE FACTOR 6 (ARF6) and PHYTOCHROME INTERACTING FACTOR 4 (PIF4) promotes hypocotyl elongation via activating transcription of genes such as *SMALL AUXIN UPREGULATED 15* (*SAUR15*), *INDOLE-3-ACETIC ACID INDUCIBLE 19* (*IAA19*) and *PACLOBUTRAZOL RESISTANCE 1* (*PRE1*).

(1) The action of BZR1 and BES1 is inhibited by the GSK3-like kinase BRASSINOSTEROID INSENSITIVE 2 (BIN2), which phosphorylates BZR1/BES1, inhibiting their DNA binding activity and targeting them for proteasomal degradation. Brassinosteroids activate the receptor BRASSINOSTEROID INSENSITIVE 1 (BRI1) which, together with its co-receptor BBRI1-ASSOCIATED RECEPTOR KINASE 1 (BAK1), initiates a cascade which leads to the inhibition of BIN2, de-repressing BZR1 and BES1.

(2) ARF6 (along with other auxin response factors) is inhibited by Aux/IAA proteins. Auxin binding to TRANSPORT INHIBITOR RESPONSE 1 (TIR1) receptor promotes the degradation of Aux/IAA proteins, de-repressing ARF-mediated transcription.

(3) Light causes the activation of PHYTOCHROMES (PHYs) and their conversion to the biologically active Pfr form. Pfr-PHYs then enter the nucleus and inhibit PIF4 and other PIFs by inhibiting their DNA binding activity and promoting their degradation

(4) DELLAs inhibit the activity of the BAP module transcription factors. Giberellins (GAs) bind to GA INSENSITIVE DWARF 1 (GID1) and promote the degradation of DELLAs, relieving this inhibitory effect.

The various interactions between hormones, PIFs, and other light signalling factors is still an active area of research, and new findings continue to be presented which will further our understanding of this complex network. What is clear, however, is that there is a vast, meticulously controlled network of signalling factors showing significant overlap and redundancy, and regulating considerable rearrangements at the genetic and protein level to facilitate hypocotyl elongation in darkness, and its inhibition by light.

1.3 Epigenetic regulation of plant light signalling

1.3.1 Overview of chromatin structure in *Arabidopsis*

In the nucleus, DNA exists in a complex with proteins, predominantly histones, forming a macromolecule known as chromatin. Chromatin serves several crucial functions in the cell, including protection of the DNA molecule, maintaining chromosome integrity during cell division, and modulation of gene expression. This latter role is arguably the most complex and intriguing aspect of chromatin, and is an active area of research in modern genetics.

The basic unit of chromatin is the nucleosome, in which 146bp of DNA are wrapped around an octamer of histone proteins . There are 5 core histones which show conservation across the eukaryote domain, known as Histone 1 (H1), Histone 2A (H2A), Histone 2B (H2B), Histone 3 (H3) and Histone 4 (H4) (Reviewed in Zhou et al., 2013). The octamer of histone proteins in the nucleosome is composed of four dimers: 2 H2A-H2B dimers; and 2 H3H4 dimers. Meanwhile, the DNA in between nucleosomes is regulated by Histone 1, and known as “linker DNA” (Rando and Chang, 2009), (Zhou et al., 2013). The basic repeating structure of nucleosomes along the DNA gives rise to the “beads-on-a-string” model of chromatin, also known as the 10nm fiber (Zhou et al., 2013). This complex can then be packaged into higher order chromatin structures, and this

remodelling plays a crucial role in regulating transcriptional activity by modifying the accessibility of chromatin to transcription factors and replication machinery. It was previously thought that chromatin existed in a structure known as the 30nm fiber, which involved tight packaging of nucleosomes into a solenoid structure (Fussner et al., 2011). However, the evidence for this occurrence *in situ* has been questioned and it is now thought that the 10nm fiber "beads-on-a-string" form is the predominant form of chromatin, at least in transcriptionally active cells, and that compacting chromatin into higher order structures can be achieved by bending the 10nm fiber (Fussner et al., 2011) (Joti et al., 2012).

One of the most important features of the nucleosome is that the N-terminal tails of the histone proteins protrude out from the centre of the nucleosome. These N-terminal tails are highly susceptible to various post-translational modifications which play a significant role in chromatin compaction, and thus transcription, by affecting how chromatin fibers interact (Pazin and Kadonga, 1997). At least 9 types of histone modification have been characterised, including: Acetylation, Methylation, Phosphorylation, Ubiquitination, SUMOylation, Deimination, Ribosylation, Proline Isomerization and addition of β-N-acetylglucosamine sugar residues (Bannister & Kouzarides 2011). Many of these histone modifications are known to play distinct roles in plant development, and in recent years increasing evidence has shown that chromatin regulation forms a crucial part of the light response.

Overall, chromatin can be largely distinguished into euchromatin, which is more open, gene-rich and more actively transcribed, and heterochromatin, which is more condensed and usually contains repetitive elements (Exner and Hennig, 2008). The level of chromatin compaction is largely controlled by histone modifications, along with DNA methylation, and the pattern of these two elements together is often referred to as the "histone code"

(Exner and Hennig, 2008). The level of chromatin compaction fluctuates throughout the plant life cycle, and forms a vital regulatory factor in ensuring proper developmental transitioning. Overall, levels of heterochromatin increase during cell differentiation, representing an increase in chromatin compaction and silencing of portions of the genome (Exner and Hennig, 2008). Correspondingly, when cell de-differentiation occurs, the opposite is true, and decondensation of the genome allows for higher transcriptional activity (Exner and Hennig, 2008).

Light perception in *Arabidopsis* triggers a massive reorganisation at the transcriptional level (Ma et al., 2001), (Jiao et al., 2005). Additionally, as discussed above, a complex network of interactions between hormones and core light signalling machinery involves extensive regulation at the post-translational level. Finally, in recent years, increasing evidence highlights that a distinct epigenetic reorganisation occurs upon light perception, which also plays a crucial role in photomorphogenesis.

1.3.2 The response to light in *Arabidopsis* involves significant reorganisation of nuclear architecture

Light causes changes in condensation of chromatin in the nucleus, with higher light intensity leading to higher levels of chromatin condensation, a process which involves the photoreceptors PHYB and CRY1 (Tessadori et al., 2009) (Bourbousse et al., 2015). A significant repositioning of genes occurs, with a number of light-regulated loci being repositioned from the transcriptionally-silent chromocentres to the nuclear periphery, facilitating a distinct increase in their expression (Fang et al., 2014). This repositioning is under the control of the light signalling machinery, being promoted by Phytochromes and Cryptochromes and antagonised by key promoters of skotomorphogenesis such as COP1, PIFs and DET1, as illustrated in (Fig. 1.8) (Fang et al., 2014), (Bourbousse et al., 2015).

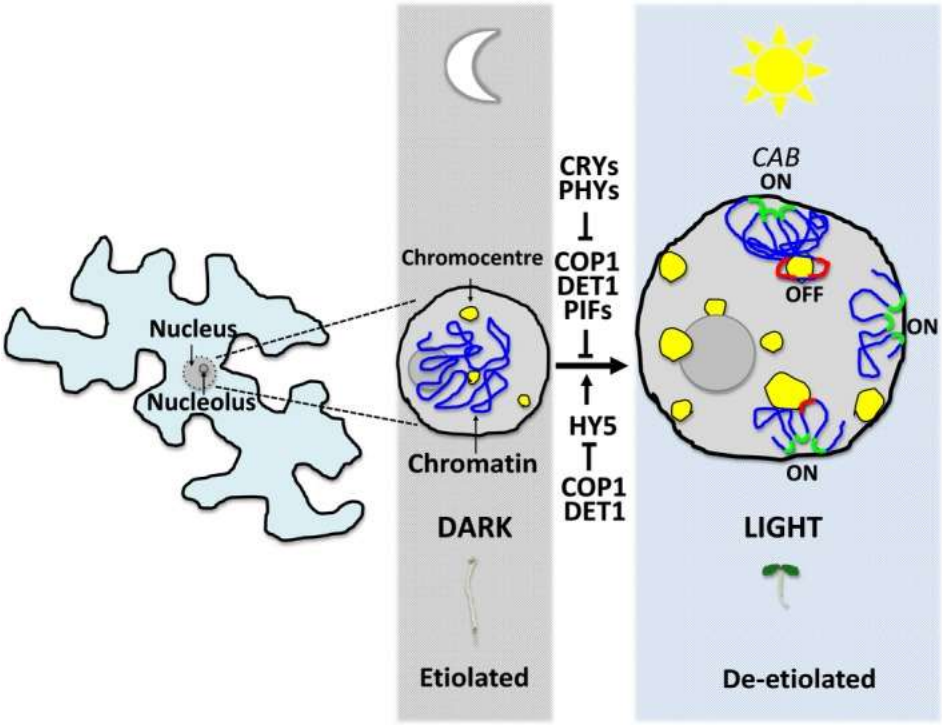

Figure 1.10 Light induces a shift in gene positioning (Figure adapted from (Perrella and Kaiserli, 2016)).

Illustration of light-dependent shift in gene positioning upon light perception. In darkness, factors such as CONSTITUTIVE PHOTOMORPHOGENIC 1 (COP1), PHYTOCHROME INTERACTNG FACTORs (PIFs) and DE-ETIOLATED 1 (DET1) maintain position of key light-responsive genes near the transcriptionally-silent chromocentres. COP1 and DET1 also inhibit the light-responsive transcription factor HY5. Upon light perception, photoreceptors such as PHYTOCHROMEs (PHYs) and CRYPTOCHROMEs (CRYs) promote the inhibition and degradation of PIFs and the nuclear exclusion of COP1 and DET1 nuclear reorganisation of light-responsive genes such as *CHLOROPHYLL A/B BINDING PROTEIN* (*CAB*) towards the nuclear periphery, facilitating increases in their transcription.

In addition, there is also one distinct nuclear event occurring after light perception the function of which is still to be fully elucidated. After light perception, various factors including photoreceptors, transcriptional regulators and other components of light signalling are known to concentrate in sub-nuclear locations known as photobodies (Reviewed in Van Buskirk et al., 2012). The purpose of these photobodies is still yet to be fully elucidated, but they have been proposed as sites of protein degradation, or transcriptional regulation, have been shown to prolong phytochrome activity upon darkness (Chen et al., 2010), (Kaiserli et al., 2015), (Van Buskirk et al., 2014).

1.3.3 Known roles of chromatin modifications during light responses

Acetylation was the first chromatin modification to be identified, and has an activating effect on transcription (Lee et al., 1993), (Roth and Allis, 1996), (Grunstein, 1997). Acetylation involves the addition of an acetyl group at lysine residues on histones, which removes the positive charge on the lysine residue. This weakens the interaction with the negatively-charged DNA, causing a relaxation of the chromatin and allowing access to transcription factors, facilitating gene expression (Roth and Allis, 1996), (Grunstein, 1997). Histone acetylation is controlled by Histone Acetyl Transferases (HATs), which add acetyl groups, and Histone De-Acetylases (HDACs), which removes them.

Histone acetylation plays a key role in light responses, including de-etiolation. The transcriptional co-repressor TOPLESS (TPL) interacts with HISTONE DEACETYLASE 19 (HDA19) to repress transcription during circadian regulation and flowering development, as well as in response to brassinosteroid signalling (Krogan et al., 2012), (Oh et al., 2014b), (Wang et al., 2013). Furthermore, HDA15, inhibits chloroplast development during skotomorphogenesis, via interaction with PIF3 (Liu et al., 2013). The HAT mutant, *gcn5,* shows elongated hypocotyls in far-red light, whilst the HDAC mutant *hd1* displays the

opposite phenotype, indicating a role for acetylation in regulating hypocotyl responses to this light wavelength (Benhamed et al., 2006). Correspondingly, histone acetylation has been shown to play a role in the light-regulated repression of PHYA transcription (Jang et al., 2011).

Histone methylation also modulates light responses. Methylation occurs primarily at lysine and arginine subunits in histone tails, and follows a more complex pattern than Acetylation. Similarly to acetylation, it is controlled by histone methyl transferases (HMTs), which add methyl groups, and histone demethylases (HDMs) which facilitate their removal. Unlike acetylation, however, methylation does not affect the charge of the protein, instead serving to affect the conformation of the chromatin macromolecule, as well as providing recruitment sites for transcription factors and other chromatin modifying factors. Additionally there are several possibilities for the methylation state of an amino acid: Lysines (K) may be mono-, di- or tri-methylated; whilst arginines (R) may be mono-, symmetrically di- or asymmetrically di-methylated (Bannister and Kouzarides, 2011). As might be expected, this also means the effects of histone methylation are more complex, with methylation having differing effects depending on the location and extent in question. In higher plants, histone methylation predominantly occurs at four lysine sites on H3 (H3K4, H3K9, H3K27 and H3K36), as well as lysine 20 on H4 (H4K20). Methylation is also observed at Arginine 17 of H3 (H3R17) and Arginine 3 of Histone 4 (H4R3) (Reviewed in Liu et al., 2010). H3K4 mono- and di- methylation H3K4me1/2) occur at both active and inactive genes, whilst trimethylation at this locus (H3K4me3) is tightly correlated with active gene expression. H3K9 methylation primarily exists as H3K9me1 and H3K9me2, which are known as silencing modifications, although some H3K9me3 can be detected, correlated with active transcription (Reviewed in Liu et al., 2010). Methylation of H3K27, whether me1, me2 or me3, is highly correlated with repression of

gene activity, and is a crucial factor in the formation and maintenance of heterochromatin. In particular, H3K27me3 plays a key role in the maintenance of repressed transcriptional states through cell division, facilitating cell memory and the maintenance of cell fates (Reviewed in Liu et al., 2010). Methylation at H3K36, meanwhile, shows the opposite pattern, and is always associated with active transcription whether me1, me2 or me3 (Reviewed in Liu et al., 2010).

During germination, PHYB mediates the deregulation of histone Arginine demethylases JUMANJI 20 (JMJ20) and JUMANJI 22 (JMJ22), which facilitate de-methylation of *GA3ox1* and *GA3ox2*, allowing an increase in GA biosynthesis which promotes germination (Cho et al., 2012). Additionally, and of particular interest for this work, regulation of the repressive chromatin modification H3K27me3 has been shown to play a key role in the control of de-etiolation. In darkness, the chromatin remodelling factor PICKLE (PKL) acts together with PIF3 and BZR1 to inhibit of H3K27me3 deposition and facilitate the expression of cell-elongation genes during skotomorphogenesis (Zhang et al., 2014). This activity was promoted by BR and GA, and inhibited by repressors of these signalling pathways, indicating a role for PKL-mediated chromatin modifications in BR and GA-induced hypocotyl elongation during skotomorphogenesis (Zhang et al., 2014).

1.4. H3K27me3 and the PRC2 complex

1.4.1 The repressive histone modification H3K27me3 is mediated by PRC2

The identification of H3K27me3 histone modifications linked to brassinosteroids and gibberellin during skotomorphogenesis is particularly intriguing. H3K27me3 is a repressive modification which facilitates gene silencing and is mediated by the Polycomb Repressive Complex 2 (PRC2). Polycomb complexes were first identified in *Drosophila* (Lewis, 1978) and are now known to represent a conserved mechanism of gene silencing across various Eukaryotes, which probably evolved before the divergence of plants and animals (Shaver et al., 2010). Correspondingly, *Arabidopsis* PRC2 components are described with reference to their homologs in Drosophila. There are three methyltransferases homologous to Enhancer of zeste [E(z)], known as CURLYLEAF (CLF), SWINGER (SWN), and MEDEA (MEA); three homologs of the complex stability protein Suppressor of Zeste 12 [Su(z)12], known as EMBRYONIC FLOWER2 (EMF2), FERTILISATION INDEPENDENT SEED2 (FIS2), and VERNALIZATION2 (VRN2); FERTILIZATION INDEPENDENT ENDOSPERM (FIE), homologous to Extra sex combs (Esc) and finally five MULTICOPY SUPRESSOR OF IRA1-5 (MSI1-5), homologous to Nucleosome Remodelling Factor 55 (Nurf55 – Also known as P55) (Mozgova and Hennig, 2015). These form three separate PRC2 complexes in Arabidopsis, determined by which homolog of Drosophila SUPPRESSOR OF ZESTE 12 [Su(z)12] is present out of EMF, VRN and FIS2. The methyltransferases also differ in which PRC2 complex they are part of: CLF and SWN both function in the VRN2 and EMF2 complexes, whilst MEA is the predominant methyltransferase in the FIS2 complex, although SWN has also been shown to associate with FIS2 (Wang et al., 2006). The composition of the three *Arabidopsis* PRC2 complexes are shown in (Fig. 1. 11)

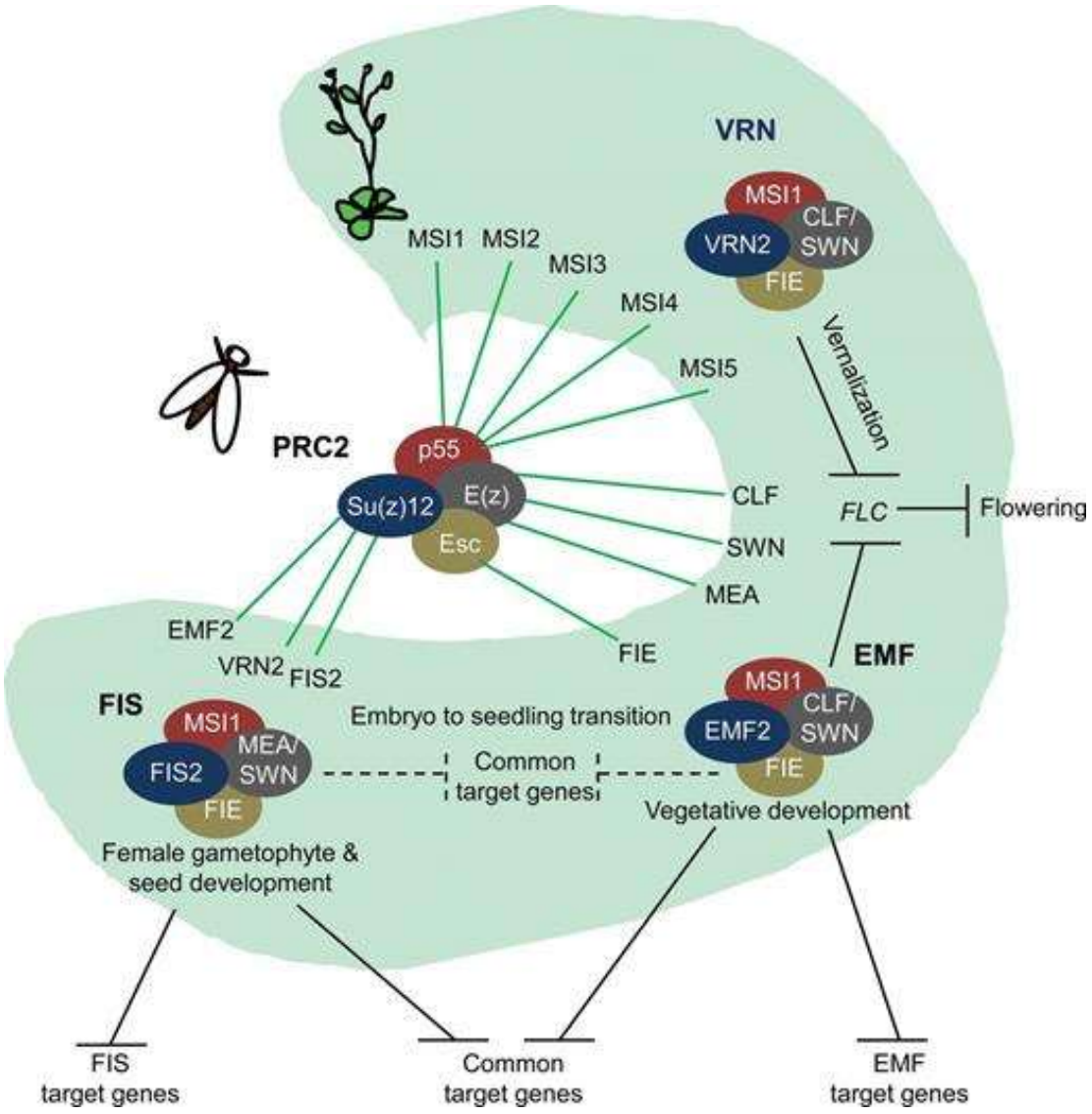

Fig 1.11 The composition of polycomb repressive complex 2 (PRC2) in *Arabidopsis* and *Drosophila* (Reproduced from Derkacheva and Hennig, 2014)

In *Arabidopsis* there are three PRC2s known as the EMBRYONIC FLOWER (EMF), VERNALIZATION (VRN) and FERTILISATION INDEPENDENT SEED DEVELOPMENT (FIS), characterized by which homolog of *Drosophila* Su(z)12 is present. All genes contain MULTICOPY SUPRESSOR OF IRA1 (MSI1) and FERTILIZATION INDEPENDENT ENDOSPERM (FIE), but differ in which histone methyltransferases are found in the complex. SWINGER (SWN) can form part of all three complexes, whilst CURLYLEAF (CLF) is restricted to the EMF and VRN complexes, and MEDEA (MEA) is only found in the FIS complex.

This figure also shows the distinctions and overlap between which processes the complexes act in. The FIS and EMF complexes both act during the embryo-seedling transition, sharing some common target genes, whilst both the EMF and VRN complexes act to regulate flowering via targeting *FLOWERING LOCUS C* (*FLC*).

1.4.2 PRC2 complexes play key roles in *Arabidopsis development*

The three PRC2 complexes have differing but overlapping functions during development, and the three methyltransferases, in particular CLF and SWN, exhibit partial redundancy (Wang et al., 2006), (De Lucia et al., 2008). Of the three PRC2 complexes FIS2 is the most distinct and primarily functions during gametophyte and seed development, inhibiting proliferation by silencing targets such as the MADS-Box transcription factor *PHERES1* (*PHE1*) and the D-type cyclin *CYCD1;1* (Grossniklaus et al., 1998), (Köhler et al., 2005) (Simonini et al., 2021). All four members of the *FIS2* complex are required for seed production, with mutations in *mea*, *fis2*, *fie* or *msi1* showing maternal effect lethality (Chaudhury et al., 1997), (Ohad et al., 1996), (Köhler et al., 2003). Notably *MEA*, the predominant methyltransferase in this complex, is primarily expressed in siliques and during seed development, and is usually silenced during vegetative growth (Roy et al., 2018). All three complexes are involved in preventing fertilisation independent seed development (Roszak and Köhler, 2011), but the other two PRC2 complexes, VRN2 and EMF2, also play key roles during sporophyte development in *Arabidopsis*. The *EMF2* complex was first identified to act in sustaining vegetative growth by repressing genes involved in the transition to flowering, such as *AGAMOUS*, *LEAFY* and *APETALA3* (Kinoshita et al., 2001). The VRN2 complex, meanwhile, is best known for its role in the vernalization process, where it is involved in accelerating flowering in response to cold by silencing *FLOWERING LOCUS C* (*FLC*) (De Lucia et al., 2008). PRCs also play important roles in establishing and maintaining cell fates during development. PRC2 is required for suppression of meristem identity genes such as *KNOX*-class genes and *WUSCHEL* (*WUS*) during meristem termination (Xu and Shen, 2008), (Sun et al., 2014), whilst *clf*/*swn* double mutants have been shown to form callus-like cell masses (Chanvivattana et al.,

2004). PRC2 has also been shown to play a key role in cell differentiation during root development (de Lucas et al., 2016).

1.4.3 Regulation of PRC2-mediated gene repression

The repression of gene expression by PRC2 is still an active area of research. It has long been understood that animals have another polycomb complex known as Polycomb Repressive Complex 1 (PRC1), which in *Drosophila* contains the eponymous Polycomb (Pc) protein, Polyhomeotic (Ph), Posterior sex combs (Psc) or Suppressor of Zeste 2 (Su(z)2), and the E3 ubiquitin ligase Sex combs extra (Sce) (Mozgova and Hennig, 2015). It was previously thought that PRC1 and PRC2 functioned in a hierarchical fashion, with PRC2-mediated deposition of H3K27me3 functioning primarily to recruit PRC1, which then mediates gene repression via ubiquitination of H2A (Wang et al., 2004). This view, however, has been challenged by observations that not all PRC2 targets require H2A ubiquitination (Gutiérrez et al., 2012) and the identification of non-canonical PRC1 complexes that can be recruited independently of H3K27me3 (Di Croce and Helin, 2013).

In plants meanwhile, for a long time whilst the PRC2 complex was well known, homologs of PRC1 had not been identified, and PRC2 in *Arabidopsis* was considered to have functioned independently of this complex (Mozgova and Hennig, 2015). This changed with the identification of the RING Proteins AtRING1A and AtRING1B as homologs of Sce (Sanchez-Pulido et al., 2008). It has since been shown that these genes function together with Psc homologs AtBMI1A, AtBMI1B and AtBMI1C to facilitate gene repression in a PRC1-like complex (Chen et al., 2010). There are still no identified homologs of Pc or Ph in plant, but two plant-specific PRC1 complex members have been described, Embryonic Flower 1 (EMF1) and Like Heterochromatin Protein 1 (LHP1), which interact with other

PRC1 members, with LHP1 fulfilling a similar H3K27me3-binding role to Polycomb in Drosophila (Turck et al., 2007), (Calonje et al., 2008).

It is known that this PRC1-like complex is responsible for at least some PcG gene repression activity in *Arabidopsis*. For example, H2A ubiquitination mediated by AtRING1A and AtBMI1 has been shown to be required for gene repression of seed maturation genes (Yang et al., 2013), and during the maintenance of cell identity (Bratzel et al., 2010).

However, as in *Drosophila*, there are observations that challenge the hierarchical model of PRC2-mediated H3K27me3 serving to recruit PRC1 to facilitate gene repression. In the repression of seed maturation genes discussed above, it appears that the H2A ubiquitination observed acts upstream of PRC2-mediated H3K27me3, with H2A ubiquitination being required for deposition of H3K27me3, but not the other way round, and Global levels of H2A actually increasing in *clf*/*swn* mutants (Yang et al., 2013). However, this was not always necessary for PRC2-mediated H32K27me3, and key targets of H3K27me3 repression such as *AGAMOUS* were not found to be marked by H2AUb (Yang et al., 2013). Overall, the exact mechanism by which PRC2-mediated deposition of H3K27me3 in plants is not fully elucidated, but probably involves the recruitment of LHP1 to facilitate condensation and increased heterochromatin formation in areas marked by this silencing modification. It is also known that LHP1 is required to maintain H3K27me3 through cell divisions, facilitating the re-establishment of this chromatin mark behind the replication fork after DNA replication (Derkacheva et al., 2013) (Derkacheva and Hennig, 2014).

PRC2-mediated gene repression is antagonized by TRITHORAX (TrxG)-group protein complexes, which are histone-modifying complexes with H3K4me3 histone

methyltransferase and/or H3K27ac histone acetyltransferase activities (Reviewed in (Mozgova and Hennig, 2015)). Transcription factors can facilitate transcriptional activation by recruiting these complexes, as has been observed for example at the *AGAMOUS* (*AG*) and *APATELA 3* (*AP3*) gene loci, both of which are targets for PRC2-mediated gene repression (Wu et al., 2012). TrxG complexes include proteins with JUMANJI-C (JmjC) domain-containing H3K27me2/3 de-methylase activity, which can remove the repressive H3K27me3 histone mark deposited by PRC2 complexes (Shen et al., 2009), (Li et al., 2013). It is thought that this is an important mechanism of regulation of PRC2-mediated gene repression in plants. For example, RELATIVE OF EARLY FLOWERING 6 (REF6) in *Arabidopsis* is an example of these H3K27me2/3 de-methylases. Overexpression of REF6 results in a reduction of H3K27me3, overexpression of PRC2-repressed target genes and an *lhp1*-like phenotype, whilst the *ref6* loss-of-function mutation can partially rescue the *clf* loss-of-function phenotype (Lu et al., 2011).

1.5 Experimental Aims of this Thesis

This chapter has discussed how the transition from skotomorphogenesis is one of the most fundamental transitions in the plant life cycle, and that this is tightly controlled by a complex and interconnected system of hormones, transcriptional regulators, ubiquitin ligase complexes and photoreceptors.

It has also been discussed that chromatin and epigenetic modifications play a key role in the regulation of transcription, and how increasing evidence is highlighting key roles for epigenetic modifications in the skotomorphogenesis-photomorphogenesis transition.

In particular, the link between H3K27me3 and light signalling is intriguing and suggests a potential role for the PRC2 complex in the light response. Previous work in our laboratory has characterised the involvement of this complex in the regulation of root development (De Lucas et al., 2016) (Brewer, 2018), and it would be desirable to carry out similar analysis of a potential PRC2 role in light signalling.

This thesis will describe various experiments to characterise this potential role. Chapter 3 will build on previous unpublished work in our laboratory to analyse the phenotypic effects of loss of PRC2 methyltransferases on hypocotyl elongation during skotomorphogenesis and photomorphogenesis, and how such components are regulated by light in combination with key photoreceptors. In Chapter 4, RNA-seq is employed to analyse how the loss of a key PRC2 component affects the transcriptional response to light in etiolated seedlings, with further investigations into how this is linked to photoreceptor activity. Finally, in Chapter 5, further investigations to characterise the potential role of a key PRC2 component in light signalling. This will involve linking transcriptional activity to PRC2-mediated chromatin modifications, analysing potential interactions between a PRC2 component and light signalling machinery, and assessing

potential roles for this component in other light-responsive processes such as phototropism.

Chapter 2 - Methods and Materials

2.1 Reagents and Suppliers

All chemical supplies other than restriction enzymes used in this thesis were obtained from SIGMA-ALDRICH (Gillingham, UK) or Fisher Scientific (Loughborough, UK) unless stated otherwise.

All primers used in this thesis were obtained from Integrated DNAs Technologies (IDT) (Coralville, Iowa, USA). All primers were ordered as 25nM DNA Oligos, purified by standard desalting.

All restriction enzymes and buffers used in this Thesis were obtained from New England Biolabs.

2.2. Plant material and growth conditions

2.2.1 Plant Lines used in this thesis

Wild Type Col0 *Arabidopsis thaliana* seeds were obtained from lab stocks of Colombia ecotype (Col0). All *Arabidopsis thaliana* seeds used in this thesis were of the Col0 ecotype.

Loss of function mutants for *PHYTOCHROME A* (*phyA*, *phyA-211* (Reed et al., 1994)), *PHYTOCHROME B* (*phyB*, *phyB-9*, (Reed et al., 1993)), *CRYPTOCHROME 1* (*cry1*, *cry1-hy4-b104*, (Bruggemen et al., 1996)), *CRYPTOCHROME 2* (*cry2*, *cry2-1*, (Guo et al., 2008)), *SWINGER* (*swn-7*/SALK_ 109121C, (Alonso et al., 2003)) and *CURLYLEAF* (*clf29*/SALK_021003*,* (Alonso et al., 2003)) were taken from lab stocks kindly provided by François Roudier and Daniel Bouyer.

The reporter lines *pDR5::GUS* and *clf29 pDR5::GUS* used in this thesis were kindly provided by Miguel De Lucas.

2.2.2 Plant crosses

Each of the *phyA*, *phyB*, *cry1* and *cry2* lines were crossed with *clf29* lines to produce *phyAclf*, *phyBclf*, *cry1clf* and *cry2clf* lines respectively. Unopened flowers on the female plant were emasculated using forceps. Mature pollen from the male plant was then transferred manually using forceps and brushed against the stigma of the female plant. The stem was labelled using Micropore^{TM} tape, and plants were returned to the greenhouse for further growth. Silliques were removed after seeds had developed but before opening.

2.2.3 Plant genotyping

2.2.3.1 Genotyping procedures for plant lines used in this thesis

The two SALK insertion lines used in this thesis (*swn-7*/SALK_ 109121C and *clf29*/SALK_021003s) were genotyped by running two parallel PCR reactions using three primers: a Left-Border (LB) primer, a Left Primer (LP) and a Right Primer (RP). The PCR conditions are described in Chapter 2.2.3.3. Primer sequences are listed in Appendix 1. The LB primer was common for both SALK mutants. A PCR reaction using the LB and RP primer produces a PCR product when DNA from the respective SALK T-DNA insertion mutant is present, whilst a PCR using the LP and RP primers will produce a product when the wild-type gene is present. A heterozygous with both wild type and T-DNA insertion DNA will produce products in both reactions.

phyB-9 mutant plants were genotyped using the dCAPs primers and BslI digestion as described in (Neff et al., 1998). The *cry1-hy4-b104* mutant carries a deletion in the *CRY1* gene locus which removes a *HindIII* digestion site (Bruggeman et al., 1996). Primers were designed either side of this locus, and the deletion was confirmed by digestion of Col0 and *cry1-hy4-b104* DNA with *HindIII*, as described in (Bruggeman et al., 1996).

The *phyA-211* and *cry2-1* mutants both carry deletions in the *PHYA* and *CRY2* loci respectively, but the precise locations of the deletions have not been described (Reed et al., 1994), (Guo et al., 1998). Primers were designed in the gene body of the *PHYA* and *CRY2* genomic loci, and primer pairs were identified that reliably produced amplification from Col0 DNA but not from *phyA-211* or *cry2-1* mutant DNA, respectively (Sequences listed in Appendix 1). The *phyA* and *cry2* plants used in this thesis were confirmed by a combination of lack of amplification of these PCR products and their phenotypic behaviour in far-red and blue light, respectively.

The presence of *pDR5::GUS* in the reporter lines used for GUS staining were confirmed by a PCR using primers which only produced a product when the GUS construct was present (Sequences listed in Appendix 1).

All genotyping PCRs followed the conditions described in Chapter 2.2.3.3. Genotyping data for all plant lines are displayed in Appendix 4.

2.2.3.2 Plant Genomic DNA Extraction

Genomic DNA was extracted by placing a leaf from a young plant in a 1.5mL Eppendorf tube along with 2 metal beads and 100µL of DNA Extraction Buffer (20mM TRIS HCl pH 7.5, 25mM NaCl, 2.5mM Ethylenediaminetetraacetic acid (EDTA), and 0.05% Sodium Dodecil Sulfate (SDS)). The tissue was then ground in a TissueLyser II (Qiagen, UK) at 25Hz for 2 minutes. The sample was then centrifuged at 13,000G for 5 minutes to pellet residual plant matter, and 50µL of the supernatant was combined with 50µL water.

2.2.3.3 Genotyping PCR

For genotyping, DNA was extracted as described in 2.2.3.2. Genotyping PCR reactions were set up as shown in Table 2.1, and the PCR reaction was carried out as shown in Table 2.2. All primers used in genotyping reactions are listed in Appendix 1. PCR products

were ran on 1% w/v Agarose gels except where stated otherwise. Samples were ran at 150v for approximately 20 minutes, alongside a DNA ladder of known fragment size (Hyperladder^{TM} 1KB, Bioline), and visualised using ultraviolet light to confirm.

Table 2.1 Composition of the Genotyping PCR reaction

Reagant	Volume/Reaction (µL)
Taq Mix Red	6
Forward Primer (10µM)	0.1
Reverse Primer (10µM)	0.1
Water	3.8
DNA	2

Table 2.2 Composition of the Genotyping PCR reaction

Temperature (°C)	Time (s)	Number of Cycles
95	120	1
95	15	40
55	30	
72	30/kb	
72	360	1
12	∞	1

2.2.4 Plant growth conditions

2.2.4.1 Seed sterilisation

Plant seeds were sterilised by shaking first for 15 minutes in 500µL of seed sterilisation solution (70% EtOH + 0.1% v/v Tween 20) in a 1.5mL Eppendorf tube. Five hundred microlitres of 100% EtOH was then added and the tubes were shaken for another 5 minutes. This step was repeated once. The tubes were then transferred to a sterile laminar flow hood, and the EtOH was removed. Another 500µL of 100% EtOH was added, and the tubes were shaken for a final 5 minutes. This was removed and the seeds were

left to air dry in the laminar flow hood. Sterilised seeds were stored at room temperature until ready for use.

2.2.4.2 Plant growth media

Murashige and Skoog (MS) media was prepared containing 4.3g/L of basal MS media, 0.5g/L 2-(N-morpholino)ethanesulfonic acid (MES) and 10g/L of Agar unless stated otherwise. pH was adjusted to 5.8 by the addition of KOH and the media was autoclaved at 121°C for 20 minutes.

Cooled MS media was poured into square petri dishes (100x100x20mm, Sarstedt) unless stated otherwise in a sterile laminar flow hood and allowed to solidify.

2.2.4.3 Plant growth conditions

For all experiments, seeds were sterilised as described in Chapter 2.2.4.1, placed on MS agar plates prepared as described in Chapter 2.2.4.2, and stratified for 2 days in darkness at 4°C.

For Hypocotyl Measurements, seeds were exposed to white light (40 µmol m^{-2} s^{-1}) for 8 hours at 21°C to induce germination, before being moved to the relevant light condition and being grown to 5 days old at 21°C.

For all other experiments, seeds were exposed to white light (40 µmol m^{-2} s^{-1}) for 24 hours at 21°C before wrapped in two layers of foil to maintain constant darkness and grown to 5 days old at 21°C unless stated otherwise.

In all experiments, plants were grown in a Panasonic Environmental Test Chamber (MLR-352) illuminated by a daylight-white fluorescence lamp (FL40SS ENW/37; Panasonic) at a fluence rate of 40 µmol m^{-2} s^{-1} unless stated otherwise.

2.3 Hypocotyl measurements

Five-day old seedlings were sterilised and plated on MS agar plates, stratified and exposed to white light (40 µmol m^{-2} s^{-1}) for 8 hours as described in Chapter 2.2.4.3. After this, white light samples were grown to 5 days old in constant white light (40 µmol m^{-2} s^{-1}). Dark samples were then wrapped in foil to maintain constant darkness and grown to 5 days old. Other seedlings were then grown to 5 days old in monochromatic Red (660nm, 5µmol m^{-2} s^{-1}), Blue (430nm, 6.5µmol m^{-2} s^{-1}) or Far-Red light (730nm, 1µmol m^{-2} s^{-1}) using a Heliospectra Elixia (LX 6XX; Heliospectra). All seedlings were grown at a constant temperature of 21°C

After 5 days, plants were photographed alongside a ruler, and Image J software (Abramoff et al., 2004) was used to measure the length of hypocotyls.

2.4 Gene analysis via Quantitative PCR

2.4.1 mRNA isolation and cDNA synthesis

Sterilised seeds were plated on MS agar plates, exposed to 24 hours of white light (40 µmol m^{-2} s^{-1}) to induce germination and then grown to 5 days old in constant darkness as described in Chapter 2.2.4.3. At 5 days old, light samples were exposed to white light (40 µmol m^{-2}, s^{-1}) for a set period of time as described in figure legends. Dark samples were not exposed to white light. RNA extraction was carried out by a protocol similar to that described in (Townsley et al., 2015). ~20mg of seedling tissue was flash-frozen in eppendorf tubes. Several Zirconia/Silica beads were added to the tube and the tissue was lysed by grinding in a TissueLyser II (Qiagen, Cat No:85300) for 1 minute. Two hundred microlitres of Lysis Binding Buffer (LBB: 100mM Tris:HCL (pH 8.0), 1M LiCl, 10mM EDTA, 1% w/v SDS, 5mM DTT, 1.5% v/v Antifoam A, 65mM β-Mercaptoethanol) was added to the tube and the tissue was ground for another 1 minute. The samples were centrifuged

(13,000 G) for 10 minutes at 4°C and the supernatant collected. One microlitre of 12.5µM Biotin-20nt Oligo was added to 200µL of this supernatant and incubated with agitation for 10 minutes at room temperature. Twenty microlitres of Streptavidin magnetic beads (#S1420, New England Biolabs, UK) washed with 100µL LBB was added, and incubated for a further 10 minutes at room temperature with agitation. The beads were then washed sequentially in 200µL of Washing Buffer A (WBA: 10mM Tris:HCL, 150mM LiCl, 1mM EDTA, 0.1% w/v SDS), Washing Buffer B (WBB: 10mM Tris:HCl, 150mM LiCl, 1mM EDTA) and Low Salt Buffer (LSB: 20mM Tris:HCL, 150mM NaCl, 1mM EDTA). The RNA was then separated from the beads by addition of 16µL RNA Extraction Buffer (10mM Tris:HCL + 1mM β-Mercaptoethanol) and heating to 80°C for 2 minutes, before placing on a magnet and removing the supernatant. Another 200µL LBB and 1µL of 12.5µM Biotin-20nt Oligo was added to the RNA and these steps up to the final wash with LSB were repeated to minimise contamination by genomic DNA.

After this secondary wash, the LSB was removed and 10µL of cDNA reaction mix (1X Revert Aid reaction buffer, 1mM dNTPs, 0.5µL RevertAid Reverse Transcription enzyme) were added to the Beads, now bound to the isolated mRNA. Samples were mixed and placed in a thermocycler for cDNA synthesis with the following incubation steps: 60 minutes at 42°C followed by 10 minutes at 70°C.

The cDNA was then removed from the beads by incubating at 80°C for 2 minutes then immediately placing on a magnetic rack to collect the beads, and removing the supernatant. The samples were then stored at -80°C. cDNA was diluted 5-fold before use in qPCR.

2.4.2 Quantitative PCR

qPCR analysis was conducted on at least three biological replicates for each sample and three technical replicates for each biological replicate using a Rotorgene Q (Qiagen). The qPCR reaction mix and cycling conditions are detailed in Table 2.4 and Table 2.5 respectively. All qPCR primers used are listed in Appendix 1. Gene expression levels were calculated from the average of the three biological repeats. The expression of the Gene of Interest (GOI) to the expression levels of a reference gene using the critical takeoff (Ct) values for the gene of interest and the reference gene in the following equation:

Relative Expression (GOI) = 2^(Ct [Reference Gene] – Ct [GOI])

Table 2.3 Composition of the qPCR Reaction

Reagant	Volume/Reaction (µL)
qPCRBIO SyGreen Blue Mix Lo-ROX	10
Forward Primer (100µM)	0.1
Reverse Primer (100µM)	0.1
Water	7.8
cDNA	2

Table 2.4 Incubation steps in the qPCR Reaction

Temperature (°C)	Time (s)	Number of Cycles
95	180	1
95	15	40
55	20	
72	30	

Initially the gene *UBIQUITIN10* (*UB10* - AT4G05320) was selected to be the reference gene for qPCR analysis. This gene has previously been used in published work analysing *CLF* and *SWN* transcriptional activity during root development (de Lucas et al., 2016). Later in the thesis, the gene Protein Phosphatase 2A Subunit A3 (PP2AA3, AT1G13320) was selected for use as a reference gene in qPCR analysis. This gene has been studied and identified in the literature as showing stable expression in different light conditions and notably shows much lower expression than *UB10*, meaning its expression was far more similar to the genes of interest in qPCR analysis (Czechowski et al., 2005).

2.5 RNA-seq

2.5.1 mRNA Isolation and cDNA Synthesis

Sterilised seeds were plated on MS agar plates, exposed to 24 hours of white light (40 µmol m^{-2} s^{-1}) to induce germination and then grown to 5 days old in constant darkness as described in Chapter 2.2.4.3. At 5 days old, seedlings were exposed to 0 (dark samples) or 6 hours (light samples) of white light (40 µmol m^{-2} s^{-1}). RNA was extracted by a protocol identical to that described in Chapter 2.4.1 until the completion of the secondary wash. At this point, samples were separated from the magnetic beads by heating to 80°C for 2 minutes, and placing on a magnet to collect the beads. One and a half microlitres of Thermo Scientific RT buffer and 0.5µL of 100pM Random hexamers were added to 8µL RNA and heated in a thermocycler at 25°C for 1 second, 94°C for 90 seconds and 30°C for 60 seconds, then held at 4°C. cDNA synthesis was then carried out by adding 5 µL Reverse Transcription Mix (1X RT Buffer, 0.03M DTT, 2.5mM dNTPs, 10% v/v Revert Aid RT enzyme), and incubating the samples in a thermocycler for the following steps: 10 minutes at 25°C, 50 minutes at 42°C, 10 minutes at 50°C, 10 minutes at 70°C, followed by holding at 4°C.

2.5.2 Library Preparation and sequencing

cDNA was prepared as described in 2.5.1. Second strand synthesis was performed by the addition of 5µL of the following mix (2mM dNTPs, 20% v/v DNA Pol-I enzyme, 2% v/v RNAse H, 8% v/v End repair enzyme, 4% v/v Taq Polymerase enzyme, 1X End repair buffer) and placing samples in a thermocycler for the following incubation steps: 20 minutes at 16°C, 20 minutes at 20°C, 20 minutes at 72°C, then hold at 4°C. Thirty microlitres of ampure beads were then added, and samples were incubated for 5 minutes at room temperature, before collecting the beads with a magnet. The beads were washed twice with 80% ethanol in preparation for Adapter Ligation.

Adapter ligation was carried out by adding 3µL of 1µM Universal Primers to each pellet and mixing, followed by adding 7µL of the following ligation mix (1X Rapid T4 DNA Ligase Buffer, 2.5% v/v T4 DNA ligase) and incubating at room temperature for 15 minutes. Ten microlitres of 50mM EDTA and 25µL of ABR were then added to each sample and the samples were incubated for 5 more minutes at room temperature. The beads were then collected again on a magnet and washed twice with 80% ethanol, then resuspended in 22µL of 10mM Tris:HCL.

After adapter ligation, a unique indexed primer was added to each sample. Ten microlitres of adapterized cDNA was mixed with the following enrichment mix (2X Phusion HF Buffer, 0.2µM PE1 Primer, 0.8µM Enrich S1+S2 Primers, 0.5mM dNTPs, 2% v/v Phusion Polymerase enzyme) plus 0.2µM of unique indexed primer. Amplification of cDNA was carried out by placing the samples in a thermocycler for the following incubation steps: 30 seconds at 98°C, 14 cycles of the following three steps (15 seconds at 98°C, 30 seconds at 65°C, 30 seconds at 72°C), 5 minutes at 72°C. Samples were then held at 4°C until ready to proceed with the next step.

Two microlitres of cDNA was ran on a 1.5% agarose gel to check amplification was successful, then the cDNA was cleaned using ampure beads by adding 27µL of beads to 18µL of cDNA, mixing and incubating for 5 minutes at room temperature. The beads were collected with a magnet and washed twice with 80% ethanol, before being resuspended in 10µL of 10mM Tris:HCL.

The cDNA libraries were quantified usings a QUBIT Fluorimeter (Qiagen, UK) and sent for sequencing at the Vincent Coates Genomics Sequencing Lab (GSL) at the University of California, Berkeley, using an Illumina4000 50SR.

2.5.3 Bioinformatical analysis of RNA-seq

RNA-seq reads received from the GSL were mapped to the Tair10 genome using the STAR RNA-seq aligner (Dobin et al., 2013), to produce read numbers for each gene in the TAIR10 genome. This stage of the bioinformatic analysis was kindly carried out by Dr Wenbin Wei, Bioinformatics Officer in the Department of Biosciences, Durham University.

After alignment, read numbers were analysed using Bioconductor packages in R Studio. Analysis was carried out using the workflow described in (Love et al., 2019) beginning at Section 3.2 of this workflow "Starting from count matrices". All bioinformatic analysis after the mapping of reads to the TAIR10 genome was carried out by Joseph Nelson.

2.6 ChIP-qPCR

2.6.1 Growth and fixing of plant tissue

Sterilised seeds were plated on MS agar plates, exposed to 24 hours of white light (40 µmol m^{-2} s^{-1}) to induce germination and then grown to 5 days old in constant darkness as described in Chapter 2.2.4.3. At 5 days old, seeds were exposed to 0 (dark samples) or 6 hours (light samples) of white light (40 µmol m^{-2} s^{-1}), and then collected from agar plates

and fixed for 15 minutes in 37mL 1% v/v Formaldehyde. Samples were placed in a vacuum for this period to aid penetration of formaldehyde into cells. The remaining formaldeyde was then quenched by the adding Glycine to 0.125M, and incubating in a vacuum for another 5 minutes. The tissue was then washed twice with cold water using Falcon 40µM cell strainers (352340, Fisher Scientific) before being flash frozen in liquid nitrogen and thoroughly ground using a mortar and pestle. One gram of tissue was collected for Chromatin Immunoprecipitation.

2.6.2 Chromatin Immunoprecipitation

One gram of tissue prepared as described in Chapter 2.6.1 was dissolved in 5mL of Extraction Buffer 1 (0.4M Sucrose, 10mM Tris:HCl pH 8.0, 10mM MgCl2, 5mM β-Mercaptoethanol, 0.1mM Phenylmethylsulfonyl Fluoride (PMSF)), and filtered through two layers of Miracloth (Merck, UK) into a 50mL falcon tube. These were centrifuged at 3200G for 20 minutes at 4°C, and the supernatant discarded. The pellet was dissolved in 300µL of Extraction Buffer 2 (0.25M Sucrose, 10mM Tris:HCl pH 8.0, 10mM MgCl2, 1% w/v Triton X-100, 5mM β-mercaptoethanol, 0.1mM PMSF), and centrifuged for 10 minutes at 12,000G in siliconized Eppendorf tubes at 4°C. The supernatant was again discarded and the pellet dissolved in 200µL Extraction Buffer 3 (1.7M Sucrose, 10mM Tris:HCl pH 8.0, 2mM MgCl2, 0.15% w/v Triton-X-100, 5mM β-mercaptoethanol, 0.1mM PMSF). This was carefully layered on top of another 200µL of Extraction Buffer 3 in another siliconized Eppendorf tube, and centrifuged for 1 hour at 16,000G and 4°C. The supernatant was again discarded and the pellet resuspended in 100µL of Nuclei Lysis Buffer (50mM Tris:HCl pH 8.0, 10mM EDTA, 1% w/v SDS). The chromatin was then sonicated on a COVARIS M220 Focus ultra-sonicator for 6 minutes.

Ten microlitres of Protein A/G magnetic beads (Pierce Protein A/G Magnetic Beads, Thermofisher Scientific) were collected on a magnet and washed three times with 1mL ChIP Dilution Buffer, before being resuspended in 150µL ChIP Dilution Buffer and incubated with 2µL of Anti-H3K27me3 antibody for 2 hours at 4°C with gentle agitation. The sonicated chromatin was mixed with this and incubated overnight at 4°C with gentle agitation.

After overnight incubation, the magnetic beads containing the chromatin-antibody mix were collected by magtration, and then washed twice sequentially with each of the following buffers: Low Salt Buffer (20mM Tris:HCl pH 8.0, 2mM EDTA, 0.1% w/v SDS, 150mM NaCl, 1% w/v Triton-X-100); High Salt Buffer (20mM Tris:HCl pH 8.0, 2mM EDTA, 0.1% w/v SDS, 500mM NaCl, 1% w/v Triton-X-100); Lithium Chloride Buffer (10mM Tris:HCl PH8.0, 1mM EDTA, 1% w/v IGEPAL (NP40); 500mM LiCl, 1% w/v Na-Deoxycholate) and finally TE Buffer.

A 10% w/v slurry of Chelex Resin (Biorad, UK) was prepared and 75µL was used to resuspend the beads, which were then incubated at 95°C for 10 minutes, then chilled on ice for 1 minute. Two microlitres of 20mg/mL Proteinase K were added and the samples were incubated at 55°C for 1 hour, before another 10 minutes at 95°C. The samples were chilled on ice for another 1 minute. Finally, the TE was collected, and DNA was extracted in a volume of 23µL using Machery-Nagel PCR cleanup kits, with the NTC buffer.

2.6.3 Analysis of histone modifications via qPCR

DNA as prepared in Chapter 2.6.2 was diluted 5-fold for use in qPCR.

The qPCR reaction was carried out as described for transcriptional analysis in Chapter 2.4. The reference gene *UB10* (AT4G05320) was used to normalise the signal obtained.

Enrichment of H3K27me3 at the gene of interest was calculated using the same equation as for RT-qPCR analysis in 2.4.2

2.7 GUS Staining

Sterilised seeds were plated on MS agar plates, exposed to 24 hours of white light (40 µmol m^{-2} s^{-1}) to induce germination and then grown to 5 days old in constant darkness as described in Chapter 2.2.4.3. At 5 days old, seedlings were exposed to 0 (dark samples) or 6 hours (light samples) of white light (40 µmol m^{-2} s^{-1}), then fixed by placing in 90% Acetone for 30 minutes. Seedlings were washed twice with water, then placed in GUS Staining solution (50mM Phosphate Buffer (pH 7.0), 0.1% w/v Triton X-100, 1.5mM Potassium Ferrocyanide, 1.5mM Potassium Ferricyanide, 2mM 5-bromo-4-chloro-3-indolyl ß-D-glucuronide cyclohexamine) and incubated at 37°C for 2 hours in darkness. Tissue was then washed sequentially in 70%, 50%, 30% and 10% v/v Ethanol, followed by a final wash in water, before being mounted on Microscope slides using Hoyer's Solution (30g Gum Arabic, 200g Chloral (IV) Hydrate, 20g Glycerol, 50mL Water).

2.8 Phototropism Assays

Sterilised seeds were plated on MS agar plates as described in Chapter 2.2.4 2 with the modification that MS media with 8g/L of Agar was used and the seeds were grown in Magenta vessels rather than Square plates. Seeds were exposed to 24 hours of white light (40 µmol m^{-2} s^{-1}) to induce germination and then grown to 5 days old in constant darkness as described in Chapter 2.2.4.3.

The seedlings were then exposed to blue light from one direction (430nm, 4.5 µmol m^{-2} s^{-1}) for 24 hours by use of a blue filter. After this, seedlings were photographed with a camera alongside a ruler, and Image J software was used to measure the degree of bending displayed in each sample.

2.7 Hot fusion cloning

2.7.1 Plasmid vectors

The plasmid vectors used in this thesis were the pGBKT7 DNA-binding domain cloning vectors and pGADT7 activation domain cloning vectors (Clontech).

2.7.2 Primer design

Primer pairs were designed to incorporate 17bp homologous to the target site of the plasmid vector, followed by 22bp homologous to the gene of interest. All hot fusion cloning primers using in this thesis are listed in Appendix 1.

2.7.3 PCR amplification and product isolation

PCR was used to amplify the gene of interest from cDNA, with the composition as shown in Table 2.5 and the incubation steps in Table 2.6

Table 2.5 Composition of the cloning PCR reaction

Reagant	Volume/Reaction (µL)
5x Phusion Buffer	6
Forward Primer (10µM)	1
Reverse Primer (10µM)	1
dNTPs (10mM)	1
Phusion DNA Polymerase (New England Biolabs)	0.5
Water	35.5
cDNA	1

Table 2.6 Composition of the Genotyping PCR reaction

Temperature (°C)	Time (s)	Number of Cycles
98	120	1
98	15	40
60	30	
72	30/kb	
72	48	1
4	∞	1

PCR products were analysed by agarose gel electrophoresis. If the band on the gel was unique and corresponded with the expected size, then 100µL of magnetic beads were added to the PCR reaction and incubated at room temperature for 5 mins. The beads were then collected on a magnet, the supernatant was removed, and the beads were washed twice with 80% ethanol. The beads were then resuspended in 10µL of distilled water and placed back on the magnet, to remove the beads. The concentration of the PCR product was measured using a Nanodrop ND-1000 Spectrophotometer (Labtech).

2.7.4 Vector preparation

pGBKT7 and pGADT$_7$ plasmids were digested using the restriction enzymes NdeI and PstI (pGBKT7), or NdeI and XhoI (pGADT7). 8µL of Plasmid DNA was digested, with 1µL of each restriction enzyme, using cutsmart buffer (New England Biolabs), for 2 hours at 37°C. After digestion, the mix was heated to 70°C for 15 minutes to inactivate remaining enzyme, and the plasmid DNA was cleaned using magnetic beads as described in Chapter 2.7.4.

2.7.5 Hot fusion reaction and E. Coli transformation

The hot fusion reaction was conducted according to the protocol in Fu et al. (2014). Recombinant plasmids were then transformed into DH5α *E. Coli* cells using heat shock as follows: 20µL hot fusion reaction product was added to 100µL of E. coli Dh5α competent cells and incubated on ice for 30 minutes. The cells were then incubated for 2 minutes at 42°C before being returned to ice for 5 minutes. Two hundred microlitres of liquid Luria-Bertani (LB) broth (10g/l Tryptone, 5g/l Yeast Extract and 10g/l NaCl) was then added to each tube and the tubes were incubated for 1 hour at 37°C with shaking. The culture was then LB agar plates (10g/l Tryptone, 5g/l Yeast Extract, 10g/l NaCl and 12g/l Agar) containing the appropriate antibiotic for the selection of the plasmid. For pGBKT7

plasmids, 25µg/mL kanamycin was used, for pGADT7 plasmids 100µg/mL Carbenicillin was used. These plates were grown for 1 day at 37°C.

2.7.6 Validation of Plasmids by Colony PCR and digestion

Validation of plasmids was done in two steps. Firstly, some cells from the agar plates in 2.7.7 were resuspended in 5µL water, and 2µL of this mix was used for a colony PCR reaction, with the composition shown in Table 2.7 and the incubation steps shown in Table 2.8 All colony PCR primers used in this thesis can be found in Appendix 1.

Table 2.7 Composition of the cloning PCR reaction

Reagent	Volume/Reaction (µL)
Taq Mix Red (PCR Biosystems)	6
Forward Primer (10µM)	0.1
Reverse Primer (10µM)	0.1
Water	3.8
E. Coli cells resuspended in water	2

Table 2.8 Composition of the Genotyping PCR reaction

Temperature (°C)	Time (s)	Number of Cycles
95	120	1
95	15	40
55	30	
72	30/kb	
72	360	1
12	∞	1

The colony PCR was then ran on a 1% w/v agarose gel. If a band of the correct size was present, the colonies were grown overnight in liquid LB media at 37°C with shaking. DNA was extracted from this culture using Wizard® Plus SV Minipreps DNA Purification System following Promega's instructions. The plasmids were then digested with restriction enzymes and ran on an agarose gel to further validate that the plasmid was correct. If the

result was positive, plasmids were sent for sequencing by the DNA Sequencing laboratory, School of Biological and Biomedical sciences, Durham University (DBS, Durham University). DNA sequence data were analysed using the sblue lightAST 2 sequencing tool (www.ncbi.nlm.nih.gov/blast/bl2seq) and APE software (http://biologylabs.utah.edu/jorgensen/wayned/ape/) to confirm that there were no mutations in the cDNA sequence.

2.10 Yeast two-hybrid assay

2.10.1 Yeast strains

The yeast strains used in this two-hybrid assay were two strains of *Saccharomyces cerevisiae*: *AH109* (*MATa, trp1-901, leu2-3, 112, ura3-52, his3-200, gal4Δ, gal80Δ, LYS2::GAL1UAS-GAL1TATA-HIS3, GAL2UAS-GAL2TATA-ADE2, URA3::MEL1UASMEL1TATA-lacZ*) (Holtz, unpublished) and *Y187* (*MATα, ura3-52, his3-200, ade2-101, trp1-901, leu2-3, 112, gal4Δ, met–, gal80Δ, URA3::GAL1UAS-GAL1TATA-lacZ*) (James et al., 1996).

2.10.2 Reporter genes

The reporter genes used in this yeast two-hybrid (Y2H) system were ADE2, HIS3, and MEL1. Expression of these reporter genes in response to two-hybrid interactions allowed cells to grow on plates lacking adenine and histidine.

2.10.3 Yeast transformation and mating

pGBKT7 and pGADT7 vectors that were generated according to the hot fusion protocol in Chapter 2.7 were transformed into Y187 and AH109 cells, respectively. Pairs of positive interactions were identified by mating transformed Y187 and AH109. This was carried out according to the High-Throughput Transformations (96-Well

Format) and Two-Hybrid Matrix protocols as in (Walhout and Vidal, 2001).

2.11 Analysing the effects of monochromatic light exposure on *clf29* curled leaf phenotype

Sterilised seeds were plated on MS agar plates, stratified, and exposed to 24 hours of white light (40 µmol m^{-2} s^{-1}) to induce germination as described in Chapter 2.2.4.3. Seedlings were then grown to 1 week old in continuous white light (40 µmol m^{-2}, s^{-1}) or in monochromatic red light (7.6 µmol m^{-2}, s^{-1}) or blue light (6.5 µmol m^{-2}, s^{-1}) by use of red and blue filters. Seeds were then transferred to soil, and grown in a greenhouse with a 16h light at 22ºC/8h dark at 18ºC growth cycle. Photographs were taken 3 weeks later, once the *clf29* curled-leaf phenotype was apparent in plants grown under white light.

Chapter 3 – Identification of a role for the PRC2 methyltransferase CURLYLEAF during photomorphogenesis

3.1 Introduction

As discussed in Chapter 1, the PRC2 complex is a vital regulator of development in Arabidopsis, playing important roles in seed development, flowering, and the establishment and maintenance of cell identities during meristem and root development (Kinoshita et al., 2001), (De Lucia et al., 2008), (Sun et al., 2014), (De lucas et al., 2016).

H3K27me3, the chromatin modification mediated by PRC2 has been shown to undergo distinct changes during photomorphogenesis (Charron et al., 2009). Dark-grown seedlings exposed to 6 hours white light displayed 8395 regions marked by this modification after light exposure, covering 8.1% of the genome, increased from 6238 regions covering 5.7% of the genome prior to light exposure (Charron et al., 2009). As expected, H3K27me3-marked regions correlated with transcriptional silencing, and targeted regions were notably found to include genes involved in the gibberellin biosynthesis pathway, indicating a potential role for H3K27me3 in light-regulation of hormone signalling and growth (Charron et al., 2009). Other evidence in the literature reinforces this notion, with the chromatin modifier PKL has been observed to act co-operatively with PIF3 and BZR1 during skotomorphogenesis to facilitate the expression of cell wall expansion genes by inhibiting the deposition of H3K27me3 in dark-grown plants (Zhang et al., 2014). Previous work in our laboratory, carried out by Dr Miguel de Lucas, has also provided evidence of an involvement of H3K27me3 during photomorphogenesis. Chromatin immunoprecipitation identified 75 genes in the ontology category “postembryonic development” to display increased levels of H3K27me3 in dark-grown seedlings after light exposure, whilst RNA seq analysis identified that the histone methyltransferase CLF, as

well as its upstream regulator DOF6, are transcriptionally upregulated by light (De lucas, unpublished).

Considering these findings, it was hypothesised that PRC2-mediated deposition of H3K27me3 may play a key role during photomorphogenesis. This chapter describes results of analyses to assess a potential role for PRC2 during the photomorphogenic process.

The first sections of the chapter (3.2 – 3.4) describe analysis of how disruption of PRC2 activity via loss of the methyltransferase CLF induces elongated hypocotyls in *Arabidopsis* seedlings under various light regimes, although definitively linking this to light signalling is made difficult by the presence of the phenotype in dark-grown as well as light-grown seedlings.

After this, analysis is undertaken to assess how CLF may be regulated by photoreceptors during photomorphogenesis. Firstly, further phenotypic analysis is undertaken to assess whether phenotypic effects of *clf29* mutation are affected by loss of key photoreceptors, indicating a potential connection between their action during light growth.

Finally, genetic analysis is undertaken to validate previous RNA-seq data from our laboratory indicating that *CLF* is transcriptionally induced by light, and how this is dependent on photoreceptor activity.

3.2 Loss of *CLF*, but not *SWN*, induces elongated hypocotyls in *Arabidopsis*

When an *Arabidopsis* seedling encounters light for the first time, it undergoes a number of distinct architectural changes, including inhibition of hypocotyl elongation, opening of the cotyledons and unfolding of the apical hook (Harpham et al., 1991), (Cowling and Halberd, 1999), (Wu et al., 2010). Hypocotyl length measurements have been frequently used to analyse light perception and signalling in *Arabidopsis*, with several key regulators

of skoto- and photomorphogenesis being identified due to mutants displaying elongated hypocotyls when grown in the light (Koornneef et al., 1980), (Oyama et al., 1997), (Liu et al., 2011). This approach has also been used in reverse, with mutants in negative regulators of photomorphogenesis such as *COP1* being identified to have shortened hypocotyls in the absence of light (Deng et al., 1991).

Analysis of hypocotyl lengths of seedlings grown in constant white light at 21°C was carried out to assess whether loss of the methyltransferases in the PRC2 complex had a phenotypic effect on photomorphogenesis. There are three methyltransferases in the PRC2 complex, CURLYLEAF (CLF), SWINGER (SWN) and MEDEA (MEA). Of these, only *SWN* and *CLF* are involved in sporophyte development, whilst *MEA* is usually not expressed post-embryogenically (Roy et al., 2018). Therefore, only CLF and SWN are potential candidates for mediating PRC2 activity during photomorphogenesis. Plants carrying mutations in *CLF* (*clf29*) and *SWN* (*swn7*) were grown alongside Col0 (wild type) in constant white light for 5 days, and hypocotyl lengths were measured, as described in Chapter 2.3 (Fig. 3.1).

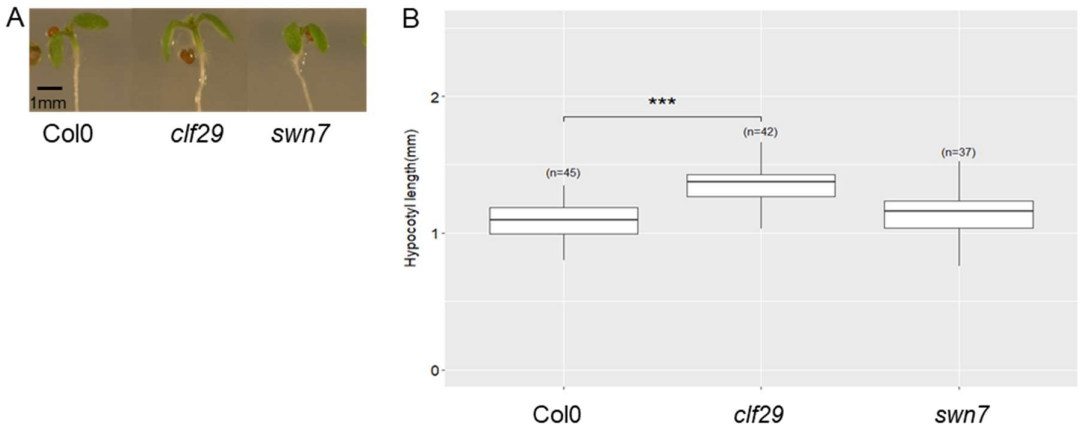

Fig 3.1 Hypocotyl lengths of Col0, *clf29* and *swn7* seedlings under white light.
A) Hypocotyls of 5-day old Col0, *clf29* and *swn7* seedlings grown in constant white light (40 µmol m^{-2} s^{-1}) at 21°C
B) Boxplot showing hypocotyl lengths of 5-day old Col0, *clf29*, and *swn7* seedlings grown in constant White Light at 21°C (40 µmol m^{-2} s^{-1}). Sample numbers displayed in graph. Asterisks indicate statistically significant differences in mean hypocotyl length as compared to WT, as determined by Independent samples T-Tests (*** = $p<0.001$).

clf29 plants had significantly elongated hypocotyls compared to Col0, whilst *swn7* lines showed no significant differences (Fig. 3.1), suggesting that only CLF function is required for full light responses in *Arabidopsis*. This is consistent with previous observations that *clf29* mutation has a more significant phenotype than *swn7*, indicating that CLF is the predominant methyltransferase acting in the PRC2 complex during sporophyte development (Derkacheva and Hennig, 2014).

3.3 *clf29* mutation causes phenotypic effects in blue light, far-red light and darkness, but not in red light

Different wavelengths of light are perceived by different photoreceptors, and initiate different downstream signalling pathways. Thus, genes involved in sensing and responding to light behave differently when exposed to different wavelengths of light. This effect can be seen prominently among the major photoreceptors, for example *phyA* loss has a marked effect on hypocotyl length in plants grown under far-red light, but not under red light, whilst the opposite is true for *phyB* loss (Reed et al., 1994).

The effect of *CLF* in darkness was also considered important. Mutations in the phytochromes and cryptochromes do not have any effect on phenotype in the absence of light (Neff and Chory, 1998), (Yu et al., 2010), but loss other key regulators of photomorphogenesis can have effects in both light and darkness. For example loss of a COP1-interacting protein SHORT HYPOCOTYL IN WHITE LIGHT 1 (SHW1) results in shortened hypocotyls in both light and darkness (Srivastava et al., 2015). Additionally, as discussed in Chapter 1.2 various hormones are crucial in regulating hypocotyl elongation in the dark, with auxin, brassinosteroids and gibberellic acid all having crucial effects on hypocotyl elongation in darkness (Nagpal et al., 2000), (Peng et al., 2008), (de Lucas et al., 2008). There are even examples of factors with differential effects in light and darkness, for example ethylene, which inhibits hypocotyl elongation in darkness, but promotes it in the light (Smalle et al., 1997).

Therefore, in order to further understand the role played by CLF during photomorphogenesis, analysis was conducted on the hypocotyl lengths of *clf29* mutants grown at different light wavelengths (Red, Blue or Far-Red) and in darkness. Col0 and *clf29* plant lines were grown under constant illumination by only a single wavelength of

light or under constant darkness (light intensity for each condition is displayed in figure legends).

Similarly to the effects observed under white light, *clf29* plants showed elongated hypocotyls under blue (Fig. 3.2) and far-red light (Fig. 3.3), indicating an involvement of *CLF* in the inhibition of hypocotyls under these wavelengths of light. This effect was also seen in the absence of light, with *clf29* lines also demonstrating elongated hypocotyls in darkness (Fig. 3. 4). Taken together, these data could indicate that *CLF* constitutively functions to inhibit hypocotyl elongation, which would explain the elongated hypocotyl phenotype of *clf29* mutants in both darkness and multiple light wavelengths.

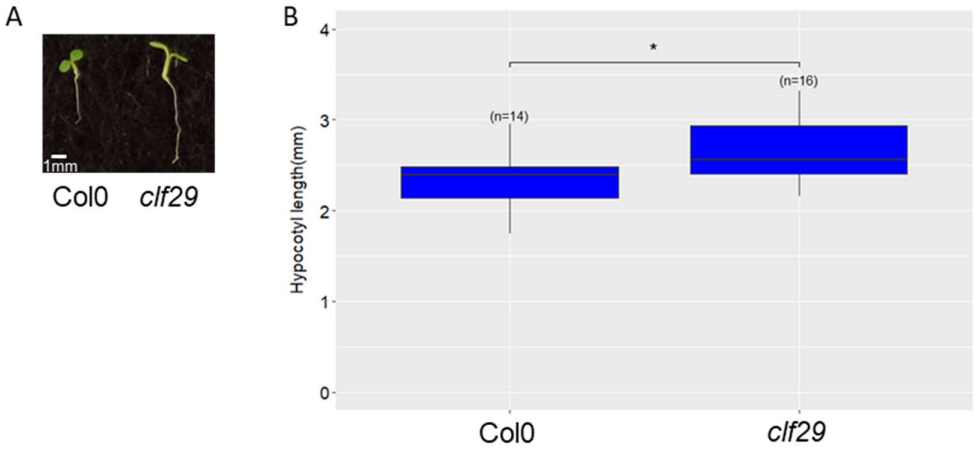

Fig 3.2 Hypocotyl lengths of Col0 and *clf29* seedlings under blue light.
A) 5-day old Col0 and *clf29* seedlings grown in constant blue light (6.5 µmol m^{-2} s-1) at 21°C
B) Hypocotyl lengths of 5-day old Col0 and *clf29* seedlings grown in constant blue light (6.5 µmol m^{-2} s-1) at 21°C. Sample numbers displayed in graph. Asterisks indicate statistically significant differences in mean hypocotyl length compared to Col0, as determined by Independent samples T-Tests (* = $p<0.05$)

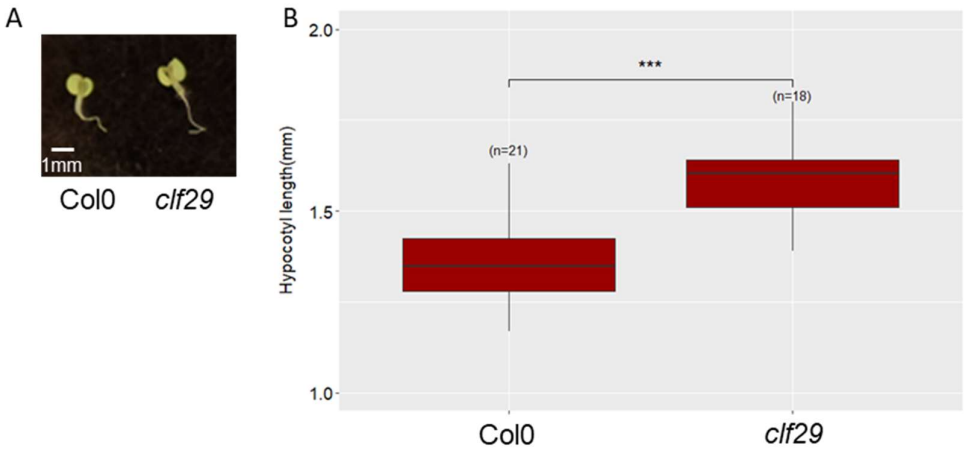

Fig 3.3 Hypocotyl lengths of Col0 and *clf29* seedlings under far-red light.
A) 5-day old Col0 and *clf29* seedlings grown in constant far-red light at 21°C (1 µmol m^{-2} s^{-1})
B) Hypocotyl lengths of 5-day old Col0 and *clf29* seedlings grown in constant far-red Light (1 µmol m^{-2} s^{-1}) at 21°C. Sample numbers displayed in graph. Asterisks indicate statistically significant differences in mean hypocotyl length compared to Col0, as determined by Independent samples T-Tests (*** = p<0.001)

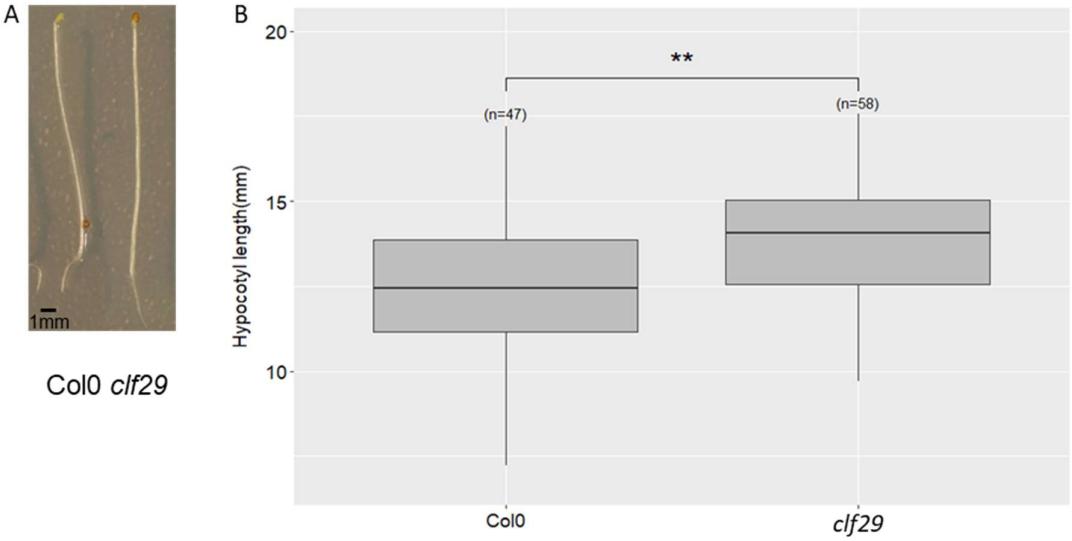

Fig 3.4 Hypocotyl lengths of Col0 and *clf29* seedlings in darkness
A) 5-day old Col0 and *clf29* seedlings grown in constant darkness at 21°C
B) Hypocotyl lengths of 5-day old Col0 and *clf29* seedlings grown in constant darkness at 21°C. Sample numbers displayed in graph. Asterisks indicate statistically significant differences in mean hypocotyl length compared to Col0, as determined by Independent samples T-Tests (** = p<0.01)

However, a different result was found in plants grown under constant red light, with *clf29* mutants showing no difference from Col0 in hypocotyl length (Fig. 3.5). Considering that *clf29* plants did exhibit elongated hypocotyls in darkness, this represents that red light abolished a *clf29* phenotype observed under all other light regimes tested. This result is intriguing, as it suggests that exposure to monochromatic red light acts in some way to inhibit CLF activity, such that under red light, *clf29* mutation has no effect.

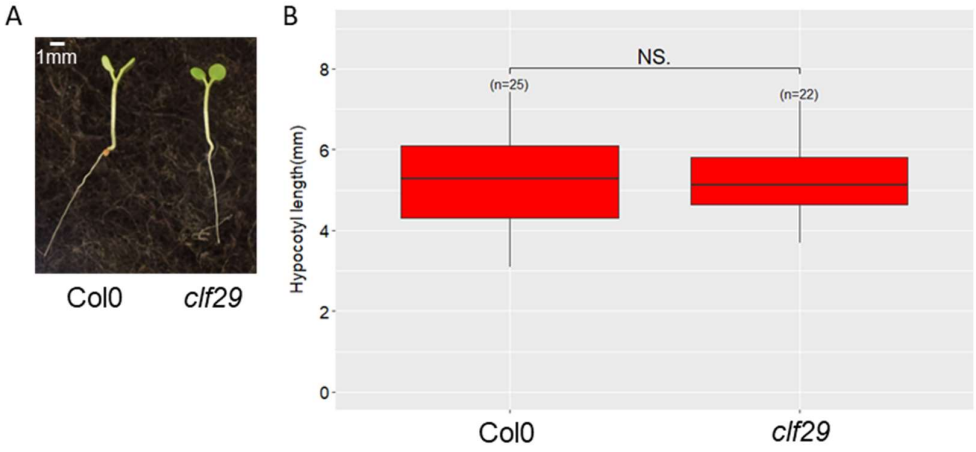

Fig 3.5 Hypocotyl lengths of Col0 and *clf29* seedlings under red light.
A) 5-day old Col0 and *clf29* seedlings grown in constant red light at 21°C (5 µmol m^{-2} s^{-1})
B) Hypocotyl lengths of 5-day old Col0 and *clf29* seedlings grown in constant red Light (5 µmol m^{-2} s^{-1}) at 21°C. Sample numbers displayed in graph. Results of independent two samples t tests between Col0 and *clf29* data displayed (NS = not significant).

3.4 *clf29* loss has no effect on hypocotyl lengths in the absence of *CRY1*

The data presented so far suggest that CLF has a distinct effect on hypocotyl elongation in white, far-red and blue light, but not in red light, indicating a potential role for CLF in the inhibition of hypocotyl elongation under some wavelengths of light, as well as in darkness.

To further understand this potential role, it was important to consider how CLF may be linked to photoreceptor activity. One way to analyse this was to assess whether the *clf29* phenotype of elongated hypocotyls in certain light wavelengths was affected by the loss of any major photoreceptors. As previously discussed, PHYB is the main red-light receptor, whilst PHYA is the predominant far-red light receptor (Reed et al., 1994). CRY1 and CRY2, meanwhile, both primarily react to blue light, with CRY1 having the most distinct effects under this wavelength (Wu and Spalding, 2007), (Yu et al., 2007). To assess whether CLF may be linked to the activity of any of these major photoreceptors, it was decided to analyse whether the elongated hypocotyls in *clf29* mutants was affected by loss of any of the main red, far-red and blue light photoreceptors. Loss of function photoreceptor mutants *cry1*, *cry2*, *phyA* and *phyB* were grown alongside double mutants also carrying a *clf29* mutation to 5 days old under constant white light at 21°C (genotyping information for these plants is displayed in Appendix 4). The theory behind this analysis was that if CLF activity is correlated with the actions of photoreceptors in light-grown seedlings, then the effect of a *clf29* mutation on the phenotype observed in light-grown seedlings may be reduced in plants lacking those photoreceptors. This approach could not be used to provide further information about CLF activity in darkness, as photoreceptors are inactive in dark-grown seedlings and do not produce phenotypically measurable effects under these conditions (Neff and Chory, 1998), (Yu et al., 2010).

In white light, *clf29* mutation resulted in significantly elongated hypocotyls in all photoreceptor-mutant backgrounds except *cry1* – with a *cry1clf29* double mutant showing no difference from a *cry1* single mutant (Fig. 3.6). In all other cases, the double mutant carrying a *clf29* mutation had significantly elongated hypocotyls compared to the single photoreceptor mutant (Fig. 3.6).

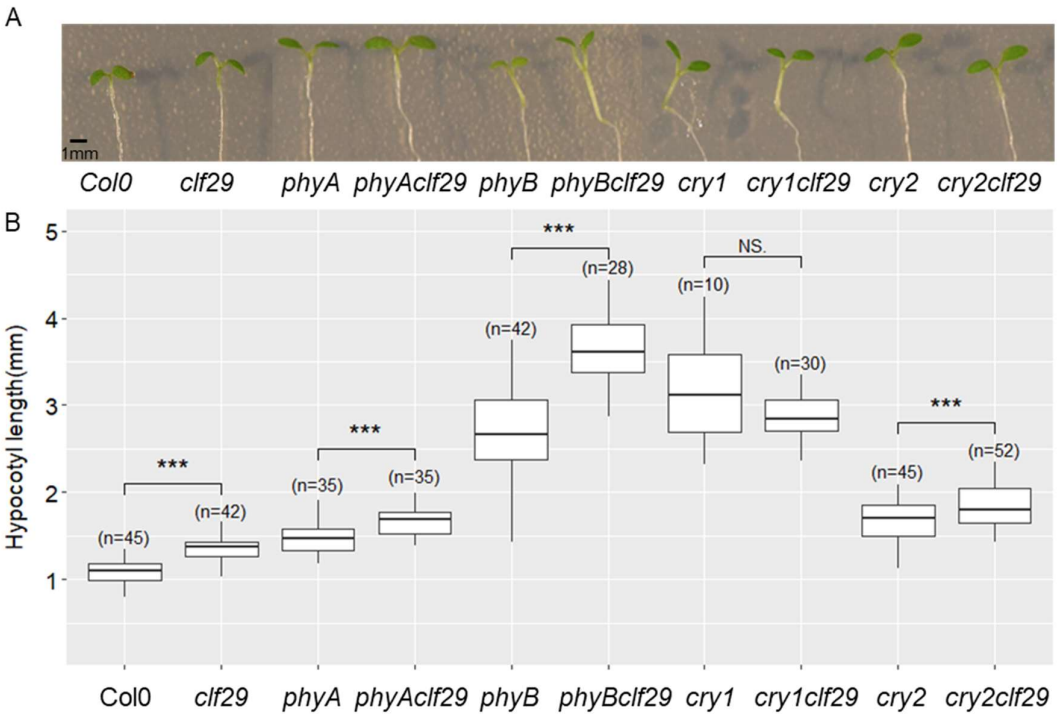

Fig. 3.6 Effect of *clf29* mutation on hypocotyl lengths in photoreceptor mutants grown under white light.
A) 5-day old seedlings carrying mutations in photoreceptors and double mutants also carrying mutations in *clf29*, grown in constant white light at 21°C (40 µmol m^{-2} s^{-1})
B) Box plot showing hypocotyl lengths of the plants in A). Sample numbers displayed in graph. Asterisks indicate statistically significant differences in mean hypocotyl length of a *clf29* mutant compared to a non-*clf29* mutant in that genetic background, as determined by Independent samples T-Tests (* = P<0.05), (** = P<0.01), (*** = P<0.001). NS. indicates no statistically significant differences between samples indicated.

This analysis was then repeated in seedlings grown under constant blue light (Fig. 3.7), far-red light (Fig. 3.8) and red light (Fig. 3.9). In seedlings grown under blue light, *clf29* mutation had no effect on hypocotyl lengths in a *cry1* or *phyA* background (Fig. 3.7), whilst in seedlings grown under far-red light *clf29* loss had a significant impact in all genetic backgrounds analysed (Fig. 3.8).

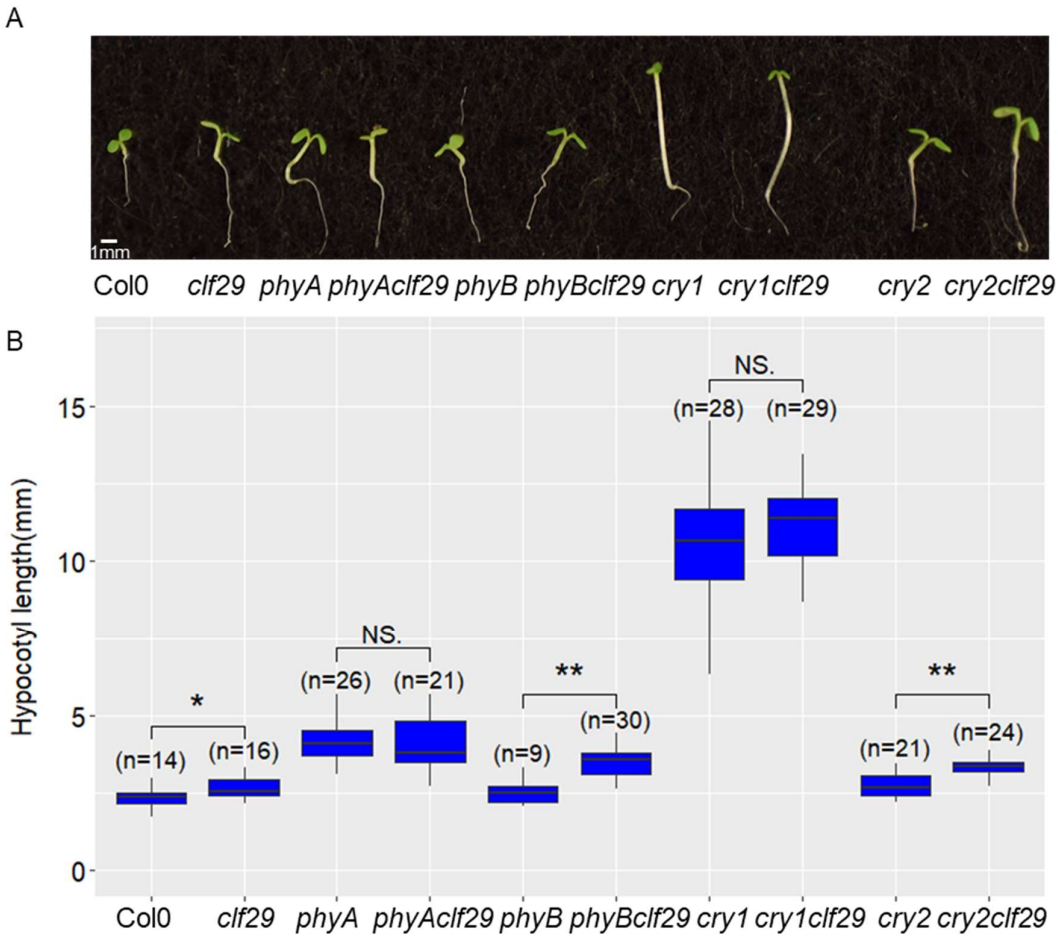

Fig. 3.7 Effect of *clf29* loss on hypocotyl lengths in photoreceptor mutants grown under blue light.
A) 5-day old seedlings carrying mutations in photoreceptors and double mutants also carrying mutations in *clf29*, grown in constant blue light at 21°C (6.5 µmol m^{-2} s^{-1})
B) Box plot showing hypocotyl lengths of the plants in A). Sample numbers displayed in graph. Asterisks indicate statistically significant differences in mean hypocotyl length of a *clf29* mutant compared to a non-*clf29* mutant in that genetic background, as determined by Independent samples T-Tests (* = P<0.05), (** = P<0.01), (*** = P<0.001). NS. indicates no statistically significant differences between samples.

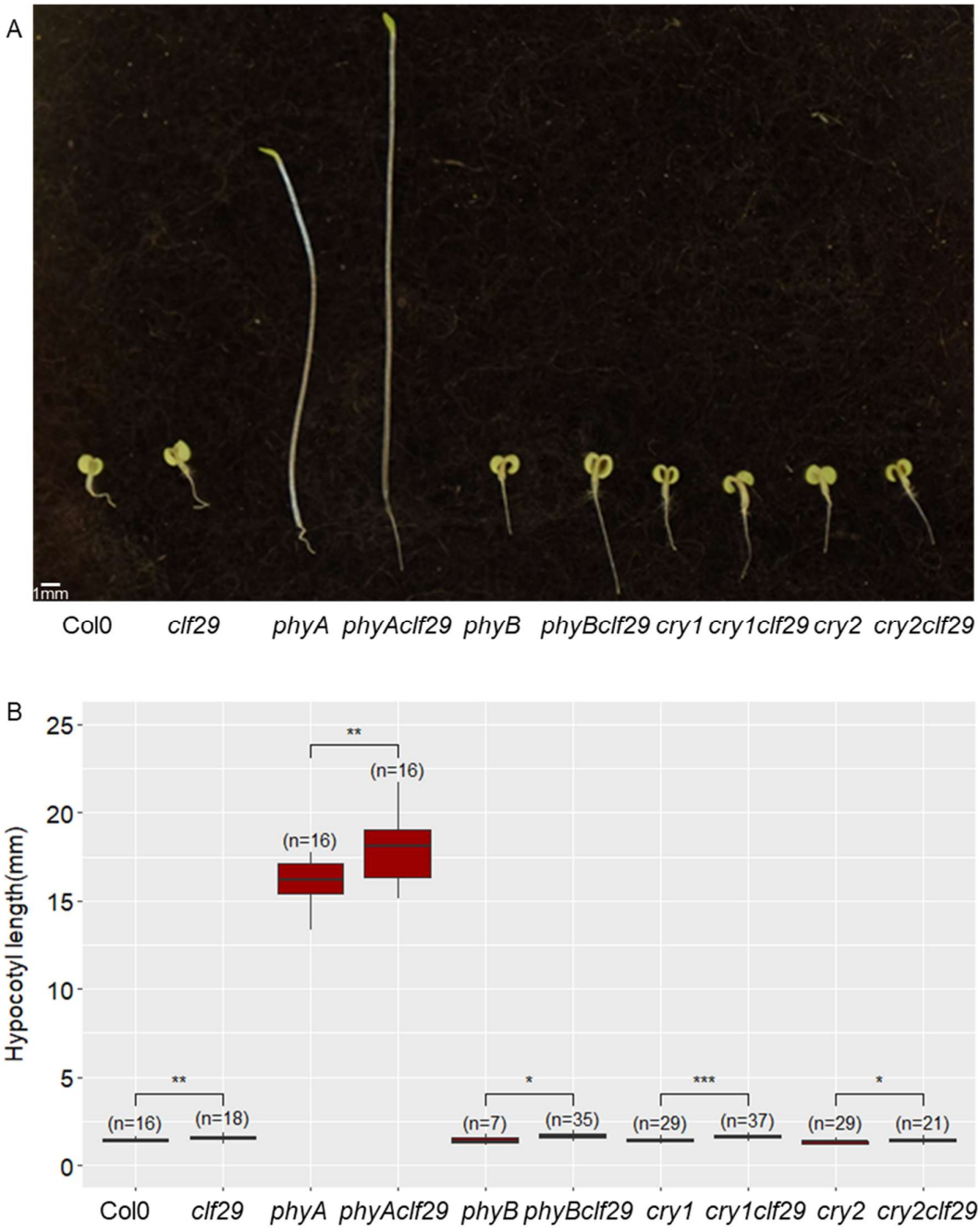

Fig. 3.8 Effect of *clf29* loss on hypocotyl lengths in photoreceptor mutants grown under far-red light.
A) 5-day old seedlings carrying mutations in photoreceptors and double mutants also carrying mutations in *clf29*, grown in constant far-red light at 21°C (1 µmol m^{-2} s^{-1})
B) Box plot showing hypocotyl lengths of the plants in A). Sample numbers displayed in graph. Asterisks indicate statistically significant differences in mean hypocotyl length of a *clf29* mutant compared to a non-*clf29* mutant in that genetic background, as determined by Independent samples T-Tests (* = P<0.05), (** = P<0.01), (*** = P<0.001).

Finally, this analysis was also carried out in seedlings grown under red light (Fig. 3.9). Considering that *clf29* plant lines are no different than Col0 when grown in red light (Fig. 3.4), it was not expected that *clf29* mutation would have a phenotypic effect on hypocotyl length in any of the genetic backgrounds analysed when grown in this wavelength of light. This expectation was borne out in the results, as shown in (Fig. 3. 9).

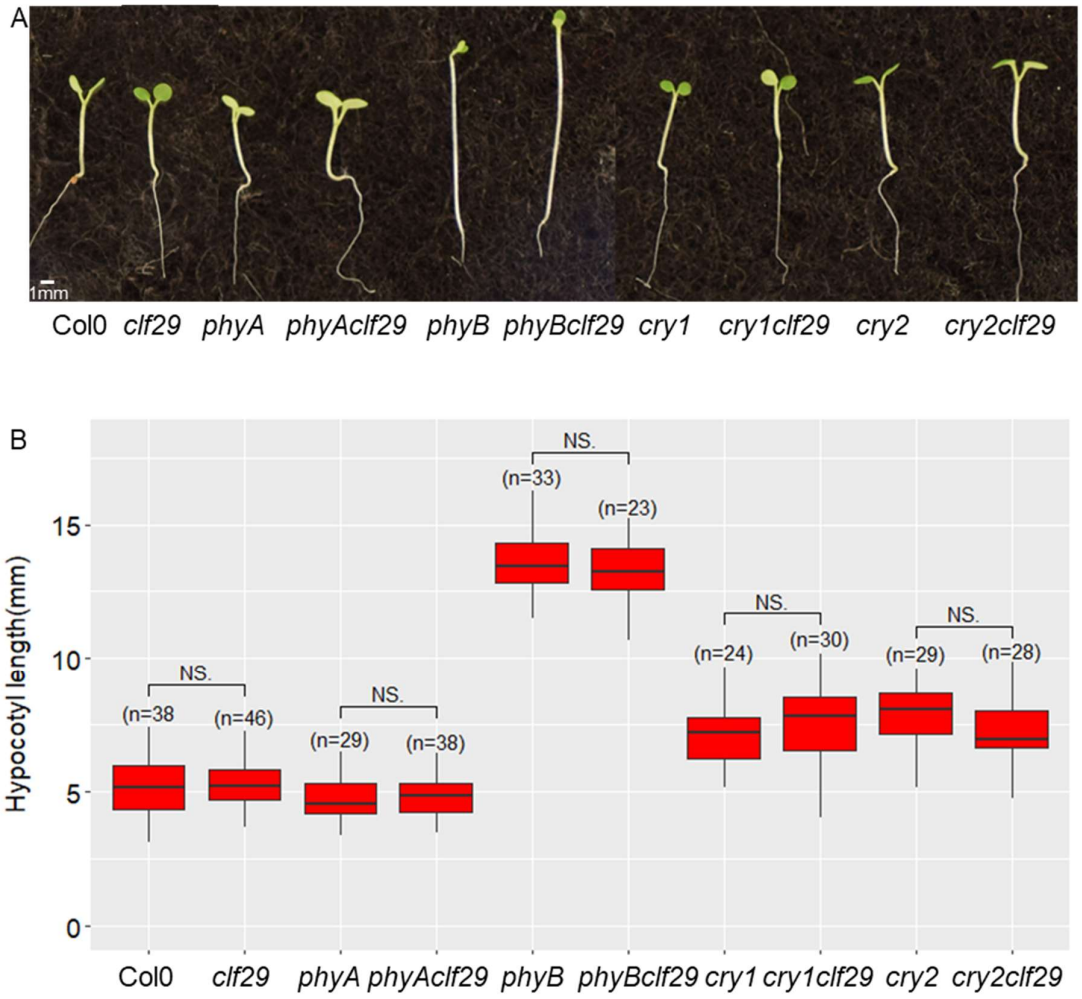

Fig. 3.9 Effect of *clf29* loss on hypocotyl lengths in photoreceptor mutants grown under red light.
A) 5-day old seedlings carrying mutations in photoreceptors and double mutants also carrying mutations in *clf29*, grown in constant red light at 21°C (5 µmol m-2 s-1)
B) Box plot showing hypocotyl lengths of the plants in A). Sample numbers displayed in graph. NS = no statistically significant differences between samples, as determined by independent samples T Tests.

3.5 *CLF* is transcriptionally induced by light in a *PHYB*- and *CRY1*- dependent manner

In Chapter 3.2 it is shown that *clf29* plants exhibit elongated hypocotyls in light (Fig. 3.1), and under monochromatic blue (Fig. 3.2) and far-red (Fig. 3.3). This phenotype is also seen in darkness (Fig. 3.4), which in Chapter 3.3 is taken to indicate that this could represent a constitutive activity of CLF that occurs regardless of the presence or absence of light. The absence of elongated hypocotyls in *clf29* plants grown under red light (Fig. 3.5) could represent a repression of CLF activity by this wavelength.

However, data presented in Chapter 3.4 indicate that under both white and blue light, the *clf29* elongated hypocotyl phenotype is abolished in a *cry1* mutant (Fig. 3. 6-7), indicating a requirement for CRY1 activity for CLF to have phenotypic effects under these wavelengths of light. A similar effect is seen for *phyA* under blue light, with *clf29* mutation showing no phenotypic effects in a *phyA* loss of function line (Fig. 3.7). This finding suggests that although *CLF* appears to have constitutive effects on hypocotyl elongation even in the absence of light, it is affected by photoreceptor activity, potentially indicating a link between CLF and light signalling machinery.

As described in Chapter 3.1, RNA-seq work in our laboratory has previously found that *CLF* transcription is rapidly induced by light, with an increase in *CLF* expression seen 15 minutes after light exposure (De Lucas, Unpublished). It was decided to verify this finding via qPCR analysis. As expected, *CLF* expression was significantly higher after exposure to 15 minutes white light in dark-grown Col0 seedlings (Fig. 3. 10) relative to the housekeeping gene *UB10*.

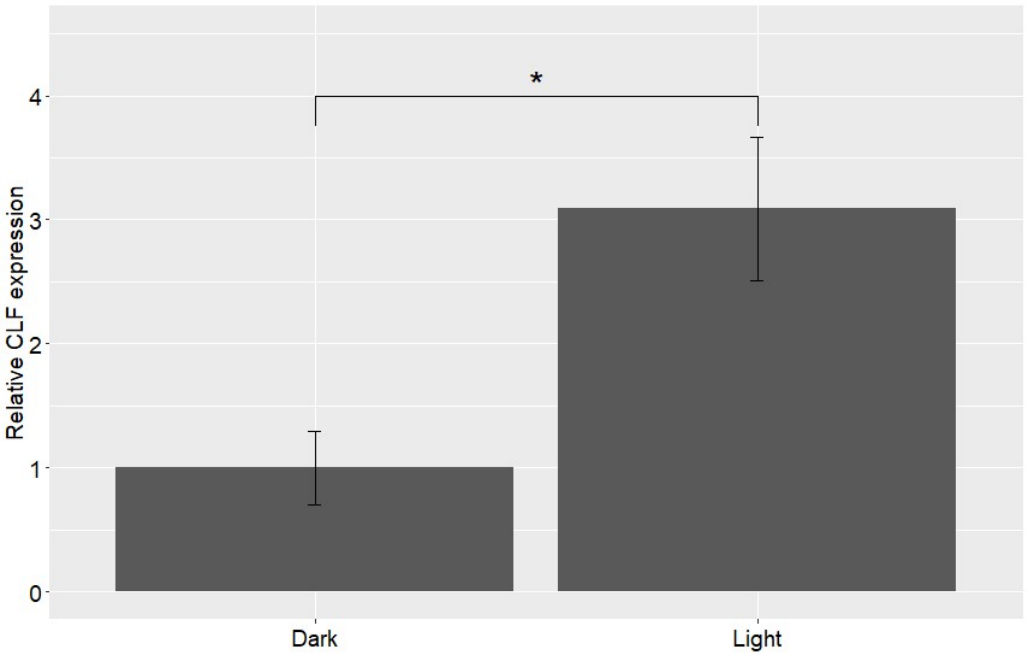

Fig. 3.10 qPCR analysis of clf29 expression in dark-grown seedlings before and after exposure to 15 minutes white light.
RNA was extracted from 5-day old dark-grown seedlings before (Dark) and after (Light) exposure to 15 minutes of white light (40µmol m^{-2} s^{-1}). *clf29* expression was analysed relative to the housekeeping gene UB10. To calculate relative expression in the light, *clf29* expression in the dark was set to 1. Error bars indicate standard error of the mean (SEM) for three biological replicates. Asterisk indicates significant difference from Dark ($p<0.05$) as determined by 2-sample unpaired t-tests

Further analysis was then carried out to assess whether this light-induced *CLF* transcription was also linked to photoreceptor activity, as observed with the elongated hypocotyl phenotype in white and blue light (Fig. 3. 6-7). Five-day old dark-grown seedlings carrying mutations in *phyA*, *phyB*, *cry1* or *cry2* were exposed to white light for 15 minutes. In *phyA* and *cry2* mutants, a significant increase in *CLF* expression was still observed after 15 minutes light (Fig. 3.11). However, in *cry1* and *phyB* mutants, this effect was abolished, and *CLF* expression actually decreased (though this decrease was not statistically significant (Fig. 3.11). These data indicate that *CRY1* and *PHYB* are required for the light-induction of *CLF* transcription seen in Col0.

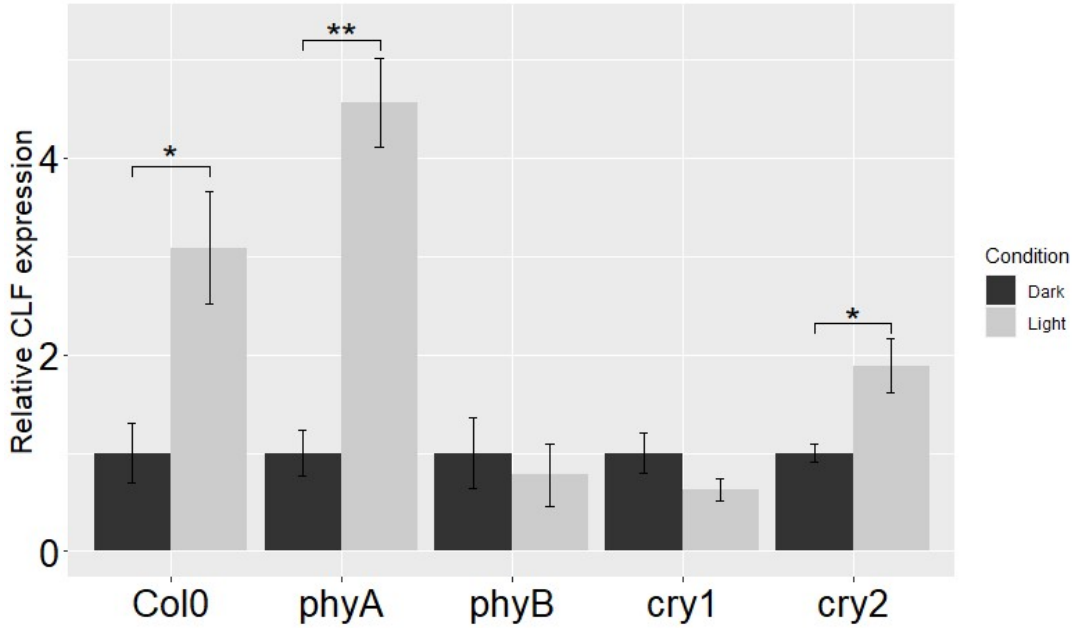

Fig. 3.11 qPCR analysis of clf29 expression before and after exposure to 15 minutes light in dark-grown photoreceptor mutants
RNA was extracted from 5-day old dark-grown Col0 seedlings and seedlings carrying mutations in *cry1*, *cry2*, *phyA* and *phyB* before (Dark) and after (Light) exposure to 15 minutes of white light (40µmol m^{-2} s^{-1}). *clf29* expression was analysed relative to the housekeeping gene UB10. To calculate relative expression in the light, *clf29* expression in the dark was set to 1. Error bars indicate standard error of the mean (SEM) for three biological replicates. Asterisks indicates significant difference from Dark as determined by independent samples t-tests T-Tests (* = p<0.05), (** = P<0.01).

The observation that *CLF* transcription is induced by light, and that this is dependent on the photoreceptors CRY1 and PHYB provides a new perspective on a potential role for CLF during light signalling. Initially, hypocotyl assays indicated that CLF may function constitutively to repress hypocotyl lengths regardless of the presence of light, meaning a link between CLF and light signalling could not be established. However, data in Chapter 3.4 and 3.5 indicate that CLF is transcriptionally induced by light in a photoreceptor-dependent manner (Fig. 3.10-11), and that loss of photoreceptors affects the phenotype of *clf29* mutants under light. Taking these data together, it can be proposed that CLF is regulated by photoreceptors during photomorphogenesis, and that upregulation of CLF may form part of the response to light.

This is most clearly seen with regards to CRY1. CRY1 is required for light-induced *CLF* transcriptional upregulation (Fig. 3.11), and *clf29* mutation has no phenotypic effect in white or blue light in a *cry1* background (Fig. 3.6-7). Taken together, these data could indicate that CRY1 is involved in activating *CLF* expression in response to blue light perception.

The observation that *CLF* shows no transcriptional induction upon light perception in a *phyB* background (Fig. 3.11) was more surprising, given that under red light, *CLF* loss shows no phenotypic differences to wild-type and, considering the role of PHYB as the primary red-light receptor. Furthermore, in any light regime where *clf29 mutation* has an effect (white, blue, or far-red light), these phenotypic effects were still apparent in a *phyB* background.

3.6 Summary

The data in this chapter have investigated a potential role for CLF in the light response.

It has been shown that loss of *CLF*, but notably not *SWN* (the other methyltransferase acting in the PRC2 complex during sporophyte development) causes significantly lengthened hypocotyls in plants grown under white light (Fig. 3.1), indicating a role for CLF in the repression of hypocotyl elongation that is not shared by SWN.

A *clf29* plant line shows elongated hypocotyls in darkness (Fig. 3.4), and in white (Fig. 3.1), blue (Fig. 3.2) or far-red light (Fig. 3.3). The presence of elongated hypocotyls in dark-grown seedlings could indicate that CLF functions constitutively to repress hypocotyl elongation, presumably via mediation of the repressive chromatin mark H3K27me3. Meanwhile, the phenotype is not seen in plants grown under red light (Fig. 3.5), which could indicate that CLF activity is repressed by red light.

It is then observed that in both white and blue light, this phenotype is abolished in a *cry1* mutant (Fig. 3.6-7), and in blue light also in a *phyA* mutant (Fig. 3.7). It is additionally shown that *CLF* is transcriptionally induced by light within 15 minutes, and that this activity is dependent on the photoreceptors CRY1 and PHYB (Fig. 3.10-11). The presence of a light-induced transcriptional activation of CLF and a *clf29* phenotype in the light, both of which are dependent on photoreceptors, is significant. Taking these observations together, it can be proposed that CLF functions to repress hypocotyl elongation, and that CLF transcription is induced by light in a photoreceptor-dependent manner as part of the light response, facilitating an increase in CLF activity which contributes to light-induced repression of hypocotyl elongation.

This model can be most confidently proposed with regards to blue light and the photoreceptor CRY1. CRY1 is the major blue light receptor, and has been shown here to be required for CLF phenotypic effects on hypocotyl lengths in both blue and white light (Fig. 3.6-7), as well as light-induced activation of CLF transcription (Fig. 3.10-11).

PHYA is also shown to be involved in the activity of CLF in blue light, with *clf29* mutants showing lacking elongated hypocotyls in a *phyA* mutant under blue light (Fig. 3.7). Notably, it has been shown that PHYA, although predominantly known for its role in responding to far-red light, does play a role in the response to blue light (Lin, 2000). It is also known to interact with CRY1 under this wavelength, and this seems to be at least partially responsible for PHYA-mediated effects under blue light. (Ahmad et al., 1998). Considering this, it is possible that PHYA contributes to CRY1-mediated induction of *CLF* transcription in response to blue light.

The picture is less clear with regards to the effects of far-red and red light on CLF, although some intriguing data are presented in this chapter.

When grown under red light, *clf29* shows no difference in hypocotyl length from Col0 (Fig. 3.5). This would suggest that red light acts in some way to repress CLF activity. However, the transcriptional induction of CLF is dependent on PHYB, the predominant red light photoreceptor (Fig. 3.11).

Meanwhile, in Far-red light, *CLF* loss does result in elongated hypocotyls (Fig. 3.4), but this effect is independent of all four photoreceptors analyse (Fig. 3. 8), and the transcriptional induction of *CLF* by white light occurs independently of PHYA, the predominant Far-Red light photoreceptor (Fig. 3.11).

Taking these data together, it is possible to propose a mechanism in which *CLF* may be involved in photomorphogenesis in *Arabidopsis*, shown in (Fig. 3. 12). Blue light induces CRY1 activation, a process which is promoted by PHYA. CRY1 then induces transcriptional upregulation of *CLF*, which mediates the repressive chromatin modification H3K27me3 as part of the PRC2 complex. The effect of CLF on its downstream targets then leads to the inhibition of hypocotyl elongation.

The effect of far-red light, meanwhile, is less clear, as discussed above, and so further investigations are required before assertions can be included in this hypothesised model. Red light is proposed to inhibit CLF activity it, given the effects of *clf29* mutation under these light conditions shown in (Fig. 3.3 and 3.5).

It must be noted that the data here have limitations and that further experiments would be desirable to increase the confidence in this model. The observation of longer hypocotyls in *clf29* plants in darkness (Fig. 3.4) indicates that inhibition of hypocotyls likely represents a constitutive activity of CLF, limiting possible conclusions with regards to CLF's role during light responses. The hypocotyl assays presented here do not consider the extend to which hypocotyls are elongated under different light regimes tested, simply

whether the differences between Col0 and *clf29* are statistically significant. Further analysis of the magnitude of hypocotyl elongation seen in darkness and light would be highly valuable in assessing whether CLF has a greater role in hypocotyl elongation in light-grown seedlings, which could be linked to the light-induced transcriptional activation observed here. Additionally, assessing the transcriptional behaviour of CLF under red, blue and far-red light individually would be desirable. It is proposed here that CLF is involved in blue light responses, due to the observation that the main blue light receptor (CRY1) is required for both its transcriptional activation (Fig. 3.11) and the *clf29* phenotype in both blue and white light (Fig. 3.6-7). Meanwhile, it is proposed that red light represses CLF activity due to the lack of a *clf29* phenotype under red light (Fig. 3.5, 3.9). Further transcriptional analysis to correlate CLF expression with phenotypes under different wavelengths of light observed would provide highly valuable evidence in support of this model.

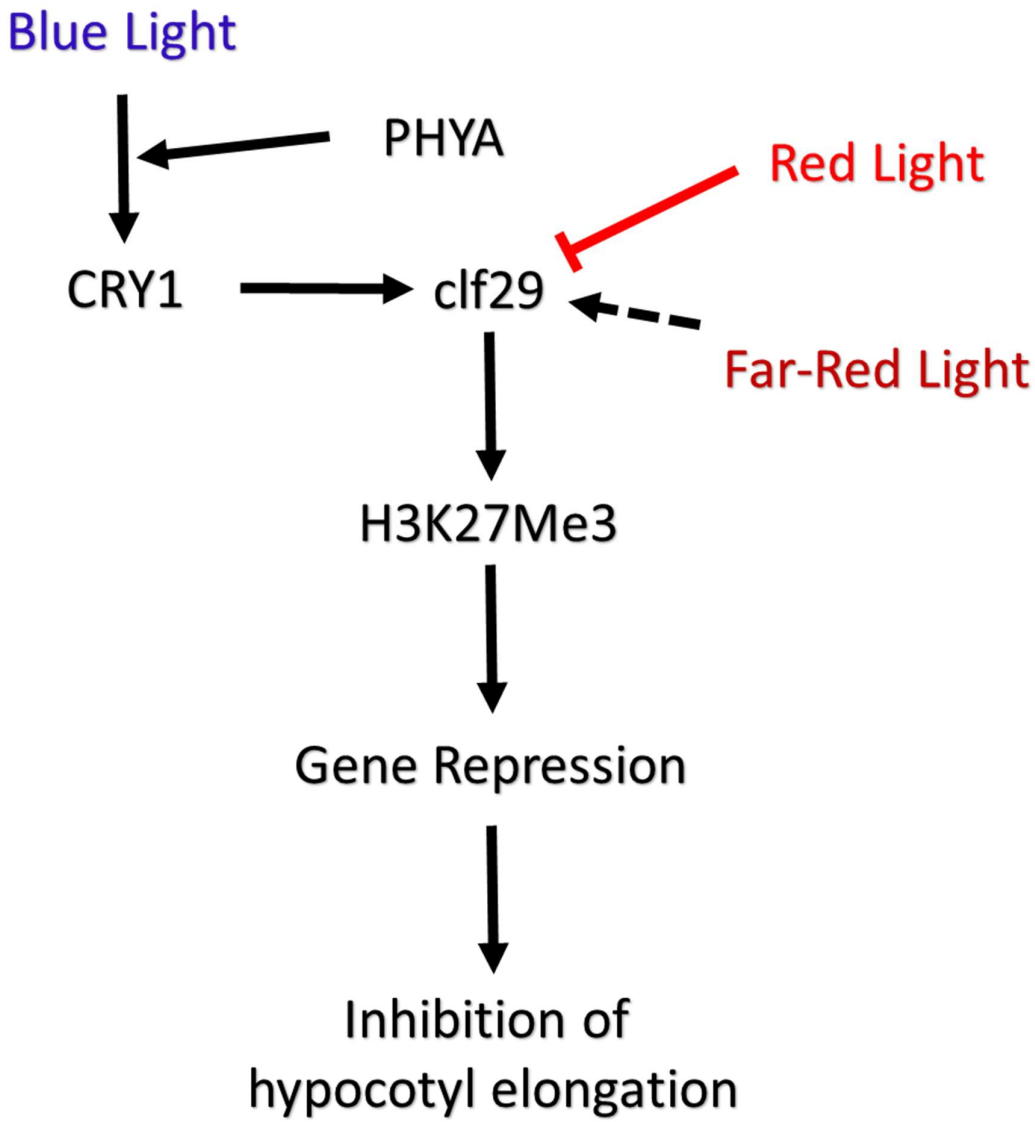
Blue Light
PHYA
Red Light
CRY1
clf29
Far-Red Light
H3K27Me3
Gene Repression
Inhibition of
hypocotyl elongation

Fig. 3.12 Proposed mechanism for clf29 involvement in light signaling during photomorphogenesis.

Black arrows indicate hypothesized positive interaction. Red T-Bars indicate hypothesised inhibition. Dashed arrows indicate potential features of this mechanism requiring further investigation.

Blue light induces CRY1 activation, a process which is promoted by PHYA. It is proposed that CRY1 then induces transcriptional upregulation of CLF. This is based on observations in this chapter that *CLF* is transcriptionally upregulated by light in a CRY1-dependent manner (Fig. 3.10-11), and that *clf29* plants exhibit elongated hypocotyls in blue light, a phenotype which is abolished in a *cry1* or *phyA* genetic background (Fig. 3.2, 7). CLF then mediates the repressive chromatin modification H3K27me3 as part of the PRC2 complex. The effect of CLF on its downstream targets then leads to the inhibition of hypocotyl elongation.

It is proposed that CLF would be repressed by red light, based on observations in this chapter that *clf29* mutation has no effect on hypocotyl lengths in plants grown under red light (Fig. 3. 5, 9), despite the elongated phenotype of *clf29* mutants observed in both darkness and under white, blue and far-red light (Fig. 3. 1-4).

The effect of far-red light is more difficult to determine. *clf29* plants do exhibit elongated hypocotyls under far-red light (Fig. 3.3), but this effect is also seen in darkness (Fig. 3. 4), and in far-red light this effect is independent of all photoreceptors analysed here (Fig. 3. 8). This means the elongated hypocotyls seen in *clf29* plants under far-red light could be due to a constitutive activity of CLF also occurring in darkness. Thus, further investigations are needed into this aspect of the proposed.

Chapter 4 – RNA-seq analysis of CLF activity during transcriptional responses to light

4.1 Introduction and background of the RNA-seq experiment

RNA-seq is a common technique for analysing the transcriptome as a whole, and was first developed in the late 2000s, making use of advances in next generation sequencing technology which made large-scale sequencing more accessible (Wang et al., 2009).

In an RNA-seq experiment, RNA is extracted from an organism and reverse-transcribed to produce cDNA using random hexamers. Adapters are added to the cDNA to produce a library of cDNA fragments, which are then sequenced on a next-generation sequencing platform. The sequenced reads are then mapped onto a genome if the organism being analysed has been sequence, or assembled *de novo* using overlapping reads (Nagalakshmi et al., 2008).

RNA-seq has a number of advantages over microarrays, including less of noise and removal of problems with cross-hybridisiation. It is also useful in that since it simply involves sequencing of RNA collected from an organism, it does not require prior knowledge of gene sequences, and provides an unbiased analysis of the transcriptome (Chee-Sang et al., 2010), (Krishnamurthy et al., 2018).

It is known that light has huge regulatory effect on the *Arabidopsis* transcriptome, with previous analyses demonstrating massive differences in the transcriptome between light- and dark-grown seedlings (Ma et al., 2001), (Jiao et al., 2005). It has also been shown that light has a distinct effect on chromatin patterns too, including the repressive histone modification H3K27me3 (Guo et al., 2008), (Charron et al., 2009). The previous chapter has identified that CLF, which mediates deposition of this mark, is involved in repressing hypocotyl elongation in darkness and under white, far-red and blue light, and that upon

light perception *CLF* transcription is upregulated in a *CRY1*- and *PHYB*-dependent manner. These data suggest that CLF is involved in the response to light, particularly in light-induced repression of hypocotyl elongation.

As such, it was hypothesised that CLF may play a key role in transcriptional responses to light. An RNA-seq analysis was planned to investigate this hypothesis, and how this may be affected by the action of Phytochromes PHYA and PHYB and cryptochromes CRY1 and CRY2. The rest of this chapter is devoted to describing the results of this RNA-seq analysis. As described in Chapter 2.5 As described in Chapter 2.5, cDNA libraries were prepared by Joseph Nelson and sent for sequencing at Vincent Coates Genomics Sequencing Lab (GSL) at the University of California, Berkeley. The raw reads were then mapped to the TAIR10 genome by Dr Wenbin Wei, Bioinformatics Officer for the Department of Biosciences, Durham University to produce read numbers for each gene in the TAIR10 genome. All bioinformatic analysis after the production of read numbers was then carried out by Joseph Nelson.

The first section will describe the results of analysing transcriptional changes upon light perception in dark-grown Col0 and *clf29* seedlings, to analyse how loss of *CLF* activity affects the transcriptional responses to light exposure in etiolated seedlings.

After this, analysis was carried out to compare Col0 and photoreceptor mutants *phyA*, *phyB*, *cry1* and *cry2*, to analyse how loss of photoreceptors affects the transcriptome after light exposure, and how this correlates with the effects of CLF discussed in the first section. Finally, analysis of *cry*/*phy*- deficient lines is compared to double mutants lacking one of the photoreceptors and *CLF*, to analyse the effect of *clf29* mutation on transcription in genetic backgrounds already lacking photoreceptors. It has been established that lack of photoreceptors *PHYA*, *PHYB*, *CRY1* or *CRY2* does not produce

measurable effects on phenotype in dark-grown seedlings (Wang et al., 2014), (Ma et al., 2016), (Yu et al., 2010), (Ponnu et al., 2019), (Li et al., 2011), (Neff and Chory, 1998), whereas each of these mutations produces effects on hypocotyl elongation under light. As such, dark-light transition was not analysed in photoreceptor mutants, and these were simply analysed after light exposure. Conversely, *clf29* mutants have been shown to have significantly elongated hypocotyls in darkness as well as light (Fig. 3. 4), so analysis of dark-light transition was considered important in this analysis.

4.2 Analysis of dark-light transcriptional changes in Col0 and *clf29*

4.2.1 Generation of lists of differentially expressed genes via RNA-seq

As described in 4.1, the first aim of the RNA-seq analysis was to profile transcriptional changes in 5-day-old dark-grown Col0 and *clf29* seedlings before and after light exposure. This will allow the identification of genes which exhibit *CLF*-dependent regulation upon light perception, allowing new insights into potential roles of *CLF* and PRC2 in photomorphogenesis.

Previous analysis in our laboratory, carried out by Miguel de Lucas, has indicated that dark-grown *Arabidopsis* undergo rapid transcriptional responses when exposed to white light, with gene expression changes detectable within 15 minutes, and reaching a "steady state" level around 6 hours after light exposure (De Lucas, unpublished). This time point of 6 hours has also been used in published analyses of both transcriptional and chromatin changes after light perception (Guo et al., 2008), (Charron et al., 2009) (Bourbousse et al., 2012). This thesis followed this precedent. RNA was extracted from 5-day old dark-grown Col0 and *clf29* seedlings before (Dark) and after (Light) exposure to 6 hours white light (40µmol m^{-2} s^{-1}), as described in Chapter 2.5. RNA-seq libraries were prepared and

samples sequenced using next generation sequencing technologies as described in Chapter 2.5.

RNA-seq analysis using DESeq2 was carried out as described in Chapter 2.5. Firstly, an analysis was carried out to compare the composition of the samples using the principal components analysis (PCA) feature in Deseq2 (Love et al., 2014) (Fig. 4.1). The PCA analysis visualises the samples by projecting them onto a 2D plane, spread out in two directions that best explain the differences observed between the transcriptomes (Love et al., 2014). As such, samples that cluster closely together on the PCA represent highly similar transcriptomes, whilst samples distant from each other are more distinct. Clear differences between different plant lines (Col0 and *clf29*) and light conditions (Dark and Light) are immediately apparent. Notably, it is clear that there is more difference between different groupings than there is between different bioreps within a single group.

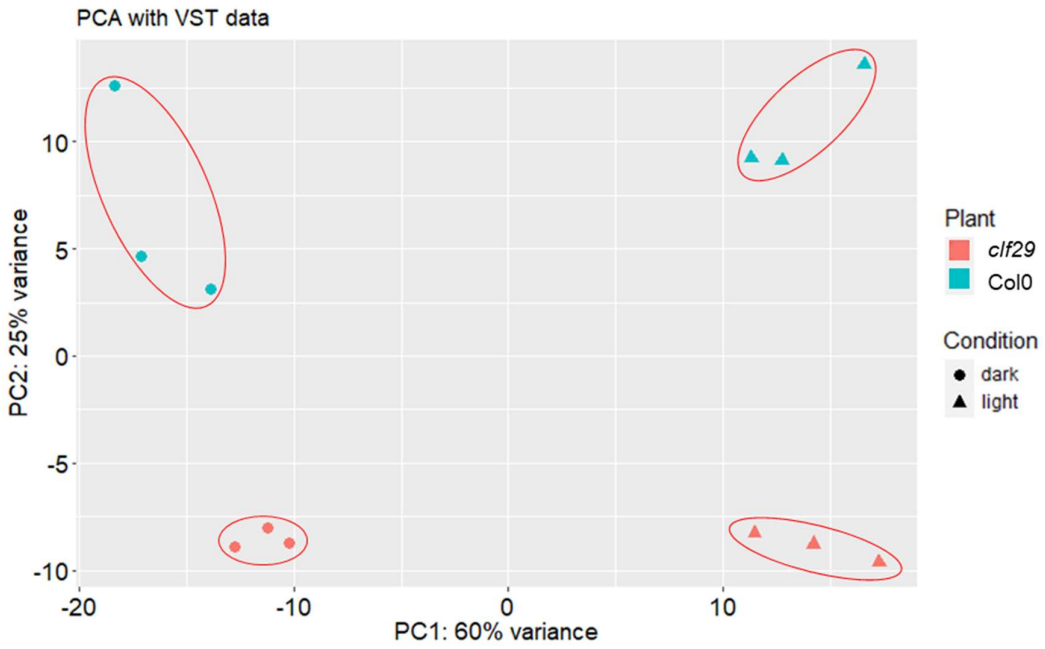

Fig 4.1 Principal component analysis of Col0 and *clf29* Dark and Light Samples

Principal component analysis (PCA) plot visualising sample distances between Col0 and *clf29* lines before and after 6 hours exposure (40µMol m^{-2} s^{-1}), analysed via RNA Seq. PCA performed on variance stabilised (vst) transformed data using the R software package DEseq2 (Love et al., 2014).

Lists of differentially expressed genes ($p<0.05$) between Dark and Light samples for Col0 and *clf29* lines were then produced, which are visualised in (Fig. 4.2 A-B). The full list of DEGs for each plant line can be found in (Appendix 2). For upregulated genes, a threshold of Log_2 Fold Change (Log2FC) < 1 was then applied, representing an actual fold change of 2, a two-fold increase in expression in light samples compared to dark samples. Similarly, for downregulated genes, a threshold of Log_2 Fold Change (Log2FC) > -1 was applied, representing an actual fold change of 0.5, a two-fold decrease in expression in light samples compared to dark samples. A total of 971 differentially expressed genes meeting these criteria were identified in Col0, with 656 upregulated genes and 315 downregulated genes (Fig. 4.2 C). Meanwhile, 882 differentially expressed genes were identified in *clf29*, with 577 upregulated genes and 305 downregulated genes.

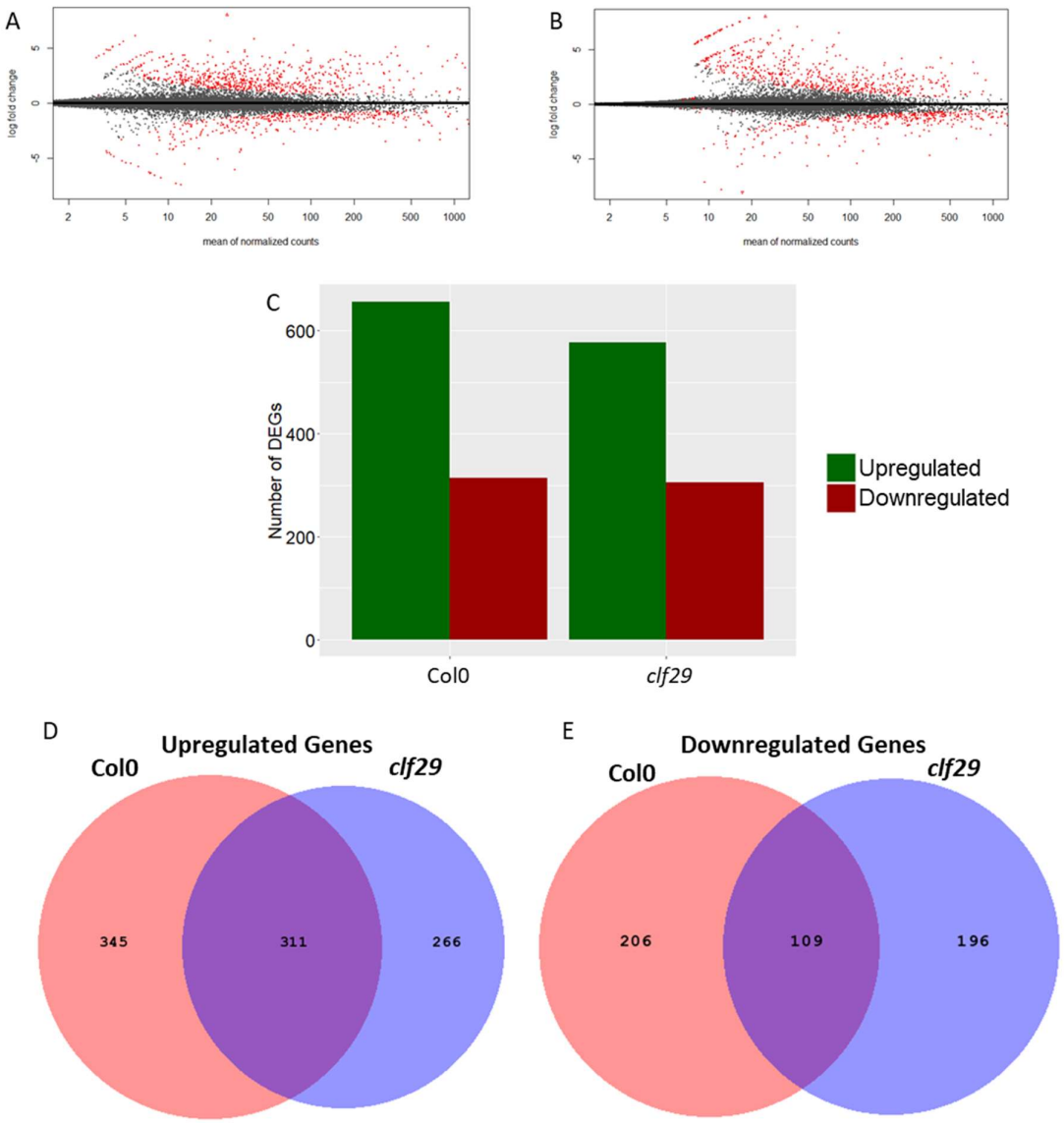

Fig 4.2 Genes differentially expressed in dark-grown Col0 and *clf29* seedlings before and after 6 hours exposure to White Light (40μMol m^{-2} s^{-1}), as identified by RNA Seq.
A) and B) Differentially expressed genes (DEGs) in dark-grown Col0 (A) and *clf29* (B) seedlings after 6 hours light exposure, calculated by the R package DESeq2 (Love et al., 2014). Red dots represent significantly DEGs, p<0.05.
C) Number of upregulated (p<0.05, Log(2) FC ≥1) or downregulated (p<0.05, Log(2) FC ≤- 1) after 6 hours white light exposure in Col0 and *clf29* seedlings.
D) Venn diagram showing overlap between genes significantly upregulated in Col0 and *clf29* dark-grown seedlings after 6 hours exposure to White Light (p<0.05, Log(2) FC ≥1).
D) Venn diagram showing number of genes significantly downregulated in Col0 and *clf29* dark-grown seedlings after 6 hours exposure to White Light (p<0.05, fold change ≤-1).

It is apparent that in both plant lines analysed, there is a massive transcriptional reorganisation upon light perception, with ~3% of the genome showing at least a two-fold change in transcription. It is also apparent that in both WT and *clf29*, more genes are upregulated in response to light than downregulated. This is in agreement with previous findings from microarray analysis of showing transcriptional responses to light (Ma et al., 2001), (Jiao et al., 2005) which have also found that more genes are upregulated than downregulated in light-grown seedlings compared to dark-grown counterparts.

Analysis of the overlap between differentially expressed genes in Col0 and *clf29* was carried out, and clear differences in both up- and down-regulated genes in Col0 and *clf29* were identified (Fig. 4.2 C-D). There was more similarity between the two plant lines among upregulated genes. Around 47% of genes showing light-induced upregulation in Col0 were also upregulated in *clf29* (311 out of 656), whilst around 54% of genes upregulated in *clf29* were also upregulated in Col0 (311 out of 577) (Fig. 4.2 D). Meanwhile, among downregulated genes Col0 and *clf29* samples were more divergent. Only around 35% of genes showing light-induced downregulation in Col0 were also downregulated in *clf29* (109 out of 315), whilst a similar proportion, 36%, of genes showing downregulation in *clf29* were also downregulated in Col0 (109 out of 305) (Fig. 4.2 E). There were no genes that showed upregulation in one of the plant lines and downregulation in the other.

4.2.2 Functional Analysis of the DEGs

Having identified lists of genes that are up- or down-regulated in response to light in Col0 and *clf29*, analysis was undertaken on the functional relevance this had and what the different transcriptional changes indicated about the light response in *clf29* plants. To do this, enrichment analysis was carried out using the Gene Ontology Resource (Ashburner et al., 2000), (Mi et al., 2019), (The Gene Ontology Consortium et al., 2021) to identify biological processes enriched among DEGs identified in Chapter 4.2.

Analysing the overlap between DEGs in Col0 and *clf29* (Fig. 4.2), it was identified that a distinct number of genes showed upregulation or downregulation in Col0, but not in *clf29*, or vice versa, as well as genes showing transcriptional changes in both plant lines. As such, there are three distinct categories of genes that could be analysed: Genes showing transcriptional changes in Col0, but not in *clf29*; genes showing transcriptional changes in both Col0 and *clf29*, and genes showing transcriptional changes in *clf29* but not in Col0. The first and last of these categories were selected for functional analysis to analyse how loss of *CLF* affects the transcriptional response to light. Genes showing transcriptional changes in both Col0 and *clf29* lines were not analysed as they likely represent genes which are independent of CLF activity.

The results were compared to assess the differences between enriched processes in Col0-specific and *clf29*-specific DEGs (Fig. 4.3). Meanwhile, the top 20 most enriched processes (if present) are shown for upregulated genes in (Fig. 4.4) and downregulated genes in (Fig. 4.5), and all enriched processes with a false discovery rate (FDR) of less than 0.5 are shown in Appendix 3.

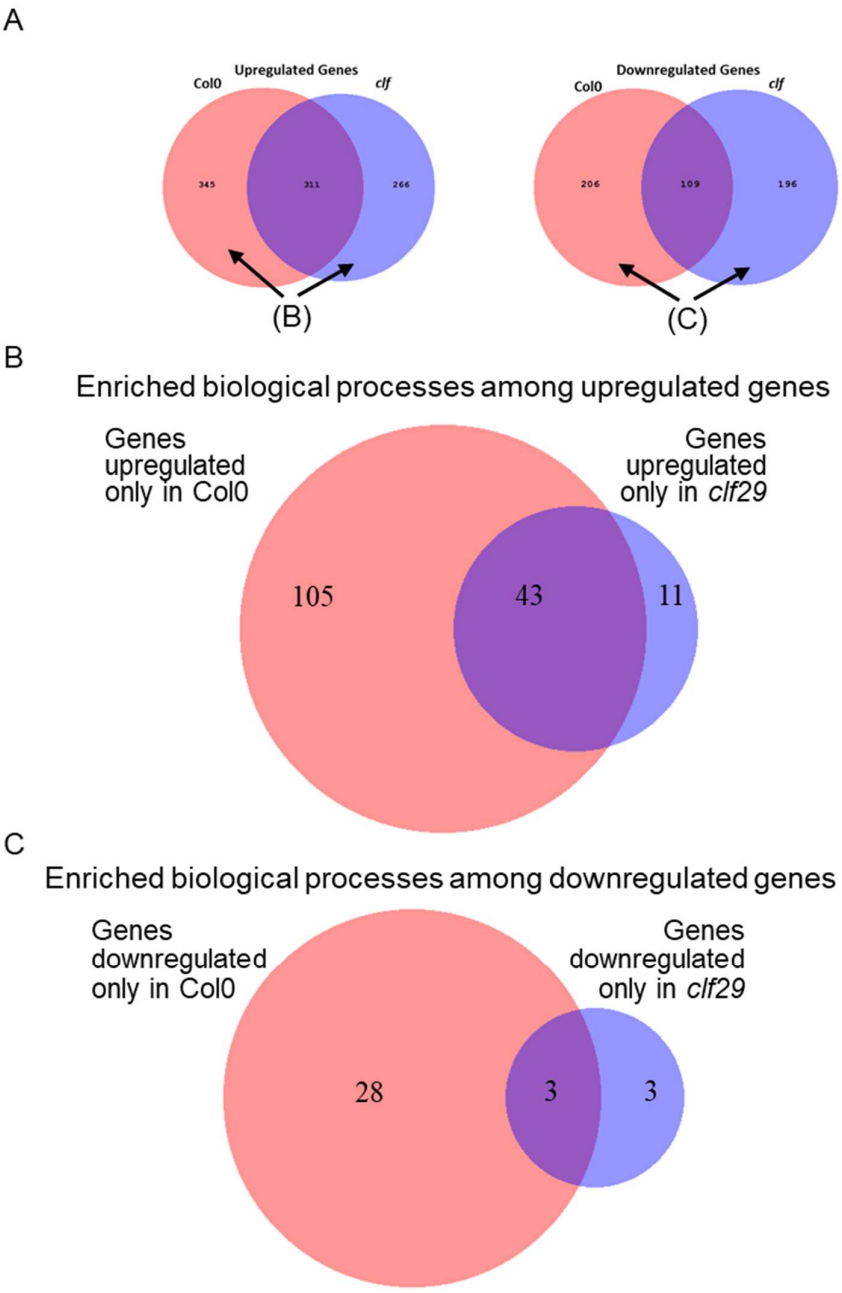

Fig 4.3 Number of enriched biological processes among Col0- and *clf29*-specific DEGs.

A) Visual representation of the genes being analysed in 4.3 B) and C).
B) Number of enriched biological processes (FDR < 0.05) among genes showing transcriptional upregulation only in Col0 or *clf29* plant lines.
C) Number of enriched biological processes (FDR < 0.05) among genes showing transcriptional downregulation only in Col0 or *clf29* plant lines.

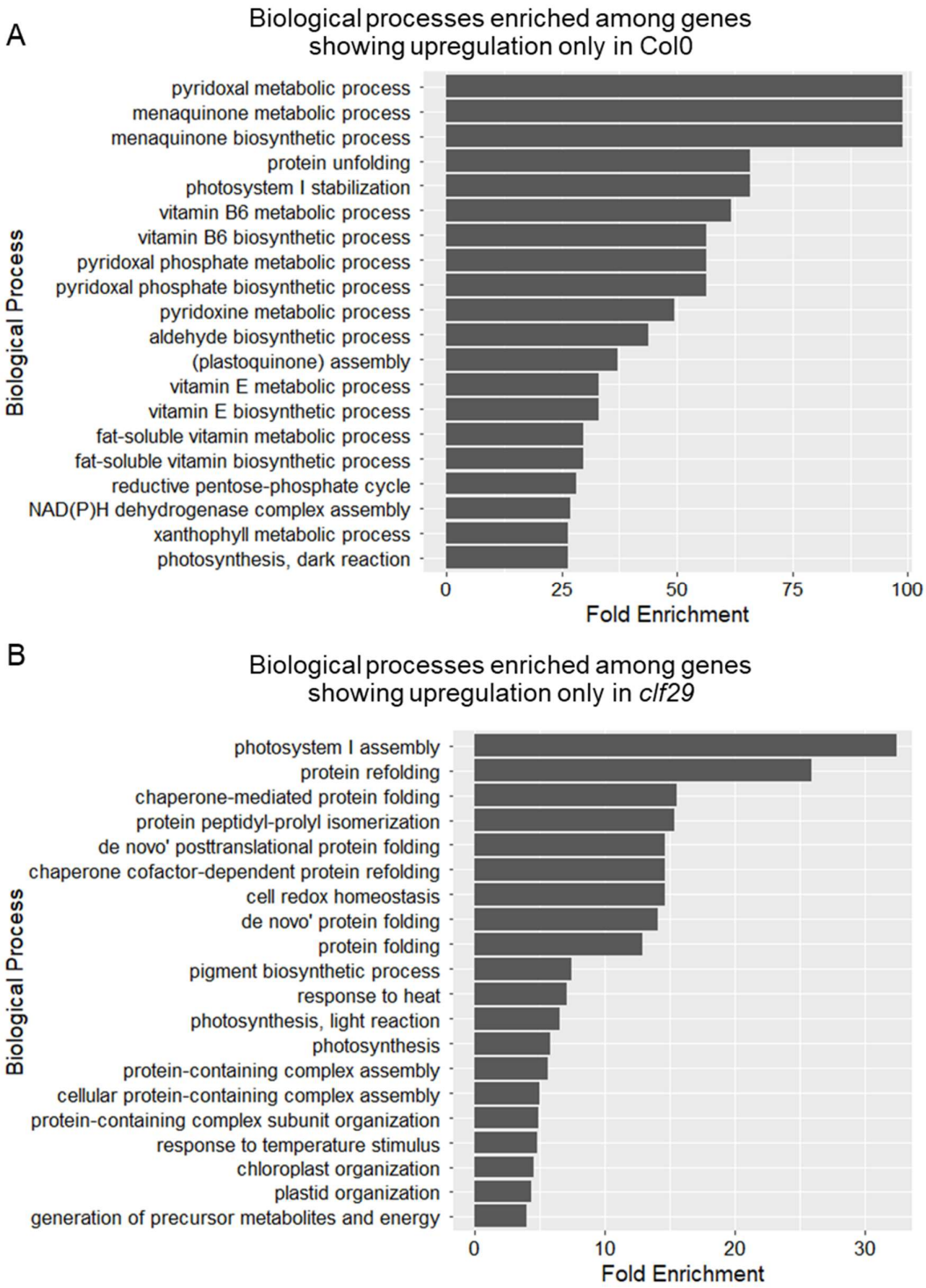

Fig 4.4 Most highly enriched processes genes showing upregulation only in Col0 or *clf29* plant lines, as identified by gene ontology analysis

Biological processes enriched among genes showing upregulation in dark-grown Col0 seedlings after exposure to 6 hours white light but not in *clf29* seedlings (A) or vice versa (B). Processes with FDR rate <0.05 sorted by enrichment score, top 20 results shown

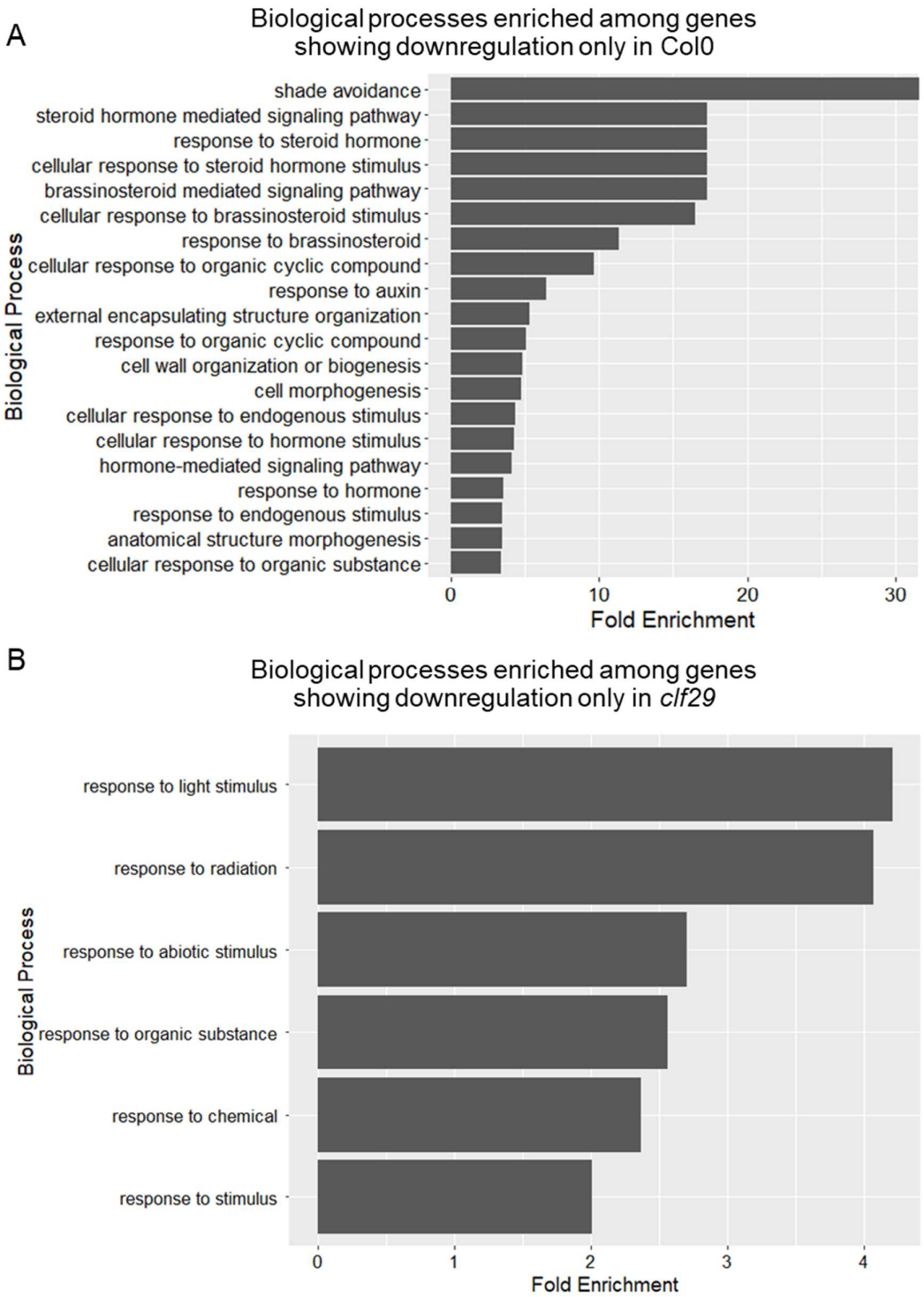

Fig 4.5 Most highly enriched processes genes showing downregulation only in Col0 or *clf29* plant lines, as identified by gene ontology analysis

Biological processes enriched among genes showing downregulation in dark-grown Col0 seedlings after exposure to 6 hours white light but not in *clf29* seedlings (A) or vice versa (B). Processes with FDR rate <0.05 sorted by enrichment score, top 20 results shown

Looking at this dataset, it is apparent that *clf29* loss has a substantial effect on the functionality of the transcriptome during the light response. *clf29*-specific DEGs had a substantial reduction in terms of the number of enriched biological processes (Fig. 4.3). This effect is particularly apparent among *clf29*-specific downregulated genes, with only 6 biological processes showing enrichment at a false discovery rate (FDR) of less than 0.05 (Fig. 4.3 C). Meanwhile there were 31 enriched biological processes among Col0-specific genes. There was also a substantial reduction in enriched biological processes among upregulated genes, with 148 enriched biological processes being found among Col0-specific upregulated genes, compared to 54 among *clf29*-specific upregulated genes (Fig. 4.3 B).

These effects are in spite of the fact that the number of DEGs in Col0 and *clf29* is similar, both for upregulated genes and downregulated genes (Fig. 4.2). This dataset perhaps indicates a dysregulation to transcriptional changes during light perception in a *clf29* line. The number of DEGs remains roughly similar, but targeting of distinct biological processes via transcriptional changes is heavily disrupted.

The observation that this effect seems more prominent among downregulated genes is likely due to the fact that CLF and the PRC2 complex mediate the repressive chromatin modification H3K27me3. Thus it would be expected that most direct targets of CLF would exhibit transcriptional downregulation as a result of its activity, and it is therefore unsurprising that the largest functional effect of loss of *clf29* during light perception would be among downregulated genes.

4.2.3 Hypothesis generation from Col0 and *clf29* dark-light transcriptional analysis

4.2.3.1 Transcriptional analysis provides evidence for a role of CLF in repressing hypocotyl growth via inhibition of cell wall elongation

One immediate observation in this dataset is that the most highly enriched process among Col0-specific downregulated genes is shade avoidance, with a >30-fold enrichment of genes involved in this process compared to what would be expected from a gene set of this size (Fig. 4.5 A). This enrichment is notably absent in *clf29*-specific downregulated genes (Fig. 4.5 B), and represents three genes involved in shade avoidance: *PHYTOCHROME RAPIDLY REGULATED1* (*PAR1*); the *HOMEOBOX-LEUCINE ZIPPER* gene *HAT2*; and *PECTIN METHYLESTERASE INHIBITOR 7* (*PMEI7*) shown in (Fig. 4.6).

Gene	AtID	Log(2)FC Dark-Light in Col0 (If $p < 0.05$)
PAR1	AT2G42870	-3.34
HAT2	AT5G47370	-2.68
PMEI7	AT4G25260	-6.00

Fig 4.6 Shade avoidance genes showing light-induced downregulation only in Col0

Genes identified by Gene Ontology Analysis of Col0-specific downregulated genes under the category "Shade Avoidance", along with their Log(2)FC in Col0, representing a 33.01-fold enrichment compared to what would be expected from a gene set of this size.

This observation is particully notable considering the findings presented in Chapter 3 that CLF has a role in repressing hypocotyl elongation. The shade avoidance response at the seedling stage primarily involes and increase in hypocotyl length (Casal, 2012), as seen in dark-grown seedlings, and so the identification of several genes relating to this process showing *CLF*-dependent downregulation provides further evidence for a role of *CLF* in inhibiting this process.

HISTONE ACETYLASE 2 (*HAT2*) is known to be transcriptionally induced in response to shade, and upon auxin perception auxin. Plants overexpressing this gene show elongated hypocotyls and other phenotypic traits characteristic of excessive auxin production, indicating it promotes hypocotyl elongation (Sawa et al., 2002). *PECTIN METHYLESTERASE INHIBITOR 7* (*PMEI7*), meanwhile, is a member of the pectin methylesterase inhibitor family. The level of pectin esterification is a key component of cell wall elongation and thus hypocotyl elongation. Demethylesterified pectin can more easily form crosslinks, stiffening the cell wall and inhibiting cell elongation (Willats et al., 2001). This is promoted by Pectin Methylesterases. As such, Pectin methylesterase inhibitors promoter hypocotyl elongation by inhibiting this activity of Pectin methylesterases (Derbyshire et al., 2007). It is clear to see how repression these genes in a *CLF*-dependent fashion could be part of CLF's role during the photomorphogenic transition.

Another intriguing and likely related observation from analysis of Col0-specific downregulated genes was enrichment of the biological process "Cell wall organisation or biogenesis", with 14 genes in this category showing light-induced downregulation in Col0, but not *clf29* (Fig. 4.7). Elongation of hypocotyls during etiolation is driven by cell elongation, with very little change in cell number (Gendreau et al., 1997). The process of cell wall elongation is tightly controlled by cell wall dynamics, and several of the genes in (Fig. 4.7) showing light-induced downregulation are key promoters of cell elongation.

Gene	AtID	Log(2)FC Dark-Light in Col0 (If p < 0.05)
CEL1	AT1G70710	-1.84
EXPA4	AT2G39700	-2.08
EXLA1	AT3G45970	-1.87
PAE9	AT5G23870	-1.67
XTH8	AT1G11545	-1.98
CSLC4	AT3G28180	-1.89
GALS2	AT5G44670	-2.86
FLA9	AT1G03870	-1.35
XTH30	AT1G32170	-1.24
XYL1	AT1G68560	-1.87
PIP5K5	AT2G41210	-1.26
EXPA11	AT1G20190	-2.40
XTH19	AT4G30290	-3.09
PME1	AT1G53840	-1.03

Fig 4.7 Genes in the category "Cell wall organisation or biogenesis" showing light-induced downregulation only in Col0

14 genes identified by Gene Ontology Analysis of Col0-specific downregulated genes under the category "Cell wall organisation or Biogenesis", along with their Log(2)FC in Col0, representing a 4.79-fold enrichment compared to what would be expected from a gene set of this size.

Firstly, there are several expansin genes, including the alpha-expansins *EXPANSIN 4* and *11* (*EXPA4* and *EXPA11*), as well as *EXPANSIN-LIKE1* (*EXPL1*). Expansins were first discovered for their actions in promoting cell wall growth in cucumbers (McQueen-Mason et al., 1992), and are now known to constitute a large superfamily of genes which facilitate cell wall growth via loosening of the cell wall (Li et al., 1993), (Choi et al., 2008). There are also three xyloglucan endotransglucosylase-hydrolase genes (*XTH8*, *XTH19* and *XTH30*) (Fig. 4.7). This is another family of genes which promote cell elongation, and

several members of this family have previously been shown to be upregulated in darkness-treated *Arabidopsis* plants, notably including the three shown here (Lee et al., 2004). Several more genes identified in (Fig. 4.7) have also been linked to cell expansion, including *CELLULASE 1* (*CEL1*) (Shani et al., 2006), *ALPHA-XYLOSIDASE 1* (*XYL1*) (Shigeyama et al., 2016) and *PHOSPHATIDYLINOSITOL- 4-PHOSPHATE 5-KINASE 5* (*PIPK5*) (Ischebeck et al., 2008).

Considering these results together provides genetic evidence to support the phenotypic evidence presented in Chapter 3 a role of CLF in photomorphogenesis. The process of shade avoidance in seedlings also involves a distinct elongation of hypocotyls, similarly to etiolation (hypocotyl elongation in darkness is driven by cell elongation (Gendreau et al., 1997), a process which involves reorganisation of the cell wall. As such, the identification of genes involved with these processes which show downregulation upon light perception in a *CLF*-dependent manner reinforces the hypothesis that CLF activity forms part of the light-induced repression of hypocotyl elongation that is characteristic of photomorphogenesis.

4.2.3.2 Auxin and Brassinosteroid signalling are enriched among Col0-specific downregulated genes

Another key result from analysis of light-downregulated genes is that there are various processes relating to plant hormone signalling enriched among Col0-specific downregulated genes. These processes include “Response to Auxin” and three categories relating to Brassinosteroid signalling: “Response to Brassinosteroid”; “Cellular Response to Brassinosteroid Signalling” and “Brassinosteroid mediated signalling pathway” (Fig. 4.5 A). Several more processes related to hormones and steroid hormones are also enriched in this geneset. All of these processes are absent from the results for *clf29*-specific downregulated genes (Fig. 4.5 B). This is an intriguing set of results. As discussed in Chapter 1, both of these hormones are known to be crucial in regulating cell and hypocotyl elongation in *Arabidopsis*, collaborating along with the PIF transcription factor in the in the BAP (Brassinosteroids-Auxin-PIFs) regulatory module (Bouré et al., 2019).

The enrichment of these categories shown in (Fig. 4.5 A) represent 11 genes in the category “Response to Auxin” and 6 genes under the category “Response to Brassinosteroids”, which are shown along with their Log(2)Fold changes between dark and light in Col0 in (Fig. 4.8) and (Fig. 4.9) respectively. The categories “Cellular Response to Brassinosteroid Signalling” and “Brassinosteroid Mediated Signalling Pathway” were found to also represent the same 6 genes as “Response to Brassinosteroids” (Fig. 4.9). This was not surprising, as categories in Gene Ontology analysis are known to display redundancy and overlap (Zeeberg et al., 2011).

Gene	AtID	Log(2)FC Dark-Light in Col0 (If p < 0.05)
GH3.5/WES1	AT4G27260	-1.87
IAA6	AT1G52830	-7.38
SAUR25	AT4G13790	-6.50
IAA13	AT2G33310	-1.33
TTL3	AT2G42580	-1.33
HAT2	AT5G47370	-2.68
IAA2	AT3G23030	-1.41
IAA4	AT5G43700	-1.01
XTH19	AT4G30290	-3.09
IAA17	AT1G04250	-1.16
IAA1	AT4G14560	-3.66

Fig 4.8 Auxin response genes showing light-induced downregulation only in Col0

11 genes identified by Gene Ontology Analysis of Col0-specific downregulated genes under the category “Response to Auxin”, along with their Log(2)FC in Col0.

Gene	AtID	Log(2)FC Dark-Light in Col0 (If $p < 0.05$)
BRI1	AT4G39400	-1.06
BRH1	AT3G61460	-1.57
IBL1	AT4G30410	-2.06
TTL3	AT2G42580	-1.33
BSK8	AT5G41260	-2.16
BSK5	AT5G59010	-1.49

Fig 4.9 Brassinosteroid response genes light-induced downregulation only in Col0

6 genes identified by Gene Ontology Analysis of Col0-specific downregulated genes under the category “Response to Brassinosteroids”, along with their Log(2)FC in Col0.

The categories “Cellular Response to Brassinosteroid Signalling” and “Brassinosteroid mediated signalling pathway” contained the same genes.

Examining the genes in these categories showing *CLF*-dependent downregulation presented some intriguing results. Auxin signalling is known to promote cell elongation and, correspondingly, hypocotyl elongation (reviewed in Majda and Robert, 2018). As such, given the evidence presented so far for CLF's involvement in repressing hypocotyl elongation, it was initially expected that *CLF* loss would result in a defect to this light-induced repression of auxin signalling. Several of the identified genes do follow this pattern, notably *SAUR25*, part of a family of *SAUR* genes which have been shown to be induced by auxin, and linked to cell wall expansion (Spartz et al., 2012). Increased expression of each of *HAT2* (Sawa et al., 2002), *XTH19* (Miedes et al., 2013) and *TTL3* (Amorim-Silva et al., 2019) has also been shown to promote hypocotoyl elongation.

A similar pattern was found with Brassinosteroid signalling genes shown in (Fig. 4.9). Again, as discussed in Chapter 1.1, Brassinosteroid signalling has been identified as a key factor in promoting hypocotyl elongation in darkness, often acting synergistically with auxin signalling (Nemhauser et al., 2004). Several genes represented in (Fig. 4.9) represent crucial components of the brassinosteroid signalling pathway, in particular *BRI1*. BRI1 is receptor for brassinosteroids located in the cell membrane, and loss of this receptor results in dwarf plants which are insensitive to brassinosteroids (Clouse et al., 1996). There are also two brassinosteroid signaling kinase (BSK) genes, *BSK5* and *BSK8*, which are part of a group of kinases known to redundantly promote brassinosteroid signalling, including the elongation of hypocotyls (Sreeramulu et al., 2013).

Taken together, these data provide evidence for a role of CLF in repressing some auxin and brassinosteroid signalling genes during photomorphogenesis. Given the crucial roles these signalling pathways play in hypocotyl elongation, this offers further insight into how CLF may act in this process, via transcriptional repression of various target genes after light perception.

However, some of the other genes in this category show behaviour that is more complicated to explain.

Firstly was the presence of *GH3.5* (also known as *WES1*) in this geneset (Fig. 4.6). *WES1* is part of a family of genes involved in repressing hypocotyl growth, and a *wes1* loss of function line has been observed to show elongated hypocotyls after growth in the light, whilst a *wes1-D* overexpression line had reduced hypocotyl length (Park et al., 2007). Meanwhile, among brassinosteroid signalling genes, the *CLF*-dependent downregulation of *BRH1* was surprising, as *BRH1* is known to be repressed by brassinosteroid signalling (Molnár et al., 2002). *IBH1*, meanwhile, has been shown to antagonize brassinosteroid-mediated cell elongation, possibly by repressing the activity of PIF4 (Zhiponova et al., 2014).

The presence of several *AUX*/*IAA* genes among Col0-specific downregulated genes, including *IAA1*, *IAA2*, *IAA6*, *IAA13* and *IAA17* also initially appears contradictory. As discussed in Chapter 1, *AUX*/*IAA* genes are canonically known as antagonists of auxin signalling, and ubiquitination and degradation of these factors to facilitate de-repression of auxin-responsive genes is a major part of auxin signal transduction (Tan et al., 2007). Considering this, and the fact that auxin promotes hypocotyl elongation, it might initially be expected that the activity of *AUX*/*IAA* genes would be enhanced in a *CLF*-dependent manner, rather than repressed, as part of a light-mediated repression of auxin signalling, to facilitate inhibition of hypocotyl elongation.

Some of these observations are difficult to reconcile with the phenotypic data from Chapter 3 and genetic data presented here that *CLF* inhibits hypocotyl elongation, possibly by contributing to light-induced repression of auxin and brassinosteroid signalling. However, previous observations in the literature can offer more context for

some of these apparently contradictory results, and suggest that this may actually be consistent with what is known about light and hormone signalling.

In particular, whilst *AUX*/*IAA* genes are repressors of auxin signalling, they are actually transcriptionally induced by auxin, whilst their repression by auxin takes place at the protein level via ubiquitination (Abel et al., 1994). A number of GH3 genes, including *WES1* are also transcriptionally induced by auxin (Hagen et al., 1984), (Park et al., 2007), which may represent a negative feedback loop regulating auxin signalling (Liscum et al., 2016). This means it could be that the lack of light-induced downregulation of these genes in a *clf29* mutant could be the result of a lack of repression of auxin-signalling in this plant line, which would be consistent with the elongated hypocotyl phenotype shown in this thesis. Notably, the expression of several *AUX*/*IAA* genes, as well as *WES1*, has been shown to be *decreased* in light-grown seedlings compared with dark-grown counterparts (Iglesias et al., 2018). This correlation with previous observations in the literature gives confidence in the data presented here, and reinforces the hypothesis that this may be due to *CLF*-dependent repression of auxin signalling leading to a lower expression level of auxin-induced genes such as *AUX*/*IAA* and *GH3* genes.

In order to verify and give confidence in the RNA seq analysis, four genes were selected for qPCR analysis. Two Aux/*IAA* genes (*IAA1* and *IAA6*) and the brassinosteroid-signaling gene *BRH1* were all identified in the RNA seq as showing light-induced downregulation in a Col0 plant (Log(2)FC<-1, p<0.05), but not in a *clf29* plant (Fig. 4.8-9, full lists of DEGs shown in appendix 2). qPCR analysis of all three gene loci, normalised against the reference gene *PP2AA3* found similar results. All three genes display genes showing statistically significant downregulation in Col0, with at least a 50% reduction in expression after light exposure (representing a log(2) fold change of less than -1) but not in a *clf29* plant (Fig. 4.10 A-C). Notably, this seems clearer for IAA1, which appears to have

drastically reduced/absent downregulation in a *clf29* plant line, whilst for *IAA6*, high variance between bioreps prevents the identification of statistically significant changes. Meanwhile, *BRH1* displays significant downregulation in both plant lines, but the extent of light-induced downregulation is substantially reduced in a *clf29* plant line such that there is not a 50% reduction in expression, meaning it no longer meets the threshold for inclusion in the lists of DEGs presented here (Log(2) Fold Change of less than -1). Finally a fourth gene, *GAST1 PROTEIN HOMOLOG 4* (*GASA4*), was also analysed by qPCR (Fig. 4.10 D). Unlike the first three genes, *GASA4* was identified in the lists of DEGs showing light-induced downregulation for both Col0 and *clf29*. *GASA4* was identified as displaying a Log(2)FC of -3.36 in Col0 and -2.18 in *clf29* after light exposure (Full lists of Log(2) fold changes for all DEGs provided in Appendix 2), indicating that it displays light-induced downregulation ($p<0.05$, $\log(2)FC < -1$) in both plant lines, but the extent of downregulation was reduced in a *clf29* plant line. qPCR analysis found a similar result, with both genes showing light-induced downregulation, but the extent of downregulation is reduced in a *clf29* plant line (Fig. 4.10 D).

The qPCR validation gives confidence in the RNA Seq data presented here. Three genes have been identified as showing light induced downregulation ($p<0.05$, $Log(2)FC < -1$) in Col0 but not in *clf29* in the RNA seq analysis (*IAA1*, *IAA6* and *BRH1*) and in qPCR analysis (Fig. 4. 10 A-C). Meanwhile a fourth gene (*GASA4*) has been identified in as showing light induced downregulation ($p<0.05$, $Log(2)FC < -1$) in both plant lines, but at a reduced in extent in a *clf29* plant line (Fig. 4.10 D).

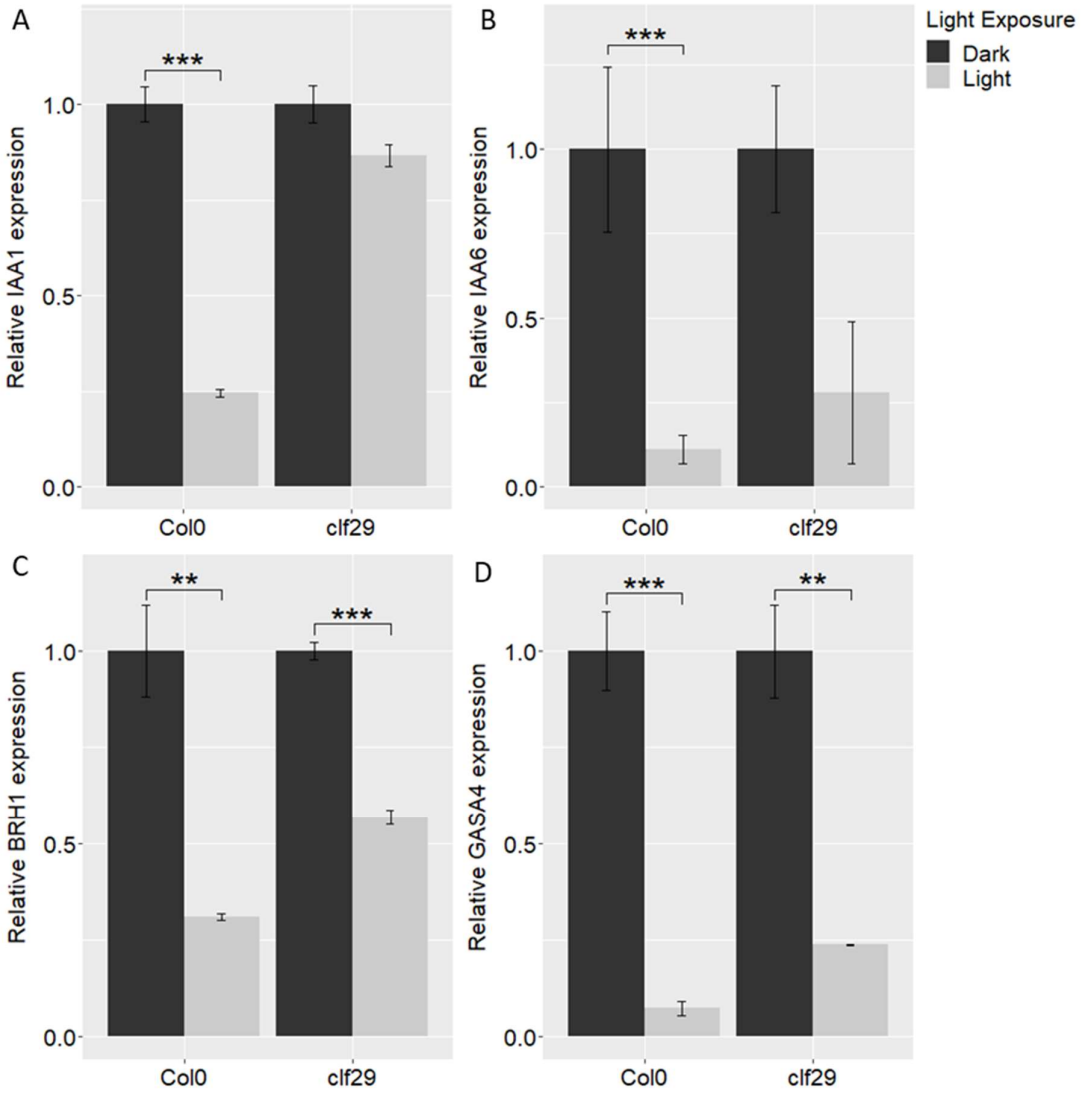

Fig 4.10 qPCR Analysis of candidate genes to confirm RNA seq analysis in Col0 and *clf29* seedlings

qPCR analysis of *IAA1* (A), *IAA6* (B), *BRH1* (C) and *GASA4* (D) in dark-grown Col0 and *clf29* seedlings before (Dark) and after (Light) exposure to 6 hours white light (40μMol m^{-2} s^{-1}).
Data normalised against the reference gene PP2AA3, expression in the dark set to 1. Error bars show the standard error of the mean (SEM) of three biological replicates. Asterisks indicate statistical significance as determined by independent samples T Tests (** = $p<0.01$), (*** = $p<0.001$).

4.3 Analysis of transcriptional misregulation in photoreceptor mutants after light perception, and how this is correlates with CLF activity

4.3.1 Generation of lists of differentially expressed genes between Col0 and photoreceptor mutants

After analysing the effect of CLF on light induced transcriptional changes, the next objective was to analyse whether CLF-mediated transcriptional changes displayed correlation with that controlled by photoreceptors. As previously discussed, photoreceptors CRY1, CRY2, PHYA and PHYB are all inactive in the dark, and mutants lacking these factors show no phenotypic differences in dark-grown seedlings, and so the dark-state transcriptome in photoreceptor mutants was considered unimportant for this analysis (Neff and Chory, 1998), (Yu et al., 2010), (Wang et al., 2014), (Ma et al., 2016). Instead, the transcriptome of each photoreceptor mutant after light 6 hours light exposure was analysed, to be compared to the Col0 transcriptome after the same exposure, and analyse differentially expressed genes.

The first step in this analysis was to compare the transcriptomes of Col0 after light exposure with the photoreceptor mutants *phyA*, *phyB*, *cry1* and *cry2*. As before, an initial analysis was done on these samples using the Principal Components Analysis function in Deseq2 (Love et al., 2014), which is shown in (Fig. 4.11). For this analysis, the transcriptome of *clf29* after light exposure was also included. Considering that in Chapter 3 it was shown that *clf29* displays elongated hypocotyls indicating deficiency in the light response, it was hypothesised that the *clf29* transcriptome after light perception may be more similar to photoreceptor mutants than to Col0, which are also deficient in the light response.

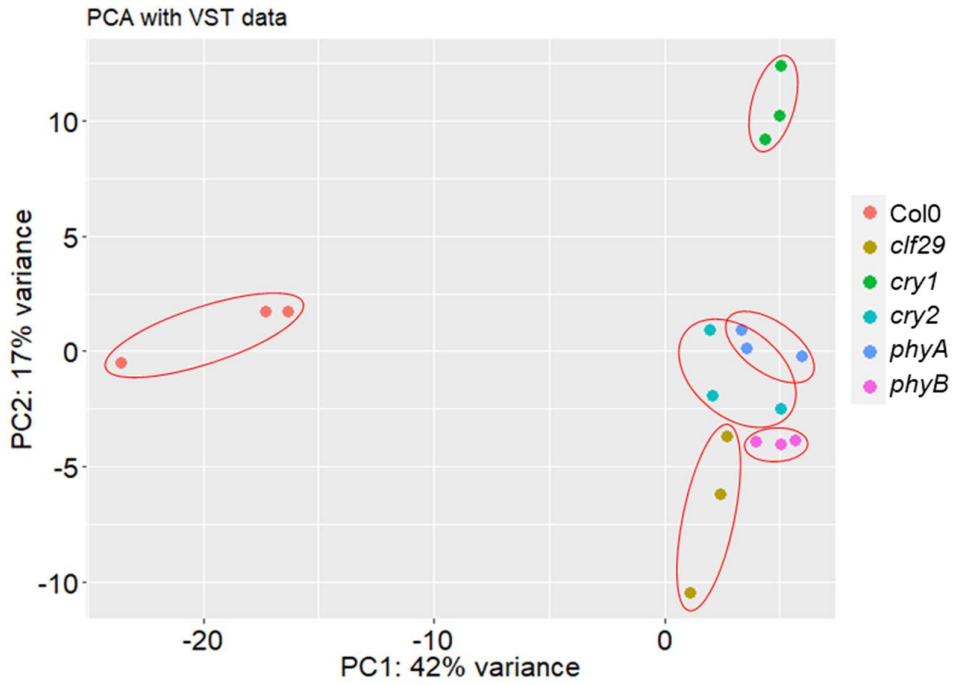

Fig 4.11 Principal component analysis of Col0, *clf29* and photoreceptor mutants after 6 hours white light exposure

Principal Components analysis (PCA) plot visualising sample distances between Col0, *clf29* and photoreceptor mutants after 6 hours white light exposure (40µMol m^{-2} s^{-1}). PCA performed on variance stabilised (vst) transformed data using the R software package DEseq2 (Love et al., 2014).

The principal component analysis shows that, as expected, the transcriptomes of photoreceptor mutants are distinctly different from that of Col0 (Fig. 4.11). Additionally, the transcriptome of *clf29* plants is also distinctly different, and appears much more similar to that of the photoreceptor mutants than to Col0. This provides further genetic evidence that *clf29* plants are deficient in photomorphogenesis.

Lists of differentially expressed genes ($p<0.05$) were then generated for each of *cry1*, *cry2*, *phyA* and *phyB*, compared to Col0, to establish the effect of loss of the major photoreceptors on the transcriptome after light perception. As before, a threshold of Log(2) Fold Change of 1 was applied to upregulated genes, representing an actual fold change of 2, a two-fold increase in expression. For downregulated genes, a threshold of Log(2) Fold Change of -1 was applied, representing an actual fold change of 0.5, a two-fold decrease in expression. The genes showing differential expression after light perception in photoreceptor mutants could then be analysed in comparison with the transcriptional behaviour of Col0 and *clf29* seedlings during light perception, discussed in Chapter 4.2.

The results of this analysis are shown in (Fig. 4.12). Notably, in all photoreceptor mutants, a larger number of genes exhibited downregulation compared to Col0 than upregulation. This supports our previous observation that more genes are upregulated in response to light than downregulated in Col0 (Ma et al., 2001), (Jiao et al., 2005) (Fig. 4.2). If the majority of these light-induced transcriptional changes are dependent on the actions of phytochromes and cryptochromes, it would be expected to see more downregulated genes in these mutants. Out of the plants analysed, *phyB* had the largest numbers of genes both upregulated and downregulated, followed by *cry1* (Fig. 4.4)

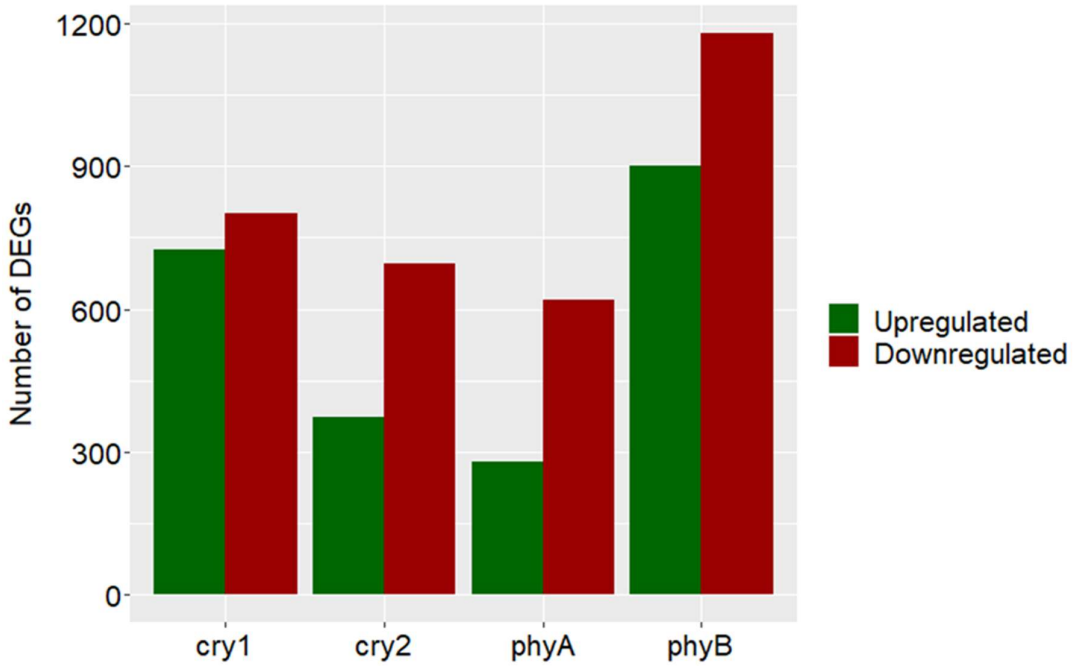

Fig 4.12 Number of DEGs in light-treated photoreceptor mutants compared to Col0. Number of genes showing higher expression ($p<0.05$, Log(2) FC ≥1) or or lower expression ($p<0.05$, Log(2) FC ≤- 1) in dark-grown *clf*, *cry1*, *cry2*, *phyA* and *phyB* mutants exposed to 6 hours white light (40μMol m_{-2} s_{-1}), compared to Col0.

In order to analyse the correlation between CLF-mediated and photoreceptor-mediated transcriptional during the light response, these lists of DEGs were compared to the transcriptional changes in Col0 and *clf29* upon light perception described earlier. The list of Col0-specific and *clf29*-specific downregulated genes were compared with genes showing upregulation in photoreceptor mutants and vice versa. This was done as it was hypothesised that if for example a gene is downregulated in the light in a *CLF*-dependent manner, and this also requires a given photoreceptor, it would be likely to show higher expression in that photoreceptor mutant compared to Col0 after light perception.

The results of this analysis are shown in (Fig. 4.13) for light-upregulated genes (compared to downregulated genes in the photoreceptor mutants) and in (Fig. 4.14) for light-downregulated genes (compared to upregulated genes in the photoreceptor mutants).

Examining the light-downregulated genes (Fig. 4.13), it is notable that genes showing higher expression in all photoreceptors have distinctly more overlap with light-induced downregulation occurring only in Col0 plants than with downregulation occurring only in *clf29* plants. This shows that *CLF* is involved in the downregulation upon light perception of a number of genes also repressed by photoreceptors, providing further genetic evidence that CLF is involved in the photomorphogenesis response.

Another notable feature is that this overlap is largest for *cry1*, with 92 genes showing *CLF*-dependent upregulation upon light perception, and lower expression in a *cry1* plant (Fig. 4.13 B). This is in spite of the fact that *phyB* plants had the highest number of genes with lower expression (Fig. 4. 12), suggesting that a greater correlation between CRY1 and CLF-mediated transcriptional regulation during the light response.

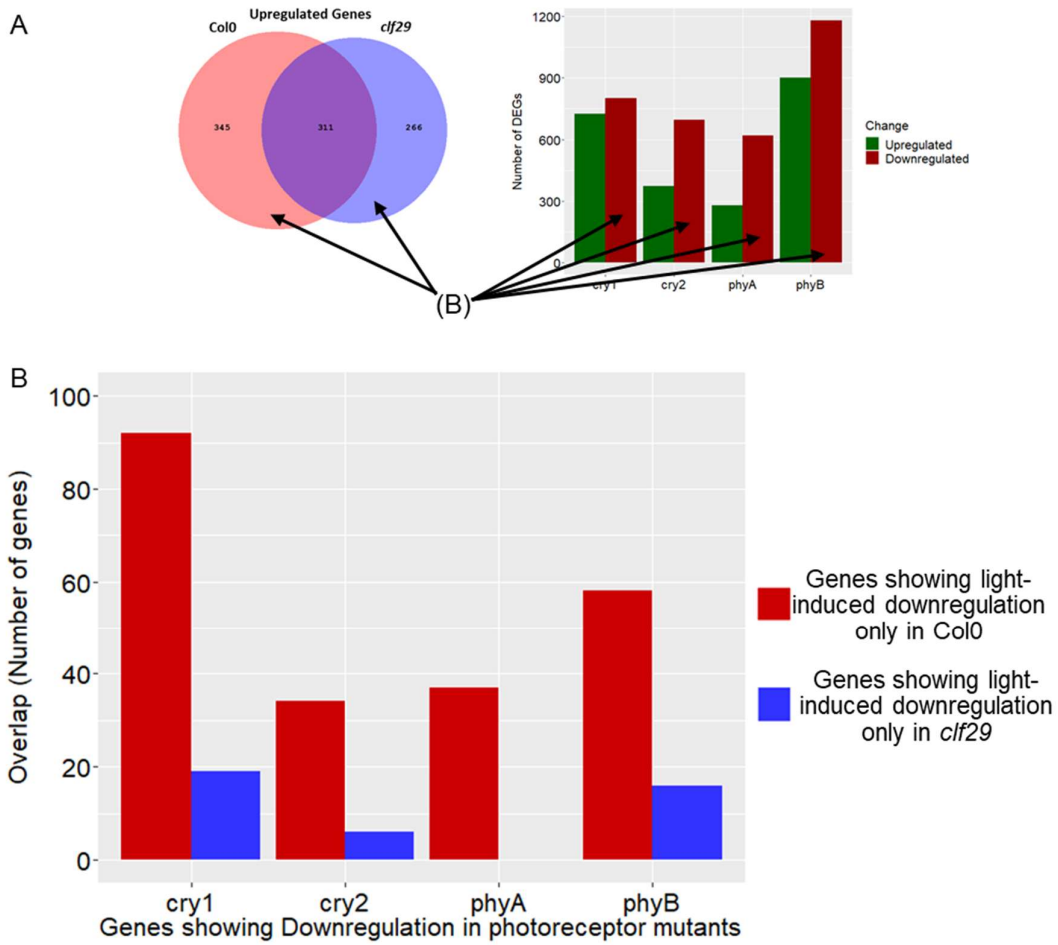

Fig 4.13 Overlap between genes showing upregulation upon light perception in Col0 or *clf29* background, and genes showing lower expression in photoreceptor mutants after light perception
A) Visual representation of the genesets being compared in this analysis.
B) Overlap between genes showing light induced transcriptional upregulation in Col0 and *clf29* and genes showing lower expression in photoreceptor mutants after light perception.

Assessing the results for genes showing light-induced transcriptional repression shows a similar pattern. Genes showing higher expression in each of the photoreceptor mutants show higher overlap with genes showing light-induced downregulation in only Col0, than those showing light-induced repression only in *clf29* (Fig. 4.14). However in this instance, the difference is not as pronounced for most photoreceptor mutants, particularly in a *cry2* mutant. However, once again higher expression in a *cry1* plant line after light perception shows strikingly higher overlap with genes downregulated only in a Col0 plant,

with 56 genes showing light-induced downregulation only in Col0 and higher expression after light perception in a *cry1* line (Fig 4. 14). This is compared to only 7 genes showing light-induced downregulation only in a *clf29* plant line and higher expression in a *cry1* line after 6 hours light (Fig. 4.14).

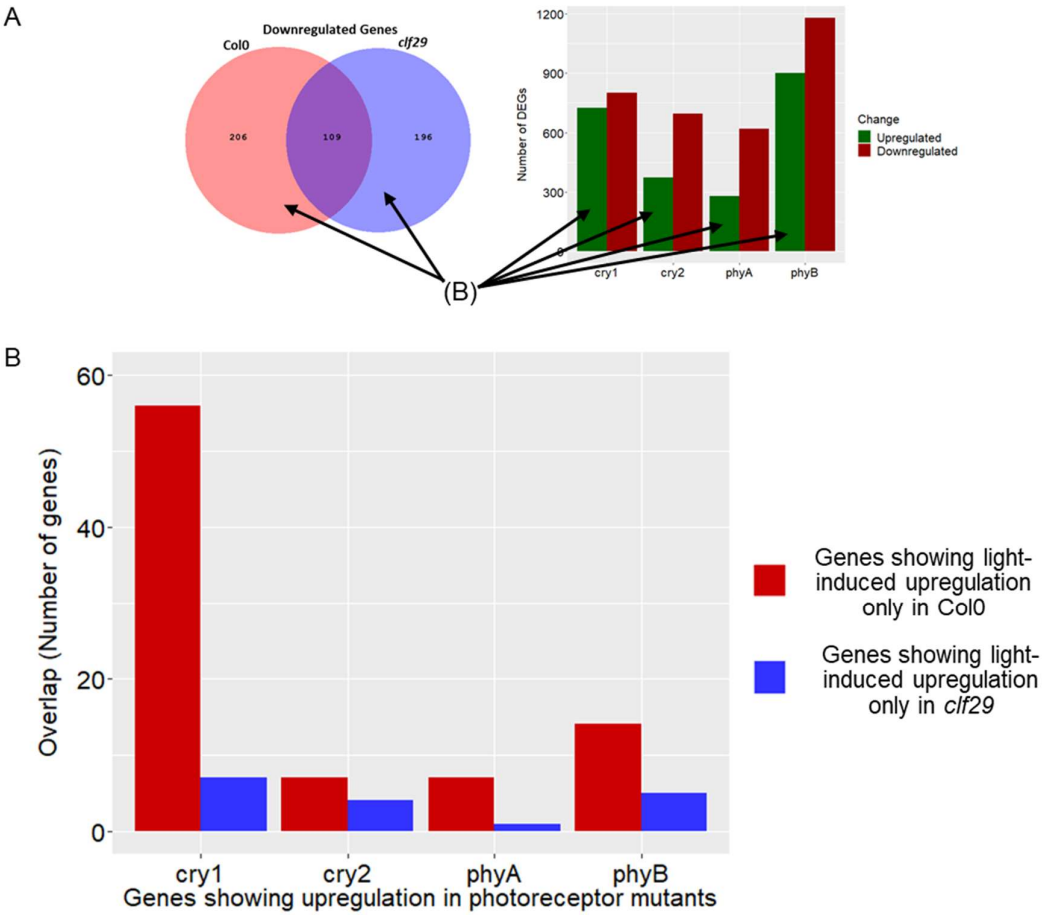

Fig 4.14 Overlap between genes showing downregulation upon light perception in Col0 or *clf29* background, and genes showing higher expression in photoreceptor mutants after light perception.
A) Visual representation of the genesets being compared in this analysis.
B) Overlap between genes showing light induced transcriptional downregulation in Col0 and *clf29* and genes showing higher expression in photoreceptor mutants after light perception.

These observations show that there is substantial overlap between *CLF*-dependent transcriptional regulation and *CRY1*-dependent transcriptional regulation upon light perception. This is notable considering the findings presented in Chapter 3 that *CLF* loss has no phenotypic impact in a *cry1* genetic background, and that *CRY1* is required for light-induced transcriptional upregulation of *CLF*. The data presented in (Fig. 4.13) and (Fig. 4.14) provide strong genetic evidence to reinforce the hypothesis proposed in Chapter 3 that CLF acts together with CRY1 during the light response.

4.3.2 Generation of lists of differentially expressed genes in *clf29* plants in various genetic backgrounds after light perception

The data presented in the previous section suggest that CRY1-mediated transcriptional regulation after light perception has the greatest correlation with CLF-mediated transcriptional changes upon light perception among the photoreceptors. This correlates with genetic evidence presented in Chapter 3 that found CRY1 was required for light-induced transcriptional upregulation of *CLF* (Fig. 3.11).

The final analysis that was undertaken via RNA-seq was to investigate the effect of *clf29* mutation on the transcriptome post-light-exposure in Col0 and photoreceptor mutants. In Chapter 3, it was found that *clf29* has no effect on hypocotyl lengths in a *cry1* genetic background under white and blue light. RNA-seq analysis was used to investigate whether a similar pattern was seen with regards to transcriptional changes, by analysing the effect of *clf29* mutation on the transcriptome post-light exposure in genetic backgrounds lacking photoreceptors. Given the findings in chapter 3 and the observation that the transcriptome of *clf29* after light exposure more closely resembles photoreceptor

mutants than Col0 (Fig. 4. 11), it was hypothesised that *clf29* mutation would have less effect in genetic backgrounds already lacking photoreceptors.

As before, first a Principal Components Analysis was carried out to visualise the distance between a *clf29* mutant and a non-*clf29* plant (WT) in Col0 (WT), *phyA*, *phyB*, *cry1* and *cry2* genetic backgrounds. The results are shown in (Fig. 4. 5). It is apparent that the distance between *clf29* and WT samples are largest in a genetic background not carrying mutations in any photoreceptors (WT Photoreceptor Background). In all photoreceptor mutants (*cry1*, *cry1*, *phyA* and *phyB*), the difference between *clf29* samples and the respective WT samples are less pronounced. This is particularly apparent in a *cry1* background. In fact, in the *cry1* background (yellow colour on the PCA), the difference between the three bioreps within each group (*clf29* and WT) appear more pronounced than the differences between these groupings, indicating that the *cry1* and *cry1clf29* transcriptome post light-exposure are very similar. This fits with the observations in Chapter 3 that under white light there is no phenotypic difference between *cry1* and a *cry1clf29* double mutant, as well as observations in Chapter 4.3.1 that *CRY1*-mediated transcriptional regulation shows substantial overlap with *CLF*-mediated transcriptional changes during the light response.

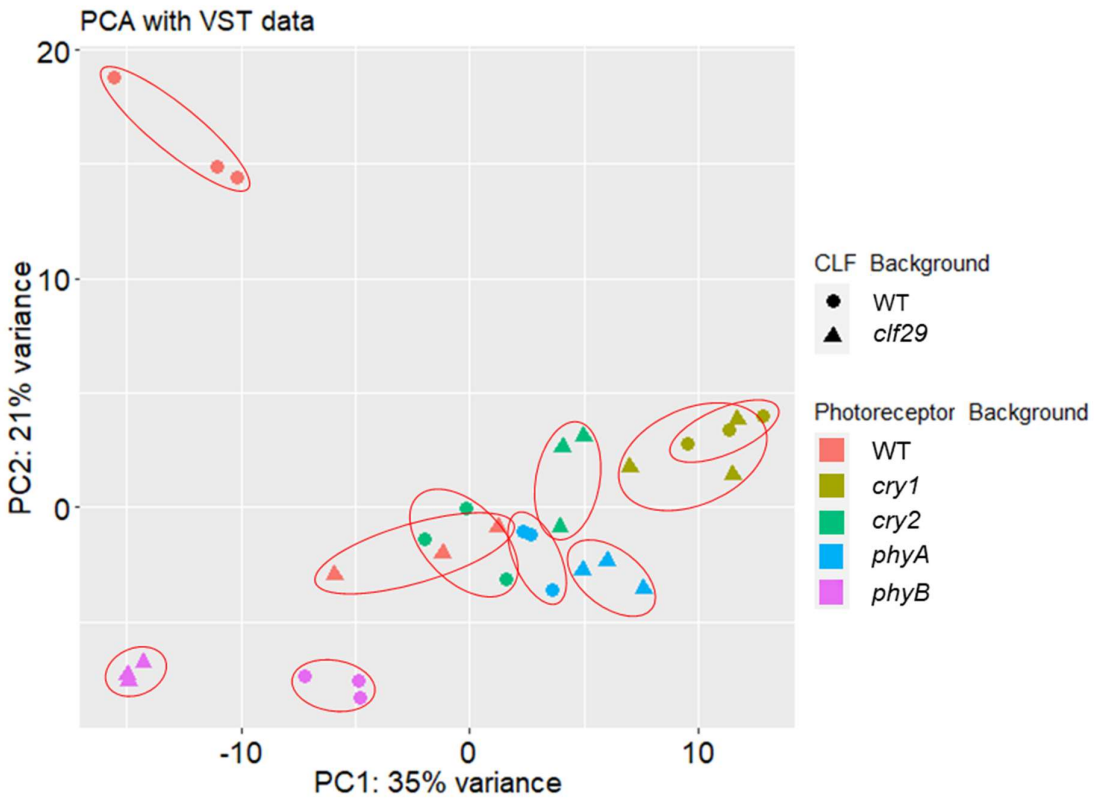

Fig 4.15 Principal Component Analysis of clf29 and *CLF*+ plants in Col0 and photoreceptor mutants after 6 hours light exposure

Principal Components analysis (PCA) plot visualising sample distances between photoreceptor mutants and double mutants also carrying a *clf29* loss of function mutation. PCA performed on variance stabilised (vst) transformed data using the R software package DEseq2 (Love et al., 2014). Shape indicates whether the plant carries a *clf29* loss of function mutation (*clf29*) or not (WT). Colour indicates whether the plant is Wild type for all four photoreceptors (WT) or a photoreceptor mutant.

Lists of upregulated ($p<0.05$, $Log_2FC \geq 1$) and downregulated ($p<0.05$, $Log_2FC \leq -1$) genes for each of these backgrounds were then generated (Fig. 4.6 – Full lists of DEGs contained in Appendix 2). In each case, the results indicate the number of transcriptional changes in a *clf29* mutant, compared to the WT plant for that genetic background (i.e. the *cry1 clf29* results indicate the number of DEGs in a *cry1clf29* double mutant compared to a *cry1* mutant, whilst the *clf29* results indicated the number of DEGs in a *clf29* mutant compared to a Col0 plant).

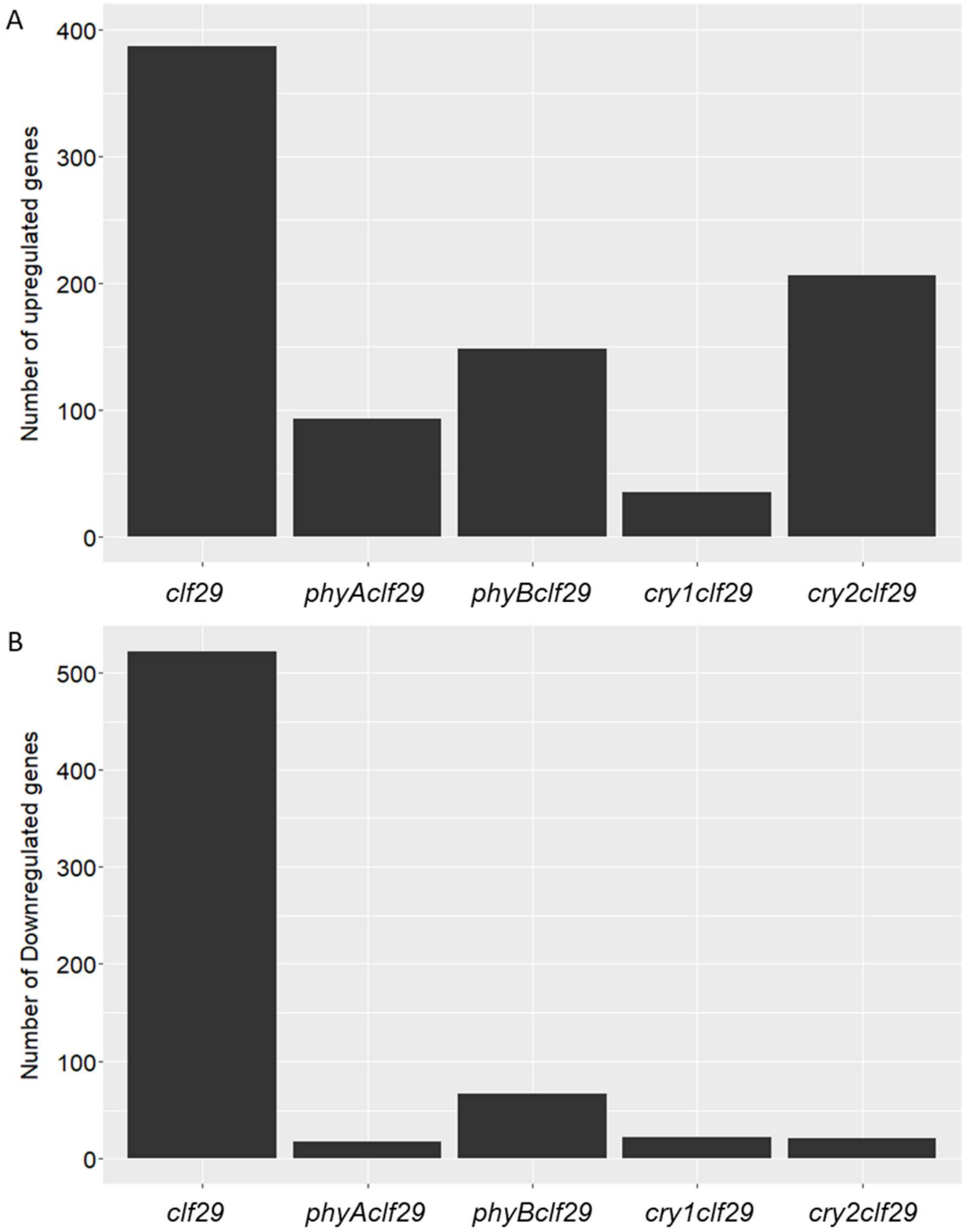

Fig 4.16 – Number of differentially expressed genes in *clf29* plants in various genetic backgrounds, compared to *CLF+* plants.

Number of genes showing significant upregulation (A), ($p<0.05$, Log(2) FC >1) or downregulation (B), ($p<0.05$, Log(2) FC < -1) in various plant lines carrying *clf29* loss-of-function mutations, compared to plants with WT *CLF* gene.

In all cases the number of DEGs in a *clf29* background is substantially reduced in genetic backgrounds containing mutations in any of the photoreceptors tested (Fig. 4. 16). This effect is particularly apparent among downregulated genes (Fig. 4.15 B) with less than 50 downregulated genes in the *phyAclf29*, *cry1clf29* and *cry2clf29* background. Among upregulated genes the effect is most notable in a *cry1* background, with only 35 genes showing upregulation in a *cry1clf29* double mutant compared to a *cry1* single mutant (Fig. 4. 16 A). This shows that in a *cry1* mutant background, a *clf29* mutation has very little effect on the transcriptome, which is consistent with the lack of a phenotype as shown in Chapter 3. This adds further genetic evidence to support the hypothesis of a requirement for CRY1 in CLF-mediated effects on photomorphogenesis.

To verify the data seen here, the genes *IAA1* and *GASA4* were analysed via qPCR. As seen in Chapter 4.2.3.2, this gene shows light-induced downregulation in a Col0 plant, but not in a *clf29* plant (Fig. 4.10 A), whilst *GASA4* displays light-induced downregulation in both plant lines, but to a reduced extent in a *clf29* plant line (Fig. 4.10 D). RNA-seq analysis using DESeq2 (Love et al., 2014) indicated that the *IAA1* gene showed higher expression in *phyA*, *phyB*, *cry1* and *cry2* plants after exposure to 6 hours light, compared to Col0 (Fig. 4.17 A). This finding was verified by RT-qPCR analysis, with all four photoreceptor mutants showing higher expression of *IAA1* after light exposure than Col0 (Fig 4. 17 C). *GASA4*, meanwhile, displayed higher expression in a *phyA*, *cry1* and *cry2* plant line, compared to Col0, but not in a *phyB* plant line (Fig. 4.17 B). Again, this was verified by qPCR, with *phyA*, *cry1* and *cry2* showing higher expression of *GASA4* compared to Col0, but not *phyB* (Fig. 4. 17 D). The validation of two candidate genes showing similar results in qPCR analysis to that identified in the RNA seq gives confidence in the RNA-seq analysis presented here.

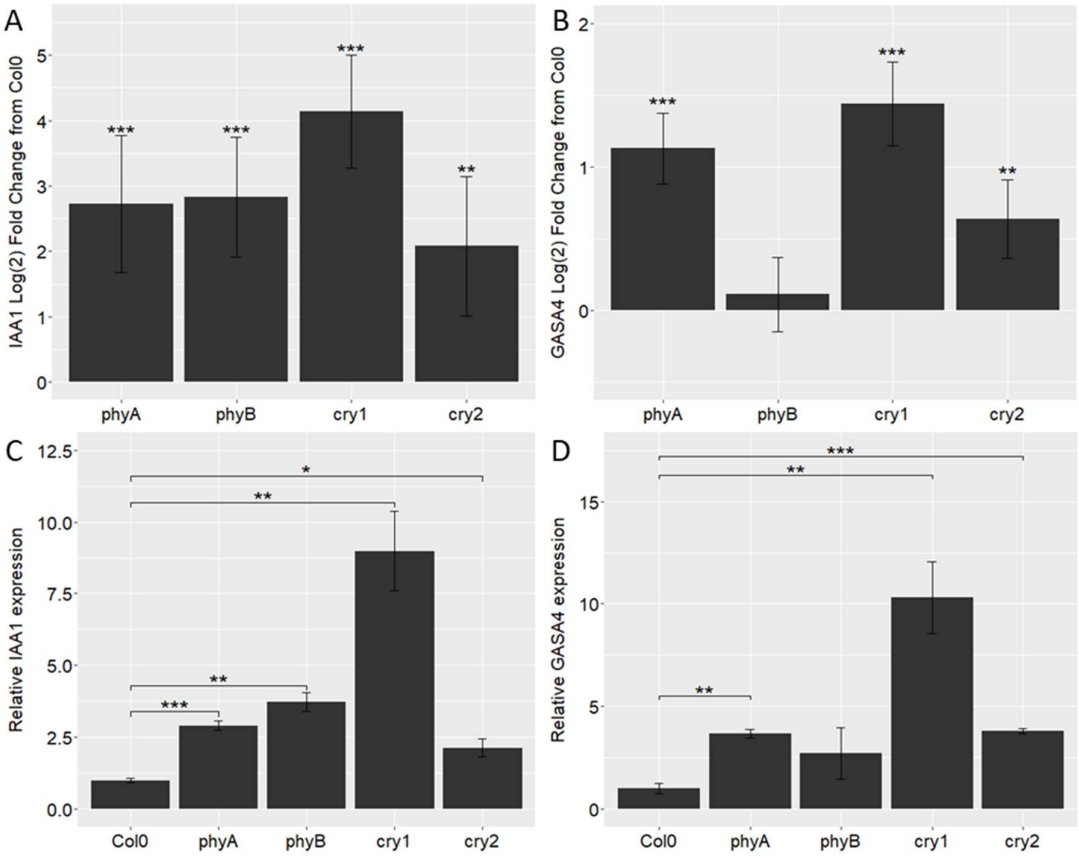

Fig 4.17 Analysis of candidate genes *IAA1* and *GASA4* in seedlings carrying mutations in phytochromes or cryptochromes.

A) Log(2)FC of *IAA1* in dark-grown *phyA*, *phyB*, *cry1* and *cry2* seedlings after exposure to 6 hours white light (40μMol m^{-2} s^{-1}), compared to Col0, as identified by Deseq2 (Love et al., 2014).
B) Log(2)FC of *GASA4* in dark-grown *phyA*, *phyB*, *cry1* and *cry2* seedlings after exposure to 6 hours white light (40μMol m^{-2} s^{-1}), compared to Col0, as identified by Deseq2 (Love et al., 2014).
C) qPCR analysis of *IAA1* in dark-grown Col0, *phyA*, *phyB*, *cry1* and *cry2* seedlings exposed to 6 hours white light (40μMol m^{-2} s^{-1}). Col0 expression set to 1.
D) qPCR analysis of *GASA4* in dark-grown Col0, *phyA*, *phyB*, *cry1* and *cry2* seedlings exposed to 6 hours white light (40μMol m^{-2} s^{-1}). Col0 expression set to 1.

Error bars indicate standard error of the mean for 3 biological replicates. Asterisks indicate statistically significant differences from Col0, as determined by Deseq2 (A), (B) or Independent samples T-Tests (C), (D).

qPCR analysis was also used to analyse the behaviour of these two genes in *clf29* plants in varying genetic backgrounds. RNA-seq analysis indicated that both *IAA1* and *GASA4* showed significantly higher expression in a *clf29* plant compared to Col0 after 6 hours light exposure (Fig. 4. 18 A-B), but that this was not true in any of the double mutants carrying a *clf29* mutation along with loss of a photoreceptor, compared to the single mutant with WT *CLF* gene (Fig. 4.18 A-B). qPCR analysis of these double mutants mostly corroborated these results with *clf29*-photoreceptor double mutants not displaying higher expression of either gene, compared to the same photoreceptor mutant not carrying the *clf29* mutation (Fig. 4.18 C-D). The only discrepancy was that a *phyBclf29* double mutant compared to a *phyB* single mutant showed significantly lower expression of *IAA1*, which was not detected by the RNA-seq analysis (Fig. 4. 18 C)

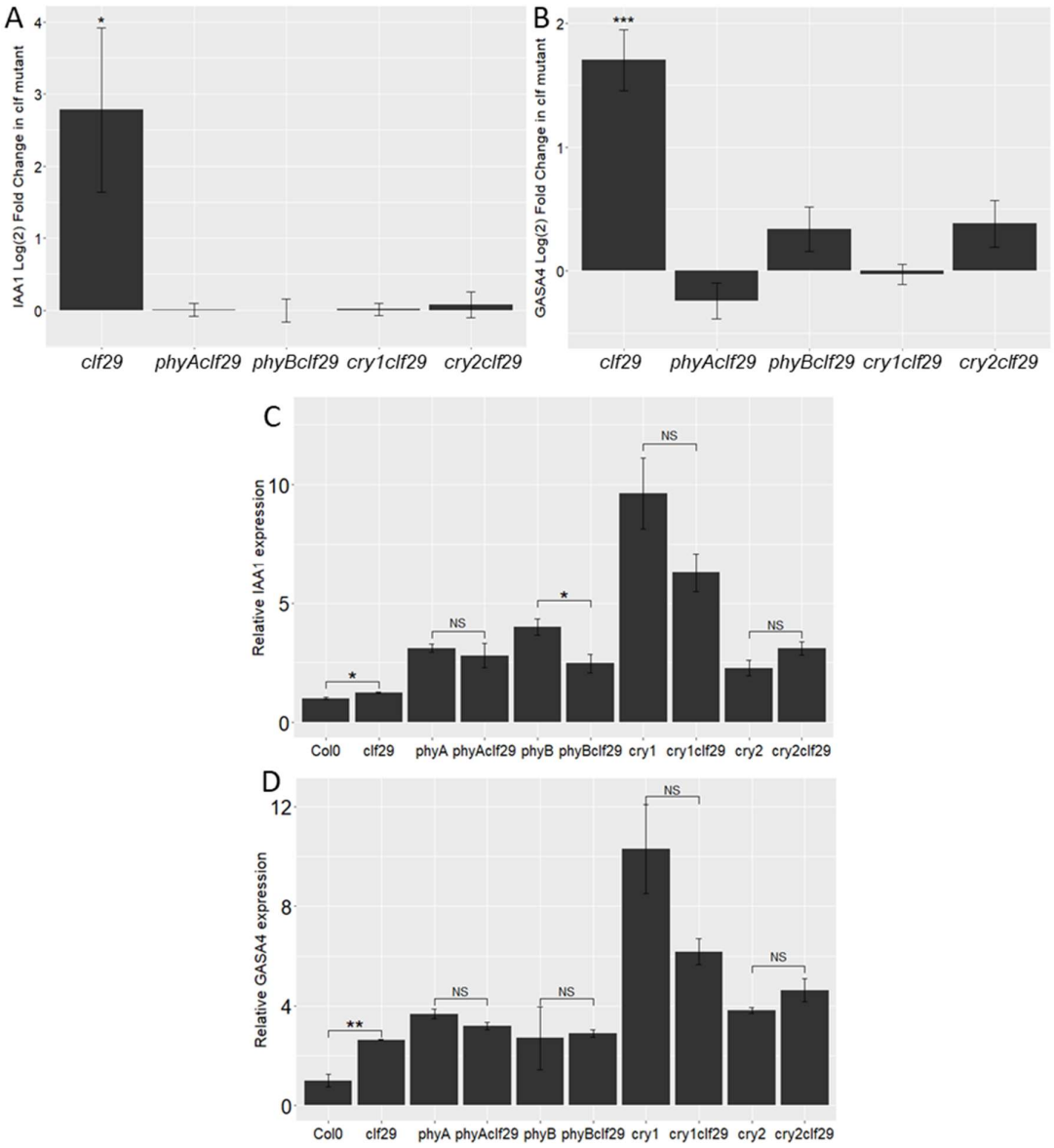

Fig 4.18 Analysis of the effects of *clf29* mutation on *IAA1* and *GASA4* expression in different genetic backgrounds.

A) Log(2)FC of *IAA1* in dark-grown *clf29*, *phyAclf29*, *phyBclf29*, *cry1clf29* and *cryclf29* seedlings after exposure to 6 hours white light (40μMol m-2 s-1), compared to a plant carrying WT *CLF*, as identified by Deseq2 (Love et al., 2014)
B) Log(2)FC of *GASA4* in dark-grown *clf29*, *phyAclf29*, *phyBclf29*, *cry1clf29* and *cryclf29* seedlings after exposure to 6 hours white light (40μMol m-2 s-1), compared to a plant carrying WT *CLF*, as identified by Deseq2 (Love et al., 2014).
C) qPCR analysis of *IAA1* in dark-grown seedlings exposed to 6 hours white light (40μMol m-2 s-1). Col0 expression set to 1.
D) qPCR analysis of *GASA4* in dark-grown seedlings exposed to 6 hours white light (40μMol m-2 s-1). Col0 expression set to 1.
Error bars indicate standard error of the mean for 3 biological replicates. Asterisks indicate statistically significant differences from Col0, as determined by Deseq2 (A), (B) or Independent samples T-Tests (C), (D).

4.4 Summary

The data presented here provide genetic evidence suggesting a role for CLF during photomorphogenesis. The number of DEGs after light exposure in a *clf29* remains similar (Fig. 4.2), but the number of enriched biological processes among *clf29*-specific DEGs is drastically reduced compared to that seen for Col0 (Fig. 4.3). This suggests that transcriptional changes upon light perception in a *clf29* plant line are more dysregulated, with the targeting of specific biological processes heavily disrupted.

Analysis of the genes showing *CLF*-dependent downregulation offers genetic evidence to further support the hypothesis that CLF is involved in light-induced repression of hypocotyl elongation. The biological processes of shade avoidance and Cell wall organisation/biogenesis were both enriched among Col0-specific downregulated genes (Fig. 4.5), with various genes known to promote hypocotyl elongation or cell expansion showing *CLF*-dependent downregulation.

This analaysis also indicates that CLF activity may occur through regulation of hormone signalling pathways, particularly auxin and Brassinosteroids (Fig. 4.5). A number of genes involved in these two signalling pathways also exhibit *CLF*-dependent downregulation upon light perception. Some of these results are surprising, with negative regulators of both processes identified among these gene-sets. However, some of these negative regulators (such as *AUX*/*IAA* and *GH3* genes) are known to exhibit transcriptional induction by auxin, meaning that this could reflect a reduction light-induced, CLF-dependent reduction of auxin levels, which is abolished in a *clf29* mutant plant.

Further analysis focused on the relationship between *CLF*-regulated transcription and photoreceptor-regulated transcription. First, composition analysis of Col0, *clf29* and photoreceptor mutants shows that *clf29* plants are more similar to photoreceptor

mutants after light perception (Fig. 4. 11). It is particularly shown that genes upregulated in a *cry1* mutant after light exposure show high overlap with genes showing *CLF*-dependent downregulation upon light exposure (Fig. 4.12-13). This adds further evidence to the hypothesis presented in Chapter 3 that *CLF* and *CRY1* activity during photomorphogenesis are linked. This is then reinforced further by analysing the effect of a *clf29* mutation on the transcriptome post light-exposure in genetic backgrounds lacking photoreceptors. *clf29* is found to have a distinctly lessened effect in all photoreceptor mutants (Fig. 4.16). In particular, *clf29* mutation results in very few genes showing upregulation in a *cry1* genetic background (Fig. 4.16 A). Taking these data together, along with the observation in Chapter 3 that *clf29* shows no light-induced upregulation in a *cry1* background (Fig. 3. 11), suggests that CRY1 action is required for light-induced activation of CLF activity.

Overall, considering these data together contributes genetic evidence to support the model presented in Chapter 3. Light is hypothesised to induce CLF activity in a CRY1-dependent manner. CLF then mediates transcriptional regulation which results in the repression of hypocotyl elongation by the repression of various genes involved in cell expansion, as well as modulation of hormone signalling.

Chapter 5 – Further investigations to characterise CLF activity during plant light responses

5.1 Introduction

Data presented in Chapters 3 and 4 indicate a role for CLF in the light response. *clf29* mutant plants exhibit elongated hypocotyls in darkness, and under white light, blue light and far-red light. It is also demonstrated that *CLF* is transcriptionally upregulated upon light perception in a CRY1 and *PHYB*-dependent manner. It is then shown that *clf29* mutation has a distinct effect on the transcriptional response to light, and in particular that light induced downregulation of genes involved in cell expansion and auxin and brassinosteroid signalling are curtailed. Finally, it is shown that genes with higher expression after light perception in a *cry1* mutant line are highly correlated with genes showing *CLF*-dependent downregulation, and that *clf29* mutation has very little effect on the transcriptome in a *cry1* genetic background, suggesting a link between CRY1- and CLF-mediated transcriptional responses to light. This suggests a model in which *CLF* acts downstream of *CRY1* upon blue light perception to inhibit hormone signalling and cell expansion, thus contributing to the inhibition of hypocotyl elongation.

This Chapter presents the results of investigations to further clarify and expand this model. First, chromatin immunoprecipitation is carried out to link *CLF*-mediated transcriptional changes with chromatin modifications. Then, several lines of further investigation are carried out to assess other potential links between CLF and light-signalling, and to implicate CLF in a wider range of light-regulated processes beyond the inhibition of hypocotyl elongation.

5.2 Linking *CLF*-dependent transcriptional regulation with chromatin modifications

Data in Chapter 4.2 analyse transcriptional changes upon light perception, and how this is affected in a *clf29* plant line. Among these genes showing *CLF*-dependent downregulation are various genes involved in Auxin signalling, including the *AUX*/*IAA* gene *IAA1* (Fig. 4. 6), which was confirmed by RT-qPCR (Fig 4.10 and reproduced in Fig. 5.1 A). CLF triggers H3K27me3 deposition, and so it was investigated whether deposition of this silencing chromatin mark correlated with the *CLF*-dependent transcriptional repression observed in Chapter 4.

IAA1 was previously identified as H3K27me3 marked gene in *Arabidopsis* seedlings via ChIP-microarray analysis (Zhang et al., 2007), and recently has also been identified as a CLF binding site (Shu et al., 2019). This made *IAA1* an excellent candidate for linking CLF-mediated chromatin modifications with transcriptional behaviour upon light perception.

Chromatin Immunoprecipitation was carried out on dark-grown Col0 and *clf29* seedlings before and after exposure to 6 hours light as described in Chapter 2.6, with antibodies targeting H3K27me3. In previous ChIP experiments, both H3K27me3 and CLF-binding have been shown to be highest in transcribed regions, with a peak around the transcriptional start-site (TSS) (Zhang et al., 2007), (Shu et al., 2019). Thus, primers for qPCR analysis were designed in the gene body of *IAA1* using primer3 (Untergasser et al., 2012). The primers were located shortly downstream of the TSS, flanking the first intron, as shown in (Fig. 5. 1 B). The signal was normalised against the reference gene *UB10* and the amplification in the Dark for each plant line set to 1. A distinct increase in H3K27me3 levels at the *IAA1* gene locus is notable after 6 hours in Col0, which was abolished in *clf29* (Fig. 5.1 C).

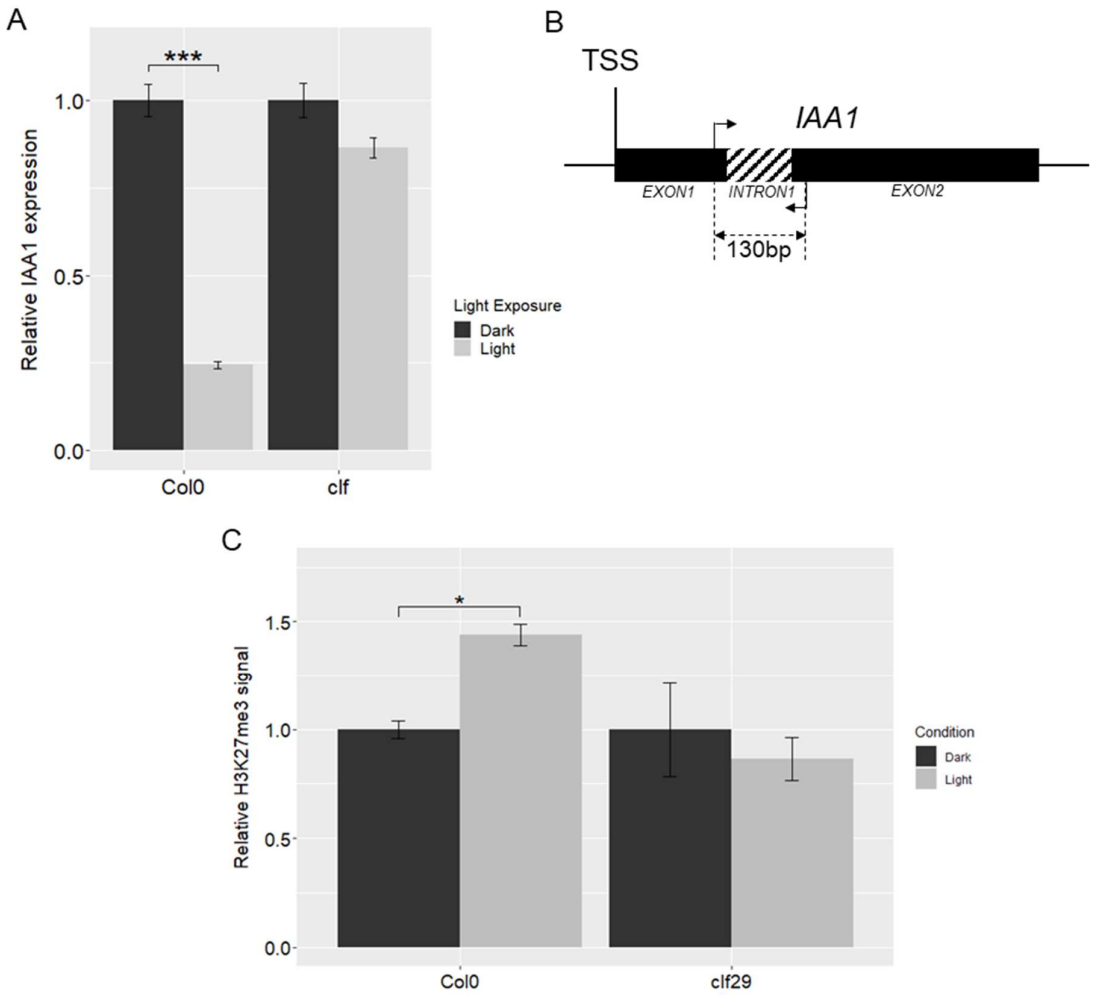

Fig. 5.1 *IAA1* shows *CLF*-dependent accumulation of H3K27me3 and transcriptional repression upon light perception.

A) qPCR analysis showing *CLF*-dependent transcriptional downregulation of *IAA1*, reproduced from (Fig. 4.10). B) binding sites for primers used for ChIP-qPCR analysis of *IAA1.* C) H3K27me3 signal at the *IAA1* gene body before (Dark) and after (Light) 6 hours light exposure in dark-grown Col0 and *clf29* seedlings, relative to the reference gene UB10. For each plant line, dark samples were set to 1, and light samples expressed relative to the dark samples. Asterisks indicate statistically significant differences from dark samples (* = $p < 0.05$) as determined by independent samples t tests

This result indicates a link between *CLF*-dependent deposition of H3K27me3 and *CLF*-dependent transcriptional repression of *IAA1* in the photomorphogenesis response of etiolated seedlings, with both of these responses being abolished in a *clf29* plant line.

Another relevant dataset for this analysis is presented in (Charron et al., 2009). Here it was found that light induces a large reorganisation of four chromatin modifications in etiolated seedlings, including H3K27me3 (Charron et al., 2009). In this dataset, over 2000 more genomic were found to be marked by H3K27me3 in samples exposed to light, compared to dark samples, with H3K27me3 displaying a negative correlation with transcription (Charron et al., 2009). To further demonstrate a link between CLF-mediated histone modifications and CLF-mediated transcriptional changes, two further candidate genes were selected from this for analysis via chromatin immunoprecipitation. The two genes selected were *EXP11* (AT1G20190), which features in the gene ontology category "Cell wall organisation or biogenesis", and *WES1* (AT4G27260), which features in the "Response to Auxin" category. Both genes exhibit CLF-dependent transcriptional downregulation upon light perception in the RNAseq data presented here (Fig. 4. 5-6) (Fig. 5. 2 A), and both were found to display increases in H3K27me3 upon light perception in (Charron et al., 2009). Additionally, both of these genes offer further insight into how CLF may mediate light-induced transcriptional reorganisation. In particular, direct transcriptional regulation of genes such as *EXP11* by CLF would provide a useful mechanistic link as to how CLF may be involved in the repression of hypocotyl elongation. Meanwhile, regulation of *WES1* by CLF would offer more evidence that CLF plays a role in regulating auxin signalling. A similar analysis to that used for *IAA1* was carried out for these two genes. It was found that H3K27me3 deposition at these loci showed CLF-dependent increases upon light perception, relative to the reference gene *UB10* (Fig. 5.2 B), as seen for *IAA1*.

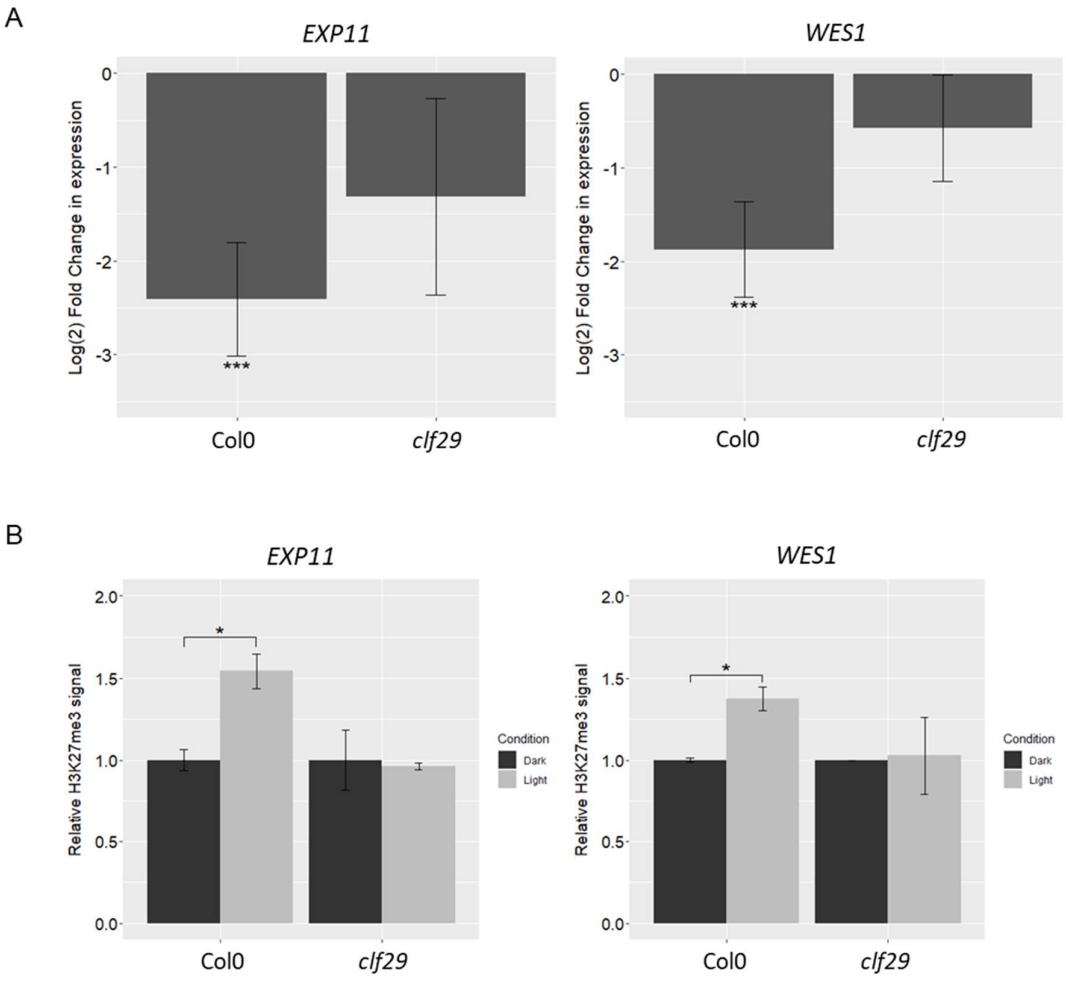

Fig. 5.2 *WES1* and *EXP11* both exhibit *CLF* dependent transcriptional downregulation and increases in H3K27me3 after light perception.

A) Log(2) fold changes in *WES1* and *EXP11* during the dark to light transition in Col0 and *clf29*, as identified by RNA Seq. Asterisks indicate statistically significant changes in expression from dark samples, as determined by Deseq2 (Love et al., 2014).
B) H3K27me3 signal at the *WES1* and *EXP11* gene loci before (Dark) and after (Light) 6 hours light exposure in dark-grown Col0 and *clf29* seedlings, relative to the reference gene UB10. For each plant line, dark samples were set to 1, and light samples expressed relative to the dark samples. Asterisks indicate statistically significant differences from dark samples (* = $p < 0.05$) as determined by independent samples t tests

The linking of *CLF*-mediated deposition of H3K27me3 and transcriptional changes at several gene loci reinforces confidence in the model presented in Chapters 3 and 4 whereby light induces an increase in *CLF* activity, which contributes to photomorphogenesis via the deposition of H3K27me3 at key light-repressed genes.

This leads to new questions about how CLF is activated and targeted by light signalling machinery. Data in Chapters 3 and 4 strongly suggest that CRY1, and potentially PHYA and PHYB to a lesser extent, are involved in this process, but there are likely to be other layers of regulation beyond these factors mediating a transcriptional increase in CLF. Additionally, *clf29* mutants are also observed to have elongated hypocotyls in darkness, where PHYs and CRYs are inactive. As such, it was deemed highly valuable to carry out further investigations into how CLF activity is integrated with light signalling. The rest of this Chapter describes further investigations carried out towards this purpose. Firstly, a yeast two-hybrid assay is undertaken to identify how CLF activity may be linked to light signalling machinery at the protein level, in addition to photoreceptor-dependent transcriptional changed discussed earlier. Then, analysis is carried out to further assess the role of CLF in regulating auxin signalling via GUS staining to assay auxin levels in Col0 and *clf29* plants, and analysing the effect of *clf29* mutation on another auxin-regulated process (phototropism).

5.3 CLF interacts with the skotomorphogenesis transcription factor PIF4

One way to analyse potential integration between CLF and light signaling machinery at the protein level was to test for protein-protein interactions between CLF and core light signalling components. As discussed in Chapter 1.2, the downstream signalling activated by endogenous hormones crosslinks with light signalling partially via physical interactions between signalling components in the different pathways. In particular, ARF6 and BZR1, whose activity is de-repressed by Auxins and Brassinosteroids respectively, both interact with PIF4 in the BAP transcriptional regulation module (Oh et al., 2012) (Oh et al., 2014).

A Yeast-two-hybrid assay was carried out to search for physical interactions between CLF and light and hormone signalling hubs such as COP1 and PIFs 3, 4 and 5, as well as the photoreceptors PHYA, PHYB, CRY1 and CRY2. These genes were cloned into the $pGAD_{T7}$ and $pGBK_{T7}$ yeast two-hybird vectors and introduced into yeast strains AH109 and Y187 respectively, which were then mated together as described in Chapter 2.9-10. Only the C-terminal regulatory domains were cloned for PHYs and CRYs, as these are responsible for downstream protein interactions observed with these proteins (Reviewed in (Quail, 2010) and (Wang and Lin, 2020)). The yeast were then grown on agar plates lacking specific amino acids for auxotrophic of mated yeast colonies (-L/W) and for protein-protein interaction analysis (-L/W/A/H).

An initial experiment highlighted potential interactions between CLF and PIF3, PIF4 and CRY1 (Fig. 5. 2 A). Unfortunately, further analysis of the CLF-PIF3 and CLF-CRY1 interactions displayed autoactivation from the PIF3-BD and CRY1-BD plasmids when negative controls were introduced (Fig. 5.2 B), meaning these cannot be assigned to an interaction between these two factors and CLF. However, the CLF-PIF4 interaction was

successfully reproduced in a second Y2H experiment (Fig. 5.2 C), representing a novel interaction at the protein level between CLF and light signalling machinery.

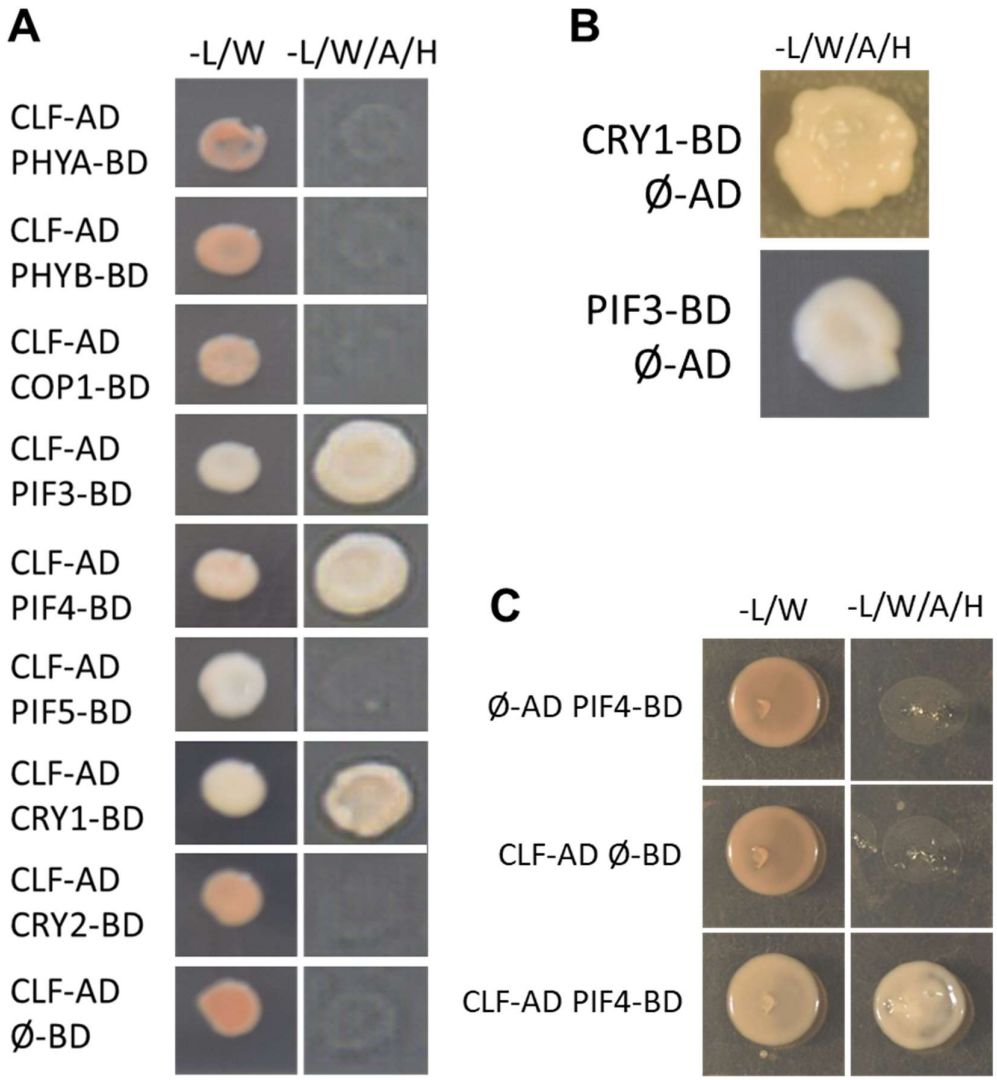

Fig. 5.3 Yeast-Two-Hybrid assay for protein-protein interactions between CLF and core light signalling machinery

A) Yeast Two hybrid screen testing for protein-protein interactions between CLF and PIFs, COP1, PHYs and CRYs. Growth on –L/W plate indicates successful transformation of plasmids and mating of yeast strains, growth on –L/W/A/H plate indicates interaction. CLF-AD Ø-BD included as a negative control.

B) Indication that potential CLF-PIF3 and CLF-CRY1 interactions were due to autoactivation from PIF3- and CRY1-BD plasmids.

C) Confirmation of potential CLF-PIF4 interaction in a second yeast-two-hybrid assay, with PIF4-BD Ø-AD and CLF-AD Ø-BD negative controls

5.4 Analysing the effects of *clf29* mutation on auxin signalling

In Chapter 4, it is shown that auxin signalling genes are enriched among genes showing *CLF*-dependent downregulation upon light perception (Fig. 4. 6). Some of these findings were noted as being potentially contradictory given *clf29* mutants also displayed elongated hypocotyls, a phenotype enhanced by auxin signalling, however, with the consideration that some of these genes (such as *AUX*/*IAA* genes) are transcriptionally upregulated by auxin, it was hypothesised that this could perhaps be due to *clf29* plants showing a lower level of auxin.

In order to investigate this further, an assay was carried out to visualise auxin signalling in Col0 and *clf29* plants utilising plant lines that carried a *pDR5* promoters fused to the β-glucuronidase (GUS) reporter gene (*pDR5::GUS*). DR5 is a synthetic auxin-responsive promoter containing a strong auxin responsive element (AuxRE) based on the D1-4 AuxRE from the *GH3* promoter (Ulmasov et al., 1997). *pDR5* fused to several reporter genes such as GUS, Green Fluorescent Protein (GFP) and Yellow Fluorescent Protein (YFP) is a commonly used method of visually analysing auxin levels across different tissues in *Arabidopsis* (e.g. (Yu and Wen, 2013) (Vandenbussche et al., 2010) (Hayashi et al., 2014)). A GUS staining assay was carried out in dark-grown Col0 and *clf29* seedlings containing the *pDR5::GUS* construct before (Dark) and after (Light) 6 hours of white light exposure as described in Chapter 2.7. In all cases, the most staining was observed in the cotyledons and at the top of the hypocotyl (Fig 5.3 A). In comparison, relatively little staining was seen lower in the hypocotyl (Fig. 5.3 B). In both dark and light-treated samples, staining was drastically reduced in a *clf29* seedling in the cotyledons, indicating lower levels of auxin (Fig. 3.5 A).

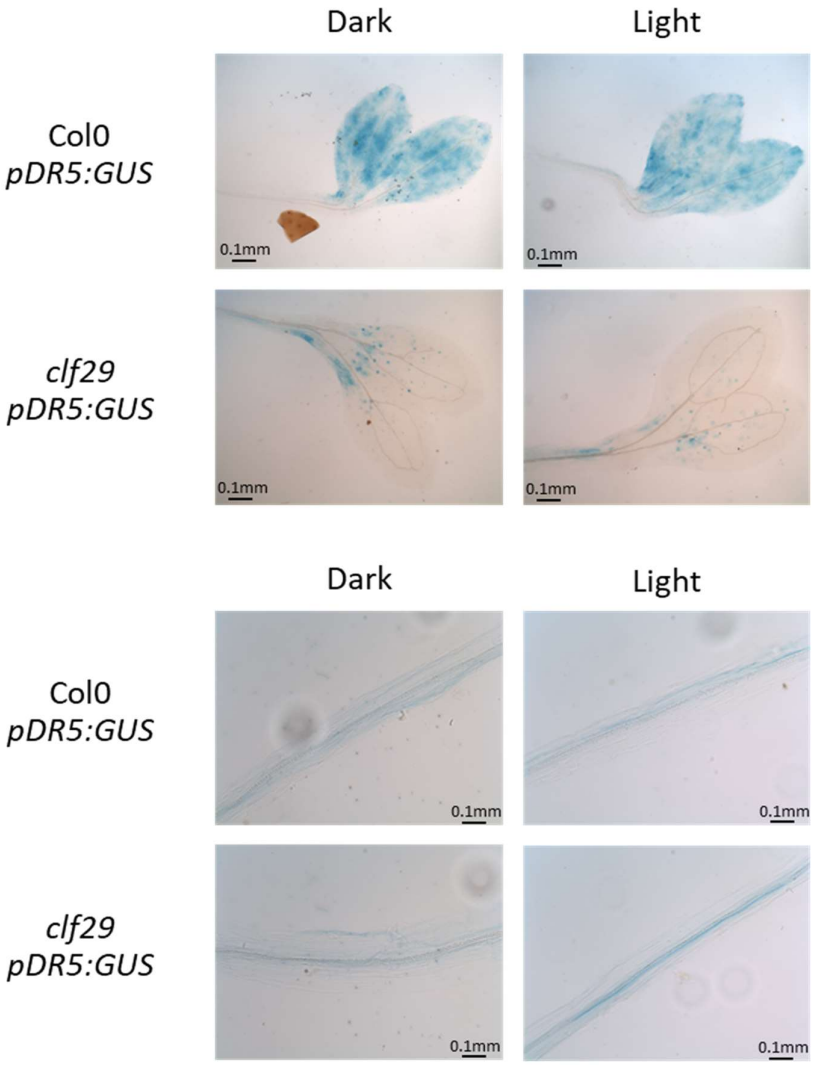

Fig. 5.4 Analysis of Auxin levels in Col0 and *clf29* plants before and after light perception via GUS staining.

GUS staining in cotyledons (A) and hypocotyls (B) of dark-grown Col0 and *clf29* seedlings carrying the *pDR5:GUS* reporter construct before (dark) and after (light) exposure to 6 hours white light (40µmol m^{-2} s^{-1}).

This is an intriguing finding. Thus far, work in this thesis has focused on hypocotyl expansion, a process which is promoted by auxin, and repressed by light (Nemhauser et al., 2006). Auxin also plays a key role in the expansion of cotyledons, another key process induced by light. In the dark, cotyledons are small and folded around the shoot tip, whilst light induces them to unfold and expand (Harpham et al., 1991). The mechanism by which light induces differential responses in different organs is still an active area of research, and notably light has been observed to induce different genetic expression patterns in each organ (Ma et al., 2005). Auxin promotes both hypocotyl elongation and cotyledon expansion by facilitating cell expansion, and differential regulation of auxin levels and auxin-responsive genes has been shown to be play a key role in this regulation (Sun et al., 2016). In particular, a number of SAUR genes show light-induced upregulation only in cotyledons *and*/*or* light-induced downregulation only in hypocotyls (Sun et al., 2016). The observation that *clf29* plants exhibit distinctly reduced auxin signalling in cotyledons (Fig. 5.3 A) suggests that CLF may play a role in promoting auxin signalling at the cotyledons. This hypothesis is consistent with the observations in Chapter 4 that a number of auxin repressors such as *WES1* and several *AUX*/*IAA* genes show CLF-dependent downregulation upon light, and the observation in chapter 4 that this is linked to CLF-dependent increases in H3K27me3 at the *IAA1* and *WES1* locus. This finding also suggests the intriguing possibility that CLF is involved in differential regulation of light-mediated processes in different organs.

Another observation from the GUS staining analysis is that a different pattern can be observed at the top of the hypocotyl with strong staining apparent in a *clf29* plant, which is localised to one side of the hypocotyl (Fig. 5.3 A). Notably, this pattern is maintained even after 6 hours of light exposure (Fig. 5.3 A). This potentially indicates an involvement of CLF with another light-regulated process, the opening of the apical hook. As mentioned in Chapter 1.1, etiolated seedlings display a hooked structure at the top of their hypocotyls, with the apical end of the hypocotyl bent to protect the shoot tip as it moves through the soil. Auxin is crucial to this process, but unlike with hypocotyl elongation or cotyledon expansion does not follow a simple pattern where increasing auxin levels uxhypocotyl is established, with higher auxin levels seen on the inner side of the apical hook (Schwark and Schierle, 1992), (Vandenbussche et al., 2010), (Gallego-Bartolomé et al., 2011). This gradient is crucial to the establishment of differential growth on the two sides of the apical hook, in combination with other hormones, particularly ethylene and GAs (Abbas et al., 2013). Plants grown in the presence of exogenous auxin and mutants which accumulate high levels of auxin both such as *superroot-1* (*sur-1*) both fail to develop the apical hook (Schwark and Schierle, 1992) (Boerjan et al., 1995), showing that it is the gradient across the hypocotyl that is important, not simply high levels of auxin. Perception of light induces the abolition of this auxin gradient and opening of the apical hook, with the gradient observed to be lost within 4 hours of light perception in dark-grown seedlings (Wu et al., 2010). This is notably affected in the *clf29* seedlings observed here, with a distinct gradient of GUS staining observed at the top of the hypocotyl even after 6 hours of light exposure (Fig. 5.3 A). The observation that *clf29* plants display lower auxin levels in the cotyledons, but higher levels at the top of the hypocotyl further suggests that CLF may be involved in differential regulation of hormone signalling in different organs. Furthermore, it also raises the possibility that CLF activity may be linked

to auxin transport, which plays a key role in the establishment, maintenance and abolition of the apical hook (Vandenbussche et al., 2010).

Another well-characterized process governed by light-mediated effects on auxin transport is phototropism. As far back as the 19th century, it was described that redistribution of a mysterious substance was responsible for directional growth towards a light source observed in plants (Darwin, 1880). This substance was later identified to be auxin, which is redistributed from the lit side of the stem to the shaded side, where it promotes a greater degree of cell elongation and thus curvature towards the light source (Went and Thimann, 1937), (Holland et al., 2009). This redistribution, in contrast to the other processes discussed in this thesis, is primarily regulated by the blue-light photoreceptors PHOT1 and PHOT2, with PHOT1 being the primary receptor under low fluence blue light, and the two acting redundantly under moderate-to-high fluence blue light (Liscum and Briggs, 1996), (Sakai et al., 2000).

Dark-grown Cola0 and *clf29* seedlings were illuminated from one side with blue light for 24 hours, as described in Chapter 2. 8. As shown in (Fig. 5.4), *clf29* plants exhibited a heightened phototropic response. In Chapter 3 it is shown that *CLF* activity in repressing hypocotyl elongation under blue light is likely downstream of CRY1 and PHYA, with a *clf29* mutation having no effect on hypocotyl lengths under blue light in a *cry1* or *phyA* genetic background (Fig. 3. 9). A similar analysis of the phototropic response of photoreceptor mutants and double mutants also carrying *clf29* mutation was carried out. Again, *clf29* mutation had no effect in a *cry1* or *phyA* genetic background (Fig 5.5).

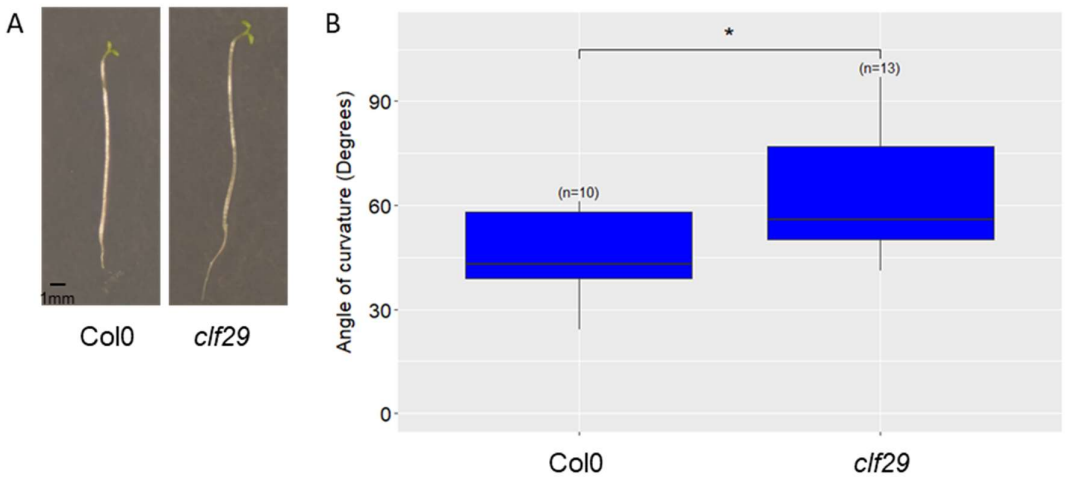

Fig. 5.5 *clf29* mutation results in enhanced blue-light phototropism in etiolated seedlings

A) Phototropism response in 5-day old dark-grown Col0 and *clf29* seedlings illuminated on one side with blue light (4.5µmol m-2 s-1) for 24 hours
B) Degree of curvature of 5-day old dark-grown Col0 and *clf29* seedlings illuminated on one side with blue light for 24 hours. Sample numbers displayed in graph. Asterisks indicate statistically significant differences from Col0 (* = $p < 0.05$)

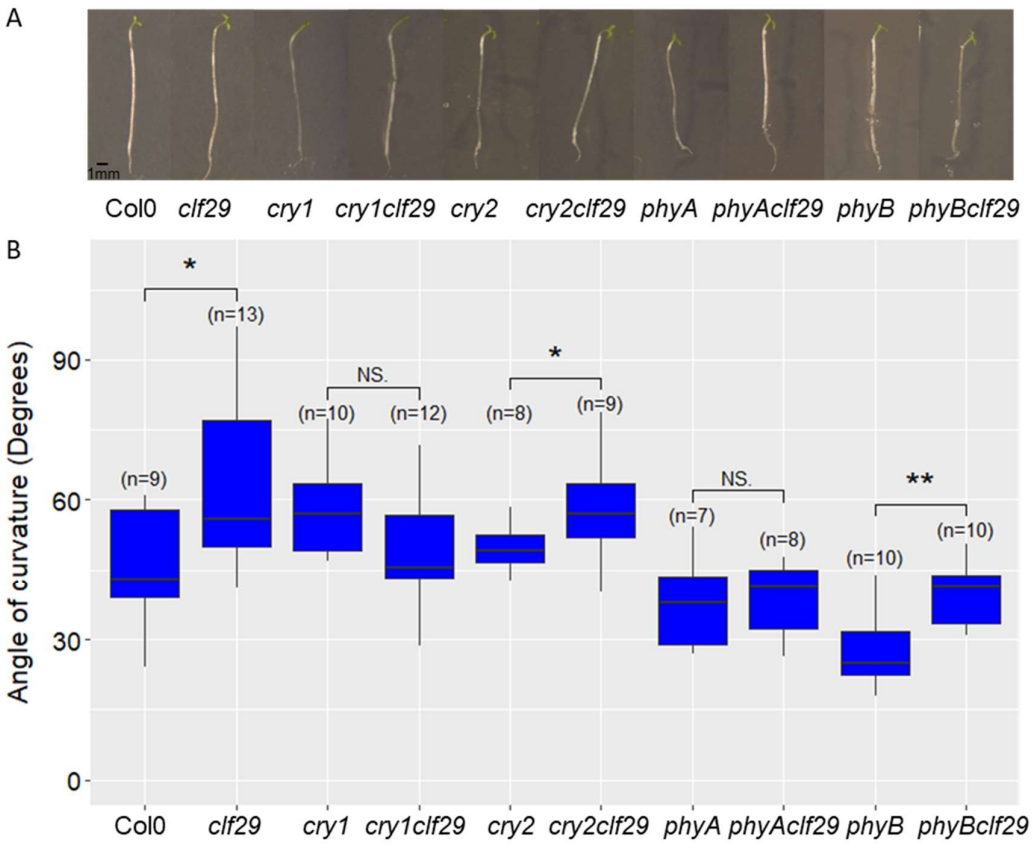

Fig. 5.6 *clf29* plant lines show no differences in blue-light phototropism in *cry1* and *phyA* genetic backgrounds

A) Phototropism response in 5-day old dark-grown plants exposed to blue light (4.5µmol m^{-2} s^{-1}) on one side for 24 hours.
B) Boxplots showing the degree of curvature in plants in (A). Sample numbers displayed in graph. Asterisks indicate statistically significant differences from the plants carrying a *clf29* mutation and the same plant line with WT *CLF* gene, as determined by independent samples T Tests (* = $p < 0.05$, ** = $p < 0.01$).

This figure provides further evidence that CLF plays a role in the response to blue light, acting downstream of CRY1 and PHYA. It also demonstrates further that CLF is involved in regulation of various auxin-related processes.

Additionally, as mentioned above, these data also raised the possibility for a CLF role in auxin transport. Auxin transport plays a crucial role in two processes discussed here – the maintenance and abolishment of the apical hook and phototropism. This auxin transport is primarily regulated in these processes by the AUX/LAX genes and the PIN genes

(Vandenbussche et al., 2010), (Zádníková et al., 2010), (Liscum et al., 2014), whilst the efflux carrier ATP-BINDING CASSETTE B19 (ABCB19) has also been shown to act in both processes (Wu et al., 2010), (Christie et al., 2011). However, analysis of the RNA-seq from chapter 4 identified that none of the AUX/LAX or PIN genes, nor *ABCB19* were present in the lists of DEGs for either Col0 or *clf29* (Full lists of DEGs are shown in Appendix 2). As such, the data in this thesis cannot provide any genetic evidence to support a hypothesis of CLF directly regulating auxin transport via transcriptional modification of auxin influx/efflux carriers.

5.5 Further analysis of the effect of Red Light on *clf29* phenotype

In Chapter 3, it is shown that *clf29* plants have no difference in hypocotyl length when grown under red light (Fig. 3.5). In addition, it is found that *clf29* mutation has no effect on hypocotyl lengths under white or blue light in a *cry1* genetic background (Fig. 3.7). *clf29* plants are also shown to be elongated under far-red light (Fig.3.3), but the fact that this phenotype was not dependent on any photoreceptors tested made this harder to interpret (Fig. 3.8). These data together are taken to indicate that CLF is primarily activated by blue light, and acts downstream of CRY1, a finding which is reinforced in Chapter 4 by high correlation between transcriptional misregulation in *clf29* and *cry1* plant lines (Fig. 4.13-14). Meanwhile, it is proposed in Chapter 3 that *CLF* may be downregulated by red light due to the lack of an observable phenotype in *clf29* seedlings grown under red light, especially considering that *clf29* plants show elongated hypocotyls in darkness (Fig. 3.4). As such, the work in this thesis has thus far focused on processes which are most strongly regulated by blue light. Hypocotyl elongation is repressed by both blue and red wavelengths, but blue light has the highest impact, with less than one minute of light being required for inhibition of hypocotyl elongation in dark-grown (Parks et al., 1998) seedlings compared to several minutes for red light (Parks and Spalding,

1999). Correspondingly, as shown in Chapter 3 seedlings grown under blue light are far shorter than those grown under red light (Fig. 3.2), (Fig. 3.5). Equally, continuous blue light has a much greater effect on both opening of the apical hook and the opening of the cotyledons in Col0 seedlings (Liscum and Hangarter, 1993). However, the lack of a *clf29* phenotype in red light is intriguing, and a further investigation was carried out to see if this was limited to hypocotyls. The primary phenotype of *clf* loss-of-function mutants is small, upwardly-curved leaves, after which the gene is named, which is caused by expression of the CLF-silenced gene *AGAMOUS* (*AG*) in these plants (Coupland et al., 1993), (Kim et al., 1998). In order to further analyse the effect of red light on CLF, analysis was carried out to see if this phenotype was also affected in seedlings grown under monochromatic red light. To analyse this, Col0 and *clf* lines were exposed to white light for 24 hours to induce germination, then grown for one week under constant red light, as described in Chapter 2.11. As controls, the same lines were also grown in constant white light and blue light – both conditions under which *clf29* mutants had been shown to exhibit elongated hypocotyls (Fig. 3.1) (Fig. 3.2). Following this, they were transferred to a greenhouse and grown in soil under long-day conditions. After four weeks, the *clf29* lines initially grown under white or blue light showed the distinctive phenotype of upwardly curled leaves (Fig. 5.6). However, this phenotype was drastically reduced in the plants initially grown under red light, with *clf29* lines showing very little difference from WT in the frequency of leaf curvature under these conditions (Fig. 5.6).

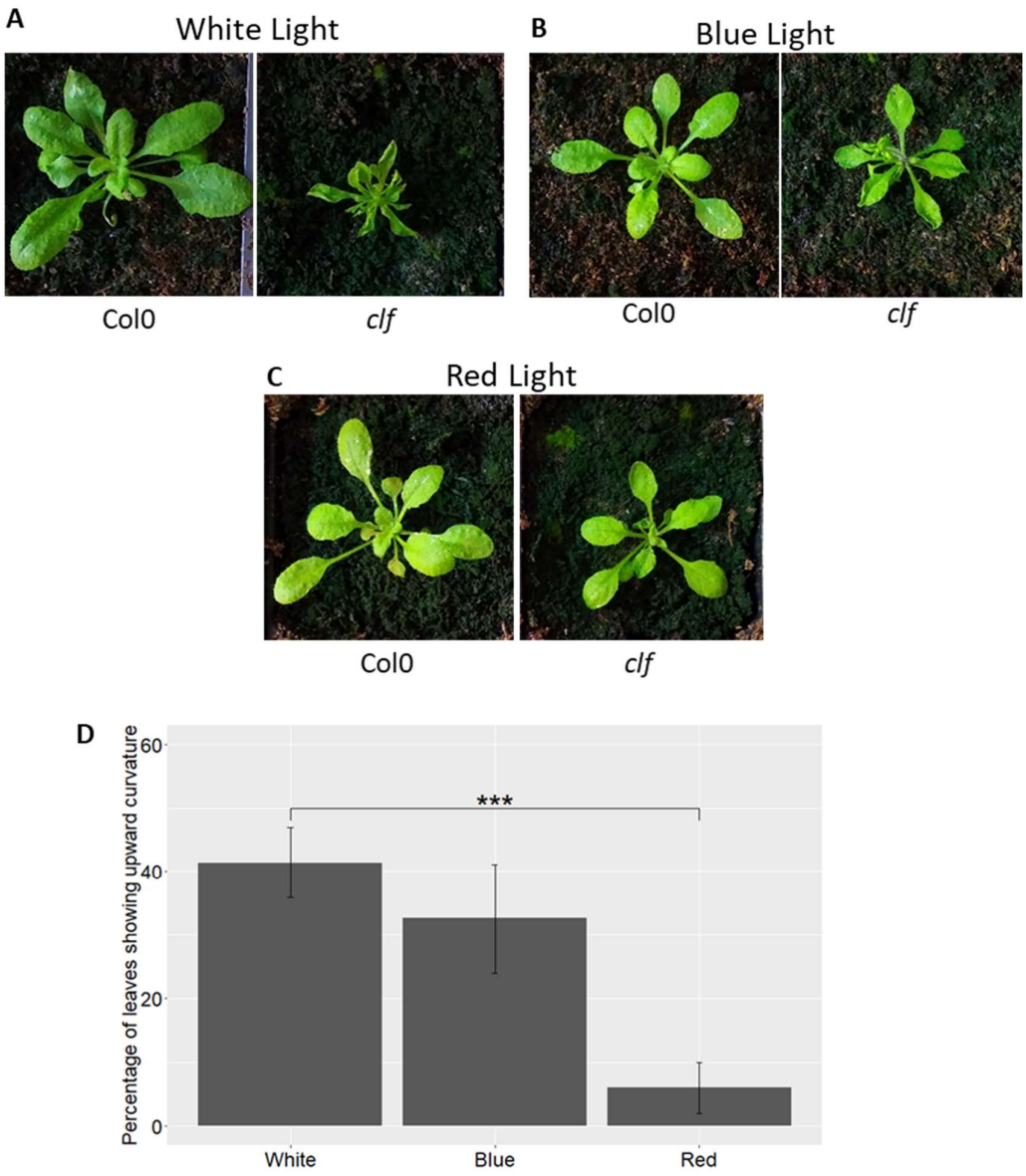

Fig. 5.7 Analysis of effects of white, blue and red light exposure during early development on prevalence of *clf29* curled-leaf phenotype.
(A)-(C) Col0 and *clf29* seeds on MS Agar plates were grown to 7 days old in constant white (A - 40µmol m-2 s-1), Blue (B – 6.5µmol m-2 s-1) or Red (C – 7.6µmol m-2 s-1) light at 21°C in a light chamber, then transferred to soil and grown under long-day conditions in a greenhouse and photographed at 4-weeks old
(D) Thee percentage of leaves showing upwards curvature in *clf29* plants after growth in these conditions. Error bars indicate standard error of the Mean (SEM) from 5 biological replicates. Asterisks indicate significant differences from plants grown under constant white light, as determined by independent samples t-tests (***=p<0.001)

5.6 Summary

Data presented in this Chapter provide a link between *CLF*-mediated chromatin regulation and transcription, and sought to expand the analysis of light-regulated CLF activity beyond the focus on hypocotyl elongation in earlier chapters.

Firstly data are presented that identify a *CLF*-dependent, light-induced increase in H3K27me3 at several gene loci shown to exhibit *CLF*-dependent transcriptional repression in Chapter 4 (Fig. 5. 1-2). This demonstrates that *CLF*'s role in transcriptional regulation is mediated by its histone modification activity, and reinforces the model for CLF activity during the light response presented in Chapter 3 (Fig. 3. 13)

Analysis is then carried out to further analyse how *CLF* may be regulated during transcriptional activity by screening for physical interactions between *CLF* and key regulators of skotomorphogenesis and photomorphogenesis. An intriguing interaction is found between CLF and PIF4(Fig. 5. 3 C), which could play a key role in the targeting of CLF activity to certain genomic loci.

The analysis of CLF activity, so far predominantly restricted to hypocotyl elongation, is then expanded into other pathways. GUS staining is used to analyse the levels of auxin before and after light perception in WT and *clf29* mutants, with the finding that *clf29* plants show massively reduced auxin levels in the cotyledons, but higher levels at the tip of the hypocotyl, where the apical hook is located during skotomorphogenesis (Fig. 5. 4). The reduction of auxin levels at the cotyledon correlates with findings from RNA-seq and ChIP-qPCR analysis that key repressors of auxin signalling undergo light induced accumulation of H3K27me3 and transcriptional repression, both in a *CLF*-dependent manner (Fig. 4. 8), (Fig. 5.2-3).

Meanwhile, the identification of higher auxin signalling at the top of the hypocotyl in *clf29* plants, and in particular the maintenance of this after light perception (Fig. 5. 4 A) suggests that *clf29* may also play a role in other light-regulated processes involving auxin. To further this analysis, the effects of *clf29* mutation on blue light-induced phototropism are assayed, and it is found that *clf29* has an enhanced phototropic response (Fig. 5.5). However, as seen earlier with hypocotyls of blue-light-seedlings, this effect is lost in a *cry1* and *phyA* genetic background (Fig. 5. 6).

Finally, a further analysis is carried out on the effects of blue light and red light early in development on the archetypal *clf29* phenotype – leaf curvature. In Chapter 3 it was hypothesised that CLF activity is repressed by red light, based on observations that *clf29* mutation has no effect on hypocotyl lengths on seedlings grown under red light. This hypothesis is reinforced here by observations that exposure to red light early in life abolishes the curled leaf phenotype in *clf29* seedlings even after they are removed from the red light (Fig. 5.7). It would be intriguing to carry out further investigations as to whether red light also impacted other phenotypes resulting from loss of *CLF*, such as early flowering (Bian et al., 2016). It would also be intriguing to analyse how *phyB* mutation affected this phenotype, given how red light signalling is heavily affected in a *phyB* plant line. Finally, it would be valuable to assess how *CLF*-regulated genes such as *AGAMOUS*, as well as other candidate genes identified in this thesis such as *EXPANSINs* and *XTH* genes are affected by early light exposure to monochromatic red light, in order to further assess how downstream *CLF* activity is affected.

Chapter 6 – Discussion

6.1 – Introduction

As discussed in Chapter 1, increasing evidence in recent years has demonstrated that chromatin modifications play a key role in light signalling in *Arabidopsis thaliana*. Work in this thesis has aimed to provide a contribution to this growing field, identifying a novel role for the chromatin remodelling complex PRC2 in light signalling, acting via the histone methyltransferase CLF.

A variety of experiments are used to present evidence for the involvement of PRC2 activity in plant light responses, acting via the histone methyltransferase CLF, and regulated by photoreceptors. Chapter 3 presents phenotypic and genetic data identifying a role for CLF in a key light-regulated process, repression of hypocotyl elongation, how it is regulated at the transcriptional level by the effects of light, and the involvement of photoreceptors in this process. Chapter 4 uses RNA-seq analysis to investigate if *clf29* mutation affects the transcriptional responses to light. This analysis is then expanded to analyse light responses in photoreceptor mutants, and how this correlates with that seen in *clf29* plants, before concluding with an analysis of the effects of *clf29* mutation in genetic backgrounds already lacking individual photoreceptors. Finally, in Chapter 5, the transcriptional regulation discussed in Chapter 4 is correlated with changes in the chromatin modification H3K27me3. Further investigations are then carried out to understand how CLF may modulate light responses.

The aim of this chapter is to review and summarise the data presented in Chapters 3-5, discuss the findings in the context of current knowledge from the literature, and assess what conclusions can be drawn. Finally, it will also be discussed what further evidence is

required to support the hypotheses presented, and suggestions will be made for future research in this area.

6.2 CLF is involved in light signalling in *Arabidopsis thaliana*

6.2.1 CLF displays light induced transcriptional activation and *clf29* mutants have elongated hypocotyl

It is known that the silencing histone modification H3K27me3 is involved in plant light responses. A significant reorganisation of this chromatin mark in has been identified in etiolated seedlings exposed to light, with 8395 regions marked by this modification after light exposure, covering 8.1% of the genome (Charorn et al., 2009). This was increased from 6238 regions covering 5.7% of the genome prior to light exposure and correlated with transcriptional silencing (Charron et al., 2009). This chromatin modification is regulated by the PRC2 complex, acting through the methyltransferases CLF, SWN and MEA. Previous work in our laboratory has identified via RNA-seq analysis that among these chromatin modifiers, CLF shows rapid transcriptional induction by white light in etiolated seedlings (De Lucas, unpublished). In Chapter 3, this observation is confirmed by RT-qPCR analysis (Fig. 3.10), demonstrating that CLF is regulated at the transcriptional level by light.

As well as the observation of a massive reorganisation in H3K27me3 upon light perception, it has also been shown that key factors involved in promoting skotomorphogenesis such as PIF3 and BZR1 function to repress the deposition of H3K27me3 in darkness (Zhang et al., 2014). Combining this observation with the light-induced upregulation of *CLF* transcription suggested a potential role for CLF in light signalling.

In Chapter 3, it is shown that CLF has a repressive effect on hypocotyl elongation, with *clf29* loss-of-function mutants displaying elongated hypocotyls in both light grown and dark-grown seedlings (Fig. 3.1) (Fig. 3.4). This potentially indicates that CLF plays a role in repressing hypocotyl elongation, representing a novel role for CLF. However, it must be noted that these data alone cannot provide evidence of a role for CLF in light-mediated regulation of plant development, due to the limitations of the data presented here. The hypocotyl assays presented in Chapter 3 do not consider the scale of hypocotyl elongation seen in *clf29* plants, and this phenotype is observed in both light and darkness. As such, this data could indicate a constitutive role for CLF in repression of hypocotyl elongation, and it cannot be concluded from this that CLF activity during this process is regulated by light, or that CLF acts during the dark-light transition. As discussed in chapter 3, it would be highly valuable to carry out further hypocotyl assays considering the magnitude of the elongation seen in *clf29* plants in both dark and light-grown seedlings.

6.2.2 CLF has phenotypic effects in blue and far-red light, but is likely repressed by red light

After demonstrating that CLF displays a role in repression of hypocotyl elongation, further analysis is carried out in Chapter 3 into the phenotypic effects of *clf29* mutation under specific light wavelengths. *clf29* mutation is shown to result in elongated hypocotyls in seedlings grown under constant blue and far-red light (Fig. 3. 2 – 3), but not under red light (Fig. 3. 5). This is taken to show that CLF acts to repress hypocotyl elongation in plants grown under blue and far-red light. The elongated hypocotyl of *clf29* seedlings grown in darkness but not in red light instead suggests a model in which CLF has a constitutive effect in repressing hypocotyl elongation and that red light acts to repress its activity in some way. This analysis is expanded in Chapter 5, where it is shown that growing seedlings under monochromatic red light abolishes the *clf29* curled leaf

phenotype which develops in seedlings later transferred to long-day growth (Fig. 5.6). This supports the hypothesis that red light suppresses CLF activity and provides evidence that this is not limited to the hypocotyl elongation phenotype shown in this thesis, but also affects other CLF-regulated processes later in development.

6.2.3 CLF likely acts downstream of the photoreceptor CRY1 in blue light signalling

As such, it is shown that CLF has a repressive effect on hypocotyl elongation, but this alone cannot demonstrate that CLF plays a role in light signalling. However, other data presented in this thesis allow a hypothesis to be proposed in which CLF functions during light responses, and is regulated by the blue-light photoreceptor CRY1.

Firstly, there is the observation that light-induced increases in CLF expression are dependent on CRY1 (Fig. 3.10-11). Additionally, it is observed that the *clf29* elongated hypocotyl phenotype in both white and blue light is also dependent on CRY1 with *cry1clf29* double mutants showing no significant differences from a *cry1* single mutant (Fig. 3.6-7). As such, it has been shown that CLF is regulated by light in a photoreceptor-dependent manner, and loss of *CLF* results in a photoreceptor-dependent phenotype in the light, indicating that CLF may be linked to that of photoreceptors acting during the light response.

Further evidence for a role of CLF in light responses is then provided by the RNA seq analysis in Chapter 4. It is shown that *clf29* plants are distinctly affected in their transcriptional responses to light, providing clear evidence for a role of CLF in mediating this process. As discussed in Chapter 4, although the number of genes showing significant changes in expression is not substantially affected (Fig. 4.2), the targeting of specific biological processes is (Fig. 4.3). A number of genes relating to cell expansion and hormone signalling are discussed which exhibit *CLF*-dependent downregulation upon light

perception (Fig. 4. 6-9). This evidence clearly demonstrates a role for *CLF* in responses to light in *Arabidopsis*.

The RNA-seq-data also show a high correlation between CLF- and CRY1-mediated transcriptional responses to light, providing further evidence linking CLF and CRY1 activity. Out of 345 genes showing *CLF*-dependent transcriptional upregulation, 92 of them also show lower expression in a *cry1* plant after light perception (Fig. 4.13). Meanwhile, out of 206 genes showing *CLF*-dependent downregulation upon light perception, 56 of them also show higher expression in a *cry1* mutant after light perception (Fig. 414). These observations, together with the fact that *clf29* has CRY1-dependent phenotypic effects in blue light strongly suggest that CLF acts in the same light signalling pathways as CRY1.

This hypothesis is reinforced by the data showing that *clf29* mutation has very little effect on other phenotypic or genetic responses to light in a plant already lacking CRY1. In addition to the hypocotyl assays already discussed, Chapter 5 analyses blue light-induced phototropism. *clf29* plants are found to exhibit heightened phototropism, but this phenotype is abolished in a *cry1* plant line (Fig. 5. 5-6). This is also reinforced by genetic data, with the transcriptomes of *cry1* and *cry1clf29* plant lines after light perception showing very little distinction, and very few genes showing transcriptional changes (Fig. 4. 15-16).

These data together suggest a model in which CLF acts downstream of CRY1 in the response to blue light. It is also possible that the phytochromes are involved in this process, but their role in this pathway is less clear. PHYB is required for light-induced upregulation of *CLF* transcription (Fig. 3. 12), but in all data presented in this thesis, phenotypic effects of *clf29* mutation appear independent of PHYB (Fig. 3. 6-8), (Fig. 5.6).

Furthermore, PHYB primarily acts in response to Red light, and data in this thesis show that red light abolishes the phenotype of *clf29* plants (Fig. 3.5), (Fig. 5.7).

Meanwhile, PHYA is shown to be required for *clf29* mutation to exhibit phenotypic effects on hypocotyl length and phototropism under blue light (Fig. 3. 8), (Fig. 5. 6). However, this is conflicted by the observation that *clf29* mutation still results in longer hypocotyls under white light in a *phyA* genetic background (Fig. 3. 7), and that PHYA is dispensable for the light-induced activation of *CLF* activity (Fig. 3. 11). Furthermore, under far-red light, the primary wavelength promoting PHYA activity, a *phyAclf29* has longer hypocotyls than the *phyA* single mutant, indicating that under this wavelength CLF has an repressive effect on hypocotyl elongation that is independent of PHYA. (Fig. 3.8). This intriguing result suggests that *PHYA* is only required for CLF activity in blue light. Although the primary absorption spectrum for phytochromes is in the longer red and far-red wavelengths, PHYA does have a secondary peak of absorption in blue wavelengths and has been shown to play a role in mediating various blue light responses. Notably, these include inhibition of hypocotyl elongation, cotyledon expansion and phototropism (Whitelam et al., 1993), (Neff and Chory, 1998) (Sullivan et al., 2016). PHYA activity under blue wavelengths is at least partially dependent on interaction with CRY1 and promotion of blue-light-induced CRY1 activation (Ahmad et al., 1998). Thus, these observations could indicate that PHYA contributes to CRY1-mediated induction of CLF activity under blue light.

As discussed, there is evidence that CLF acts downstream of CRY1 in blue light signalling, and evidence that CLF is repressed by red light. It is also shown that *clf29* mutation results in hypocotyl elongation in dark-grown seedlings, suggesting that CLF has a constitutive effect on this process. This observation, combined with the lack of photoreceptor involvement in *clf29* phenotype under far-red light (Fig. 3.8) could indicate that far-red light has no effect on CLF activity, and that the elongated hypocotyl phenotype seen in

clf29 plants grown under far-red light simply represents a continuation of CLF activity on repressing hypocotyl elongation in darkness.

6.2.4 Summary

Overall, this thesis does provide evidence for a role of CLF activity in photomorphogenesis, representing a novel role for PRC2 activity during *Arabidopsis* development.

Taking these data together, a model can be proposed in which CLF functions to repress hypocotyl elongation, and upon blue-light perception is transcriptionally induced in a CRY1-dependent fashion. CLF then forms a key part of downstream CRY1-signalling, to promote blue-light induced developmental changes. Meanwhile, PHYA is proposed to contribute to this process via promotion of blue-light activation of CRY1.

Red light is proposed to have a repressive effect on CLF activity, whilst the role of far-red light cannot be conclusively determined. *clf29* mutation does result in elongated hypocotyls under far-red light (Fig. 3.3) but this independent of all photoreceptors, and could simply represent constitutive CLF activity on this process, which is also apparent in darkness (Fig. 3.4).

This thesis does not provide any data indicating a requirement for CRY2 in this process, and thus this pathway is proposed to act independently of this photoreceptor. Meanwhile, the activity of PHYB cannot be determined, as PHYB appears required for light-induced transcriptional induction of *CLF* (Fig. 3.11), but dispensable for *clf29* phenotypic effects (Fig. 3.7-8), (Fig. 5.6).

This model for light-regulation of CLF activity during photomorphogenesis is displayed in (Fig. 6.1).

As discussed earlier, it must be noted that further experimentation is needed to increase confidence in these assertions. In particular, it would be desirable to carry out a more focused hypocotyl assay calculating the scale of hypocotyl elongation seen in darkness and under different light wavelengths, in order to further link the light-induced transcriptional upregulation of CLF with an increase in its activity in repressing hypocotyls. It would also be highly valuable to carry out qPCR assays to analyse CLF transcriptional responses to individual wavelengths of light, and correlate transcriptional changes with *clf29* phenotypes.

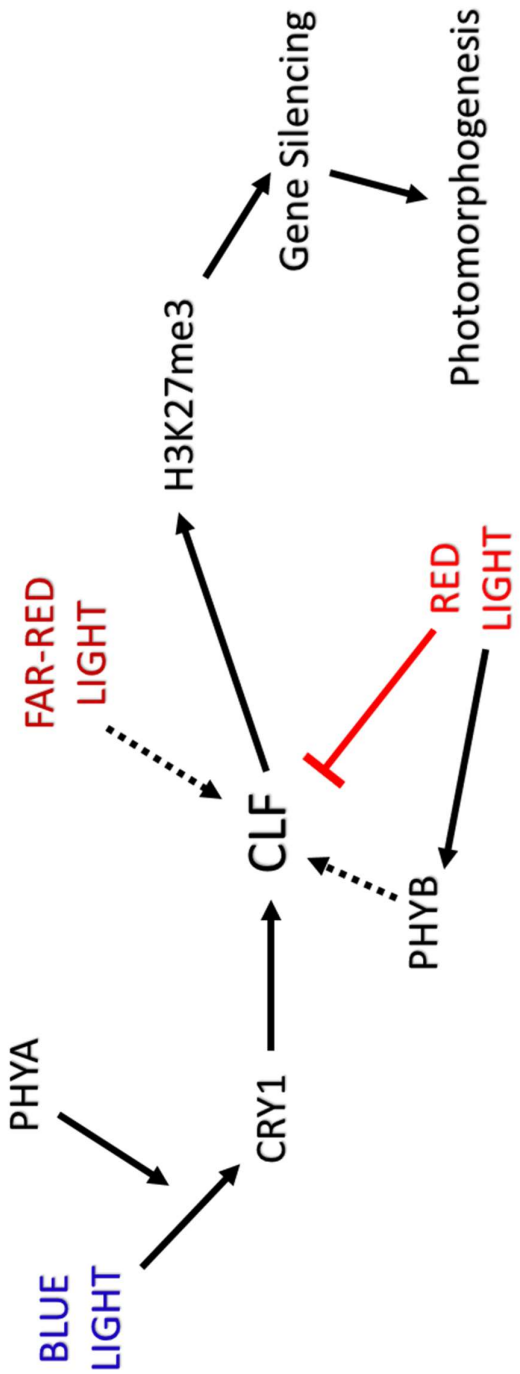

Fig. 6.1 (figure legend on next page)

Fig. 6.1 Hypothesised pathway of CLF regulation by light during photomorphogenesis

Black arrows indicate hypothesised positive interaction. Red T-Bars indicate hypothesised inhibition. Dashed arrows indicate potential interaction requiring further investigation.

CLF is hypothesised to contribute to photomorphogenesis by inhibiting hypocotyl elongation, based on data presented in Chapter 3 that *clf29* plants exhibit elongated hypocotyls in darkness and under continuous white, blue, and far-red light (Fig. 3.1-4). It is proposed that CLF acts downstream of CRY1 during light signalling, and is transcriptionally upregulated by blue light in a CRY1-dependent fashion. This is based on data in Chapter 3 showing that *CLF* is transcriptionally upregulated by white light in a CRY1-dependent fashion (Fig. 3. 10-11) and that the phenotypic effects on hypocotyl length in *clf29* plants under both blue and white light are abolished in a *cry1* genetic background (Fig. 3.6-7). Additionally, data in Chapter 4 shows that the transcriptomes of *cry1* and *cry1clf29* plants after light perception are very similar, with very few differentially expressed genes (Fig. 4.16). Finally, it is shown in Chapter 5 that *clf29* effects on blue-light induced phototropism are also abolished in a *cry1* genetic background (Fig. 5.5-6). Together, these data indicate that a *clf29* mutation has very little effect in a *cry1* genetic background, indicating a requirement for CRY1 in CLF activity during light signalling.

Meanwhile, PHYA is hypothesised to contribute to this process via promotion of blue-light activation of CRY1, based on data in Chapter 3 and Chapter 5 showing that *clf29* phenotypic effects on hypocotyl lengths and phototropism in blue light are abolished in a *phyA* genetic background (Fig. 3. 7) (Fig. 5.6).

Red light is proposed to have a repressive effect on CLF activity, based on data in Chapter 3 indicating that *clf29* mutation has no effect on hypocotyl lengths under monochromatic red light (Fig. 3. 5, 9), and data in Chapter 5 indicating that exposure to monochromatic red light suppresses the *clf29* curled-leaf phenotype (Fig. 5.7). The role of PHYB cannot be determined. In Chapter 3 it is shown that *PHYB* is required for light-induced *CLF* transcriptional upregulation (Fig. 3.11) but *phyB* mutation has no effect on the *clf29* elongated hypocotyl phenotype under any conditions tested (Fig. 3.6-9). Additionally, PHYB activity is highest under red light, which is hypothesised to repress CLF activity.

The role of far-red light in regulating CLF activity cannot be determined. *clf29* mutation does result in elongated hypocotyls under far-red light (Fig. 3. 3) but this independent of all photoreceptors (Fig. 3. 8) and could simply represent constitutive CLF activity on this process, which is also apparent in darkness (Fig. 3. 4).

No data presented here indicate a role for CRY2 in regulation of CLF, and so CLF is proposed to act independently of this photoreceptor.

6.3 CLF mediates repression of hypocotyl elongation via repression of genes such as expansins and *XTH* genes

6.3.1 RNA-seq shows CLF is required for downregulation of key cell-expansion promoting gene families

Chapter 6.2 discusses evidence from this thesis that the histone methyltransferase CLF is involved in light signalling in *Arabidopsis thaliana*, especially in response to blue light, acting downstream of CRY1.

One of the major lines of evidence in this discussion is the effect of *clf29* mutation on hypocotyl elongation, shown in Chapter 3, with *clf29* loss of function mutants observed to display elongated hypocotyls when grown in darkness (Fig. 3.4) or in white (Fig. 3.1), blue (Fig. 3.2) or far-red light (Fig. 3.3). In Chapter 4, RNA-seq analysis provides genetic evidence to support this model, and a number of findings are presented which suggest a mechanistic explanation of how CLF acts during this process.

Gene ontology analysis of genes showing light-specific downregulation identified the category of cell wall organisation or biogenesis as enriched among genes showing *CLF*-dependent downregulation (Fig. 4. 5-6). The process of hypocotyl elongation is primarily driven by a loosening of the cell wall to increase its extensibility and facilitate turgor-driven cell expansion (Gendrau et al., 1997), (Derbyshire et al., 2007), (Refrégier et al., 2004). Correspondingly, genes in the category of cell wall organisation or biogenesis are major players in cell expansion, as discussed in Chapter 4.2.3.1.

Several members of two prominent gene families involved in cell expansion are present in the data in (Fig. 4.7), displaying CLF-dependent downregulation. Firstly are the expansins. The alpha-expansins *EXPA4* and *EXPA11* are both represented in this dataset, along with one member of the EXPANSIN-LIKE A sub-family *EXLA11*. Expansins are the major

regulators of a phenomenon referred to as “acid-growth”, whereby lowering of the pH in the cell wall by a H+ ATP-ases results in cell elongation (Rayle and Cleland, 1992). Expansins promote this process by mediating a pH-dependent loosening of the cell wall (Li et al., 1993), which is thought to occur via weakening of hydrogen bonds between polysaccharides, allowing them to slide more easily (Wang et al., 2013). Correspondingly, overexpression of expansins has been shown to induce massive hypocotyl elongation in etiolated seedlings in *Arabidopsis* (Boron et al., 2015).

Additionally, three members of the *XYLOGLUCAN ENDO-TRANSGLYCOSYLASE/HYDROLASE* gene family are also found to exhibit CLF-dependent downregulation – *XTH8*, *XTH19* and *XTH30* (Fig. 4.7). Like the expansins, the *XTH* gene family are another key group of enzymes promoting cell elongation by promoting polysaccharide-to-polysaccharide transglycosylation, which facilitates sliding of the polysaccharides within the cell wall, loosening the cell wall and facilitating cell expansion (Fry et al., 1992). Notably, all three of these *XTH* genes have been previously shown to be upregulated in darkness-treated *Arabidopsis* seedlings (Lee et al., 2004).

6.3.2 ChIP-qPCR data and previous data from the literature provide evidence for CLF-dependent transcriptional repression of cell elongation via deposition of H3K27me3 on expansins and XTH genes

The *CLF*-dependent light-induced repression of several genes within two major gene families regulating cell elongation is strong genetic evidence for a role of CLF in repressing hypocotyl elongation. However, these data alone do not provide a definite answer as to how this *CLF*-mediated transcriptional regulation occurs. One possible explanation could be that this repression of cell-wall elongated genes is due to CLF-mediated effects on hormone signalling, as both brassinosteroid and auxin signalling are also enriched among

genes showing *CLF*-dependent downregulation upon light perception (Fig. 4.7). Both of these hormones promote cell expansion and hypocotyl elongation, and notably both have been shown to transcriptionally upregulate both expansins and XTH genes (Nemhauser et al., 2006).

Thus, in order to show a direct link between CLF activity and light-induced transcriptional silencing, analysis of chromatin modifications was required. In Chapter 5, ChIP-qPCR analysis is used to show that a CLF-dependent increase in H3K27me3 deposition occurs at *EXP11* upon light perception (Fig. 5.2). The identification of light-induced transcriptional repression and accumulation of this silencing histone modification, both in a *CLF*-dependent manner, provides strong evidence that this gene is a direct target of CLF.

Furthermore, considering this finding together with several published datasets suggests that this CLF-mediated silencing via H3K27me3 accumulation may also occur at several more genes discussed here. Firstly, as mentioned in Chapter 5.2, *EXP11* had been previously identified as displaying accumulation of H3K27me3 upon light exposure in dark-grown seedlings (Charron et al., 2009), which is also true for *XTH30*. Additionally, another dataset has identified *XTH8* as a target gene for H3K27me3 in seedlings grown under long day conditions (Zhang et al., 2008). Finally, both *EXP11* and *XTH30* have also previously been identified in a screen for CLF binding sites across the genome (Shu et al., 2019). Considering these data, it is highly tempting to propose that many of the discussed genes exhibiting CLF-dependent transcriptional repression upon light perception may also show *CLF*-dependent accumulation of H3K27me3.

Taking these genetic and epigenetic data together, it can be hypothesised that CLF exhibits a repressive effect on hypocotyl elongation by directly targeting genes involved in cell wall expansion such as expansins and XTH genes. These genes would be proposed to

exhibit H3K27me3 accumulation and transcriptional silencing in a CLF-dependent manner, thus restricting the extensibility of the cell wall, and repressing cell expansion. Considering data discussed in Chapter 6.2, blue light would be proposed to promote CLF activity in a CRY1-dependent manner, and this would play a major role in the light-induced repression of these genes and ensuing inhibition of hypocotyl elongation. This hypothesised pathway is illustrated in (Fig. 6.2)

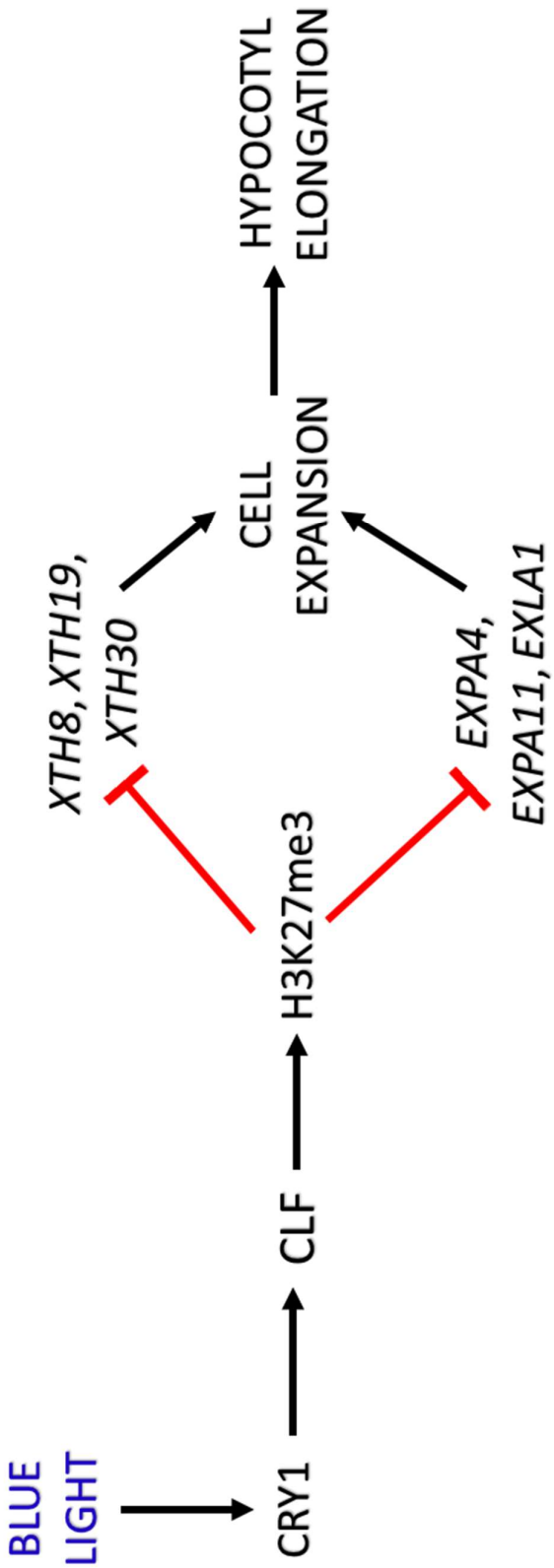

(Fig. 6.2 legend on next page)

Fig. 6.2 Hypothesised pathway of CLF activity during light-induced repression of hypocotyl elongation.

Black arrows indicate hypothesized positive interaction. Red T-Bars indicate hypothesised inhibition.

As discussed, in this thesis it is proposed that CLF is to plays a role in repressing hypocotyl elongation and CLF activity is promoted by blue light in a CRY1-dependent fashion (more detail provided in Fig. 6.1).

It is hypothesised that one mechanism for this activity is via CLF-mediated deposition of H3K27me3 at *EXPANSINS* and *XTH* genes. It is shown in Chapter 3 that *CLF* is transcriptionally induced by white light in a photoreceptor-dependent manner (Fig. 3.10-11) and in Chapter 4 that *clf29* mutation has a significant effect on transcriptional responses to light (Fig. 4.2-5). Further analysis in Chapter 4 indicates that several *EXPANSINS* and *XTH* genes display *CLF-dependent* downregulation upon light exposure (Fig. 4.7), including those displayed in this figure. In Chapter 5 it is shown that at the *EXP11* locus, there is also *CLF*-dependent accumulation of the repressive chromatin mark H3K27me3 upon light exposure (Fig. 5.2). It is hypothesised that the other *EXPANSINS* and *XTH* genes displayed here may also display CLF-dependent accumulation of H3K27me3 after light exposure, based on their CLF-dependent downregulation identified in Chapter 4. This is reinforced by published literature identifying members of these gene classes as both CLF-binding sites and marked by H3K27me3 (Zhang et al., 2008), (Charron et al., 2009), (Shu et al., 2019).

This model is discussed in Chapter 6.3

6.4 CLF regulates auxin signalling in *Arabidopsis*

6.4.1 CLF enhances auxin signalling in cotyledons via deposition of H3K27me3 at Auxin-repressive genes

As well as direct targeting of genes involved in cell expansion, the genetic analysis in Chapter 4 presented another key finding that CLF mediated transcriptional changes at hormone signalling genes. In particular, RNA-seq identified a CLF-dependent downregulation of auxin and brassinosteroid (BR) signalling genes (Fig. 4.5, 8-9). Initially, some of these data appeared difficult to interpret alongside the phenotypic observations presented in Chapter 3 that CLF plays a repressive role on auxin signalling. For example, the downregulation of several auxin-repressive genes, including several *AUX*/*IAA* genes in a *CLF*-dependent manner appeared contradictory with the observation that *clf29* mutation results in increased hypocotyl elongation (Fig. 3.2), a process which is promoted by auxin. In Chapter 4, it was initially hypothesised that since the *AUX*/*IAA* genes are transcriptionally induced by auxin, that this could be a result of a CLF-mediated reduction in auxin levels, which would correlate with the *clf29* phenotype of longer hypocotyls (Fig. 3.1-4).

However, data in Chapter 5 present a different perspective on this data. It is shown that the regulation of *IAA1* and *WES1* is directly linked to CLF activity, as these genes display a *CLF*-dependent increase in H3K27me3 levels (Fig. 5.1-2) as well as the *CLF*-dependent transcriptional repression. This shows that these genes are direct targets of CLF-mediated gene repression, rather than a by-product of CLF-mediated effects on other processes such as auxin synthesis. Previous data in the literature reinforce this view, particularly with regards to CLF-mediated regulation of *AUX*/*IAA* genes. In addition to *IAA1*, *IAA6* and *IAA17* have been identified as marked by H3K27me3 in a whole-genome analysis (Zhang

et al., 2007), whilst *IAA17* has also been identified in a second dataset as displaying an increase in H3K27me3 upon light perception (Charron et al., 2009). Meanwhile, *IAA6* and *IAA2* have been identified as CLF-binding targets (Shu et al., 2019). All these *AUX*/*IAA* genes are identified in this thesis as showing CLF-dependent downregulation upon light perception (Fig. 4.8). As such it can be hypothesised that some, or all, of these genes will also experience CLF-dependent H3K27me3 accumulation upon light perception. As such, it can be concluded that silencing of *AUX*/*IAA* genes via deposition of H3K27me3 represents a key mechanism of CLF action during light signalling.

In Chapter 5, analysis of auxin levels in Col0 and *clf29* plants via GUS staining in Col0 shows that this CLF-mediated repression of *AUX*/*IAA* genes has a massive effect on auxin signalling. *clf29* plants have distinctly reduced auxin in the cotyledons of *clf29* mutants both before and after light perception (Fig. 5.3).

Another CLF target identified in the RNA-seq and ChIP-qPCR analyses is that the GH3 gene *WES1* (*GH3.5*) also displays *CLF*-mediated repression upon light perception. Similarly to *IAA1*, *WES1* is shown in this thesis to display reduced transcription (Fig. 4.8) and accumulation of H3K27me3 after light perception (Fig. 5.2), both in a *CLF*-dependent manner.

In the context of the cotyledons, this is consistent with the model discussed above. WES1 functions to repress auxin signalling by facilitating conjugation of IAA to Asp residues, which leads to the degradation of IAA (Staswick et al., 2005), (Park et al., 2007b). As such, it can be proposed that *WES1* represents another target gene during CLF-mediated promotion of auxin signalling in the hypocotyls.

The enhancement of expression of *GH3* and *AUX*/*IAA* genes is thought to represent a key negative feedback mechanism during auxin signalling in plants. Auxin-induced expression

of GH3 genes such as *WES1* limits the pool of active endogenous auxin, whilst auxin-induced expression of *AUX*/*IAA* genes represses the activation of ARFs (Park et al., 2007b) (Zhou et al., 2015). In this context, an intriguing the repression of these genes by CLF could be proposed to inhibit a key negative feedback mechanism limiting the scale of auxin signalling, leading to an enhancement of auxin signalling and the promotion of processes such as cotyledon expansion.

Overall, there is clear evidence to support a hypothesised molecular pathway in which CLF promotes auxin signalling in cotyledons by mediating H3K27me3 accumulation at auxin-repressive genes, including *AUX*/*IAA* genes and the GH3 gene *WES1*, as illustrated in (Fig. 6.3). It can be hypothesised that this would result in *clf29* plants being deficient in the process of cotyledon opening due to lack of auxin-promoted cell expansion, and that this activity would be promoted by blue light in a CRY1-dependent manner. Further phenotypic analysis to provide evidence for these two hypothesised elements of this pathway would be desirable.

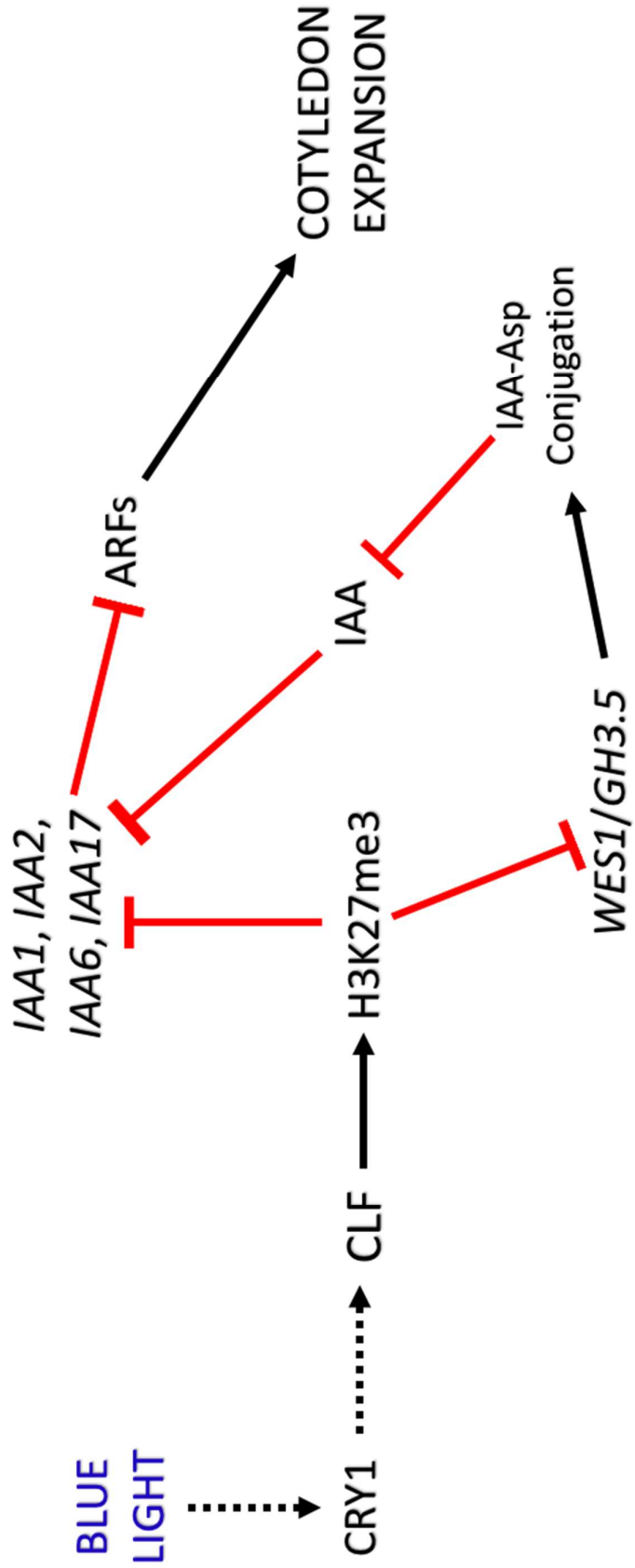

Fig 6.3 (Legend on next page)

Fig. 6.3 Hypothesised CLF effects on auxin signaling during cotyledon expansion.

Black arrows indicate hypothesized positive interaction. Red T-Bars indicate hypothesised inhibition. Dashed arrows indicate potential interaction requiring further investigation.

CLF is proposed to contribute to cotyledon expansion upon light perception based on transcriptional data presented in Chapter 4, and chromatin immunoprecipitation and DR5::GUS assays presented in Chapter 5. In Chapter 4 it is shown that several genes involved in auxin signaling display CLF-dependent downregulation upon light exposure (Fig. 4.8). These genes include several *AUX*/*IAA* genes and the GH3 gene *WES1*/*GH3.5*. In Chapter 5, chromatin immunoprecipitation data show that alongside this *CLF*-dependent downregulation there is also a *CLF*-dependent accumulation of the repressive chromatin mark H3K27me3 at the *IAA1* and *WES1* loci (Fig. 5.1-2). It is hypothesised that other *AUX*/*IAA* genes displayed here may also display CLF-dependent accumulation of H3K27me3 after light exposure, based on their CLF-dependent downregulation identified in Chapter 4. This is reinforced by published literature identifying *AUX*/*IAA* genes as both CLF-binding sites and marked by H3K27me3 (Zhang et al., 2008), (Charron et al., 2009), (Shu et al., 2019).

Both *IAA* genes and *GH3* genes repress auxin signaling, and so CLF-dependent repression of these genes is hypothesised to lead to activation of *AUXIN RESPONSE FACTORS* (*ARFs*), facilitating downstream auxin signaling. In Chapter 5 data from DR5::GUS staining assays indicate that *clf29* plants exhibit significantly reduced levels of auxin signaling in cotyledons (Fig. 5.3). Taking this together with the transcriptional and chromatin immunoprecipitation data discussed above, it is hypothesised that CLF promotes auxin signaling in cotyledons by inhibition of auxin-repressive genes such as *AUX*/*IAA* genes and *WES1*.

Other data in this thesis indicate that CLF plays a role in inhibiting hypocotyl elongation in response to blue light, and that this is dependent on CRY1 (Fig. 3. 2, 7) (discussed in Chapter 6.1). It is possible that a similar pathway could occur here, and that CLF could promote cotyledon expansion by enhancing auxin signaling in response to blue light in a CRY1-dependent fashion. However, no phenotypic data is presented in this thesis that links CRY1 activity and CLF's role in auxin signaling, or to show that *clf29* mutation has an effect on cotyledon expansion, so these points cannot be conclusively determined and require further investigation.

6.4.2 *CLF* represses blue-light induced phototropism

To further investigate the role of CLF in auxin signalling, in Chapter 5 an analysis is made on the effect of *clf29* mutation in blue-light induced phototropism. Phototropism, primarily regulated by the photoreceptors PHOT1 and PHOT2, is driven by a build up of auxin on the shaded side of the hypocotyl, which promotes a higher degree of cell elongation on the shaded side, which causes the hypocotyl to bend towards the light (Went and Thimann, 1937), (Holland et al., 2009). As such, these data provide further evidence for a role of CLF in mediating light signalling.

It was considered that this could indicate a role for CLF in regulation of auxin transport, a possibility also suggested by the maintenance of a strong apical gradient of auxin at the top of the hypocotyl 6 hours after light perception (Fig. 5.4). However, no light-mediated regulation of PIN genes or *AUX*/*LAX* genes is identified by the RNA-seq data in either Col0 or *clf29* seedlings (full lists of DEGs can be found in Appendix 2), meaning that there is no genetic evidence to support a hypothesis of CLF-mediated regulation of auxin transport.

As such, the mechanism by which CLF mediates repression of phototropism cannot be conclusively determined by data presented in this thesis, and is worthy of further investigation. In particular, it would be valuable to carry out GUS staining assays of Col0 and *clf29* plants carrying the *pDR5::GUS* construct as they are undergoing phototropism in response to directional blue light. This would provide evidence as to whether redistribution of auxin during blue light-induced phototropism is affected in a *clf29* plant line.

Additionally, it is also possible that this enhancement of phototropism is due to the effect of *CLF* in mediating blue-light inhibition of hypocotyl elongation. As discussed in Chapter 6.2, this thesis provides strong evidence that CLF acts downstream of CRY1 to facilitate

repression of hypocotyl elongation via silencing of cell-expansion-related genes such as expansins and *XTH* genes, an activity which is promoted by blue light and also requires PHYA (Fig. 6.1-2). Abolition of this *CLF*-mediated repression of hypocotyl elongation could lead to enhanced growth on the shaded side of the hypocotyl, causing the enhanced phototropism response seen here. Furthermore, *clf29* mutation has no phenotypic effect on either blue-light hypocotyl lengths or blue-light phototropism in a *phyA* or a *cry1* genetic background (Fig. 3. 7) (Fig. 5.6). This could be interpreted as evidence that CLF effects on phototropism occur via its repressive effect on blue-light mediated hypocotyl elongation, downstream of these two photoreceptors.

The observed light-induced repression of the auxin-repressive gene *WES1* is also worth considering further at this point, with regards to both phototropism and hypocotyl elongation. As discussed in Chapter 6.2, CLF-dependent repression of *WES1* would be consistent with CLF playing a role in enhancement of auxin signalling at the cotyledons, resulting in the drastically reduced levels of auxin seen in this organ in a *clf29* plant (Fig. 5.4).

However, as mentioned in Chapter 4, this *CLF*-dependent repression of *WES1* upon light perception represents an apparent contradiction to the long-hypocotyl phenotype observed in *clf29* mutants, which is worthy of further consideration due to strong parallels with a previous finding in the literature. WES1 has a repressive effect on hypocotyl elongation, with *wes1-D* gain-of-function mutants displaying shorter, and *wes1* loss-of-function mutants longer hypocotyls in light grown seedlings (Park et al., 2007a). However, in an apparent contradiction to this, *WES1* is known to be transcriptionally repressed upon light perception, and it is also known that this occurs specifically in the hypocotyls, with two published analyses of organ-specific transcriptional regulation upon light perception finding that *WES1* transcription is repressed both in the cotyledons and

the hypocotyl (Ma et al., 2005), (Sun et al., 2016). Furthermore, *WES1* transcription was distinctly higher in a *phyB* mutant, and slightly higher in both a *cry1* and *cry2* mutants compared to Col0 wild type (Park et al., 2007a). This suggests that photoreceptors are involved in the transcriptional repression of *WES1* in the hypocotyl after light perception, despite the fact that higher *WES1* expression represses hypocotyl elongation. CLF appears to display a similar paradox – CLF is required for the light-induced repression of *WES1* transcription via deposition of H3K27me3, despite the fact that WES1 promotes the same phenotypic effect as CLF in the hypocotyls (repression of elongation).

A similar phenomenon is observed with *WES1* during phototropism. *WES1*, along with another GH3 gene, *GH3.6*/*DFL1*, has been observed to accumulate on the side showing enhanced growth during tropic responses (Esmon et al., 2006). Given the repressive role of *WES1* on auxin signalling by promoting degradation of auxin, this would be expected to inhibit auxin-induced cell elongation in the shaded section of the hypocotyl. Correspondingly, this is thought to represent a negative feedback mechanism limiting the scale of tropic responses (Esmon et al., 2006), (Liscum et al., 2016). Again, the direct targeting of *WES1* for transcriptional repression by CLF-mediated deposition of H3K27me3 (Fig. 5.2) is difficult to reconcile with the observation that *clf29* mutation results in enhancement of phototropism, a trait which would be expected to be promoted by the CLF-mediated repression of *WES1*.

6.5 CLF activity may be regulated by interaction with PIF4

Finally, another intriguing finding is presented in Chapter 5 from a yeast two hybrid experiment analysing protein-protein interactions between CLF and core components of light signalling pathways. A candidate interaction is presented between CLF and PIF4 (Fig. 5.3). If confirmed *in vivo*, this would represent a novel interactive partner of CLF.

This interaction presents a potential mechanism for the regulation of CLF activity during light signalling. Further work is required to demonstrate physiological significance interaction, but an intriguing possibility can be hypothesised based on PIF4 interactions with other key factors functioning during light signalling. In particular, PIF4 interacts with the BR-responsive transcription factor *BZR1* and the auxin-responsive transcription factor *ARF6*, with these three factors being descried as forming a single transcriptional module called the BAP module, as discussed in Chapter 1.2 (Boure et al., 2019). This interaction with PIF4 has a distinct effect on the activity of these transcription factors, and these transcription factors together with PIF4 co-operatively regulates a number of their target genes (Oh et al., 2012) (Oh et al., 2014). It is highly tempting to propose that a CLF-PIF4 interaction could have a similar effect, and play a role in regulating the activity of either CLF or PIF4 as transcriptional regulators. Additionally, it is possible that PIF4 could play a role in guiding CLF to target genes. It is of great relevance to this hypothesis that CLF does not possess intrinsic DNA-binding activity (Schubert et al., 2006), (Zhou et al., 2018). Although reports in recent years have identified sequences enriched at H3K27me3 and CLF/SWN binding regions, there no currently known consensus recruitment sites for PRC2, and the mechanisms by which CLF and SWN are recruited to specific gene loci remain under investigation (Deng et al., 2013), (Zhou et al., 2018), (Shu et al., 2019).

However, it must be noted that here an opposite relationship would be expected than that seen between PIF4 and other members of the BAP transcriptional module. *ARF6*, *BZR1* and *PIF4* are all key promoters of skotomorphogenesis, and as such function to synergistically regulate a number of target genes (Oh et al., 2012), (Oh et al., 2014). In contrast, data in this thesis indicate that CLF plays a role in characteristics of photomorphogenesis, such as inhibition of hypocotyls and auxin signalling in the cotyledons. As such, it would be hypothesised that CLF and PIF4 would play antagonistic

roles at common target genes, potentially similar to that seen with HY5 (Toledo-Ortiz et al., 2014).

In further support of this hypothesis, previous knowledge in the literature has shown that PIFs can regulate modification of chromatin in response to light signals via physical interaction. Several PIFs, including PIF4, were shown to interact with members of the INO80C complex to facilitate removal of H2A.Z during low red:far-red responses (Willige et al., 2021), whilst PIF3 has also been shown to interact with the histone deacetylase HDA15 to facilitate repression of chloroplast biogenesis in etiolated seedlings (Liu et al., 2013).

6.6 Priorities for further work in this area

The data presented in this thesis identify a number of priorities for further work, in order to confirm hypotheses presented in this thesis, or answer questions raised by the data.

6.6.1 CLF regulation by light and photoreceptors

As has been discussed previously, there are limitations to the conclusions presented here that CLF is involved in light signalling due to *clf29* plants also exhibiting elongated hypocotyls in darkness. Photoreceptor-dependent increases in transcription and light phenotypes provide evidence that CLF is regulated by light signalling, but it would be desirable to further demonstrate this by more detailed analysis of phenotypes. Hypocotyl assays examining the magnitude of hypocotyl elongation seen in *clf29* plants under darkness and different wavelengths of light should be carried out to analyse whether the increase in CLF transcription seen upon light perception translates to a more severe *clf29* phenotype with regards to hypocotyl elongation.

Another experimental priority would be to identify how individual wavelengths of light regulate *CLF* transcription. This work has shown that *CLF* is transcriptionally induced by

light and has phenotypic effects under blue and far-red light, but not under red light, which suggests that red light may repress *CLF* activity. To confirm this, further qPCR analysis could be used to analyse changes in *CLF* transcription in dark-grown seedlings exposed separately to monochromatic red, blue and far-red light. This analysis could also then be repeated in photoreceptor mutants in each light condition, in order to further understand potential roles of PHYA and PHYB in the regulation of CLF activity, alongside that shown for CRY1. The candidate genes identified as differentially expressed during light responses in WT and *clf29* mutants, such as *IAA1* and *WES1* could also be analysed before and after exposure to individual wavelengths of light, to correlate CLF transcriptional regulation in different light regimes with effects on downstream target genes. This would also allow further demonstration that CLF functions during light signalling, and its activity is regulated by light.

Many of the analyses in Chapter 5 should also be carried out in other plant lines to analyse the effects of photoreceptors on *CLF* activity as well. The acquisition of H3K27me3 at the gene loci in Chapter 5.2 (*IAA1*, *WES1* and *EXP11*) should be analysed in a *cry1* and *cry1clf29* loci. Based on phenotypic and transcriptional data, it is concluded throughout this thesis that CRY1 activity is highly correlated with CLF activity, and that a *clf29* mutation has little to no effect in a CRY1 mutant. If it was found that the abolition of H3K27me3 deposition at CLF-repressed gene loci was also abolished in a *cry1* plant line, this would further reinforce this hypothesis, particularly if the same abolition of H3K27me3 was not detected in photoreceptor mutants which do not appear linked to CLF, such as *cry2*. Furthermore, it is proposed that several genes not directly analysed in this thesis may also display accumulation of H3K27me3 in a CLF-dependent manner, based on previous observations in the literature. Confirmation of this via further ChIP-qPCR analysis at other genomic locations would reinforce this hypothesis.

6.6.2 CLF activity during auxin signalling

GUS staining indicates that *clf29* plants exhibit reduced auxin levels in the cotyledons, but the auxin-gradient at the top of the hypocotyl involved in apical hook formation still seems prevalent. To investigate the phenotypic effects of this, it would be desirable to analyse the rate of cotyledon expansion and unfolding of the apical hook in a *clf29* plant compared to Col0. GUS staining of plants exhibiting phototropism would also be desirable to further assess a potential role for *CLF* in auxin transport and spatio-temporal effects of CLF activity on auxin signalling during photomorphogenesis. In particular, it would be interesting to observe whether *clf29* mutants displayed enhanced or reduced auxin signalling during phototropism, and whether the establishment of a gradient of auxin across the hypocotyl during the process was affected by *clf29* mutation.

6.6.3 Candidate CLF-PIF4 interaction

Finally, the PIF4 interaction identified in Chapter 5 presents an intriguing area for further study, and an immediate priority would be to further validate this interaction by co-immunoprecipitation and also demonstrate the interaction *in plantae* via a split-luciferase assay. If verified, further experiments to assess the biological meaning of this interaction could include analysis of the relationship between PIF4- and CLF- mediated transcription. This could be examined by analysing the effect of *clf29* mutation on transcription of key CLF-mediated target genes identified here in both a *pif4* loss-of-function mutant and a PIF4ox mutant, to investigate potential roles for PIF4 in targeting of CLF to specific genes.

6.6.4 Use of a second *clf*- knockout line to increase confidence in conclusions

Finally, it must be acknowledged that there is a caveat to conclusion drawn from data in this thesis regarding CLF activity. This work has made use of a SALK insertion line carrying a T-DNA insertion at the *CLF* gene locus, SALK_021003. This plant line has been confirmed

to carry the T-DNA insertion at the *CLF* gene locus, and to lack the WT *CLF* gene (genotyping data provided in Appendix 4). However, it must be noted that no complementation analysis is presented in this thesis to verify that the plant line does not carry additional T-DNA insertions at other genomic loci.

clf29 is an established plant line in the literature and has been used in published studies as the sole single *clf*- knockout line (e.g. (Chen et al., 2014), (De lucas et al., 2016), (Jiang et al., 2019), (Shu et al., 2019), (Shu et al., 2020)). However, no work in this thesis has been carried out to conclusively identify that there are no off-target insertions in the genetic background of this plant line.

In order to increase confidence in conclusions drawn from this study, it would thus be desirable to repeat some of the assays presented here with a separate *clf* loss-of-function line, such as *clf-28* (SALK_139371) (Doyle and Amasino, 2009). In particular, it would be desirable to repeat the hypocotyl assays presented in Chapter 3. If *clf28* showed the same phenotypic effects as *clf29* in these assays, it would increase confidence in asserting these as the effect of a *clf* loss of function mutation.

6.7 Concluding Remarks

The data presented in this thesis present an exciting novel role for PRC2 activity, functioning through the histone methyltransferase CLF, in the regulation of light signalling during *Arabidopsis* development. It is shown that CLF activity is likely induced by blue light, but repressed by red light, offering a novel mechanism by which specific light wavelengths may regulate chromatin modification.

In particular, data are presented supporting a molecular pathway in which CLF functions downstream of CRY1 during blue light signalling to repress the elongation of hypocotyls via deposition of the silencing histone modification H3K27me3 at expansins and *XTH*

genes. Potential roles for PHYA and PHYB are identified, and suggestions made for further studies to fully elucidate how these photoreceptors may be related to CLF activity, as well as the action of far-red light.

Additional data show that CLF is involved in the enhancement of auxin signalling in the cotyledons via the H3K27me3-mediated silencing of *AUX*/*IAA* and *GH3* genes, potentially serving to inhibit a natural negative feedback loop which limits the scale of auxin signalling in the plant. Data also indicate a role for CLF in further auxin-regulated processes including blue light-mediated phototropism, and potentially in the regulation of the apical hook, and its light-induced abolition. Again, suggestions are made for additional investigations to further clarify and understand this function of CLF.

Finally, a Yeast-Two-Hybrid assay identifies an intriguing candidate interaction between CLF and PIF4, a key transcriptional regulator of skotomorphogenesis, which may play a role in the targeting of CLF to key gene loci during this process.

Overall, this thesis presents an exciting novel link between chromatin modification and light during plant development, and opens up a number of potential areas for further research.

Appendix 1 – Primers used in this Thesis

Primers used for genotyping SALK mutants *clf29* and *swn7*

Plant Line	Primer	Sequence
All SALK Mutants	*LB*	ATTTTGCCGATTTCGGAAC
clf29 (SALK_021003)	*LP*	AAGAAACTTGCTAGTTCCGCC
	RP	GAGGCATTGACTTTGATTTGC
swn7 (SALK_109121C)	*LP*	TGATTATTGCTCCGTTTCCAC
	RP	CGAGGAATTTTCTAATTCCGG

Primers used for genotyping photoreceptor mutants

Plant Line	Primer	Sequence
phyA-211	*LP*	TGCAGGAGATAGCTTCATGGT
	RP	CAGCGGGTTTGGATTTTGGA
phyB-9	*LP*	AAGAAACTTGCTAGTTCCGCC
	RP	GAGGCATTGACTTTGATTTGC
cry1-hy4-b104	*LP*	AGCGGTTCGATCATTCAACG
	RP	TGAGAGAGTCGGATTTGCGA
cry2-1	*LP*	AAGGGGTATACGAGGATTCAAAGT
	RP	ACAACTAGTGGCGTGTGTTC

Primers used for genotyping plants carrying the *pDR5:GUS* construct

Plant Line	Primer	Sequence
pDR5:GUS construct	*LP*	
	RP	

Primers used for RT-qPCR Analysis

Gene	Primer	Sequence
UB10	*LP*	AAAGAGATAACAGGAACGGAAACATAGT
	RP	GGCCTTGTATAATCCCTGATGAATAAG
CLF	*LP*	ACCACACCCACGAAGTTCTC
	RP	ACCTTTGGCGATGATGAAAC
PP2AA3	*LP*	TAACGTGGCCAAAATGATGC
	RP	GTTCTCCACAACCGCTTGGT
IAA1	*LP*	GACACAGAGCTTCGTTTGGG
	RP	GGCCATCCAACGATTTGTGT
IAA6	*LP*	TCACAGAGCTTCGATTGGGT
	RP	CTTGACTCTTCACAACCGGC

Primers used for ChIP-qPCR Analysis

Gene	Primer	Sequence
UB10	*LP*	TGCAGGAGATAGCTTCATGGT
	RP	CAGCGGGTTTGGATTTTGGA
IAA1	*LP*	GCTCCTCCTCCTGCAAAGTA
	RP	GGCCATCCAACGATTTGTGT
EXP11	*LP*	CGCCAATCCAGCTAGAGACT
	RP	CGCTTCCCACCTTTATTTAAACA
WES1	*LP*	AGCGTTCACTTAATTCCTCGA
	RP	GCAAGCTTTTAGTGTGTGAGGA

Primers used for hot fusion cloning I – Amplification of cDNA sequences

Gene	Vector	Primer	Sequence
CLF	*pGADT7*	*LP*	GTACCAGATTACGCTCATATGGCGTCAGAAGCTTCGCCTT
		RP	ATTCATCTGCAGCTCGACTAAGCAAGCTTCTTGGGTCTA
	pGBKT7	*LP*	CAGAGGAGGACCTGCATATGGCGTCAGAAGCTTCGCCTT
		RP	GCTAGTTATGCGGCCGCCTAAGCAAGCTTCTTGGGTCTA
PIF3	*pGADT7*	*LP*	GTACCAGATTACGCTCATATGCCTCTGTTTGAGCTTTTCA
		RP	ATTCATCTGCAGCTCGATCACGACGATCCACAAAACTGA
	pGBKT7	*LP*	CAGAGGAGGACCTGCATATGCCTCTGTTTGAGCTTTTCA
		RP	GCTAGTTATGCGGCCGCTCACGACGATCCACAAAACTGA
PIF4	*pGADT7*	*LP*	GTACCAGATTACGCTCATATGGAACACCAAGGTTGGAGTT
		LP	ATTCATCTGCAGCTCGACTAGTGGTCCAAACGAGAACCG
	pGBKT7	*LP*	CAGAGGAGGACCTGCATATGGAACACCAAGGTTGGAGTT
		RP	GCTAGTTATGCGGCCGCCTAGTGGTCCAAACGAGAACCG
PIF5	*pGADT7*	*LP*	GTACCAGATTACGCTCATATGGAACAAGTGTTTGCTGATT
		RP	ATTCATCTGCAGCTCGATCAGCCTATTTTACCCATATGA
	pGBKT7	*LP*	CAGAGGAGGACCTGCATATGGAACAAGTGTTTGCTGATT
		RP	GCTAGTTATGCGGCCGCTCAGCCTATTTTACCCATATGA
COP1	*pGADT7*	*LP*	GTACCAGATTACGCTCATATGGAAGAGATTTCGACGGATC
		RP	ATTCATCTGCAGCTCGACCAGCAAACCGCACTAATAAAG
	pGBKT7	*LP*	CAGAGGAGGACCTGCATATGGAAGAGATTTCGACGGATC
		RP	GCTAGTTATGCGGCCGCCCAGCAAACCGCACTAATAAAG
PHYA	*pGADT7*	*LP*	GTACCAGATTACGCTCATATGTTGGAAATGAAAGAATTCA
		RP	ATTCATCTGCAGCTCGACTACTTGTTTGCTGCAGCGAGT
	pGBKT7	*LP*	CAGAGGAGGACCTGCATATGTTGGAAATGAAAGAATTCA
		RP	CAGAGGAGGACCTGCATATGTTGGAAATGAAAGAATTCA

PHYB	*pGADT7*	*LP*	GTACCAGATTACGCTCATATGGAAGAGTTTTTCCTTGGAA
		RP	ATTCATCTGCAGCTCGACTAATATGGCATCATCAGCATC
	pGBKT7	*LP*	CAGAGGAGGACCTGCATATGGAAGAGTTTTTCCTTGGAA
		RP	GCTAGTTATGCGGCCGCTCAGCCAGGAGCTGTTGAATCC
CRY1	*pGADT7*	*LP*	GTACCAGATTACGCTCATTCAGATGTGGCAACTAGAAGCTG
		RP	ATTCATCTGCAGCTCGATTACCCGGTTTGTGAAAGCCGT
	pGBKT7	*LP*	ATCTCAGAGGAGGACCTGCATCAGATGTGGCAACTAGAAGCTG
		RP	TATGCTAGTTATGCGGCCGCTTACCCGGTTTGTGAAAGCCGT
CRY2	*pGADT7*	*LP*	GTACCAGATTACGCTCATTCAAGAACCCGTGAAGCACAGA
		RP	ATTCATCTGCAGCTCGATCATTTGCAACCATTTTTTCCC
	pGBKT7	*LP*	ATCTCAGAGGAGGACCTGCATTCAAGAACCCGTGAAGCACAGA
		RP	TATGCTAGTTATGCGGCCGCTCATTTGCAACCATTTTTTCCC

Primers used for hot fusion cloning II – Colony PCR

Primer	**Sequence**
T7 Promoter	TAATACGACTCACTATAGGG
pGADT7 Reverse	AGATGGTGCACGATGCACAG
pGBKT7 Reverse	TAAGAGTCACTTTAAAATTTGTATC

Appendix 2 – Full list of differentially expressed genes in RNA-seq analysis

The full lists of differentially expressed genes identified by RNA-seq can be found in the excel file "Appendix 2 - List of differentially expressed genes identified by RNA-seq". The following lists of DEGs are included:

Sheet 1: Col0 dark-light upregulated genes

Sheet 2: Col0 dark-light downregulated genes

Sheet 3: *clf29* dark-light upregulated genes

Sheet 4: *clf29* dark-light downregulated genes

Sheet 5: Col0 Light – *cry1* Light upregulated genes

Sheet 6: Col0 Light – *cry1* Light downregulated genes

Sheet 7: Col0 Light – *cry2* Light upregulated genes

Sheet 8: Col0 Light – *cry2* Light downregulated genes

Sheet 9: Col0 Light – *phyA* Light upregulated genes

Sheet 10: Col0 Light – *phyA* Light downregulated genes

Sheet 11: Col0 Light – *phyB* Light upregulated genes

Sheet 12: Col0 Light – *phyB* Light downregulated genes

Sheet 13: *cry1* Light – *cry1clf29* Light upregulated genes

Sheet 14: *cry1* Light – *cry1clf29* Light downregulated genes

Sheet 15: *cry2* Light – *cry2clf29* Light upregulated genes

Sheet 16: *cry2* Light – *cry2clf29* Light downregulated genes

Sheet 17: *phyA* Light – *phyAclf29* Light upregulated genes

Sheet 18: *phyA* Light – *phyAclf29* Light downregulated genes

Sheet 19: *phyB* Light – *phyBclf29* Light upregulated genes

Sheet 20: *phyB* Light – *phyBclf29* Light downregulated genes

Appendix 3 – Full results of ontology analysis of differentially expressed genes in RNA-seq Analysis

The full results of gene ontology analysis of DEGs identified by RNA-seq can be found in the excel file "Appendix 3 Appendix 3 - Results of gene ontology analysis of DEGs in Col0 and *clf29*"

The following lists of ontology analysis results are included:

Sheet 1: Col0 dark-light upregulated genes

Sheet 2: Col0 dark-light downregulated genes

Sheet 3: *clf29* dark-light upregulated genes

Sheet 4: *clf29* dark-light downregulated genes

Appendix 4 – Genotyping data for plant lines used in this study

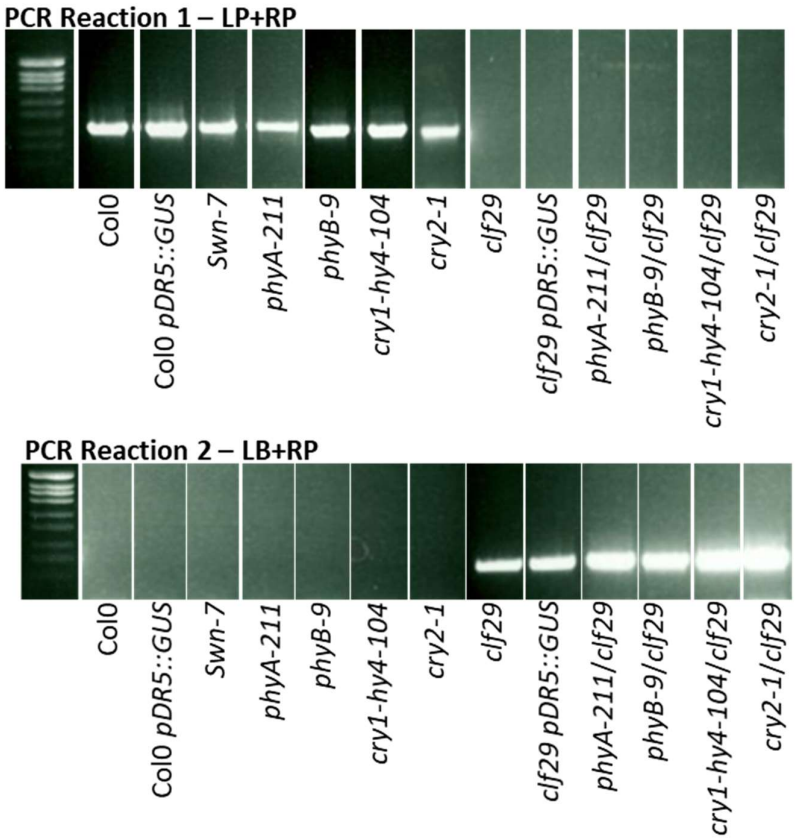

Fig. S1 *clf29* genotyping

As described in Chapter 2.2.3.1, plants carrying *clf29* SALK insertions (SALK_021003) and their respective wild-types were genotyped using two separate PCR reactions, with primers designed using the tDNA express primer design tool (http://signal.salk.edu/tdnaprimers.2.html)

In Reaction 1, a PCR is performed using two primers that bind within the *CLF* gene locus (LP and RP). The sequences for these primers are found in Appendix 1. This PCR reaction gives a product of 1154bp if the wild-type *CLF* gene is present.

In Reaction 2, a PCR is performed using the Right-hand Primer (RP) from reaction 1 along with a primer that binds within the T-DNA insertion found in SALK_021003 (LB). The sequences for these primers are listed in Appendix 1. This PCR reaction gives a product of 538-838bp if the SALK_021003 T-DNA insertion is present.

Genomic DNA from a heterozygous mutant produces a product in both PCR reactions.

As shown, all *CLF+* plants used in this study are shown to produce a PCR product in Reaction 1, but not in reaction 2, indicating that the SALK_021003 T-DNA insertion is not present in any of these lines, and they all possess a wild-type *CLF* gene. The presence of *swn-7*, another SALK mutant in this assay demonstrates that this PCR reaction does not produce amplification from T-DNA insertions at the *SWN* gene locus.

All plants carrying a *clf29* mutation used in this study are shown to produce a PCR product in Reaction 2, ut not in reaction 1, indicating that they carry the SALK_021003 T-DNA insertion and do not possess a wild-type *CLF* gene.

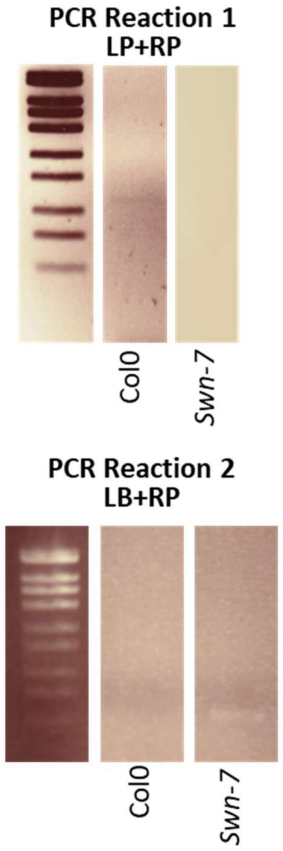

Fig. S2 *swn7* genotyping

As described in Chapter 2.2.3.1, plants carrying *swn-7* SALK insertions (SALK_109121) and their respective wild-type was genotyped using two separate PCR reactions, with primers designed using the tDNA express primer design tool (http://signal.salk.edu/tdnaprimers.2.html)

In Reaction 1, a PCR is performed using two primers that bind within the *SWN* gene locus (LP and RP). The sequences for these primers are found in Appendix 1. This PCR reaction gives a product of 1146bp if the wild-type *SWN* gene is present.

In Reaction 2, a PCR is performed using the Right-hand Primer (RP) from reaction 1 along with a primer that binds within the T-DNA insertion found in SALK_021003 (LB). The sequences for these primers are listed in Appendix 1. This PCR reaction gives a product of 464-764bp if the SALK_021003 T-DNA insertion is present.

Genomic DNA from a heterozygous mutant produces a product in both PCR reactions.

As shown, the Col0 plants used in this study are shown to produce a PCR product in Reaction 1, but not in reaction 2, indicating that the SALK_021003 T-DNA insertion is not present in these lines, and they possess a wild-type *CLF* gene. *swn-7* plants used in this study are shown to produce a PCR product in Reaction 2, but not in reaction 1, indicating that they carry the SALK_021003 T-DNA insertion and do not possess a wild-type *SWN* gene.

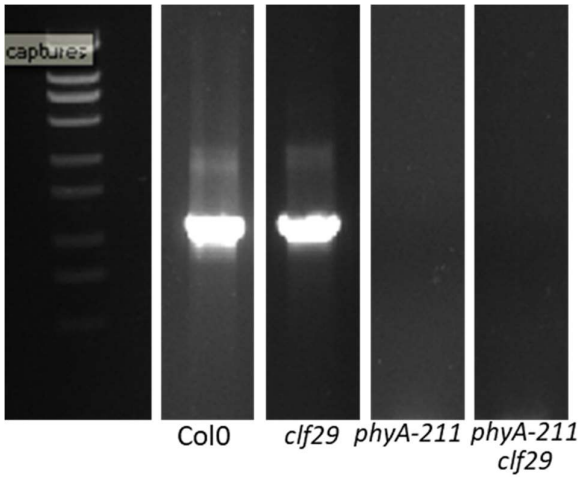

Fig. S3 *phyA-211* genotyping.

As discussed in Chapter 2.2.3.1, *phyA-211* contains a deletion in the *PHYA* locus, but the exact location has not been described (Reed et al., 1994).

Primers were designed amplifying within the *PHYA* locus, and primer pairs were identified that reliably produced amplification from both Col0 DNA and *clf29* DNA, but did not produce amplification from plants carrying a *phyA-211* deletion (shown above). PCR reactions were ran as described in 2.2.3.3 then ran on a 1% w/v agarose gel.

Genomic DNA from *phyA-211* single mutants and *phyA-211clf29* double mutants failed to produce amplification using these primers, indicating that both of these plant lines carry the *phyA-211* deletion.

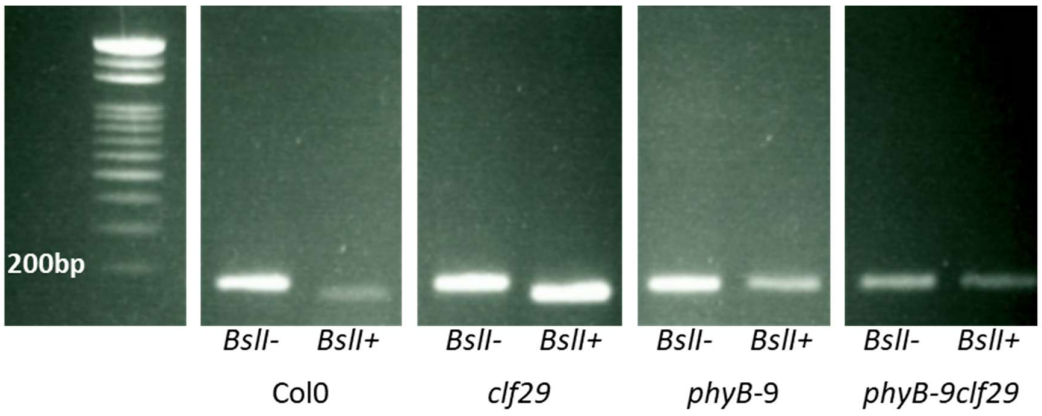

Fig. S4 *phyB-9* genotyping

Plants were genotyped for the presence of the *phyB*-9 point mutation using dCAPs primers as and *BslI* digestion as described in (Neff et al., 1998).

DNA from Col0, *phyB-9, clf29* and *phyBclf29* double mutants was used to carry out a PCR reaction using dCAPs primers (sequences listed in Appendix 1). In a plant containing the WT *PHYB* gene, this produces a PCR product 160bp in length containing a *BslI* digestion site ~20bp from one end. In a *phyB-9* plant, a point mutation removes this digestion site, and digestion does not occur. In a heterozygous plant, both digested and undigested product would be present.

PCR reactions were ran as described in Chapter 2.2.3.3, then digested with *BslI* for 1 hour at 55°C. PCR products were then ran on a 2.5% w/v agarose gel. Due to the proximity of the point mutation to the end of the PCR product, the smaller digestion product cannot be seen to verify that digestion has taken place, and so undigested PCR product (*BslI-*) was also ran alongside digested product (*BslI+*) for each plant line. PCR products from Col0 and *clf29* genomic DNA digested with *BslI,* indicating a WT *PHYB* gene. In the *phyB-9* and the *phyB-9clf29* double mutant, digestion did not occur, indicating a *phyB-9* mutation.

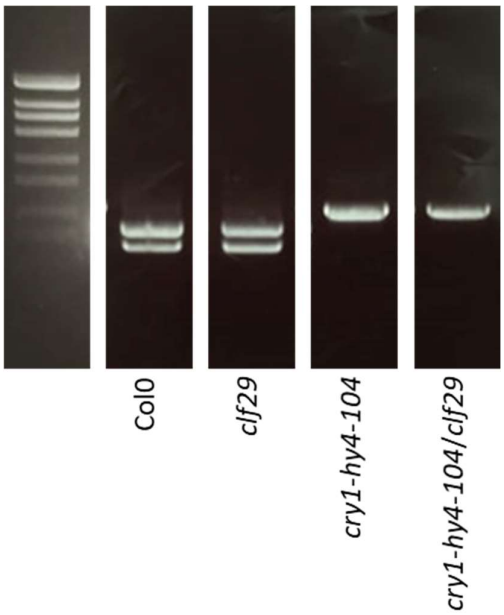

Fig. S5 *cry1-hy4-104* genotyping.

Plants carrying *cry1-hy4-104* deletions were genotyped using PCR amplification followed by *HindIII* digestion.

Plants carrying the *cry1-hy4-104* deletion have a deletion in Exon 3 which removes a *HindIII* digestion site (Bruggeman et al., 1996). Primers were designed flanking Exon 3 of the *CRY1* gene locus (sequences for these primers are listed in Appendix 1). PCR reactions were ran using these primers and genomic DNA from Col0, *clf29*, *cry1-hy4-104* and *cry1-hy4-104*/*clf29* double mutants, using the conditions described in chapter 2.2.3.3. These PCR products were then digested with *HindIII* for 1 hour at 37°C, and ran on a 1% w/v agarose gel.

PCR products from Col0 and *clf29* genomic DNA digested with *HindIII,* indicating a WT *CRY1* gene. In the *cry1-hy4-104* and the *cry1-hy4-104*/*clf29* double mutant, the PCR product did not digest with *HindIII*, indicating that these plants carry the *cry1-hy4-104* deletion that removes this *HindIII* digestion site.

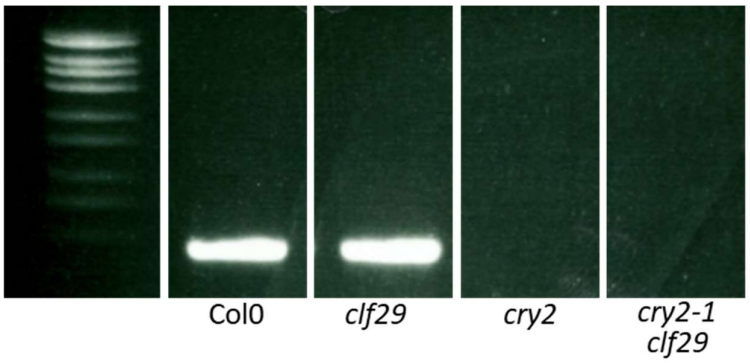

Fig. S6 *cry2-1* genotyping.

As discussed in Chapter 2.2.3.1, *cry2-1* contains a deletion in the *CRY2* locus, but the exact location has not been described (Guo et al., 1998).

Primers were designed amplifying within the *CRY2* locus, and primer pairs were identified that reliably produced amplification from both Col0 DNA and *clf29* DNA, but did not produce amplification from plants carrying a *cry2-1* deletion (shown above). PCR reactions were run as described in Chapter 2.2.2.3, then ran on a 1% w/v Agarose gel stained with ethidium bromide

Genomic DNA *cry2-1* single mutants and *cry2-1clf29* double mutants failed to produce amplification using these primers, indicating that both of these plant lines carry the *cry2-1* deletion.

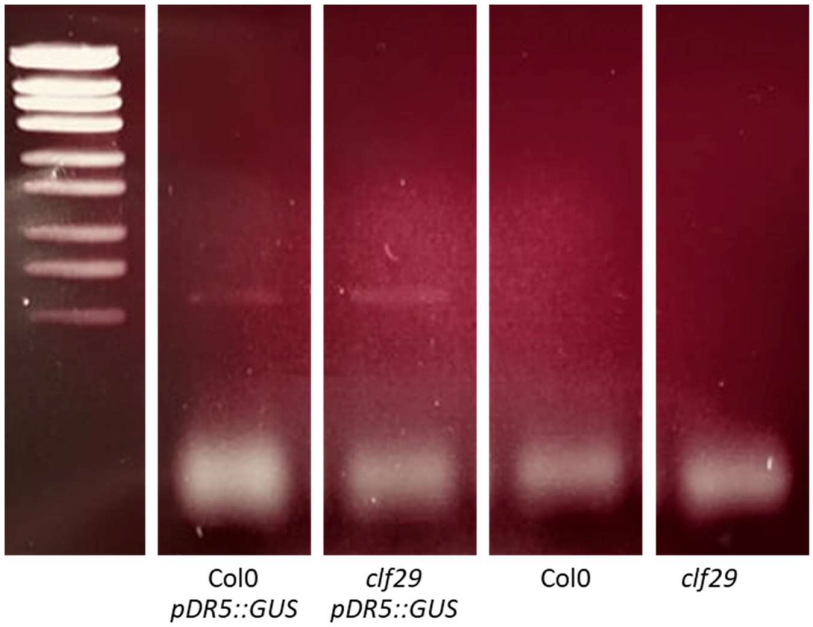

Fig. S7 *pDRF5::GUS* genotyping

The reporter lines used for GUS staining carry a *pDR5::GUS* construct. Col0 and *clf29* plants were genotyped for the presence of the *pDR5::GUS* construct using two primers which amplified within the GUS genomic sequence (sequences listed in Appendix 1). In both plant lines (Col0 and *clf29*), these primers only produced a PCR product when the *pDR5::GUS* construct was present.

PCR reactions were ran as described in Chapter 2.2.3.3, then ran on a 1% w/v agarose gel.

Bibliography

Abbas, M., Alabadí, D., and Blázquez, M.A. (2013). Differential growth at the apical hook: all roads lead to auxin. Front. Plant Sci. *0*.

Abel, S., Oeller, P.W., and Theologis, A. (1994). Early auxin-induced genes encode short-lived nuclear proteins. Proc Natl Acad Sci U S A *91*, 326–330.

Abràmoff, M.D. Image Processing with ImageJ. 7.

Ahmad, M., and Cashmore, A.R. (1993). HY4 gene of A. thaliana encodes a protein with characteristics of a blue-light photoreceptor. Nature *366*, 162–166.

Ahmad, M., Jarillo, J.A., Smirnova, O., and Cashmore, A.R. (1998). The CRY1 Blue Light Photoreceptor of Arabidopsis Interacts with Phytochrome A In Vitro. Molecular Cell *1*, 939–948.

Alabadí, D., Gil, J., Blázquez, M.A., and García-Martínez, J.L. (2004). Gibberellins Repress Photomorphogenesis in Darkness. Plant Physiol *134*, 1050–1057.

Alonso, J.M., Stepanova, A.N., Leisse, T.J., Kim, C.J., Chen, H., Shinn, P., Stevenson, D.K., Zimmerman, J., Barajas, P., Cheuk, R., et al. (2003). Genome-Wide Insertional Mutagenesis of Arabidopsis thaliana. Science *301*, 653–657.

Al-Sady, B., Ni, W., Kircher, S., Schäfer, E., and Quail, P.H. (2006). Photoactivated Phytochrome Induces Rapid PIF3 Phosphorylation Prior to Proteasome-Mediated Degradation. Molecular Cell *23*, 439–446.

Amorim-Silva, V., García-Moreno, Á., Castillo, A.G., Lakhssassi, N., Esteban del Valle, A., Pérez-Sancho, J., Li, Y., Posé, D., Pérez-Rodriguez, J., Lin, J., et al. (2019). TTL Proteins Scaffold Brassinosteroid Signaling Components at the Plasma Membrane to Optimize Signal Transduction in Arabidopsis. The Plant Cell *31*, 1807–1828.

Arsovski, A., Galstyan, A., Waite, J., and Nemhauser, J. (2012). Photomorphogenesis. The Arabidopsis Book / American Society of Plant Biologists *10*, e0147.

Ashburner, M., Ball, C.A., Blake, J.A., Botstein, D., Butler, H., Cherry, J.M., Davis, A.P., Dolinski, K., Dwight, S.S., Eppig, J.T., et al. (2000). Gene Ontology: tool for the unification of biology. Nat Genet *25*, 25–29.

Bai, M.-Y., Shang, J.-X., Oh, E., Fan, M., Bai, Y., Zentella, R., Sun, T., and Wang, Z.-Y. (2012). Brassinosteroid, gibberellin, and phytochrome impinge on a common transcription module in Arabidopsis. Nat Cell Biol *14*, 810–817.

Bannister, A.J., and Kouzarides, T. (2011). Regulation of chromatin by histone modifications. Cell Res *21*, 381–395.

Benhamed, M., Bertrand, C., Servet, C., and Zhou, D.-X. (2006). Arabidopsis GCN5, HD1, and TAF1/HAF2 Interact to Regulate Histone Acetylation Required for Light-Responsive Gene Expression. Plant Cell *18*, 2893–2903.

Bernardo-García, S., Lucas, M. de, Martínez, C., Espinosa-Ruiz, A., Davière, J.-M., and Prat, S. (2014). BR-dependent phosphorylation modulates PIF4 transcriptional activity and shapes diurnal hypocotyl growth. Genes Dev. *28*, 1681–1694.

Bian, S., Li, J., Tian, G., Cui, Y., Hou, Y., and Qiu, W. (2016). Combinatorial regulation of CLF and SDG8 during Arabidopsis shoot branching. Acta Physiol Plant 38, 173.

Boerjan, W., Cervera, M.T., Delarue, M., Beeckman, T., Dewitte, W., Bellini, C., Caboche, M., Van Onckelen, H., Van Montagu, M., and Inzé, D. (1995). Superroot, a recessive mutation in Arabidopsis, confers auxin overproduction. Plant Cell *7*, 1405–1419.

Boron, A.K., Van Loock, B., Suslov, D., Markakis, M.N., Verbelen, J.-P., and Vissenberg, K. (2015). Over-expression of AtEXLA2 alters etiolated arabidopsis hypocotyl growth. Annals of Botany *115*, 67–80.

Bourbousse, C., Mestiri, I., Zabulon, G., Bourge, M., Formiggini, F., Koini, M.A., Brown, S.C., Fransz, P., Bowler, C., and Barneche, F. (2015). Light signaling controls nuclear architecture reorganization during seedling establishment. Proc Natl Acad Sci U S A *112*, E2836–E2844.

Bouré, N., Kumar, S.V., and Arnaud, N. (2019). The BAP Module: A Multisignal Integrator Orchestrating Growth. Trends in Plant Science *24*, 602–610.

Bouyer, D., Roudier, F., Heese, M., Andersen, E.D., Gey, D., Nowack, M.K., Goodrich, J., Renou, J.-P., Grini, P.E., Colot, V., et al. (2011). Polycomb Repressive Complex 2 Controls the Embryo-to-Seedling Phase Transition. PLOS Genetics *7*, e1002014.

Bratzel, F., López-Torrejón, G., Koch, M., Del Pozo, J.C., and Calonje, M. (2010). Keeping cell identity in Arabidopsis requires PRC1 RING-finger homologs that catalyze H2A monoubiquitination. Curr Biol *20*, 1853–1859.

Bruggemann, E., Handwerger, K., Essex, C., and Storz, G. (1996). Analysis of fast neutron-generated mutants at the Arabidopsis thaliana HY4 locus. The Plant Journal *10*, 755–760.

Calonje, M. (2014). PRC1 Marks the Difference in Plant PcG Repression. Molecular Plant *7*, 459–471.

Calonje, M., Sanchez, R., Chen, L., and Sung, Z.R. (2008). EMBRYONIC FLOWER1 Participates in Polycomb Group–Mediated AG Gene Silencing in Arabidopsis. The Plant Cell *20*, 277–291.

Carter, B., Bishop, B., Ho, K.K., Huang, R., Jia, W., Zhang, H., Pascuzzi, P.E., Deal, R.B., and Ogas, J. (2018). The Chromatin Remodelers PKL and PIE1 Act in an Epigenetic Pathway That Determines H3K27me3 Homeostasis in Arabidopsis. The Plant Cell *30*, 1337–1352.

Casal, J.J. (2012). Shade Avoidance. Arabidopsis Book *10*, e0157.

Casal, J.J., and Balasubramanian, S. (2019). Thermomorphogenesis. Annual Review of Plant Biology *70*, 321–346.

Chanvivattana, Y., Bishopp, A., Schubert, D., Stock, C., Moon, Y.-H., Sung, Z.R., and Goodrich, J. (2004). Interaction of Polycomb-group proteins controlling flowering in Arabidopsis. Development *131*, 5263–5276.

Charron, J.-B.F., He, H., Elling, A.A., and Deng, X.W. (2009). Dynamic Landscapes of Four Histone Modifications during Deetiolation in Arabidopsis. The Plant Cell *21*, 3732–3748.

Chaudhury, A.M., Ming, L., Miller, C., Craig, S., Dennis, E.S., and Peacock, W.J. (1997). Fertilization-independent seed development in Arabidopsis thaliana. PNAS *94*, 4223–4228.

Chee-Seng, K., Yun, L.E., Yudi, P., and Kee-Seng, C. (2010). Next Generation Sequencing Technologies and Their Applications. In ELS, (American Cancer Society), p.

Chen, D., Molitor, A., Liu, C., and Shen, W.-H. (2010a). The Arabidopsis PRC1-like ring-finger proteins are necessary for repression of embryonic traits during vegetative growth. Cell Res *20*, 1332–1344.

Chen, M., Galvão, R.M., Li, M., Burger, B., Bugea, J., Bolado, J., and Chory, J. (2010b). Arabidopsis HEMERA/pTAC12 Initiates Photomorphogenesis by Phytochromes. Cell *141*, 1230–1240.

Chen, N., Zhou, W.-B., Wang, Y.-X., Dong, A.-W., and Yu, Y. (2014). Polycomb-group histone methyltransferase CLF is required for proper somatic recombination in Arabidopsis. Journal of Integrative Plant Biology *56*, 550–558.

Cho, J.-N., Ryu, J.-Y., Jeong, Y.-M., Park, J., Song, J.-J., Amasino, R.M., Noh, B., and Noh, Y.-S. (2012). Control of Seed Germination by Light-Induced Histone Arginine Demethylation Activity. Developmental Cell *22*, 736–748.

Choi, D., Kim, J.H., and Lee, Y. (2008). Expansins in Plant Development. In Advances in Botanical Research, (Academic Press), pp. 47–97.

Christie, J.M., Yang, H., Richter, G.L., Sullivan, S., Thomson, C.E., Lin, J., Titapiwatanakun, B., Ennis, M., Kaiserli, E., Lee, O.R., et al. (2011). phot1 Inhibition of ABCB19 Primes Lateral Auxin Fluxes in the Shoot Apex Required For Phototropism. PLoS Biol *9*, e1001076.

Clouse, S.D., Langford, M., and McMorris, T.C. (1996). A brassinosteroid-insensitive mutant in Arabidopsis thaliana exhibits multiple defects in growth and development. Plant Physiol *111*, 671–678.

Cosgrove, D.J. (1993). Wall extensibility: its nature, measurement and relationship to plant cell growth. New Phytol *124*, 1–23.

Cosgrove, D.J. (2016). Plant cell wall extensibility: connecting plant cell growth with cell wall structure, mechanics, and the action of wall-modifying enzymes. Journal of Experimental Botany *67*, 463–476.

Coupland, G., Dash, S., Goodrich, J., Lee, K., Long, D., Martin, M., Puangsomlee, P., Puterill, J., Robson, F., Sundberg, E., et al. (1993). MOLECULAR AND GENETIC ANALYSIS OF THE CONTROL OF FLOWERING TIME IN RESPONSE TO DAYLENGTH IN ARABIDOPSIS THALIANA. Flowering Newsletter 27–32.

Cowling, R.J., and Harberd, N.P. (1999). Gibberellins control Arabidopsis hypocotyl growth via regulation of cellular elongation. Journal of Experimental Botany *50*, 1351–1357.

Czechowski, T., Stitt, M., Altmann, T., Udvardi, M.K., and Scheible, W.-R. (2005). Genome-Wide Identification and Testing of Superior Reference Genes for Transcript Normalization in Arabidopsis. Plant Physiology *139*, 5–17.

Darwin, C. (2009). The Power of Movement in Plants (Cambridge: Cambridge University Press).

De Lucia, F., Crevillen, P., Jones, A.M.E., Greb, T., and Dean, C. (2008). A PHD-Polycomb Repressive Complex 2 triggers the epigenetic silencing of FLC during vernalization. Proceedings of the National Academy of Sciences *105*, 16831–16836.

Debrieux, D., and Fankhauser, C. (2010). Light-induced degradation of phyA is promoted by transfer of the photoreceptor into the nucleus. Plant Mol Biol *73*, 687–695.

Dehesh, K., Franci, C., Parks, B.M., Seeley, K.A., Short, T.W., Tepperman, J.M., and Quail, P.H. (1993). Arabidopsis HY8 locus encodes phytochrome A. Plant Cell *5*, 1081–1088.

Deng, W., Buzas, D.M., Ying, H., Robertson, M., Taylor, J., Peacock, W.J., Dennis, E.S., and Helliwell, C. (2013). Arabidopsis Polycomb Repressive Complex 2 binding sites contain putative GAGA factor binding motifs within coding regions of genes. BMC Genomics *14*, 593.

Deng, X.W., Caspar, T., and Quail, P.H. (1991). cop1: a regulatory locus involved in light-controlled development and gene expression in Arabidopsis. Genes Dev. *5*, 1172–1182.

Derbyshire, P., Findlay, K., McCann, M.C., and Roberts, K. (2007a). Cell elongation in Arabidopsis hypocotyls involves dynamic changes in cell wall thickness. Journal of Experimental Botany *58*, 2079–2089.

Derbyshire, P., McCann, M.C., and Roberts, K. (2007b). Restricted cell elongation in Arabidopsishypocotyls is associated with a reduced average pectin esterification level. BMC Plant Biology *7*, 31.

Derkacheva, M., and Hennig, L. (2014). Variations on a theme: Polycomb group proteins in plants. Journal of Experimental Botany *65*, 2769–2784.

Derkacheva, M., Steinbach, Y., Wildhaber, T., Mozgová, I., Mahrez, W., Nanni, P., Bischof, S., Gruissem, W., and Hennig, L. (2013). Arabidopsis MSI1 connects LHP1 to PRC2 complexes. EMBO J *32*, 2073–2085.

Di Croce, L., and Helin, K. (2013). Transcriptional regulation by Polycomb group proteins. Nat Struct Mol Biol *20*, 1147–1155.

Dong, J., Sun, N., Yang, J., Deng, Z., Lan, J., Qin, G., He, H., Deng, X.W., Irish, V.F., Chen, H., et al. (2019). The Transcription Factors TCP4 and PIF3 Antagonistically Regulate Organ-Specific Light Induction of SAUR Genes to Modulate Cotyledon Opening during De-Etiolation in Arabidopsis. The Plant Cell *31*, 1155–1170.

Doyle, M.R., and Amasino, R.M. (2009). A Single Amino Acid Change in the Enhancer of Zeste Ortholog CURLY LEAF Results in Vernalization-Independent, Rapid Flowering in Arabidopsis. Plant Physiol *151*, 1688–1697.

Eichenberg, K., Hennig, L., Martin, A., and Schäfer, E. (2000). Variation in dynamics of phytochrome A in Arabidopsis ecotypes and mutants. Plant, Cell & Environment *23*, 311–319.

Esmon, C.A., Tinsley, A.G., Ljung, K., Sandberg, G., Hearne, L.B., and Liscum, E. (2006). A gradient of auxin and auxin-dependent transcription precedes tropic growth responses. Proc Natl Acad Sci U S A *103*, 236–241.

Exner, V., and Hennig, L. (2008). Chromatin rearrangements in development. Current Opinion in Plant Biology *11*, 64–69.

Fairchild, C.D., Schumaker, M.A., and Quail, P.H. (2000). HFR1 encodes an atypical bHLH protein that acts in phytochrome A signal transduction. Genes Dev *14*, 2377–2391.

Favero, D.S., Lambolez, A., and Sugimoto, K. (2021). Molecular pathways regulating elongation of aerial plant organs: a focus on light, the circadian clock, and temperature. The Plant Journal *105*, 392–420.

Feng, C.-M., Qiu, Y., Van Buskirk, E.K., Yang, E.J., and Chen, M. (2014). Light-regulated gene repositioning in Arabidopsis. Nature Communications *5*, 1–9.

Folta, K.M., and Spalding, E.P. (2001). Unexpected roles for cryptochrome 2 and phototropin revealed by high-resolution analysis of blue light-mediated hypocotyl growth inhibition. The Plant Journal *26*, 471–478.

Fry, S.C., Smith, R.C., Renwick, K.F., Martin, D.J., Hodge, S.K., and Matthews, K.J. (1992). Xyloglucan endotransglycosylase, a new wall-loosening enzyme activity from plants. Biochem J *282*, 821–828.

Fu, C., Donovan, W.P., Shikapwashya-Hasser, O., Ye, X., and Cole, R.H. (2014). Hot Fusion: An Efficient Method to Clone Multiple DNA Fragments as Well as Inverted Repeats without Ligase. PLoS One *9*, e115318.

Fussner, E., Ching, R.W., and Bazett-Jones, D.P. (2011). Living without 30 nm chromatin fibers. Trends in Biochemical Sciences *36*, 1–6.

Gallego-Bartolomé, J., Arana, M.V., Vandenbussche, F., Žádníková, P., Minguet, E.G., Guardiola, V., Straeten, D.V.D., Benkova, E., Alabadí, D., and Blázquez, M.A. (2011). Hierarchy of hormone action controlling apical hook development in Arabidopsis. The Plant Journal *67*, 622–634.

Gangappa, S.N., and Botto, J.F. (2016). The Multifaceted Roles of HY5 in Plant Growth and Development. Molecular Plant *9*, 1353–1365.

Gendreau, E., Traas, J., Desnos, T., Grandjean, O., Caboche, M., and Höfte, H. (1997). Cellular basis of hypocotyl growth in Arabidopsis thaliana. Plant Physiol *114*, 295–305.

Gressel, J. (1979). Blue Light Photoreception. Photochemistry and Photobiology *30*, 749–754.

Griffiths, J., Murase, K., Rieu, I., Zentella, R., Zhang, Z.-L., Powers, S.J., Gong, F., Phillips, A.L., Hedden, P., Sun, T., et al. (2006). Genetic Characterization and Functional Analysis of the GID1 Gibberellin Receptors in Arabidopsis. The Plant Cell *18*, 3399–3414.

Guo, H., Yang, H., Mockler, T.C., and Lin, C. (1998). Regulation of Flowering Time by Arabidopsis Photoreceptors. Science *279*, 1360–1363.

Guo, L., Zhou, J., Elling, A.A., Charron, J.-B.F., and Deng, X.W. (2008). Histone Modifications and Expression of Light-Regulated Genes in Arabidopsis Are Cooperatively Influenced by Changing Light Conditions. Plant Physiol *147*, 2070–2083.

Gupta, S.K., Sharma, M., Deeba, F., and Pandey, V. (2017). Plant Response. In UV-B Radiation, (John Wiley & Sons, Ltd), pp. 217–258.

Gutiérrez, L., Oktaba, K., Scheuermann, J.C., Gambetta, M.C., Ly-Hartig, N., and Müller, J. (2012). The role of the histone H2A ubiquitinase Sce in Polycomb repression. Development *139*, 117–127.

Hagen, G., Kleinschmidt, A., and Guilfoyle, T. (1984). Auxin-regulated gene expression in intact soybean hypocotyl and excised hypocotyl sections. Planta *162*, 147–153.

HARPHAM, N.V.J., BERRY, A.W., KNEE, E.M., ROVEDA-HOYOS, G., RASKIN, I., SANDERS, I.O., SMITH, A.R., WOOD, C.K., and HALL, M.A. (1991). The Effect of Ethylene on the Growth and Development of Wild-type and Mutant Arabidopsis thaliana (L.) Heynh. Annals of Botany *68*, 55–61.

Hayashi, K., Nakamura, S., Fukunaga, S., Nishimura, T., Jenness, M.K., Murphy, A.S., Motose, H., Nozaki, H., Furutani, M., and Aoyama, T. (2014). Auxin transport sites are visualized in planta using fluorescent auxin analogs. Proc Natl Acad Sci U S A *111*, 11557–11562.

He, J.-X., Gendron, J.M., Yang, Y., Li, J., and Wang, Z.-Y. (2002). The GSK3-like kinase BIN2 phosphorylates and destabilizes BZR1, a positive regulator of the brassinosteroid signaling pathway in Arabidopsis. PNAS *99*, 10185–10190.

Helizon, H., Rösler-Dalton, J., Gasch, P., Horsten, S. von, Essen, L.-O., and Zeidler, M. (2018). Arabidopsis phytochrome A nuclear translocation is mediated by a far-red elongated hypocotyl 1–importin complex. The Plant Journal *96*, 1255–1268.

Hirano, K., Ueguchi-Tanaka, M., and Matsuoka, M. (2008). GID1-mediated gibberellin signaling in plants. Trends in Plant Science *13*, 192–199.

Hoang, Q.T.N., Han, Y.-J., and Kim, J.-I. (2019). Plant Phytochromes and their Phosphorylation. International Journal of Molecular Sciences *20*, 3450.

Hoecker, U. (2005). Regulated proteolysis in light signaling. Current Opinion in Plant Biology *8*, 469–476.

Holm, M., Ma, L.-G., Qu, L.-J., and Deng, X.-W. (2002). Two interacting bZIP proteins are direct targets of COP1-mediated control of light-dependent gene expression in Arabidopsis. Genes Dev *16*, 1247–1259.

Huq, E., Al-Sady, B., Hudson, M., Kim, C., Apel, K., and Quail, P.H. (2004). PHYTOCHROME-INTERACTING FACTOR 1 Is a Critical bHLH Regulator of Chlorophyll Biosynthesis. Science *305*, 1937–1941.

Iglesias, M.J., Sellaro, R., Zurbriggen, M.D., and Casal, J.J. (2018). Multiple links between shade avoidance and auxin networks. Journal of Experimental Botany *69*, 213–228.

Ischebeck, T., Stenzel, I., and Heilmann, I. (2008). Type B Phosphatidylinositol-4-Phosphate 5-Kinases Mediate Arabidopsis and Nicotiana tabacum Pollen Tube Growth by Regulating Apical Pectin Secretion. Plant Cell *20*, 3312–3330.

James, P., Halladay, J., and Craig, E.A. (1996). Genomic Libraries and a Host Strain Designed for Highly Efficient Two-Hybrid Selection in Yeast. Genetics *144*, 1425–1436.

Jang, I.-C., Chung, P.J., Hemmes, H., Jung, C., and Chua, N.-H. (2011). Rapid and Reversible Light-Mediated Chromatin Modifications of Arabidopsis Phytochrome A Locus[C][W]. Plant Cell *23*, 459–470.

Jensen, P.J., Hangarter, R.P., and Estelle, M. (1998). Auxin Transport Is Required for Hypocotyl Elongation in Light-Grown but Not Dark-Grown Arabidopsis. Plant Physiol *116*, 455–462.

Jiang, W., Li, Z., Yao, X., Zheng, B., Shen, W.-H., and Dong, A. (2019). jaw-1D: a gain-of-function mutation responsive to paramutation-like induction of epigenetic silencing. J Exp Bot *70*, 459–468.

Jiao, Y., Ma, L., Strickland, E., and Deng, X.W. (2005). Conservation and Divergence of Light-Regulated Genome Expression Patterns during Seedling Development in Rice and Arabidopsis. Plant Cell *17*, 3239–3256.

Josse, E.-M., and Halliday, K.J. (2008). Skotomorphogenesis: The Dark Side of Light Signalling. Current Biology *18*, R1144–R1146.

Joti, Y., Hikima, T., Nishino, Y., Kamada, F., Hihara, S., Takata, H., Ishikawa, T., and Maeshima, K. (2012). Chromosomes without a 30-nm chromatin fiber. Nucleus *3*, 404–410.

Kaiserli, E., Paldi, K., O'Donnell, L., Batalov, O., Pedmale, U.V., Nusinow, D.A., Kay, S.A., and Chory, J. (2015). Integration of light and photoperiodic signaling in transcriptional nuclear foci. Dev Cell *35*, 311–321.

Kami, C., Lorrain, S., Hornitschek, P., and Fankhauser, C. (2010). Chapter Two - Light-Regulated Plant Growth and Development. In Current Topics in Developmental Biology, M.C.P. Timmermans, ed. (Academic Press), pp. 29–66.

Kim, G.-T., Tsukaya, H., and Uchimiya, H. (1998). The CURLY LEAF gene controls both division and elongation of cells during the expansion of the leaf blade in Arabidopsis thaliana. Planta *206*, 175–183.

Kim, J., Song, K., Park, E., Kim, K., Bae, G., and Choi, G. (2016). Epidermal Phytochrome B Inhibits Hypocotyl Negative Gravitropism Non-Cell-Autonomously. Plant Cell *28*, 2770–2785.

Kim, T.-W., Guan, S., Burlingame, A.L., and Wang, Z.-Y. (2011). The CDG1 kinase mediates brassinosteroid signal transduction from BRI1 receptor kinase to BSU1 phosphatase and GSK3-like kinase BIN2. Mol Cell *43*, 561–571.

Kinoshita, T., Harada, J.J., Goldberg, R.B., and Fischer, R.L. (2001). Polycomb repression of flowering during early plant development. PNAS *98*, 14156–14161.

Kinoshita, T., Caño-Delgado, A., Seto, H., Hiranuma, S., Fujioka, S., Yoshida, S., and Chory, J. (2005). Binding of brassinosteroids to the extracellular domain of plant receptor kinase BRI1. Nature *433*, 167–171.

Klose, C., Venezia, F., Hussong, A., Kircher, S., Schäfer, E., and Fleck, C. (2015). Systematic analysis of how phytochrome B dimerization determines its specificity. Nature Plants *1*, 1–9.

Köhler, C., Hennig, L., Bouveret, R., Gheyselinck, J., Grossniklaus, U., and Gruissem, W. (2003). Arabidopsis MSI1 is a component of the MEA/FIE Polycomb group complex and required for seed development. EMBO J *22*, 4804–4814.

Köhler, C., Page, D.R., Gagliardini, V., and Grossniklaus, U. (2005). The Arabidopsis thaliana MEDEA Polycomb group protein controls expression of PHERES1 by parental imprinting. Nat Genet *37*, 28–30.

Koornneef, M., Rolff, E., and Spruit, C.J.P. (1980). Genetic Control of Light-inhibited Hypocotyl Elongation in Arabidopsis thaliana (L.) Heynh. Zeitschrift Für Pflanzenphysiologie *100*, 147–160.

Kornberg, R.D. (1974). Chromatin structure: a repeating unit of histones and DNA. Science *184*, 868–871.

Krishnamurthy, A., Ferl, R.J., and Paul, A. (2018). Comparing RNA-Seq and microarray gene expression data in two zones of the Arabidopsis root apex relevant to spaceflight. Appl Plant Sci *6*.

Krogan, N.T., Hogan, K., and Long, J.A. (2012). APETALA2 negatively regulates multiple floral organ identity genes in Arabidopsis by recruiting the co-repressor TOPLESS and the histone deacetylase HDA19. Development *139*, 4180–4190.

Lavy, M., and Estelle, M. (2016). Mechanisms of auxin signaling. Development *143*, 3226–3229.

Lee, D., Polisensky, D.H., and Braam, J. (2005). Genome-wide identification of touch- and darkness-regulated Arabidopsis genes: a focus on calmodulin-like and XTH genes. New Phytologist *165*, 429–444.

Lee, D.Y., Hayes, J.J., Pruss, D., and Wolffe, A.P. (1993). A positive role for histone acetylation in transcription factor access to nucleosomal DNA. Cell *72*, 73–84.

Legris, M., Klose, C., Burgie, E.S., Costigliolo, C., Neme, M., Hiltbrunner, A., Wigge, P.A., Schäfer, E., Vierstra, R.D., and Casal, J.J. (2016). Phytochrome B integrates light and temperature signals in Arabidopsis. Science.

Legris, M., Ince, Y.Ç., and Fankhauser, C. (2019). Molecular mechanisms underlying phytochrome-controlled morphogenesis in plants. Nat Commun *10*, 5219.

Leroy, O., Hennig, L., Breuninger, H., Laux, T., and Köhler, C. (2007). Polycomb group proteins function in the female gametophyte to determine seed development in plants. Development *134*, 3639–3648.

Leu, W.M., Cao, X.L., Wilson, T.J., Snustad, D.P., and Chua, N.H. (1995). Phytochrome A and phytochrome B mediate the hypocotyl-specific downregulation of TUB1 by light in arabidopsis. Plant Cell *7*, 2187–2196.

Lewis, E.B. (1978). A gene complex controlling segmentation in Drosophila. Nature *276*, 565–570.

Lewis, D.R., Wu, G., Ljung, K., and Spalding, E.P. (2009). Auxin transport into cotyledons and cotyledon growth depend similarly on the ABCB19 Multidrug Resistance-like transporter. The Plant Journal *60*, 91–101.

Leyser, O., and Day, S. (2009). Mechanisms in Plant Development (John Wiley & Sons).

Li, J., and Nam, K.H. (2002). Regulation of brassinosteroid signaling by a GSK3/SHAGGY-like kinase. Science *295*, 1299–1301.

Li, J., Nagpal, P., Vitart, V., McMorris, T.C., and Chory, J. (1996). A role for brassinosteroids in light-dependent development of Arabidopsis. Science *272*, 398–401.

Li, J., Terzaghi, W., Gong, Y., Li, C., Ling, J.-J., Fan, Y., Qin, N., Gong, X., Zhu, D., and Deng, X.W. (2020). Modulation of BIN2 kinase activity by HY5 controls hypocotyl elongation in the light. Nat Commun *11*, 1592.

Li, T., Chen, X., Zhong, X., Zhao, Y., Liu, X., Zhou, S., Cheng, S., and Zhou, D.-X. (2013). Jumonji C domain protein JMJ705-mediated removal of histone H3 lysine 27 trimethylation is involved in defense-related gene activation in rice. Plant Cell *25*, 4725–4736.

Li, X., Wang, Q., Yu, X., Liu, H., Yang, H., Zhao, C., Liu, X., Tan, C., Klejnot, J., Zhong, D., et al. (2011). Arabidopsis cryptochrome 2 (CRY2) functions by the photoactivation mechanism distinct from the tryptophan (trp) triad-dependent photoreduction. PNAS *108*, 20844–20849.

Li, Z.-C., Durachko, D.M., and Cosgrove, D.J. (1993). An oat coleoptile wall protein that induces wall extension in vitro and that is antigenically related to a similar protein from cucumber hypocotyls. Planta *191*, 349–356.

Lin, C. (2000). Plant blue-light receptors. Trends in Plant Science *5*, 337–342.

Lin, C., Robertson, D.E., Ahmad, M., Raibekas, A.A., Jorns, M.S., Dutton, P.L., and Cashmore, A.R. (1995). Association of flavin adenine dinucleotide with the Arabidopsis blue light receptor CRY1. Science *269*, 968–970.

Lin, C., Ahmad, M., and Cashmore, A.R. (1996). Arabidopsis cryptochrome 1 is a soluble protein mediating blue light-dependent regulation of plant growth and development. Plant J *10*, 893–902.

Lin, C., Yang, H., Guo, H., Mockler, T., Chen, J., and Cashmore, A.R. (1998). Enhancement of blue-light sensitivity of Arabidopsis seedlings by a blue light receptor cryptochrome 2. Proc Natl Acad Sci U S A *95*, 2686–2690.

Liscum, E., and Briggs, W.R. (1996). Mutations of Arabidopsis in Potential Transduction and Response Components of the Phototropic Signaling Pathway. Plant Physiology *112*, 291–296.

Liscum, E., and Hangarter, R.P. (1993). Light-Stimulated Apical Hook Opening in Wild-Type Arabidopsis thaliana Seedlings. Plant Physiol *101*, 567–572.

Liscum, E., Askinosie, S.K., Leuchtman, D.L., Morrow, J., Willenburg, K.T., and Coats, D.R. (2014). Phototropism: Growing towards an Understanding of Plant Movement[OPEN]. Plant Cell *26*, 38–55.

Liu, B., Zuo, Z., Liu, H., Liu, X., and Lin, C. (2011). Arabidopsis cryptochrome 1 interacts with SPA1 to suppress COP1 activity in response to blue light. Genes Dev. *25*, 1029–1034.

Liu, C., Lu, F., Cui, X., and Cao, X. (2010). Histone Methylation in Higher Plants. Annual Review of Plant Biology *61*, 395–420.

Liu, H., Yu, X., Li, K., Klejnot, J., Yang, H., Lisiero, D., and Lin, C. (2008). Photoexcited CRY2 Interacts with CIB1 to Regulate Transcription and Floral Initiation in Arabidopsis. Science *322*, 1535–1539.

Liu, X., Chen, C.-Y., Wang, K.-C., Luo, M., Tai, R., Yuan, L., Zhao, M., Yang, S., Tian, G., Cui, Y., et al. (2013). PHYTOCHROME INTERACTING FACTOR3 Associates with the Histone Deacetylase HDA15 in Repression of Chlorophyll Biosynthesis and Photosynthesis in Etiolated Arabidopsis Seedlings[W][OA]. Plant Cell *25*, 1258–1273.

Love, M.I., Huber, W., and Anders, S. (2014). Moderated estimation of fold change and dispersion for RNA-seq data with DESeq2. Genome Biol *15*, 550.

Lu, F., Cui, X., Zhang, S., Jenuwein, T., and Cao, X. (2011). Arabidopsis REF6 is a histone H3 lysine 27 demethylase. Nat Genet *43*, 715–719.

de Lucas, M., and Prat, S. (2014). PIFs get BRright: PHYTOCHROME INTERACTING FACTORs as integrators of light and hormonal signals. New Phytol *202*, 1126–1141.

de Lucas, M., Davière, J.-M., Rodríguez-Falcón, M., Pontin, M., Iglesias-Pedraz, J.M., Lorrain, S., Fankhauser, C., Blázquez, M.A., Titarenko, E., and Prat, S. (2008). A molecular framework for light and gibberellin control of cell elongation. Nature *451*, 480–484.

de Lucas, M., Pu, L., Turco, G., Gaudinier, A., Morao, A.K., Harashima, H., Kim, D., Ron, M., Sugimoto, K., Roudier, F., et al. (2016). Transcriptional Regulation of Arabidopsis Polycomb Repressive Complex 2 Coordinates Cell-Type Proliferation and Differentiation. Plant Cell *28*, 2616–2631.

Ma, D., Li, X., Guo, Y., Chu, J., Fang, S., Yan, C., Noel, J.P., and Liu, H. (2016). Cryptochrome 1 interacts with PIF4 to regulate high temperature-mediated hypocotyl elongation in response to blue light. Proc Natl Acad Sci U S A *113*, 224–229.

Ma, L., Li, J., Qu, L., Hager, J., Chen, Z., Zhao, H., and Deng, X.W. (2001). Light Control of Arabidopsis Development Entails Coordinated Regulation of Genome Expression and Cellular Pathways. Plant Cell *13*, 2589–2608.

Ma, L., Sun, N., Liu, X., Jiao, Y., Zhao, H., and Deng, X.W. (2005). Organ-Specific Expression of Arabidopsis Genome during Development. Plant Physiology *138*, 80–91.

Majda, M., and Robert, S. (2018). The Role of Auxin in Cell Wall Expansion. Int J Mol Sci *19*, 951.

Marowa, P., Ding, A., and Kong, Y. (2016). Expansins: roles in plant growth and potential applications in crop improvement. Plant Cell Rep *35*, 949–965.

Martínez, C., Espinosa-Ruíz, A., de Lucas, M., Bernardo-García, S., Franco-Zorrilla, J.M., and Prat, S. (2018). PIF4-induced BR synthesis is critical to diurnal and thermomorphogenic growth. EMBO J *37*, e99552.

Mazzella, M.A., and Casal, J.J. (2001). Interactive signalling by phytochromes and cryptochromes generates de-etiolation homeostasis in Arabidopsis thaliana. Plant, Cell & Environment *24*, 155–161.

McQueen-Mason, S., Durachko, D.M., and Cosgrove, D.J. (1992). Two endogenous proteins that induce cell wall extension in plants. Plant Cell *4*, 1425–1433.

Meng, Y., Li, H., Wang, Q., Liu, B., and Lin, C. (2013). Blue Light–Dependent Interaction between Cryptochrome2 and CIB1 Regulates Transcription and Leaf Senescence in Soybean. The Plant Cell *25*, 4405–4420.

Mi, H., Muruganujan, A., Ebert, D., Huang, X., and Thomas, P.D. (2019). PANTHER version 14: more genomes, a new PANTHER GO-slim and improvements in enrichment analysis tools. Nucleic Acids Research *47*, D419–D426.

Miedes, E., Suslov, D., Vandenbussche, F., Kenobi, K., Ivakov, A., Van Der Straeten, D., Lorences, E.P., Mellerowicz, E.J., Verbelen, J.-P., and Vissenberg, K. (2013). Xyloglucan endotransglucosylase/hydrolase (XTH) overexpression affects growth and cell wall mechanics in etiolated Arabidopsis hypocotyls. Journal of Experimental Botany *64*, 2481–2497.

Molnár, G., Bancoş, S., Nagy, F., and Szekeres, M. (2002). Characterisation of BRH1, a brassinosteroid-responsive RING-H2 gene from Arabidopsis thaliana. Planta *215*, 127–133.

Mozgova, I., and Hennig, L. (2015). The Polycomb Group Protein Regulatory Network. Annual Review of Plant Biology *66*, 269–296.

Müller, J., Hart, C.M., Francis, N.J., Vargas, M.L., Sengupta, A., Wild, B., Miller, E.L., O'Connor, M.B., Kingston, R.E., and Simon, J.A. (2002). Histone Methyltransferase Activity of a Drosophila Polycomb Group Repressor Complex. Cell *111*, 197–208.

Nagalakshmi, U., Wang, Z., Waern, K., Shou, C., Raha, D., Gerstein, M., and Snyder, M. (2008). The Transcriptional Landscape of the Yeast Genome Defined by RNA Sequencing. Science *320*, 1344–1349.

Nagpal, P., Walker, L.M., Young, J.C., Sonawala, A., Timpte, C., Estelle, M., and Reed, J.W. (2000). AXR2 Encodes a Member of the Aux/IAA Protein Family1. Plant Physiology *123*, 563–574.

Neff, M.M., and Chory, J. (1998). Genetic Interactions between Phytochrome A, Phytochrome B, and Cryptochrome 1 during Arabidopsis Development. Plant Physiol *118*, 27–35.

Neff, M.M., and Van Volkenburgh, E. (1994). Light-Stimulated Cotyledon Expansion in Arabidopsis Seedlings (The Role of Phytochrome B). Plant Physiol *104*, 1027–1032.

Neff, M.M., Neff, J.D., Chory, J., and Pepper, A.E. (1998). dCAPS, a simple technique for the genetic analysis of single nucleotide polymorphisms: experimental applications in Arabidopsis thaliana genetics. The Plant Journal *14*, 387–392.

Nemhauser, J., and Chory, J. (2002). Photomorphogenesis. Arbo.j *2002*.

Nemhauser, J.L., Hong, F., and Chory, J. (2006). Different Plant Hormones Regulate Similar Processes through Largely Nonoverlapping Transcriptional Responses. Cell *126*, 467–475.

Nishino, Y., Eltsov, M., Joti, Y., Ito, K., Takata, H., Takahashi, Y., Hihara, S., Frangakis, A.S., Imamoto, N., Ishikawa, T., et al. (2012). Human mitotic chromosomes consist predominantly of irregularly folded nucleosome fibres without a 30-nm chromatin structure. EMBO J *31*, 1644–1653.

Oh, E., Zhu, J.-Y., and Wang, Z.-Y. (2012). Interaction between BZR1 and PIF4 integrates brassinosteroid and environmental responses. Nat Cell Biol *14*, 802–809.

Oh, E., Zhu, J.-Y., Bai, M.-Y., Arenhart, R.A., Sun, Y., and Wang, Z.-Y. (2014a). Cell elongation is regulated through a central circuit of interacting transcription factors in the Arabidopsis hypocotyl. ELife *3*, e03031.

Oh, E., Zhu, J.-Y., Ryu, H., Hwang, I., and Wang, Z.-Y. (2014b). TOPLESS mediates brassinosteroid-induced transcriptional repression through interaction with BZR1. Nat Commun *5*, 4140.

Oh, J., Park, E., Song, K., Bae, G., and Choi, G. (2020). PHYTOCHROME INTERACTING FACTOR8 Inhibits Phytochrome A-Mediated Far-Red Light Responses in Arabidopsis. Plant Cell *32*, 186–205.

Ohad, N., Margossian, L., Hsu, Y.C., Williams, C., Repetti, P., and Fischer, R.L. (1996). A mutation that allows endosperm development without fertilization. Proceedings of the National Academy of Sciences *93*, 5319–5324.

Oravecz, A., Baumann, A., Máté, Z., Brzezinska, A., Molinier, J., Oakeley, E.J., Ádám, É., Schäfer, E., Nagy, F., and Ulm, R. (2006). CONSTITUTIVELY PHOTOMORPHOGENIC1 Is Required for the UV-B Response in Arabidopsis. The Plant Cell *18*, 1975–1990.

Osterlund, M.T., and Deng, X.-W. (1998). Multiple photoreceptors mediate the light-induced reduction of GUS-COP1 from Arabidopsis hypocotyl nuclei. The Plant Journal *16*, 201–208.

Osterlund, M.T., Hardtke, C.S., Wei, N., and Deng, X.W. (2000). Targeted destabilization of HY5 during light-regulated development of Arabidopsis. Nature *405*, 462–466.

Oyama, T., Shimura, Y., and Okada, K. (1997). The Arabidopsis HY5 gene encodes a bZIP protein that regulates stimulus-induced development of root and hypocotyl. Genes Dev *11*, 2983–2995.

Paik, I., Kathare, P.K., Kim, J.-I., and Huq, E. (2017). Expanding Roles of PIFs in Signal Integration from Multiple Processes. Mol Plant *10*, 1035–1046.

Park, E., Park, J., Kim, J., Nagatani, A., Lagarias, J.C., and Choi, G. (2012). Phytochrome B inhibits binding of Phytochrome-Interacting Factors to their target promoters. Plant J *72*, 537–546.

Park, J.-E., Seo, P.J., Lee, A.-K., Jung, J.-H., Kim, Y.-S., and Park, C.-M. (2007a). An Arabidopsis GH3 Gene, Encoding an Auxin-Conjugating Enzyme, Mediates Phytochrome B-Regulated Light Signals in Hypocotyl Growth. Plant and Cell Physiology *48*, 1236–1241.

Park, J.-E., Park, J.-Y., Kim, Y.-S., Staswick, P.E., Jeon, J., Yun, J., Kim, S.-Y., Kim, J., Lee, Y.-H., and Park, C.-M. (2007b). GH3-mediated Auxin Homeostasis Links Growth Regulation with Stress Adaptation Response in Arabidopsis*. Journal of Biological Chemistry *282*, 10036–10046.

Parks, B.M., and Spalding, E.P. (1999). Sequential and coordinated action of phytochromes A and B during Arabidopsis stem growth revealed by kinetic analysis. PNAS *96*, 14142–14146.

Parks, B.M., Cho, M.H., and Spalding, E.P. (1998). Two Genetically Separable Phases of Growth Inhibition Induced by Blue Light in Arabidopsis Seedlings. Plant Physiol *118*, 609–615.

Pazin, M.J., and Kadonaga, J.T. (1997). What's Up and Down with Histone Deacetylation and Transcription? Cell *89*, 325–328.

Pedmale, U.V., Huang, S.C., Zander, M., Cole, B.J., Hetzel, J., Ljung, K., Reis, P.A.B., Sridevi, P., Nito, K., Nery, J.R., et al. (2016). Cryptochromes Interact Directly with PIFs to Control Plant Growth in Limiting Blue Light. Cell *164*, 233–245.

Peng, P., Yan, Z., Zhu, Y., and Li, J. (2008). Regulation of the Arabidopsis GSK3-like Kinase BRASSINOSTEROID-INSENSITIVE 2 through Proteasome-Mediated Protein Degradation. Molecular Plant *1*, 338–346.

Perrella, G., and Kaiserli, E. (2016). Light behind the curtain: photoregulation of nuclear architecture and chromatin dynamics in plants. New Phytol *212*, 908–919.

Ponnu, J., Riedel, T., Penner, E., Schrader, A., and Hoecker, U. (2019). Cryptochrome 2 competes with COP1 substrates to repress COP1 ubiquitin ligase activity during Arabidopsis photomorphogenesis. PNAS *116*, 27133–27141.

Raiola, A., Camardella, L., Giovane, A., Mattei, B., Lorenzo, G.D., Cervone, F., and Bellincampi, D. (2004). Two Arabidopsis thaliana genes encode functional pectin methylesterase inhibitors1. FEBS Letters *557*, 199–203.

Rando, O.J., and Chang, H.Y. (2009). Genome-wide views of chromatin structure. Annu Rev Biochem *78*, 245–271.

Rao, X., Huang, X., Zhou, Z., and Lin, X. (2013). An improvement of the 2ˆ(–delta delta CT) method for quantitative real-time polymerase chain reaction data analysis. Biostat Bioinforma Biomath *3*, 71–85.

Rayle, D.L., and Cleland, R.E. (1992). The Acid Growth Theory of auxin-induced cell elongation is alive and well. Plant Physiology *99*, 1271–1274.

Reed, J.W., Nagpal, P., Poole, D.S., Furuya, M., and Chory, J. (1993). Mutations in the gene for the red/far-red light receptor phytochrome B alter cell elongation and physiological responses throughout Arabidopsis development. Plant Cell *5*, 147–157.

Reed, J.W., Nagatani, A., Elich, T.D., Fagan, M., and Chory, J. (1994). Phytochrome A and Phytochrome B Have Overlapping but Distinct Functions in Arabidopsis Development. Plant Physiol *104*, 1139–1149.

Refrégier, G., Pelletier, S., Jaillard, D., and Höfte, H. (2004). Interaction between Wall Deposition and Cell Elongation in Dark-Grown Hypocotyl Cells in Arabidopsis. Plant Physiol *135*, 959–968.

Rizzini, L., Favory, J.-J., Cloix, C., Faggionato, D., O'Hara, A., Kaiserli, E., Baumeister, R., Schäfer, E., Nagy, F., Jenkins, G.I., et al. (2011). Perception of UV-B by the Arabidopsis UVR8 Protein. Science *332*, 103–106.

Roszak, P., and Köhler, C. (2011). Polycomb group proteins are required to couple seed coat initiation to fertilization. Proc Natl Acad Sci U S A *108*, 20826–20831.

Roth, S.Y., and Allis, C.D. (1996). Histone Acetylation and Chromatin Assembly: A Single Escort, Multiple Dances? Cell *87*, 5–8.

Roy, S., Gupta, P., Rajabhoj, M.P., Maruthachalam, R., and Nandi, A.K. (2018). The Polycomb-Group Repressor MEDEA Attenuates Pathogen Defense1. Plant Physiol *177*, 1728–1742.

Sakai, T., Wada, T., Ishiguro, S., and Okada, K. (2000). RPT2: A Signal Transducer of the Phototropic Response in Arabidopsis. The Plant Cell *12*, 225–236.

Sanchez-Pulido, L., Devos, D., Sung, Z.R., and Calonje, M. (2008). RAWUL: A new ubiquitin-like domain in PRC1 Ring finger proteins that unveils putative plant and worm PRC1 orthologs. BMC Genomics *9*, 308.

Sawa, S., Ohgishi, M., Goda, H., Higuchi, K., Shimada, Y., Yoshida, S., and Koshiba, T. (2002). The HAT2 gene, a member of the HD-Zip gene family, isolated as an auxin inducible gene by DNA microarray screening, affects auxin response in Arabidopsis. The Plant Journal *32*, 1011–1022.

Schubert, D., Primavesi, L., Bishopp, A., Roberts, G., Doonan, J., Jenuwein, T., and Goodrich, J. (2006). Silencing by plant Polycomb-group genes requires dispersed trimethylation of histone H3 at lysine 27. EMBO J *25*, 4638–4649.

Schwark, A., and Schierle, J. (1992). Interaction of Ethylene and Auxin in the Regulation of Hook Growth I The Role of Auxin in Different Growing Regions of the Hypocotyl Hook of Phaseolus vulgaris. Journal of Plant Physiology *140*, 562–570.

Schwechheimer, C. (2012). Gibberellin Signaling in Plants – The Extended Version. Front. Plant Sci. *2*.

Shani, Z., Dekel, M., Roiz, L., Horowitz, M., Kolosovski, N., Lapidot, S., Alkan, S., Koltai, H., Tsabary, G., Goren, R., et al. (2006). Expression of endo-1,4-β-glucanase (cel1) in Arabidopsis thaliana is associated with plant growth, xylem development and cell wall thickening. Plant Cell Rep *25*, 1067–1074.

Sharrock, R.A., and Clack, T. (2002). Patterns of Expression and Normalized Levels of the Five Arabidopsis Phytochromes. Plant Physiology *130*, 442–456.

Shaver, S., Casas-Mollano, J.A., Cerny, R.L., and Cerutti, H. (2010). Origin of the polycomb repressive complex 2 and gene silencing by an E(z) homolog in the unicellular alga Chlamydomonas. Epigenetics *5*, 301–312.

Shen, X., Kim, W., Fujiwara, Y., Simon, M.D., Liu, Y., Mysliwiec, M.R., Yuan, G.-C., Lee, Y., and Orkin, S.H. (2009). Jumonji modulates polycomb activity and self-renewal versus differentiation of stem cells. Cell *139*, 1303–1314.

Shigeyama, T., Watanabe, A., Tokuchi, K., Toh, S., Sakurai, N., Shibuya, N., and Kawakami, N. (2016). α-Xylosidase plays essential roles in xyloglucan remodelling, maintenance of cell wall integrity, and seed germination in Arabidopsis thaliana. Journal of Experimental Botany *67*, 5615–5629.

Shin, J., Kim, K., Kang, H., Zulfugarov, I.S., Bae, G., Lee, C.-H., Lee, D., and Choi, G. (2009). Phytochromes promote seedling light responses by inhibiting four negatively-acting phytochrome-interacting factors. PNAS *106*, 7660–7665.

Shu, J., Chen, C., Thapa, R.K., Bian, S., Nguyen, V., Yu, K., Yuan, Z.-C., Liu, J., Kohalmi, S.E., Li, C., et al. (2019). Genome-wide occupancy of histone H3K27 methyltransferases CURLY LEAF and SWINGER in Arabidopsis seedlings. Plant Direct *3*, e00100.

Sibout, R., Sukumar, P., Hettiarachchi, C., Holm, M., Muday, G.K., and Hardtke, C.S. (2006). Opposite Root Growth Phenotypes of hy5 versus hy5 hyh Mutants Correlate with Increased Constitutive Auxin Signaling. PLOS Genetics *2*, e202.

Siegelman, H.W., and Hendricks, S.B. (1965). Purification and properties of phytochrome: a chromoprotein regulating plant growth. Fed Proc *24*, 863–867.

Siegelman, H.W., Turner, B.C., and Hendricks, S.B. (1966). The Chromophore of Phytochrome. Plant Physiology *41*, 1289–1292.

Simonini, S., Bemer, M., Bencivenga, S., Gagliardini, V., Pires, N.D., Desvoyes, B., van der Graaff, E., Gutierrez, C., and Grossniklaus, U. (2021). The Polycomb group protein MEDEA controls cell proliferation and embryonic patterning in Arabidopsis. Developmental Cell *56*, 1945-1960.e7.

Smalle, J., Haegman, M., Kurepa, J., Van Montagu, M., and Straeten, D.V.D. (1997). Ethylene can stimulate Arabidopsis hypocotyl elongation in the light. Proc Natl Acad Sci U S A *94*, 2756–2761.

Somers, D.E., Sharrock, R.A., Tepperman, J.M., and Quail, P.H. (1991). The hy3 Long Hypocotyl Mutant of Arabidopsis Is Deficient in Phytochrome B. Plant Cell *3*, 1263–1274.

Spartz, A.K., Lee, S.H., Wenger, J.P., Gonzalez, N., Itoh, H., Inzé, D., Peer, W.A., Murphy, A.S., Overvoorde, P.J., and Gray, W.M. (2012). The SAUR19 subfamily of SMALL AUXIN UP RNA genes promote cell expansion. Plant J *70*, 978–990.

Spartz, A.K., Ren, H., Park, M.Y., Grandt, K.N., Lee, S.H., Murphy, A.S., Sussman, M.R., Overvoorde, P.J., and Gray, W.M. (2014). SAUR Inhibition of PP2C-D Phosphatases Activates Plasma Membrane H+-ATPases to Promote Cell Expansion in Arabidopsis. Plant Cell *26*, 2129–2142.

Sreeramulu, S., Mostizky, Y., Sunitha, S., Shani, E., Nahum, H., Salomon, D., Hayun, L.B., Gruetter, C., Rauh, D., Ori, N., et al. (2013). BSKs are partially redundant positive regulators of brassinosteroid signaling in Arabidopsis. The Plant Journal *74*, 905–919.

Srivastava, A.K., Senapati, D., Srivastava, A., Chakraborty, M., Gangappa, S.N., and Chattopadhyay, S. (2015). Short Hypocotyl in White Light1 Interacts with Elongated Hypocotyl5 (HY5) and Constitutive Photomorphogenic1 (COP1) and Promotes COP1-Mediated Degradation of HY5 during Arabidopsis Seedling Development1[OPEN]. Plant Physiol *169*, 2922–2934.

Staswick, P.E., Serban, B., Rowe, M., Tiryaki, I., Maldonado, M.T., Maldonado, M.C., and Suza, W. (2005). Characterization of an Arabidopsis Enzyme Family That Conjugates Amino Acids to Indole-3-Acetic Acid. The Plant Cell *17*, 616–627.

Su, J., Liu, B., Liao, J., Yang, Z., Lin, C., and Oka, Y. (2017). Coordination of Cryptochrome and Phytochrome Signals in the Regulation of Plant Light Responses. Agronomy *7*, 25.

Suetsugu, N., and Wada, M. (2013). Evolution of Three LOV Blue Light Receptor Families in Green Plants and Photosynthetic Stramenopiles: Phototropin, ZTL/FKF1/LKP2 and Aureochrome. Plant and Cell Physiology *54*, 8–23.

Sullivan, S., Hart, J.E., Rasch, P., Walker, C.H., and Christie, J.M. (2016). Phytochrome A Mediates Blue-Light Enhancement of Second-Positive Phototropism in Arabidopsis. Front. Plant Sci. *0*.

Sun, B., Looi, L.-S., Guo, S., He, Z., Gan, E.-S., Huang, J., Xu, Y., Wee, W.-Y., and Ito, T. (2014). Timing Mechanism Dependent on Cell Division Is Invoked by Polycomb Eviction in Plant Stem Cells. Science *343*.

Sun, N., Wang, J., Gao, Z., Dong, J., He, H., Terzaghi, W., Wei, N., Deng, X.W., and Chen, H. (2016). Arabidopsis SAURs are critical for differential light regulation of the development of various organs. PNAS *113*, 6071–6076.

Sun, Y., Fan, X.-Y., Cao, D.-M., Tang, W., He, K., Zhu, J.-Y., He, J.-X., Bai, M.-Y., Zhu, S., Oh, E., et al. (2010). Integration of brassinosteroid signal transduction with the transcription network for plant growth regulation in Arabidopsis. Dev Cell *19*, 765–777.

Szekeres, M., Németh, K., Koncz-Kálmán, Z., Mathur, J., Kauschmann, A., Altmann, T., Rédei, G.P., Nagy, F., Schell, J., and Koncz, C. (1996). Brassinosteroids Rescue the Deficiency of CYP90, a Cytochrome P450, Controlling Cell Elongation and De-etiolation in Arabidopsis. Cell *85*, 171–182.

Takahashi, K., Hayashi, K., and Kinoshita, T. (2012). Auxin activates the plasma membrane H+-ATPase by phosphorylation during hypocotyl elongation in Arabidopsis. Plant Physiol *159*, 632–641.

Tan, X., Calderon-Villalobos, L.I.A., Sharon, M., Zheng, C., Robinson, C.V., Estelle, M., and Zheng, N. (2007). Mechanism of auxin perception by the TIR1 ubiquitin ligase. Nature *446*, 640–645.

Tang, W., Kim, T.-W., Oses-Prieto, J.A., Sun, Y., Deng, Z., Zhu, S., Wang, R., Burlingame, A.L., and Wang, Z.-Y. (2008). BSKs mediate signal transduction from the receptor kinase BRI1 in Arabidopsis. Science *321*, 557–560.

Tessadori, F., van Zanten, M., Pavlova, P., Clifton, R., Pontvianne, F., Snoek, L.B., Millenaar, F.F., Schulkes, R.K., van Driel, R., Voesenek, L.A.C.J., et al. (2009). PHYTOCHROME B and HISTONE DEACETYLASE 6 Control Light-Induced Chromatin Compaction in Arabidopsis thaliana. PLoS Genet *5*, e1000638.

The Gene Ontology Consortium, Carbon, S., Douglass, E., Good, B.M., Unni, D.R., Harris, N.L., Mungall, C.J., Basu, S., Chisholm, R.L., Dodson, R.J., et al. (2021). The Gene Ontology resource: enriching a GOld mine. Nucleic Acids Research *49*, D325–D334.

Toledo-Ortiz, G., Johansson, H., Lee, K.P., Bou-Torrent, J., Stewart, K., Steel, G., Rodríguez-Concepción, M., and Halliday, K.J. (2014). The HY5-PIF regulatory module coordinates light and temperature control of photosynthetic gene transcription. PLoS Genet *10*, e1004416.

Turck, F., Roudier, F., Farrona, S., Martin-Magniette, M.-L., Guillaume, E., Buisine, N., Gagnot, S., Martienssen, R.A., Coupland, G., and Colot, V. (2007). Arabidopsis TFL2/LHP1 Specifically Associates with Genes Marked by Trimethylation of Histone H3 Lysine 27. PLOS Genetics *3*, e86.

Ulmasov, T., Murfett, J., Hagen, G., and Guilfoyle, T.J. (1997). Aux/IAA proteins repress expression of reporter genes containing natural and highly active synthetic auxin response elements. The Plant Cell *9*, 1963–1971.

Untergasser, A., Cutcutache, I., Koressaar, T., Ye, J., Faircloth, B.C., Remm, M., and Rozen, S.G. (2012). Primer3—new capabilities and interfaces. Nucleic Acids Res *40*, e115.

Van Buskirk, E.K., Decker, P.V., and Chen, M. (2012). Photobodies in Light Signaling1. Plant Physiol *158*, 52–60.

Van Buskirk, E.K., Reddy, A.K., Nagatani, A., and Chen, M. (2014). Photobody Localization of Phytochrome B Is Tightly Correlated with Prolonged and Light-Dependent Inhibition of Hypocotyl Elongation in the Dark. Plant Physiology *165*, 595–607.

Vandenbussche, F., Petrášek, J., Žádníková, P., Hoyerová, K., Pešek, B., Raz, V., Swarup, R., Bennett, M., Zažímalová, E., Benková, E., et al. (2010). The auxin influx carriers AUX1 and LAX3 are involved in auxin-ethylene interactions during apical hook development in Arabidopsis thaliana seedlings. Development *137*, 597–606.

Wang, Q., and Lin, C. (2020). Mechanisms of Cryptochrome-Mediated Photoresponses in Plants. Annu Rev Plant Biol *71*, 103–129.

Wang, R., and Estelle, M. (2014). Diversity and specificity: auxin perception and signaling through the TIR1/AFB pathway. Current Opinion in Plant Biology *21*, 51–58.

Wang, Y., and Folta, K.M. (2013). Contributions of green light to plant growth and development. American Journal of Botany *100*, 70–78.

Wang, Y., and Guo, H. (2019). On hormonal regulation of the dynamic apical hook development. New Phytologist *222*, 1230–1234.

Wang, D., Tyson, M.D., Jackson, S.S., and Yadegari, R. (2006). Partially redundant functions of two SET-domain polycomb-group proteins in controlling initiation of seed development in Arabidopsis. PNAS *103*, 13244–13249.

Wang, H., Ma, L.G., Li, J.M., Zhao, H.Y., and Deng, X.W. (2001a). Direct interaction of Arabidopsis cryptochromes with COP1 in light control development. Science *294*, 154–158.

Wang, L., Brown, J.L., Cao, R., Zhang, Y., Kassis, J.A., and Jones, R.S. (2004). Hierarchical Recruitment of Polycomb Group Silencing Complexes. Molecular Cell *14*, 637–646.

Wang, L., Kim, J., and Somers, D.E. (2013a). Transcriptional corepressor TOPLESS complexes with pseudoresponse regulator proteins and histone deacetylases to regulate circadian transcription. Proc Natl Acad Sci U S A *110*, 761–766.

Wang, S., Li, L., Xu, P., Lian, H., Wang, W., Xu, F., Mao, Z., Zhang, T., and Yang, H. (2018a). CRY1 interacts directly with HBI1 to regulate its transcriptional activity and photomorphogenesis in Arabidopsis. Journal of Experimental Botany *69*, 3867–3881.

Wang, T., Park, Y.B., Caporini, M.A., Rosay, M., Zhong, L., Cosgrove, D.J., and Hong, M. (2013b). Sensitivity-enhanced solid-state NMR detection of expansin's target in plant cell walls. PNAS *110*, 16444–16449.

Wang, X., Wang, Q., Nguyen, P., and Lin, C. (2014). Cryptochrome-mediated light responses in plants. Enzymes *35*, 167–189.

Wang, Y., Li, J., Deng, X.-W., and Zhu, D. (2018b). Arabidopsis noncoding RNA modulates seedling greening during deetiolation. Sci China Life Sci *61*, 199–203.

Wang, Z., Gerstein, M., and Snyder, M. (2009). RNA-Seq: a revolutionary tool for transcriptomics. Nature Reviews Genetics *10*, 57–63.

Wang, Z.-Y., Seto, H., Fujioka, S., Yoshida, S., and Chory, J. (2001b). BRI1 is a critical component of a plasma-membrane receptor for plant steroids. Nature *410*, 380–383.

Wang, Z.-Y., Bai, M.-Y., Oh, E., and Zhu, J.-Y. (2012). Brassinosteroid Signaling Network and Regulation of Photomorphogenesis. Annual Review of Genetics *46*, 701–724.

Whitelam, G.C., Johnson, E., Peng, J., Carol, P., Anderson, M.L., Cowl, J.S., and Harberd, N.P. (1993). Phytochrome A null mutants of Arabidopsis display a wild-type phenotype in white light. Plant Cell *5*, 757–768.

Willats, W.G.T., McCartney, L., Mackie, W., and Knox, J.P. (2001). Pectin: cell biology and prospects for functional analysis. Plant Mol Biol *47*, 9–27.

Willige, B.C., Zander, M., Yoo, C.Y., Phan, A., Garza, R.M., Trigg, S.A., He, Y., Nery, J.R., Chen, H., Chen, M., et al. (2021). PHYTOCHROME-INTERACTING FACTORs trigger environmentally responsive chromatin dynamics in plants. Nat Genet *53*, 955–961.

Wu, G., and Spalding, E.P. (2007). Separate functions for nuclear and cytoplasmic cryptochrome 1 during photomorphogenesis of Arabidopsis seedlings. Proc Natl Acad Sci U S A *104*, 18813–18818.

Wu, G., Cameron, J.N., Ljung, K., and Spalding, E.P. (2010). A role for ABCB19-mediated polar auxin transport in seedling photomorphogenesis mediated by cryptochrome 1 and phytochrome B. The Plant Journal *62*, 179–191.

Wu, M.-F., Sang, Y., Bezhani, S., Yamaguchi, N., Han, S.-K., Li, Z., Su, Y., Slewinski, T.L., and Wagner, D. (2012). SWI2/SNF2 chromatin remodeling ATPases overcome polycomb repression and control floral organ identity with the LEAFY and SEPALLATA3 transcription factors. PNAS *109*, 3576–3581.

Xu, L., and Shen, W.-H. (2008). Polycomb Silencing of KNOX Genes Confines Shoot Stem Cell Niches in Arabidopsis. Current Biology *18*, 1966–1971.

Yang, C., Bratzel, F., Hohmann, N., Koch, M., Turck, F., and Calonje, M. (2013). VAL- and AtBMI1-mediated H2Aub initiate the switch from embryonic to postgerminative growth in Arabidopsis. Curr Biol *23*, 1324–1329.

Yang, H.-Q., Wu, Y.-J., Tang, R.-H., Liu, D., Liu, Y., and Cashmore, A.R. (2000). The C Termini of Arabidopsis Cryptochromes Mediate a Constitutive Light Response. Cell *103*, 815–827.

Yin, Y., Wang, Z.-Y., Mora-Garcia, S., Li, J., Yoshida, S., Asami, T., and Chory, J. (2002). BES1 Accumulates in the Nucleus in Response to Brassinosteroids to Regulate Gene Expression and Promote Stem Elongation. Cell *109*, 181–191.

Yin, Y., Vafeados, D., Tao, Y., Yoshida, S., Asami, T., and Chory, J. (2005). A new class of transcription factors mediates brassinosteroid-regulated gene expression in Arabidopsis. Cell *120*, 249–259.

Yu, J., and Wen, C.-K. (2013). Arabidopsis aux1rcr1 mutation alters AUXIN RESISTANT1 targeting and prevents expression of the auxin reporter DR5:GUS in the root apex. J Exp Bot *64*, 921–933.

Yu, X., Klejnot, J., Zhao, X., Shalitin, D., Maymon, M., Yang, H., Lee, J., Liu, X., Lopez, J., and Lin, C. (2007). Arabidopsis Cryptochrome 2 Completes Its Posttranslational Life Cycle in the Nucleus. Plant Cell *19*, 3146–3156.

Yu, X., Liu, H., Klejnot, J., and Lin, C. (2010). The Cryptochrome Blue Light Receptors. Arabidopsis Book *8*, e0135.

Zádníková, P., Petrásek, J., Marhavy, P., Raz, V., Vandenbussche, F., Ding, Z., Schwarzerová, K., Morita, M.T., Tasaka, M., Hejátko, J., et al. (2010). Role of PIN-mediated auxin efflux in apical hook development of Arabidopsis thaliana. Development *137*, 607–617.

Zeeberg, B.R., Liu, H., Kahn, A.B., Ehler, M., Rajapakse, V.N., Bonner, R.F., Brown, J.D., Brooks, B.P., Larionov, V.L., Reinhold, W., et al. (2011). RedundancyMiner: De-replication of redundant GO categories in microarray and proteomics analysis. BMC Bioinformatics *12*, 52.

Zhang, D., Jing, Y., Jiang, Z., and Lin, R. (2014). The Chromatin-Remodeling Factor PICKLE Integrates Brassinosteroid and Gibberellin Signaling during Skotomorphogenic Growth in Arabidopsis. Plant Cell *26*, 2472–2485.

Zhang, H., He, H., Wang, X., Wang, X., Yang, X., Li, L., and Deng, X.W. (2011). Genome-wide mapping of the HY5-mediated genenetworks in Arabidopsis that involve both transcriptional and post-transcriptional regulation. The Plant Journal *65*, 346–358.

Zhang, X., Clarenz, O., Cokus, S., Bernatavichute, Y.V., Pellegrini, M., Goodrich, J., and Jacobsen, S.E. (2007). Whole-Genome Analysis of Histone H3 Lysine 27 Trimethylation in Arabidopsis. PLoS Biol *5*.

Zhao, L., Peng, T., Chen, C.-Y., Ji, R., Gu, D., Li, T., Zhang, D., Tu, Y.-T., Wu, K., and Liu, X. (2019). HY5 Interacts with the Histone Deacetylase HDA15 to Repress Hypocotyl Cell Elongation in Photomorphogenesis1[OPEN]. Plant Physiol *180*, 1450–1466.

Zhao, Y., Mou, M., Li, P., Huang, Y., Zhai, X., Ma, Y., Liu, J., and Yu, X. (2015). Theoretical modeling of the Aux/IAA negative feedback circuit in plants. South African Journal of Botany *100*, 16–19.

Zhiponova, M.K., Morohashi, K., Vanhoutte, I., Machemer-Noonan, K., Revalska, M., Van Montagu, M., Grotewold, E., and Russinova, E. (2014). Helix–loop–helix/basic helix–loop–helix transcription factor network represses cell elongation in Arabidopsis through an apparent incoherent feed-forward loop. PNAS *111*, 2824–2829.

Zhou, B.-R., Feng, H., Kato, H., Dai, L., Yang, Y., Zhou, Y., and Bai, Y. (2013). Structural insights into the histone H1-nucleosome complex. PNAS *110*, 19390–19395.

Zhou, P., Song, M., Yang, Q., Su, L., Hou, P., Guo, L., Zheng, X., Xi, Y., Meng, F., Xiao, Y., et al. (2014). Both PHYTOCHROME RAPIDLY REGULATED1 (PAR1) and PAR2 Promote Seedling Photomorphogenesis in Multiple Light Signaling Pathways. Plant Physiology *164*, 841–852.

Zhou, Y., Wang, Y., Krause, K., Yang, T., Dongus, J.A., Zhang, Y., and Turck, F. (2018). Telobox motifs recruit CLF/SWN–PRC2 for H3K27me3 deposition via TRB factors in Arabidopsis. Nat Genet *50*, 638–644.